



Afdelingen for Bærende Konstruktioner
Department of Structural Engineering
Danmarks Tekniske Højskole · Technical University of Denmark

Plastic Analysis of Shear in Beams
Deep Beams and Corbels

Chen Ganwei

Serie R

No 237

1988

PLASTIC ANALYSIS OF SHEAR IN BEAMS
DEEP BEAMS AND CORBELS

by

Chen Ganwei

Plastic Analysis of Shear in Beams Deep Beams and Corbels
Copyright © by Chen Ganwei 1988

Tryk:

Afdelingen for Bærende Konstruktioner
Danmarks Tekniske Højskole
Lyngby
ISBN 87-7740-003-8

	Page
<u>CONTENTS</u>	
Acknowledgements	5
Notation	6
I. Introduction	13
II. Plastic Theory for Concrete	16
2.1 Failure and Yield Criteria	16
2.1.1 Coulomb's Failure Hypothesis and Coulomb Materials	16
2.1.2 Coulomb's Modified Failure Hypothesis and Modified Coulomb Materials	18
2.1.3 Failure Criterion for Concrete	24
2.2 Theory of Plasticity	26
2.3 Internal Work for Plain Concrete	28
2.3.1 The Dissipation of Concrete in Plane Strain Fields	31
2.3.2 The Dissipation of Concrete in Plane Stress Fields	35
2.4 Dissipation of Curved Yield Line Corresponding to Rotation Around an Arbitrary Point in the Plane	40
2.5 The Plastic Strengths of Concrete	44
2.6 Basic Assumptions	46
III. Bending Carrying Capacity of Beams, Deep Beams and Corbels	48
3.1 Members with Only Tensile Reinforcement	48
3.1.1 Beams and Deep Beams with Rectangular Section	48
3.1.2 Corbels with Rectangular section	49
3.2 Beams with Compression Reinforcement	50
3.3 Deep Beams with Horizontal Web Reinforcement	51
3.4 The Effectiveness Factor for Bending	53
3.5 Experimental Verification	54
IV. Shear Carrying Capacity of Beams, Deep Beams and Corbels without Web Reinforcement	56
4.1 Shear Capacity Considering the Tensile Strength of Concrete	56
4.1.1 Lower Bound Solution	57
4.1.2 Upper Bound Solution	67
4.1.3 The Complete Plastic Solutions	76
4.1.4 The p^* and v Values in the Plastic Solutions	87
4.2 Shear Capacity Neglecting the Tensile Strength of Concrete	104
4.2.1 Lower Bound Solution	104
4.2.2 Upper Bound Solution	107
4.2.3 Modified Simple Formula	110
4.3 The Influence of Normal Forces on the Shear Capacity	114
4.3.1 Theoretical Solutions	114
4.3.2 Experimental Verification	129
4.4 The Influence of Prestress to Shear Capacity of Beams	134
4.5 Shear Capacity of Joints	143

V. Shear Carrying Capacity of Beams with Web Reinforcement	147
5.1 Theoretical Solutions	148
5.2 The Effective Shear Depth h^* and the Effectiveness Factor μ	152
5.3 Experimental Verification of the Theory	155
5.3.1 Conventional Thin-Webbed Beams	155
5.3.2 Deep Beams with Web Reinforcement	158
5.3.3 Prestressed Beams with Web Reinforcement	161
5.4 Some Discussion on μ	164
SUMMARY	167
RESUME	168
REFERENCES	170
APPENDIX A. Test Data of Deep Beams Failed in Flexure	188
B. Test Data of Beams, Deep Beams and Corbels Failed in Shear	191
C. Test Data of Beams and Corbels with Normal Force	210
D. Test Data of Prestressed Beams without Shear Reinforcement	213
E. Test Data of Conventional Thin-Webbed Beams with Web Reinforcement	221
F. Test Data of Deep Beams with Web Reinforcement	224
G. Test Data of Prestressed Beams with Web Reinforcement	225

ACKNOWLEDGEMENTS

This research was sponsored by the Danish Council for Scientific and Technical Research (STVF) under grants to Professor M.P. Nielsen. The study work was carried out at the Department of Structural Engineering of the Technical University of Denmark, under the guidance of Professor M.P. Nielsen. I wish to express my deep gratitude and sincere appreciation to him for giving me the possibility of completing my Ph.D studies and for his advice, encouragement and constant help, without which it would have been impossible to finish this work. I also wish to thank Dr. Bjarne Chr. Jensen for serving as examiner of my thesis.

In connection with my studies I received a lot of help from many colleagues at the Department of Structural Engineering. In particular, Mr. Bent S. Andreasen and Mr. Bent Feddersen greatly inspired me and contributed with many valuable suggestions. I would like to take this opportunity to thank all those who have assisted me in my work.

Thanks are due to Mrs. Karen Perris and Mrs. Bente Jensen for their fast typing and to Mr. Benny Leisten for his excellent drawings.

Financial assistance from the Danish Council for Scientific and Technical Research (STVF) is gratefully acknowledged.

NOTATIONS

The symbols are defined when they first occur in the text. The frequently used notations are listed alphabetically below.

- a: Clear shear span
- A: Internal work
- A_c : Area of cross-section
- a_{cc} : Shear span, measured from concentrated load to the reaction for beams or measured from concentrated load to the face of column for corbels
- A_s : Cross-sectional area of main tensile reinforcement
- A_{cs} : Cross-sectional area of compressive reinforcement
- A_{swh} : Cross-sectional area of horizontal web reinforcement per unit depth
- A_{swv} : Cross-sectional area of vertical web reinforcement per unit length
- b: Web width of beam
- b_l: Width of compressive flange
- c: Internal cohesion of material
- C: Resultant compressive force of concrete.

$$\text{Parameter, } C = \begin{cases} 1-2\phi^* & \phi^* \leq \frac{1}{2} \\ 0 & \phi^* > \frac{1}{2} \end{cases}$$

c_1, c_2 : Constants

$$C_1 = \begin{cases} 1-2(n^*+\phi^*) & , & n^*+\phi^* < \frac{1}{2} \\ 0 & , & n^*-\phi^* \leq \frac{1}{2} \leq n^*+\phi^* \\ 1-2(n^*-\phi^*) & , & \frac{1}{2} < n^*-\phi^* \end{cases}$$

C_y : Coefficient of variation

d: Effective depth of beam. Length of line

$$D = \begin{cases} \frac{\mu-2\phi^*}{\lambda} & \phi^* \leq \frac{\mu}{2} \\ 0 & \phi^* > \frac{\mu}{2} \end{cases}$$

D: Parameter, $D =$

$$D_0 = \begin{cases} \frac{\mu_0-2T/bhf_c^*}{\lambda_0} & T/bhf_c^* \leq \frac{\mu_0}{2} \\ 0 & T/bhf_c^* > \frac{\mu_0}{2} \end{cases}$$

D_0 : Parameter, $D_0 =$

$$D_1 = \begin{cases} \frac{\mu-2(n^*+\phi^*)}{\lambda} & n^*+\phi^* < \frac{\mu}{2} \\ 0 & n^*-\phi^* \leq \frac{\mu}{2} \leq n^*+\phi^* \\ \frac{\mu-2(n^*-\phi^*)}{\lambda} & \frac{\mu}{2} < n^*-\phi^* \end{cases}$$

D_1 : Parameter, $D_1 =$

d_c : Distance from extreme compression fibre to centroid of compression reinforcement

d_s : Stirrup depth

f_A : Separation resistance

f_C : Uniaxial compressive strength of concrete

f_C^* : Plastic compressive strength of concrete, defined as $f_C^* = \nu f_C$

F_{se} : Effective prestress acting on the section
 f_c : Tensile strength of concrete
 f_c^* : Plastic tensile strength of concrete, defined as $f_c^* = \nu_t f_c$
 f_y : Yield strength of tensile reinforcement
 f_{yc} : Yield strength of compressive reinforcement
 f_{yw} : Yield strength of web reinforcement
 f_{ywh} : Yield strength of horizontal web reinforcement
 h : Depth of cross-section
 h_1 : Depth of compressive flange
 h^* : Effective shear depth
 k : Material constant, $k = (1 + \sin\omega) / (1 - \sin\omega)$. Length of loading platen
 k_1, k_2 : Constants
 l : Material constant, $l = 1 - (k-1)f_c/f_c$
 L_o : Span of beam
 m : Material constant, $m = 1 - (k+1)f_c/f_c$
 M_p : Bending yield moment
 m_p^* : Effective dimensionless bending yield moment, defined as

$$m_p^* = M_p / b d^2 f_c$$

 n : Normal direction. Number of tests

N : Normal force
 n^* : Effective normal force degree, defined as $n^* = N / b h f_c$
 P : External load
 r : Function of curved yield line. Polar coordinate
 r_o, r_1 : Parameters in polar coordinate system
 r_m : Length of line
 S_y : Equivalent yield stress of web reinforcement, defined as

$$S_y = A_{sw} f_{yw} / b \text{ or } S_y = A_{sw} f_{yw} / b$$

 t : Tangential direction. Distance
 T : Resultant force of tensile reinforcement
 v : Relative displacement in yield line
 V : Ultimate load. Volume
 V_{cal} : Calculated ultimate load
 V_t, V_{test} : Observed ultimate load in test
 W : Internal plastic work per unit volume (dissipation)
 W_E : External work
 W_I : Internal work
 W_1 : Dissipation per unit length
 x : Depth of rectangular stress block. Cartesian coordinate. Distance

- x_0 : Distance
- \bar{x} : Mean
- y : Distance measured from bottom of cross section to centroid of tensile reinforcement. Cartesian coordinate
- y_0 : Distance from top of cross section to neutral axis
- z : Internal moment lever arm
- α : Angle. Ratio, $\alpha = d_c/d$
- α_1 : Ratio, $\alpha_1 = \phi_{hw}^*/\phi_b^*$
- α_m, β, τ : Angles
- γ_{nt} : Shear strain in n,t-coordinate system
- $\delta, \delta_m, \delta_s$: Relative displacement rates.
- A : Width of deforming zone idealized as yield line
- $\epsilon_1, \epsilon_2, \epsilon_3$: Principal strains
- ϵ_n, ϵ_t : Strains in n- and t-directions, respectively
- η : Rotation rate. Ratio, $\eta = \frac{\lambda}{\mu}$
- θ : Angles. Polar coordinate
- θ_0, θ_1 : Angles

- λ : Proportionality factor in flow law. Material constant, $\lambda = 1 - (k-1)\rho^*$
- λ_1 : Proportionality factor in flow law
- λ_0 : Material constant, $\lambda_0 = 1 - k \frac{\sigma_1^*}{f_c^*} + \frac{\sigma_1^*}{f_c^*}$
- μ : Coefficient of friction, $\mu = \tan\phi$. Material constant $\mu = 1 - (k+1)\rho^*$
- μ_0 : Material constant, $\mu_0 = 1 - k \frac{\sigma_1^*}{f_c^*} - \frac{\sigma_1^*}{f_c^*}$
- ν : Effectiveness factor for the compressive strength of concrete
- ν_b : Effectiveness for bending
- ν_t : Effectiveness factor for the tensile strength of concrete
- ξ : Parameter, $\xi = \begin{cases} n^{*+\phi^*} & , & n^{*+\phi^*} < \frac{k-1}{4k} \\ \frac{k-1}{4k} & , & n^{*+\phi^*} \leq n^{*+\phi^*} \\ n^{*-\phi^*} & , & \frac{k-1}{4k} < n^{*+\phi^*} \end{cases}$
- ρ^* : Effectiveness factor, $\rho^* = f_c^*/f_c^*$
- σ : Normal stress. Standard deviation
- $\sigma_1, \sigma_2, \sigma_3$: Principal stresses
- $\sigma_{I, II}$: Principal stresses
- σ_b, σ_y : Stresses
- σ_x, σ_y : Normal stresses in x,y-coordinate system

τ : Shear stress

τ_{xy} : Shear stress in x,y-coordinate system

φ : Angle of friction for concrete. Reinforcement ratio, defined as $\varphi = A_s/bh$

φ_b : Reinforcement ratio for bending, defined as $\varphi_b = A_s/bd$

φ_{wh} : Horizontal web reinforcement ratio, defined as $\varphi_{wh} = A_{sw}h/b$

φ_{wv} : Vertical web reinforcement ratio, defined as $\varphi_{wv} = A_{sw}v/b$

ϕ^* : Effective reinforcement degree, defined as $\phi^* = A_s f_y / b h f_c$

ϕ_b^* : Effective reinforcement degree for bending, $\phi_b^* = A_s f_y / b d f_c$

ϕ_c^* : Effective compressive reinforcement degree, $\phi_c^* = A_{sc} f_c / b d f_c$

ϕ_h^* : Effective horizontal reinforcement degree, $\phi_h^* = A_s f_y / b h f_c + A_{sw} f_{yw} / b f_c$

ϕ_{hw}^* : Effective horizontal web reinforcement degree, $\phi_{hw}^* = A_{sw} f_{yw} / b f_c$

ϕ_v^* : Effective vertical web reinforcement degree, $\phi_v^* = A_{swv} f_{yw} / b f_c$

ϕ_{yo}^* : Critical web reinforcement degree

χ : Parameter, $\chi = \begin{cases} n^* + \phi^* & \frac{2}{h} \leq \tan \varphi \\ n^* - \phi^* & \frac{2}{h} > \tan \varphi \end{cases}$

ω : Angle

CHAPTER I. INTRODUCTION

During shear tests on deep concrete beams without web reinforcement in 1985, I became interested in limit state analysis for concrete inspired by the achievements of plastic theory of concrete in shear, which had been developed since the 1960's in Denmark [67.1], [74.3], [75.1], [75.4], [76.3], [76.6], [77.1], [77.2], [78.3] and [79.1].

Deep beam is the beam having a depth comparable to its span. It has been widely used in such structures as tanks, bins, silos and in buildings. Because of the geometry, deep beams may have relatively low shear span-to-depth ratio compared with conventional slender beams and relatively low reinforcement ratio because of the bigger concrete web. Shear is very often a dominant factor in deep beams without web reinforcement.

For a long time deep beams were classified and treated as an independent kind of structural members different from beams and corbels. Shear in reinforced concrete deep beams has been studied extensively for decades. There have been conducted a lot of work on shear behavior and shear capacity of deep beams. The literature on the subject is almost overwhelming. Most papers, however, report specific test series and supply empirical formulae to fit the results obtained. Just as most building codes contain little more than empirical formulae deduced from a large number of tests. The traditional design approach for deep concrete beams based on accumulated experience may be sufficiently safe, but they need not be particularly economical.

Compared to the hitherto dominating empirical methods, the rational mathematical theory of plasticity has considerable advantages. Firstly, as a general theory, it unifies the shear analysis in beams with that of deep beams and corbels. According to the limit state analysis, so far as the shear problem is concerned, the only difference between beams, deep beams and

corbels is the shear span-to-depth ratio. Normal beams have relatively large shear span-to-depth ratios, while corbels have very small shear span-to-depth ratios and deep beams lie between them. Secondly, as a rational mathematical model describing the mechanism of the shear members, it leads to a thorough understanding of the failure mechanism in concrete. Therefore, by means of this theory one can calculate the ultimate shear capacity effectively and simply, and also dimension and detail the shear members economically.

Furthermore, it is easy to extend the theory into applications within related areas not directly covered by cases studied, while such an extension is more or less impossible or at least extremely difficult and uncertain when dealing with empirical methods. An example of extending the plastic solution to fibre reinforced concrete can be found in [87.3]. Since many examples [73.7], [76.6], [77.7], [78.5] and [80.2] have fully proved that the plastic approach is simple, consistent and able to predict remarkably well the shear failure load of reinforced concrete beams, it is natural to investigate whether the ultimate strength of deep beams with and without web reinforcement can also be solved by this theory. It has been found that the simple plastic solutions [78.2] with the so-called square yield locus and corresponding v formula in [79.4] are not suitable for deep beams and corbels, because they neglect the tensile strength of concrete in the web. Therefore, the exact solutions regarding the concrete as a perfectly plastic modified Coulomb-material with a small, but non-zero tension cut off have been derived in Chapter IV. The complete solutions are compared with the simple solutions and the modified simple solutions for conventional beams are then presented.

Results derived by plastic theory have to be modified in an empirical manner because of the well known fact that concrete is not perfectly plastic and the whole failure surface will not be fully active. To take this into account in a simple way the uniaxial compressive strength f_c is reduced by the effectiveness factor v , which must be correlated with the experimental evidence.

Therefore, in this paper a big effort has been done to develop a more general and rational approach for evaluating an approximate v -value in some shear cases, especially for shear members without web reinforcement.

The theoretical calculations are compared with a wide range of available test results of beams, deep beams and corbels found in literature. A satisfactorily good agreement has been found.

2.1 Failure and yield criteria

Failure and yield criteria are the criteria that must be satisfied for the stress field at yielding. The purpose of formulating failure and yield criteria for a material is to enable us to determine their behavior by means of simple tests from which we can evaluate the risk of failure or yielding for complicated stress fields.

Since our knowledge of the structure and composition of materials does not yet enable us to develop the failure criteria based on known natural laws, most failure criteria appear as hypotheses whose application to various materials will have to be evaluated from tests.

2.1.1 Coulomb's failure hypothesis and Coulomb material

Coulomb's failure hypothesis was presented in 1773 by C.A. Coulomb, who had remarked that failure in stone prisms subjected to uniaxial compression took place along certain surfaces. These surfaces are called sliding surfaces, and this type of failure is known as sliding failure.

Sliding failure is assumed to occur in a section if the shear stress $|\tau|$ in this section exceeds the sliding resistance, which can be determined by two contributions. One contribution is the internal cohesion, denoted c , which is a material constant. The other contribution comes from a kind of internal friction and equals a certain fraction μ of the normal stress σ in the sliding plane. The quantity μ is called the coefficient of friction. If σ is a compressive stress, it gives a positive contribution; if σ is a tensile stress, it gives a negative contribution. The condition for sliding failure therefore is

$$|\tau| = c - \mu\sigma \tag{2.1.1}$$

where c and μ are positive constant and σ is counted positive as a tensile stress. A material complying with failure condition (2.1.1) is called a Coulomb material. Coulomb's failure hypothesis is governed entirely by two parameters, e.g. c and μ .

Fig. 2.1 shows Coulomb's failure hypothesis depicted in a (σ, τ) coordinate system. The figure includes Mohr's circles for the stresses at a point at which the failure hypothesis is satisfied.

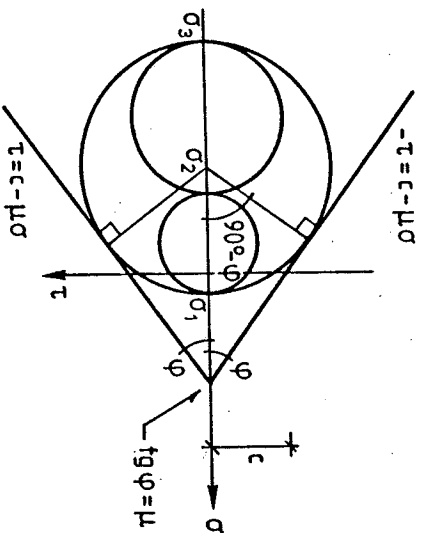


Figure 2.1. Coulomb's failure hypothesis with Mohr's circles.

The angle ϕ given by $\tan\phi = \mu$ is called the angle of friction.

A more general hypothesis was formulated by O. Mohr in 1882. Mohr assumed that failure occurs when the stresses in a section satisfy the condition

$$f(\sigma, \tau) = 0 \tag{2.1.2}$$

where $f(\sigma, \tau)$ is a function characteristic of the material, and

where σ and τ are normal stress and the shear stress, respectively, in the section. Coulomb's failure hypothesis is thus a special case of Mohr's theory.

2.1.2 Coulomb's modified failure hypothesis and modified Coulomb material

For a large group of materials it appears that reasonable failure conditions are obtained by combining Coulomb's sliding hypothesis with a bound for the maximum tensile stress. The resulting failure criterion makes it natural to distinguish between two failure modes, sliding failure and separation failure. In both cases the name of the failure refers to what we imagine the relative motion between particles on each side of the failure surface to be. At sliding failure there is motion parallel to the failure surface, while at the separation failure motion is perpendicular to the failure surface.

Separation failure occurs when the biggest tensile stress σ_1 in a section exceeds the separation resistance f_A , i.e.

$$\sigma_1 = f_A \quad (2.1.3)$$

This failure hypothesis, which results from a combination of (2.1.1) and (2.1.3), is called Coulomb's modified failure hypothesis.

A material complying with (2.1.1) and (2.1.3) is called a modified Coulomb material. As is clear, Coulomb's modified failure hypothesis requires three parameters to be determined, e.g., c , μ and f_A . Fig. 2.2 shows the modified Coulomb's failure hypothesis illustrated in a (σ, τ) -coordinate system.

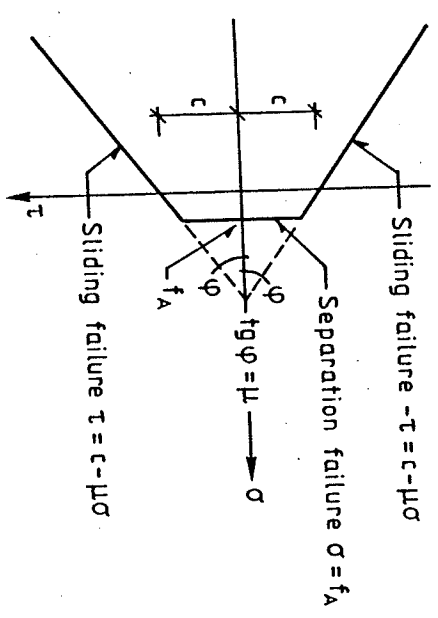


Figure 2.2. Failure criterion for a modified Coulomb material.

The straight lines, which represent the failure criterion, divide the plane into two regions. When the stresses in a section correspond to a Mohr's circle lying within the boundary lines, no failure will occur, while stresses corresponding to circles touching the lines represent stress combinations which in fact involve failure. The failure mode depends on whether the contact point lies on the lines $|\tau| = c - \mu\sigma$, which involve sliding failure, or on the line $\sigma = f_A$, which involves separation failure.

By means of drawing Mohr's circle it is easy to investigate whether the stress field in a point, given by the principal stresses σ_1, σ_2 and σ_3 , where $\sigma_1 > \sigma_2 > \sigma_3$, will cause failure. Because on Mohr's circles the points closest to the boundary lines lie on the circle with $(\sigma_1 - \sigma_3)$ as diameter, we have only to focus on the points on this circle. If the circle with diameter $(\sigma_1 - \sigma_3)$ lies within the boundary lines, failure will not occur (see Fig. 2.3).

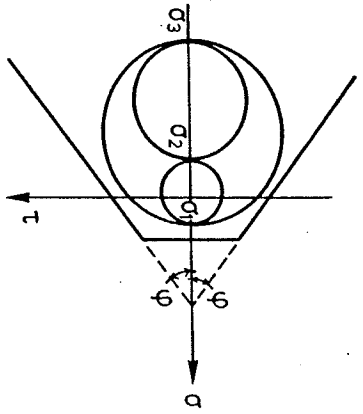


Figure 2.3. Mohr's circles of principal stresses and the failure criterion.

If the circle with diameter $(\sigma_1 - \sigma_3)$ touches the boundary lines corresponding to sliding failure, a sliding failure may occur in two sections for reasons of symmetry, (see Fig. 2.4).

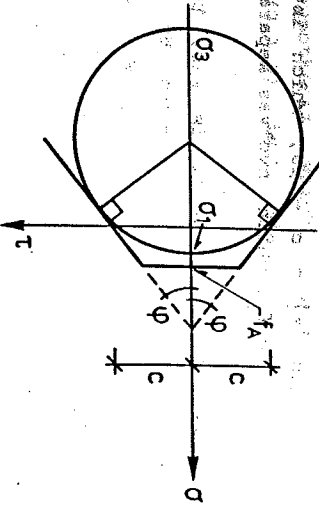


Figure 2.4. Mohr's circles at sliding failure.

If the circle touches the line corresponding to separation failure, a separation failure will then take place, (see Fig. 2.5).

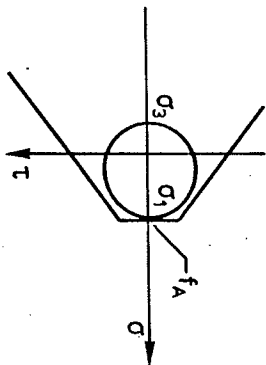


Figure 2.5. Mohr's circles at separation failure.

By means of the Fig. 2.4, we find that equation (2.1.1) for sliding failure can be written in principal stress form in the following way:

$$\frac{1}{2}(\sigma_1 - \sigma_3) = c \cos \varphi - \frac{1}{2}(\sigma_1 + \sigma_3) \sin \varphi \quad (2.1.4)$$

which is valid for $\sigma_1 > \sigma_2 > \sigma_3$. If the mutual magnitudes of the principal stresses are altered, equation (2.1.4) must be altered correspondingly.

Introducing

$$k = \left(\frac{\cos \varphi}{1 - \sin \varphi} \right)^2 = \frac{1 + \sin \varphi}{1 - \sin \varphi} = \tan^2 \left(\frac{\pi}{4} + \frac{\varphi}{2} \right) \quad (2.1.5)$$

The condition for sliding failure can be written in the simple form

$$k\sigma_1 - \sigma_3 = 2c\sqrt{k} \quad (2.1.6)$$

While the condition for separation failure is

$$\sigma_1 = f_A \quad (2.1.7)$$

The uniaxial compression strength f_C of a material is determined by a test, where the stress field at failure is given by $(\sigma_1, \sigma_2, \sigma_3) = (0, 0, -f_C)$. Since the uniaxial compression test always involves sliding failure (see Fig. 2.6), we find from equation (2.1.6)

$$-f_C = 2c\sqrt{K} \quad (2.1.8)$$

whereupon equation (2.1.6) can be written as

$$k\sigma_1 - \sigma_3 = f_C \quad (2.1.9)$$

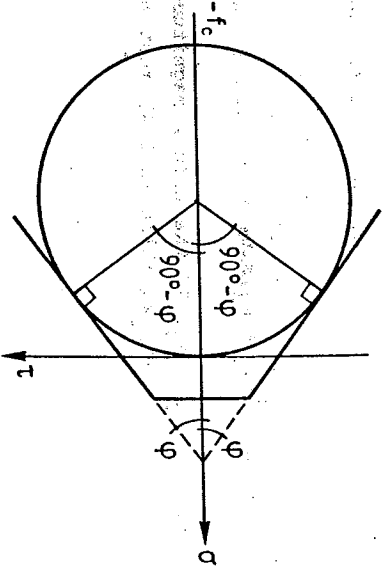
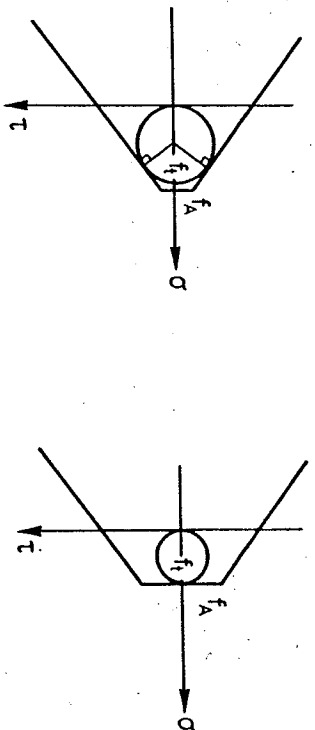


Figure 2.6. Mohr's circle at pure compression.

In a similar way the uniaxial tensile strength of a material f_t can be introduced as the stress field at failure that is given by $(\sigma_1, \sigma_2, \sigma_3) = (f_t, 0, 0)$.

As seen clearly from Fig. 2.7, the tensile test holds the possibility of sliding failure as well as separation failure.



Sliding failure.

Separation failure.

Figure 2.7. Mohr's circle at pure tension.

In the case of sliding failure we have, applying equation (2.1.6)

$$f_t = \frac{1}{k} f_C \quad (2.1.10)$$

In the case of separation failure we get, applying equation (2.1.7)

$$f_t = f_A \quad (2.1.11)$$

This means that the tensile failure is a sliding failure when

$$\frac{1}{k} f_C < f_A \quad (2.1.12)$$

and a separation failure when

$$\frac{1}{k} f_C > f_A \quad (2.1.13)$$

In the case of $\frac{1}{k} f_C < f_A$, the equation (2.1.6) can then be written as

$$\frac{\sigma_1}{f_t} - \frac{\sigma_3}{f_C} = 1 \quad (2.1.14)$$

2.1.3 Failure criterion for concrete

A lot of tests have shown that in many respects concrete can be considered as a modified Coulomb material, the parameter k being about 4 [84.1]. The agreement has been found to be reasonable. The modified Coulomb's failure hypothesis can thus be used as yield condition for concrete.

With $k = 4$, we find the constant $\mu = \tan\varphi$

$$\mu = 0.75 \quad (2.1.15)$$

corresponding to an angle of friction

$$\varphi = 37^\circ \quad (2.1.16)$$

From equation (2.1.8), we get

$$c = \frac{f_c}{2\sqrt{k}} = \frac{1}{4}f_c \quad (2.1.17)$$

In the tests we find that both the tension failure and the shear failure are separation failure. If the tensile strength is f_t , we therefore have

$$f_A = f_t \quad (2.1.18)$$

The failure condition (2.1.6) and (2.1.7) then get the final form

$$4\sigma_1 - \sigma_3 = f_c \quad (2.1.19)$$

$$\sigma_1 = f_A = f_t \quad (2.1.20)$$

The failure condition for concrete in the (σ, τ) -coordinate system is shown in Fig. 2.8.

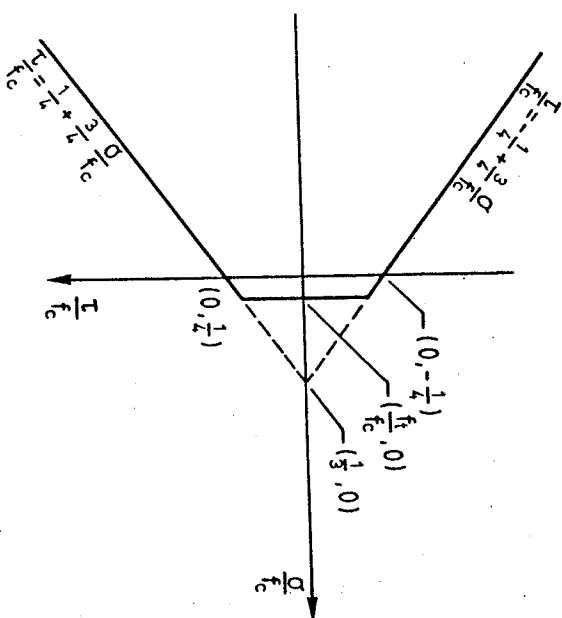


Figure 2.8. Failure condition for concrete in a (σ, τ) -coordinate system.

It's worth to notice that Coulomb's modified failure hypothesis does not completely describe the failure criterion for concrete. According to Coulomb's failure hypothesis the intermediate stress σ_2 has no effect on the carrying capacity. However, tests show that it has an effect in disagreement with the hypothesis. Some biaxial compression tests show that $\sigma_3/f_c = -1.2$ to -1.4 for $\sigma_1/f_c = -0.6$, whereas Coulomb's failure hypothesis gives $\sigma_3/f_c = -1.0$. Biaxial tensile tests and tensile/compressive tests also show that the Coulomb's modified failure hypothesis is not always convex and is a little on the unsafe side when tensile stresses occur.

Even then, the hypothesis must anyway be described as usable because the deviations are often moderate, and because there is a great dependence of the strength properties on the test circumstances [77.1]. Furthermore, in plastic theory we do not need a very accurate failure condition because of the large empirical modifications necessary for getting agreement between tests and theory (the v -value).

In the following chapters we will throughout assume that the concrete is a rigid, perfectly plastic material with the modified Coulomb's failure criterion as yield condition and the associated flow rule (normality condition) as constitutive equations.

2.2 Theory of plasticity

A rigid-plastic material is defined as a material in which no deformations occur for stresses up to a certain limit, the yield point. The yield condition describes the states of stress which may result in failure of the material. For stresses at the yield point, arbitrarily large deformations are possible without any change in the stresses.

A rigid-plastic material does not exist in reality. However, it is possible to use the model if the plastic strains are much larger than the elastic strains.

For an isotropic material we may express the failure condition in terms of the principal stresses as

$$f(\sigma_1, \sigma_2, \sigma_3) = 0 \quad (2.2.1)$$

This means that stresses rendering $f < 0$ correspond to stresses that can be sustained by the material and thus these stress combinations give no strain, while $f > 0$ corresponds to stress fields which the material cannot sustain and $f = 0$ means that plastic deformation may take place.

The relationship between the strains is then determined by the yield law (also called associated flow rule)

$$\epsilon_1 = \lambda \frac{\partial f}{\partial \sigma_1} \quad (i = 1, 2, 3) \quad (2.2.2)$$

In a 3 dimensional representation, with σ_1 , σ_2 and σ_3 as coordinate axes, (2.2.1) produces a so-called yield surface. If we

regard (2.2.2) as a vector in the $\sigma_1, \sigma_2, \sigma_3$ -coordinate system, it is a normal vector to the yield surface at the point $(\sigma_1, \sigma_2, \sigma_3)$. Equation (2.2.2) is therefore called the normality condition.

As the plastic work $\sigma_i \epsilon_i$ is assumed to be non-negative, it is seen that

$$\lambda \geq 0 \quad (2.2.3)$$

Thus the vector $(\epsilon_1, \epsilon_2, \epsilon_3)$ becomes an outward-directed normal to the yield surface. If the yield surface is a differentiable surface, the normality criterion uniquely determines the direction of the strain vector for a given stress field on the yield surface. If the yield surface consists of piece wise differentiable surfaces, the strain vector for stress fields lying on the curve of intersection of two surfaces must be located in the angle between the normals to the adjacent surfaces.

The load carrying capacity of a body consisting of a rigid-plastic material is the load at which plastic deformations become possible. The load carrying capacity is also called the yield load or the failure load. For determination of the yield load of a rigid-plastic body the following extremum principles are very useful.

First we define some important concepts which will be used in formulating the extremum principles.

A safe and statically admissible stress field is a stress field corresponding to stresses within or on the yield surface and satisfying the equilibrium conditions and the statical boundary conditions.

A geometrically admissible failure mechanism is a deformation field that satisfies the compatibility conditions and the geometrical boundary conditions.

The extremum principles can be described as follows:

The Upper-Bound Theorem:
 Any load found from the work equation for an arbitrary, geometrically admissible failure mechanism is greater than or equal to the yield load of the body.

The Lower-Bound Theorem:
 Any load corresponding to a safe and statically admissible stress field is smaller than or equal to the yield load of the body.

The Uniqueness Theorem:

If the lowest upper bound and the highest lower bound coincide, then an exact solution has been found, the coinciding upper and lower bound being the yield load of the body.

2.3 Internal work for plain concrete

Here, concrete is identified as a rigid-plastic modified Coulomb material. A yield line in concrete is a kinematical discontinuity separating two rigid parts. One part is moving relatively to the other with the displacement rate v inclined at the angle α to the yield line, (Fig. 2.9).

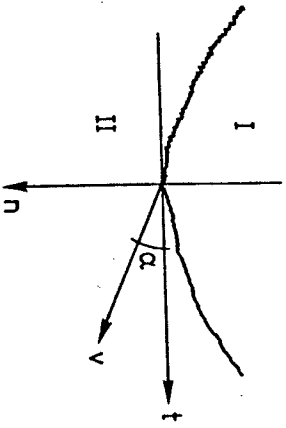


Figure 2.9. Yield line in concrete.

The discontinuity is a mathematical idealization of a narrow deformation zone, (Fig. 2.10).

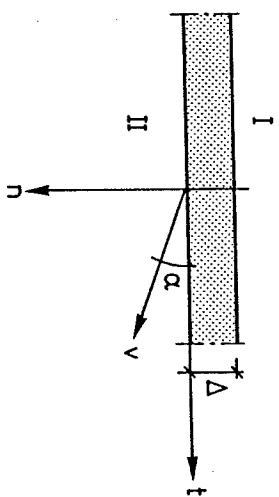


Figure 2.10. Mathematical idealization of a narrow deforming zone.

Now let us consider a narrow deforming zone of yield line in plain concrete having the width Δ , the length one and breadth b , (Fig. 2.11).

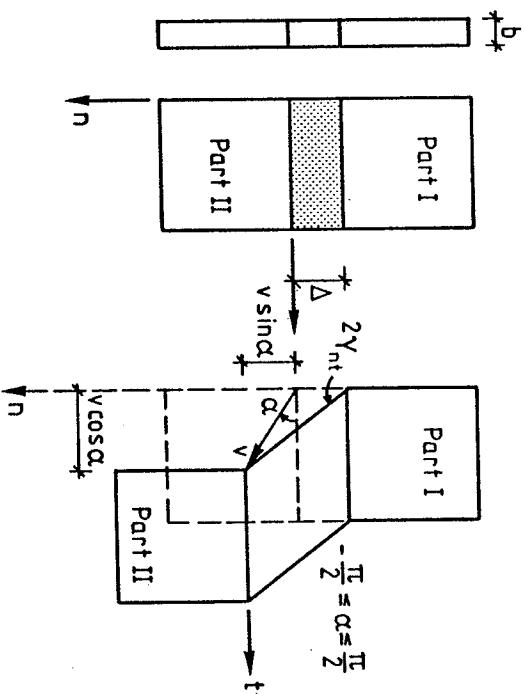


Figure 2.11. Deforming zone of yield line in plain concrete.

The strains in this narrow deforming zone are

$$\left. \begin{aligned} \epsilon_n &= \frac{v \sin \alpha}{A} \\ \epsilon_t &= 0 \\ 2\epsilon_{nt} &= \frac{v \cos \alpha}{A} \end{aligned} \right\} \quad (2.3.1)$$

The principal strains are found from (2.3.1)

$$\epsilon_1 = \frac{v}{2A}(\sin \alpha + 1) \quad (2.3.2)$$

$$\epsilon_2 = \frac{v}{2A}(\sin \alpha - 1) \quad (2.3.3)$$

From equations (2.3.2) and (2.3.3) we find that

$$\epsilon_1 - \epsilon_2 = \frac{v}{A} \quad (2.3.4)$$

$$\frac{\epsilon_1}{\epsilon_2} = -\frac{1 + \sin \alpha}{1 - \sin \alpha} \quad (2.3.5)$$

The internal work (dissipation) for a material deformed corresponding to the strains $(\epsilon_1, \epsilon_2, \epsilon_3)$ is

$$A = \int_V (\sigma_1 \epsilon_1 + \sigma_2 \epsilon_2 + \sigma_3 \epsilon_3) dV = \int_V W dV \quad (2.3.6)$$

W is the internal work per unit volume being

$$W = \sum_{i=1}^3 \sigma_i \epsilon_i \quad (i = 1, 2, 3) \quad (2.3.7)$$

Using Mohr's strain circle, we find

$$\tan 2\beta = \cot \alpha \quad (2.3.8)$$

Here, β is the angle between the displacement rate vector and the first principal axis, (Fig. 2.12).

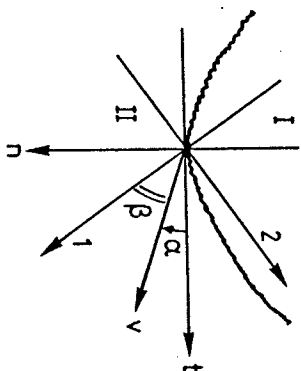


Figure 2.12. The relation between the relative displacement rate vector and the principal axes.

Solving equation (2.3.8) yields

$$\beta = \frac{1}{2} \left(\frac{\pi}{2} - \alpha \right) \quad (2.3.9)$$

It means the first principal axis bisects the angle between the relative displacement rate vector and the yield line normal.

2.3.1.1 The dissipation of concrete in plane strain fields

A plane strain field is defined as a strain field in which the strains in directions perpendicular to a plane are zero. For simplicity we assume $\epsilon_3 = 0$ and $\sigma_1 \geq \sigma_3 \geq \sigma_2$. In this case the yield criterion is composed of the following two criteria

$$k\sigma_1 - \sigma_2 - f_c = 0 \quad (2.3.10)$$

$$\sigma_1 - f_c = 0 \quad (2.3.11)$$

The equation (2.3.10) corresponds to sliding failure while equation (2.3.11) corresponds to separation failure.

For the sliding failure, the related strains can be found directly from the normality criterion (2.2.2).

Here, we get

$$(\epsilon_1, \epsilon_2, \epsilon_3) = (\lambda k, -\lambda, 0) \quad (2.3.12)$$

It is easy to find that

$$\epsilon_1 - \epsilon_2 = \lambda(k + 1) \quad (2.3.13)$$

and

$$\frac{\epsilon_1}{\epsilon_2} = -k = -\frac{1 + \sin\varphi}{1 - \sin\varphi} \quad (2.3.14)$$

Comparing equation (2.3.13) with (2.3.4) and equation (2.3.14) with (2.3.5), we have

$$\lambda = \frac{Y}{\Delta(k+1)} = \frac{Y}{\Delta} \frac{1 - \sin\varphi}{2} \quad (2.3.15)$$

and

$$\sin\alpha = \sin\varphi \quad (2.3.16)$$

Equation (2.3.16) yields

$$\alpha = \begin{cases} \varphi \\ \pi - \varphi \end{cases} \quad (2.3.17)$$

Inserting equations (2.3.12) and (2.3.15) into (2.3.7), we get

$$W = \lambda(\sigma_1 k - \sigma_2) = \frac{Y}{\Delta} \frac{1 - \sin\varphi}{2} f_c \quad (2.3.18)$$

For the separation failure, the related strains will be

$$(\epsilon_1, \epsilon_2, \epsilon_3) = (\lambda_1, 0, 0) \quad (2.3.19)$$

Comparing equation (2.3.19) with (2.3.2) and (2.3.3), we find that

$$\alpha = \frac{\pi}{2} \quad (2.3.20)$$

and

$$\lambda_1 = \frac{Y}{\Delta} \quad (2.3.21)$$

Then the internal work is easily found by inserting equations (2.3.19) and (2.3.21) into (2.3.7)

$$W = \lambda_1 f_c = \frac{Y}{\Delta} f_c \quad (2.3.22)$$

At the intersection of the two yield surfaces, corresponding to equations (2.3.10) and (2.3.11) being satisfied simultaneously, the strain vector will be an arbitrary positive linear combination of the strain vectors belonging to the two surfaces. The related strains then can be found to be

$$(\epsilon_1, \epsilon_2, \epsilon_3) = (\lambda k + \lambda_1, -\lambda, 0) \quad (2.3.23)$$

Comparing equation (2.3.23) with (2.3.3) and (2.3.2), we find that

$$\lambda = \frac{Y}{2\Delta} (1 - \sin\alpha) \quad (2.3.24)$$

and

$$\lambda_1 = \frac{Y}{2\Delta} (1 + \sin\alpha) \quad -\lambda k = \frac{Y}{\Delta} \frac{\sin\alpha - \sin\varphi}{1 - \sin\varphi} \quad (2.3.25)$$

In this case, the ranges of α are

$$\left. \begin{aligned} \varphi &\leq \alpha \leq \frac{\pi}{2} \\ \text{or } \frac{\pi}{2} &\leq \alpha \leq \pi - \varphi \end{aligned} \right\} \quad (2.3.26)$$

The internal work will be found by inserting equations (2.3.23), (2.3.24) and (2.3.25) into (2.3.7)

$$W = \frac{Y f_c}{2\Delta} [(1 - \sin\alpha) + 2 \frac{f_c}{f_c} \frac{\sin\alpha - \sin\varphi}{1 - \sin\varphi}] \quad (2.3.27)$$

It should be noticed that when $\alpha = \frac{\pi}{2}$, equation (2.3.27) is identical to equation (2.3.22), and when $\alpha = \varphi$ or $\pi - \varphi$, equation (2.3.27) changes into equation (2.3.18).

The formula (2.3.27) thus gives the internal work per unit volume of concrete in plane strain field.

If σ_1 , σ_2 and σ_3 , and ϵ_1 , ϵ_2 and ϵ_3 can mean any of the principal stresses and strains, analogous derivations can be made and the solutions are the same.

The dissipation per unit length W_1 is

$$W_1 = WbA \quad (2.3.28)$$

where b is the dimension of the body in direction perpendicular to the plane. Inserting (2.3.27) into (2.3.28), we get the complete formula for the dissipation per unit length of a discontinuity line in concrete in plane strain:

$$W_1 = \frac{1}{2} b f_c V [1 - \sin \alpha + 2 \frac{f_t}{f_c} \frac{\sin \alpha - \sin \varphi}{1 - \sin \varphi}] \quad \text{valid for } \varphi \leq \alpha \leq \pi - \varphi \quad (2.3.29)$$

Introducing the parameters

$$1 = 1 - 2 \frac{f_t}{f_c} \frac{\sin \varphi}{1 - \sin \varphi} \quad (2.3.30)$$

$$m = 1 - 2 \frac{f_t}{f_c} \frac{1}{1 - \sin \varphi} \quad (2.3.31)$$

The brief version

$$W_1 = \frac{1}{2} b f_c V (1 - m \sin \alpha) \quad \text{for } \varphi \leq \alpha \leq \pi - \varphi \quad (2.3.32)$$

is obtained.

The yield condition and the associated flow rule for concrete in

plane strain are shown in Fig. 2.13.

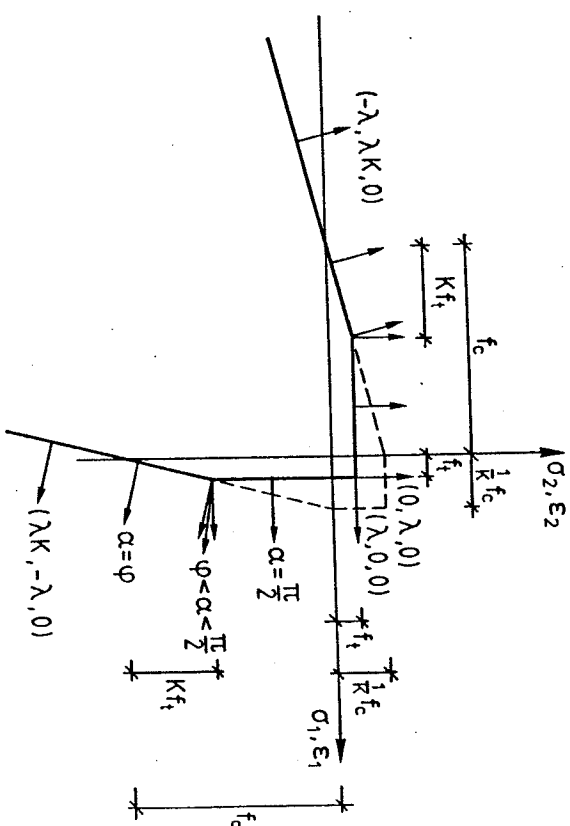


Figure 2.13. Yield condition and associated flow rule for concrete in plane strain.

2.3.2 The dissipation of concrete in plane stress fields

A plane stress field is defined as a stress field in which the stresses in sections parallel to a plane are zero; this plane is a principal section, and the normal to the plane is a principal direction with the corresponding principal stress equal to zero.

Denoting the principal stress in sections perpendicular to the plane as σ_I and σ_{II} , the yield condition can be expressed as follows:

For $\sigma_I > \sigma_{II} > 0$, we get $\sigma_1 = \sigma_I$ and $\sigma_3 = 0$, which gives

$$\sigma_I = f_c \quad (2.3.33)$$

as the condition for separation failure.

For $\sigma_I > 0 > \sigma_{II}$, we have $\sigma_1 = \sigma_I$ and $\sigma_3 = \sigma_{II}$, and the condition for sliding failure is

$$K\sigma_I - \sigma_{II} = f_c \quad (2.3.34)$$

while the condition for separation failure is the same as (2.3.33).

For $0 > \sigma_I > \sigma_{II}$, we have $\sigma_1 = 0$ and $\sigma_3 = \sigma_{II}$, and only sliding failure is possible, the condition being

$$-\sigma_{II} = f_c \quad (2.3.35)$$

With the same procedure as in plane strain, we can find the yield conditions and the corresponding strains in plane stress.

In Fig. 2.14 the yield conditions and associated flow rule have been drawn in a (σ_1, σ_2) -coordinate system.

The areas not covered by the formulae for plane strain are the lines 3-4 in Fig. 2.14.

Along 3-4, the yield condition is

$$\sigma_2 = -f_c \quad (2.3.36)$$

The related strains are found to be

$$(\epsilon_1, \epsilon_2, \epsilon_3) = (0, -\lambda, \lambda K) \quad (2.3.37)$$

The strains in the deforming zone in Fig. 2.11 are again given by equations (2.3.2) and (2.3.3).

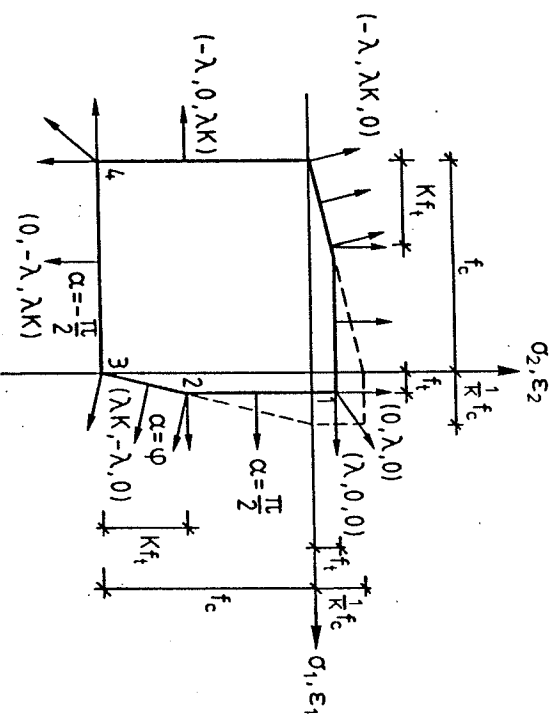


Figure 2.14. Yield condition and associated flow rule for concrete in plane stress.

Comparing (2.3.37) with (2.3.2) and (2.3.3), we get

$$\epsilon_1 = \frac{Y}{2A}(\sin\alpha + 1) = 0 \quad (2.3.38)$$

$$\epsilon_2 = \frac{Y}{2A}(\sin\alpha - 1) = -\lambda \quad (2.3.39)$$

It yields

$$\alpha = -\frac{\pi}{2} \quad (2.3.40)$$

and

$$\lambda = \frac{Y}{A} \quad (2.3.41)$$

The internal work then is

$$W = \sigma_2 \epsilon_2 = \lambda f_C = \frac{Y}{\lambda} f_C \quad \text{for } \alpha = -\frac{\pi}{2} \text{ or } \alpha = \frac{3\pi}{2} \quad (2.3.42)$$

At point 3, the strain vector can be an arbitrary positive linear combination of the strain vectors belonging to the two sides.

The related strains are

$$(\epsilon_1, \epsilon_2, \epsilon_3) = (\lambda k, -(\lambda + \lambda_1), \lambda_1 k) \quad (2.3.43)$$

Comparing equation (2.3.43) with (2.3.3), we find that

$$\lambda + \lambda_1 = \frac{Y}{2\lambda} (1 - \sin \alpha) \quad (2.3.44)$$

The internal work at point 3 then is

$$W = \sigma_2 \epsilon_2 = \frac{Y f_C}{2\lambda} (1 - \sin \alpha) \quad (2.3.45)$$

In this case α will be

$$-\frac{\pi}{2} \leq \alpha \leq \psi \text{ or } \frac{3\pi}{2} \leq \alpha \leq \pi - \psi \quad (2.3.46)$$

When $\alpha = -\frac{\pi}{2}$ or $\alpha = \frac{3\pi}{2}$, equation (2.3.45) is identical with equation (2.3.42).

The dissipation per unit length along line 3-4 and at point 3 can thus be expressed as

$$W_1 = W \Delta A = \frac{b f_C}{2} v (1 - \sin \alpha) \quad \text{for } \alpha \leq \psi \text{ or } \alpha \geq \pi - \psi \quad (2.3.47)$$

It should be noted that in a plane stress field corresponding to line 3-4 and point 3 in Fig. 2.14, there must be inhomogeneous transitional zones between the homogeneous deformation field and the rigid part I and II in Fig. 2.11, because of the strain ϵ_3 . The contribution from these transitional zones to the internal work is neglected in formula (2.3.47).

The complete dissipation per unit length of a discontinuity line for concrete in plane stress can be obtained by combining equations (2.3.32) and (2.3.47)

$$W_1 = \begin{cases} \frac{b f_C}{2} v (1 - \sin \alpha) & \text{for } \alpha \leq \psi \text{ or } \alpha \geq \pi - \psi \\ \frac{b f_C}{2} v (1 - m \sin \alpha) & \text{for } \psi \leq \alpha \leq \pi - \psi \end{cases} \quad (2.3.48)$$

The expression (2.3.48) will be strongly simplified, if $f_t = 0$, as then in the whole α -interval, we have

$$W_1 = \frac{b f_C}{2} v (1 - \sin \alpha) \quad (2.3.49)$$

In Fig. 2.15, the so-called square yield locus is depicted for concrete with a zero tension cut-off.

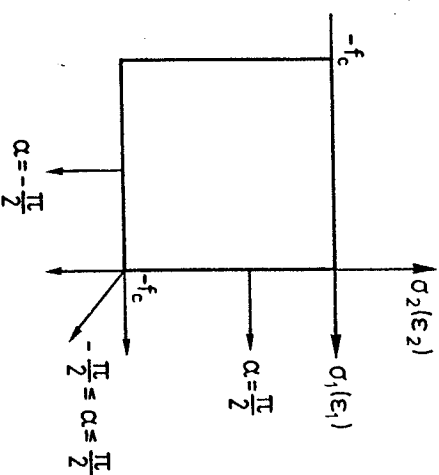


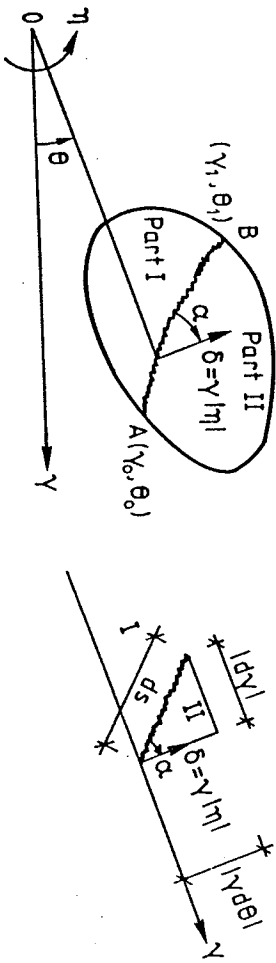
Figure. 2.15. Square yield locus for concrete in plane stress.

The dissipation formulae for yield lines in Coulomb materials and modified Coulomb materials were developed by B.C. Jensen [77.2] and Nielsen et al [78.3].

2.4 Dissipation of curved yield line corresponding to rotation around an arbitrary point in the plane.

In this section, all derivations are based on a zero tension cut-off in plane stresses.

Fig. 2.16 shows a concrete disk with breadth b in a polar-coordinate system, r, θ .



a: Concrete disk with curved yield line.

b: Element of yield line.

Figure 2.16. Curved yield line corresponding to rotation around an arbitrary point.

A curved yield line $r = r(\theta)$ separates the disk into two rigid parts I and II. The two end points are $A(r_0, \theta_0)$ and $B(r_1, \theta_1)$ separately. The part II is rotating in the plane relatively to the part I around the pole O with rotation rate η .

By using (2.3.49), the dissipation of yield line element with length ds has been found to be

$$W_I ds = \frac{\eta}{2} b f_c r (\sqrt{r'^2 + r^2} - r') d\theta \quad (2.4.1)$$

Here, $r' = \frac{dr}{d\theta}$ has been introduced.

The total dissipation of the curved yield line AB can be found by integrating along the curve

$$W_I = \frac{\eta}{2} b f_c \int_{\theta_0}^{\theta_1} F(r, r') d\theta \quad (2.4.2)$$

where

$$F(r, r') = r(\sqrt{r'^2 + r^2} - r') \quad (2.4.3)$$

The Euler equation, i.e. the necessary condition for getting an extreme value of W_I corresponding to the function $r(\theta)$, is

$$\frac{\partial F}{\partial r} - \frac{d}{d\theta} \left(\frac{\partial F}{\partial r'} \right) = 0 \quad (2.4.4)$$

Inserting equation (2.4.3) into (2.4.4) yields

$$r \cdot r''' - 3(r')^2 - 2r^2 = 0 \quad (2.4.5)$$

The solution of this differential equation (2.4.5) is

$$r = k \sqrt{\frac{C_1}{\sin[2(\theta - C_2)]}}, \quad \text{valid for } \frac{C_1}{\sin[2(\theta - C_2)]} > 0 \quad (2.4.6)$$

where C_1 and C_2 are arbitrary constants which must satisfy the edge conditions. Inserting equation (2.4.6) into (2.4.2), we get

$$W_I = \frac{\eta}{4} b f_c \left\{ \left[-C_1 \frac{\cot^2(\theta - C_2) - 1}{2 \cot(\theta - C_2)} \right]_{\theta_0}^{\theta_1} - [r^2]_{r_0}^{r_1} \right\} \quad (2.4.7)$$

Transforming the polar coordinate system into Cartesian coordinates by

$$\begin{aligned} x &= r \cdot \cos(\theta - C_2) \\ y &= r \cdot \sin(\theta - C_2) \end{aligned} \quad (2.4.8)$$

We find a simple form of the curve determined by (2.4.6) (see Fig. 2.17)

$$x \cdot y = \frac{1}{2} C_1 \quad (2.4.9)$$

In the Cartesian coordinates, equation (2.4.7) can be simplified into

$$W_I = \frac{1}{2} |\eta| b f_c r_m d \left(1 + \frac{|\eta|}{\eta} \sin(\beta - \gamma) \right) \quad (2.4.10)$$

Here, r_m , d , β and γ are 4 parameters in Cartesian coordinates (see Fig. 2.18).

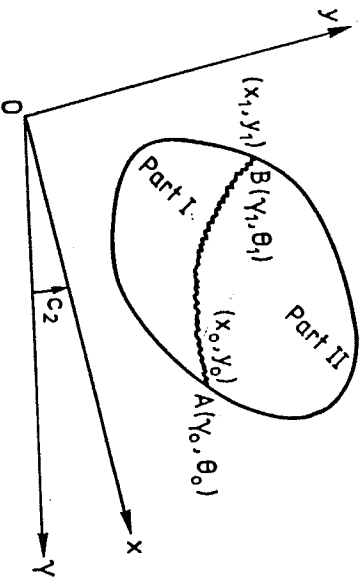


Figure 2.17. Transforming of coordinate systems.

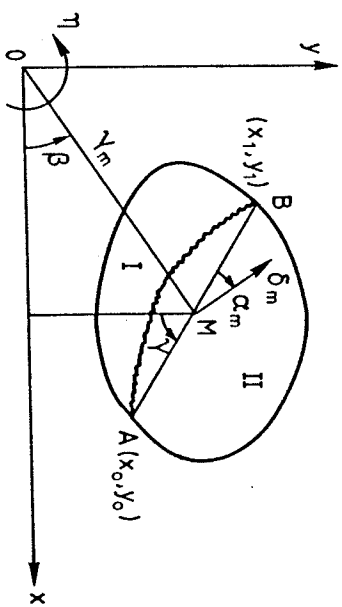


Figure 2.18. Introduction of 4 parameters.

d being the length of straight line AB , r_m the length of line OM , where M is the centre of line AB , β the angle between line OM and the x -axis, and γ is the angle between the line AB and the y -direction.

Introducing $\delta_m = r_m |\eta|$ and

$$\begin{aligned} \alpha_m &= \gamma - \beta & \text{for } \eta > 0 \\ \alpha_m &= -(\gamma - \beta) & \text{for } \eta < 0 \end{aligned} \quad (2.4.11)$$

we get the internal work of the whole curved yield line

$$W_I = \frac{1}{2} \delta_m b d f_c (1 - \sin \alpha_m) \quad (2.4.12)$$

Here δ_m is the relative displacement of point M and α_m is an angle between line AB and the direction of δ_m .

It should be noted that equation (2.4.12) is only valid when

$$r_m > \frac{1}{2} d \quad (2.4.13)$$

The dissipation of curved yield lines corresponding to rotation

around an arbitrary point in the plane was developed by J.F. Jensen [81.3].

2.5 The plastic strengths of concrete

As mentioned before, in order to apply the theory of plasticity to reinforced concrete structures, it is necessary to define concrete as a rigid, perfectly plastic material. But in fact, concrete is not a perfectly plastic material due to the fact that the stress-strain relations for concrete are characterized by strain softening; that is, as soon as the maximum value of the stresses is reached, the stresses decrease with increasing strains.

A typical stress-strain curve in uniaxial tension and compression has the form shown in Fig. 2.19 [87.2].

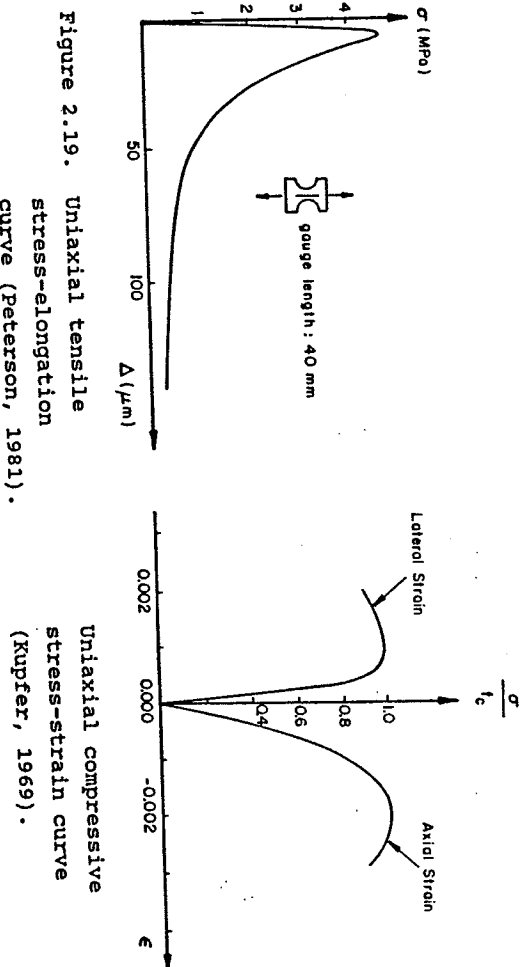


Figure 2.19. Uniaxial tensile stress-elongation curve (Peterson, 1981).

Uniaxial compressive stress-strain curve (Kupfer, 1969).

In reality, the behaviour of concrete in tension is almost brittle and the ductility of concrete in compression is very limited.

Because of the limited deformability of the concrete and the

unstable nature of the concrete failure we cannot expect the concrete stress to equal the maximum compressive strength at all points of the yield lines at failure. It means that the redistribution of stresses, as assumed in plasticity, can only take place at the expense of losing some strength.

In order that the theory may give a reasonable quantitative prediction of the observed shear capacity, a method that has been proved useful is to modify the exact plastic solutions by inserting in the theoretical formulae a concrete strength which is smaller than the strength measured by standard tests.

This suggests the introduction of the effectiveness factor ν , for the compressive strength, and ν_t , for the tensile strength, as two empirical measures of concrete ductility and as two absorbents of all other shortcomings of the theory as well.

If f_c^* is the uniaxial compressive strength of concrete measured by a standard compression test and if f_t^* is the uniaxial tensile strength of concrete measured by some standard procedure, the corresponding plastic compressive strength of concrete f_c^* and the corresponding tensile strength of concrete f_t^* are

$$f_c^* = \nu f_c \quad (2.5.1)$$

$$f_t^* = \nu_t f_t \quad (2.5.2)$$

In the remaining sections, the notations f_c^* and f_t^* are always used in formulae. Since it is difficult to determine the tensile strength of concrete by an ordinary tensile test, the plastic tensile strength of concrete f_t^* will be compared to the plastic compressive strength f_c^* by introducing the factor ρ^* defined by

$$f_t^* = \rho^* f_c^* \quad (2.5.3)$$

The quantities ν and ρ^* are called effectiveness factors. The values of ν and ρ^* normally must be determined by experiments.

2.6 Basic assumptions

Reinforced concrete beams (including deep beams and corbels) are very important structural members in concrete structures.

In the following chapters the plastic theory of reinforced concrete beams is treated based on the assumptions:

- 1) The beam is in a state of plane stress.
- 2) Anchorage failure and bearing or supporting failure are prevented by special anchorage provisions, such as steel plates welded to the bar ends, and adequate design of the bearings and load platens so that the proper transfer of reinforcement tension to concrete compression will be possible.

3) The reinforcement is rigid, perfectly plastic with a stress-strain relation for tension and compression as shown in Fig. 2.20. The yield strength of reinforcement is denoted f_y . For steels without a definite yield point, the f_y is defined in a suitable manner (e.g., as the 0.2% offset strength).

Furthermore, we assume that the reinforcing bars are only capable of carrying longitudinal tensile and compressive stresses. According to this assumption, the reinforcement bars are unable to resist any lateral forces, i.e., the dowel effects are neglected.

The assumption that the materials are rigid and perfect plastic means that any elastic deformations and work hardening effects are neglected and unlimited ductility is assumed.

4) The concrete is rigid, perfectly plastic with the modified Coulomb's failure criterion as yield condition and the associated flow rule (normality condition) as constitutive equations (see Fig. 2.14).

The tensile and compressive strength of concrete are f_t^* and f_c^* , respectively, where f_t^* and f_c^* are defined by (2.5.3) and (2.5.1).

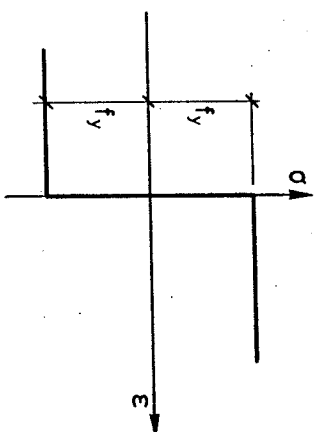


Figure 2.20. Uniaxial stress-strain relation for reinforcement.

- 5) The weight of the beam is disregarded.

CHAPTER III. BENDING CARRYING CAPACITY OF BEAMS, DEEP BEAMS AND CORBELS

In this chapter, the plastic solution of pure bending is described only briefly, since the determination of the bending capacity of reinforced concrete beams is an old problem, which may be treated by many methods described in the literature and in design codes. The purpose of reviewing the plastic theory in bending is to provide available tools to exclude the possible flexural failure when the shear problems are dealt with. The following solutions of bending were presented by M.P. Nielsen et al. [84.1], [84.6] and [78.3], except for solution of deep beams with horizontal web reinforcement, which is derived by the author at section 3.3.

3.1 Members with only tensile reinforcement

3.1.1 Beams and deep beams with rectangular section

The beams treated in this section are assumed to have a rectangular cross section $b \cdot h$ and to be loaded in pure bending. The tensile reinforcement with the yield strength f_y and area A_s is assumed to be concentrated in a stringer at a distance d from the top of the cross section as shown in Fig. 3.1.

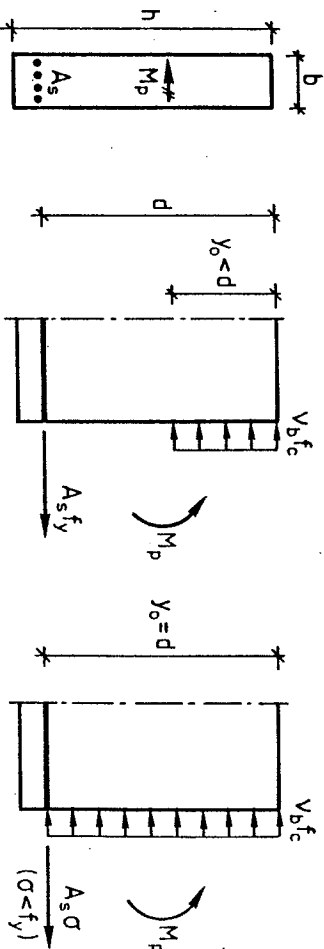
The concrete is assumed to be perfectly plastic with the compressive strength $f_c^* = v_b f_c$. Here v_b is an effectiveness factor for bending and f_c is the compressive cylinder strength of concrete.

The complete solutions for the bending failure moment are given by

$$m_p^* = \begin{cases} (1 - \frac{1}{2} \phi_b^*) \phi_b^* & \text{valid for } \phi_b^* \leq 1 \\ \frac{1}{2} & \text{valid for } \phi_b^* \geq 1 \end{cases} \quad (3.1.1)$$

Here, the effective degree of reinforcement, defined by $\phi_b^* = A_s f_y / b d f_c^*$, and the dimensionless effective yield moment m_p^*

defined by $m_p^* = M_p / b d^2 f_c^*$, have been introduced. For details concerning the derivation of (3.1.1) see, for example, [84.1].



a) Normally reinforced section b) Over reinforced section

Figure 3.1. Normal stress distribution at the yield moment.

3.1.2 Corbels with rectangular section

Fig. 3.2 shows a typical corbel with the rectangular cross section $b \cdot h$.

The complete solutions of bending capacity for such corbels are given by

$$\frac{P}{b d f_c^*} = \begin{cases} \sqrt{\left(\frac{2}{d}\right)^2 + \phi_b^* (2 - \phi_b^*)} - \frac{2}{d} & \text{valid for } \phi_b^* \leq 1 \\ \sqrt{\left(\frac{2}{d}\right)^2 + 1} - \frac{2}{d} & \text{valid for } \phi_b^* \geq 1 \end{cases} \quad (3.1.2)$$

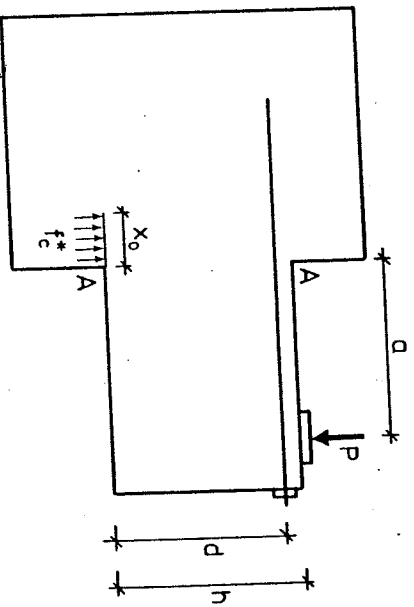


Figure 3.2. Bending capacity of rectangular corbel.

Equation (3.1.2) can easily be found by inserting equations

$$M_p = P \cdot \left(a + \frac{x_0}{2} \right) \tag{3.1.3}$$

$$x_0 = \frac{P}{b f_c^*} \tag{3.1.4}$$

into (3.1.1).

Solution (3.1.2) may be identified with the exact solution found by B.C. Jensen [79.7].

3.2 Beams with compression reinforcement

The compression reinforcement with the same tensile and compressive yield strength f_{yc} and area A_{sc} is assumed concentrated in a stringer at a distance d_c from the top of the cross section. All other data and assumptions are in agreement with those mentioned in section 3.1.1.

The dimensionless effective yield moment is found to be

$$m_p^* = \begin{cases} \phi_b^* + \alpha \phi_c^* - \frac{1}{2}(\phi_b^* + \phi_c^*)^2 & \text{valid for } (\phi_b^* + \phi_c^*) < \alpha \\ \frac{1}{2}\alpha^2 + (1 - \alpha)\phi_b^* & \text{valid for } (\phi_b^* + \phi_c^*) \geq \alpha \geq (\phi_b^* - \phi_c^*) \\ \phi_b^* - \alpha \phi_c^* - \frac{1}{2}(\phi_b^* - \phi_c^*)^2 & \text{valid for } (\phi_b^* - \phi_c^*) > \alpha \geq \alpha(\phi_b^* - \phi_c^*) \\ \frac{1}{2} + (1 - \alpha)\phi_c^* & \text{valid for } (\phi_b^* - \phi_c^*) > 1 \end{cases} \tag{3.2.1}$$

Here, the following parameters have been introduced

$$\alpha = \frac{d_c}{d} \tag{3.2.2}$$

$$\phi_c^* = \frac{A_{sc} f_{yc}}{b d f_c^*} \tag{3.2.3}$$

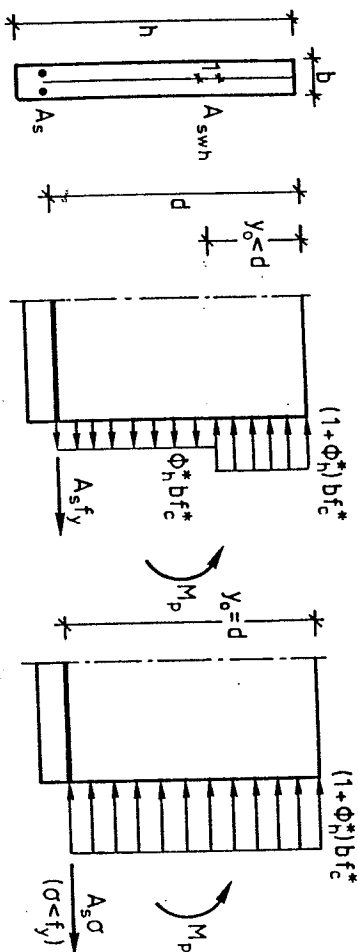
For a more detailed presentation, see [84.1].

3.3 Deep beams with horizontal web reinforcement

Because the vertical web reinforcement has no contribution to the bending capacity of the beam, we will only discuss the influence of horizontal web reinforcement.

The horizontal web reinforcement with the same tensile and compressive yield strength f_{yh} is assumed to be uniformly distributed in the cross section. The area of the horizontal web reinforcement per unit of height is denoted as A_{wh} . All other data and assumptions are the same as those mentioned in section 3.1.1.

When a flexural failure occurs, the stress distribution in the cross section will be as shown in Fig. 3.3.



a) Normally reinforced section. b) Over reinforced section

Figure 3.3. Normal stress distribution at the failure moment.

We easily obtain the dimensionless effective yield moment m_p^* as follows:

$$m_p^* = \begin{cases} \phi_b^* + \frac{1}{2} \phi_{hw}^* - \frac{1}{2} (\phi_b^* + \phi_{hw}^*)^2 / (1 + 2\phi_{hw}^*) & \text{for } \phi_b^* - \phi_{hw}^* \leq 1 \\ \frac{1}{2} (1 + \phi_{hw}^*) & \text{for } \phi_b^* - \phi_{hw}^* > 1 \end{cases} \quad (3.3.1)$$

Here the effective degree of horizontal web reinforcement ϕ_{hw}^* defined as $\phi_{hw}^* = A_{sw} \cdot f_{yw} / b f_c^*$ has been introduced.

The influence of the horizontal web reinforcement on the ultimate flexural load is shown graphically in Fig. 3.4, where $\alpha_1 = \phi_{hw}^* / \phi_b^*$ has been introduced. The three curves in Fig. 3.4 are drawn for $\alpha_1 = 0$, which corresponds to the case without horizontal web reinforcement, formula (3.1.1), $\alpha_1 = 0.5$ and $\alpha_1 = 1.0$, respectively.

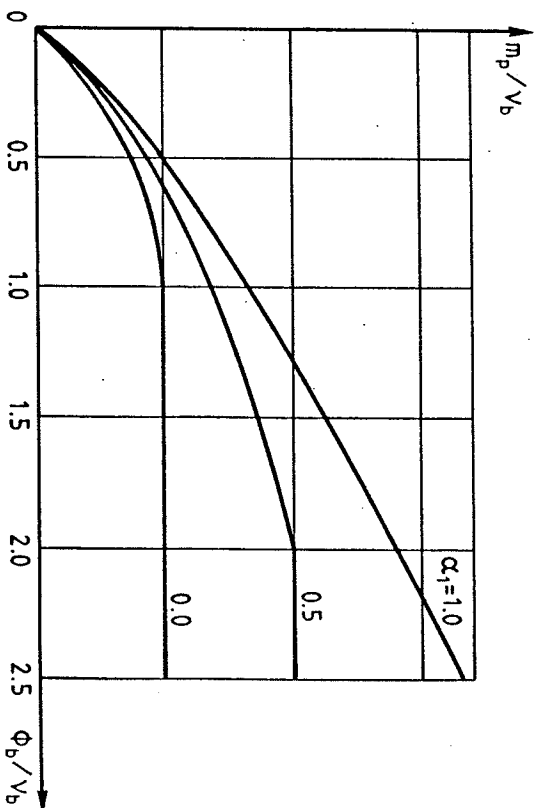


Figure 3.4. Bending capacity of beams with horizontal web reinforcement.

3.4 The effectiveness factor for bending

For pure bending of a rectangular section with only tensile reinforcement, the effectiveness factor v_b has been analytically determined by Exner [79.5] using stress-strain curves measured by P.T. Wang et al. It turns out that v_b is a function of the uniaxial compressive strength f_c' , the yield stress of the reinforcement f_y and the reinforcement ratio ρ_b , defined by $\rho_b = A_s / b d$.

For practical purpose, v_b can be calculated approximately by a simple empirical formula

$$p_d = 0.97 - \frac{f_y}{5000} - \frac{f_c}{300} \quad \text{for } \begin{cases} f_y < 900 \text{ MPa} \\ f_c < 60 \text{ MPa} \end{cases} \quad (3.4.1)$$

For most practical cases f_y will be less than 600 MPa, and conservatively we get

$$p_d = 0.85 - \frac{f_c}{300} \quad \text{for } \begin{cases} f_y < 600 \text{ MPa} \\ f_c < 60 \text{ MPa} \end{cases} \quad (3.4.2)$$

3.5 Experimental verification

Comparison between almost 300 conventional beam tests from many different test series and formula (3.1.1), using the p_d -value of (3.4.1), can be found in [84.1] and [84.6]. Here, we will only treat the deep beams with and without horizontal web reinforcement failing in flexure. The dimensions and material properties and measured ultimate loads of the tested deep beams are listed in Appendix A. The statistical values for the ratios of test to theory using (3.3.1) and the p_d -value of (3.4.2) are shown in Fig. 3.5.

Statistical values	item	number	mean	standard deviation	coeff. of variation
		n	\bar{x}	σ	C_v
cases					
deep beams without horizontal web reinforcement		74	0.999	0.069	0.069
deep beams with horizontal web reinforcement		29	0.998	0.072	0.072

Figure 3.5. The statistical values of the ratios of test to theory for deep beams with and without horizontal web reinforcement failed in flexure.

The good agreement can also be seen from Fig. 3.6, where the curve drawn is the solution (3.1.1) with the p_d -value from (3.4.2), and Fig. 3.7.

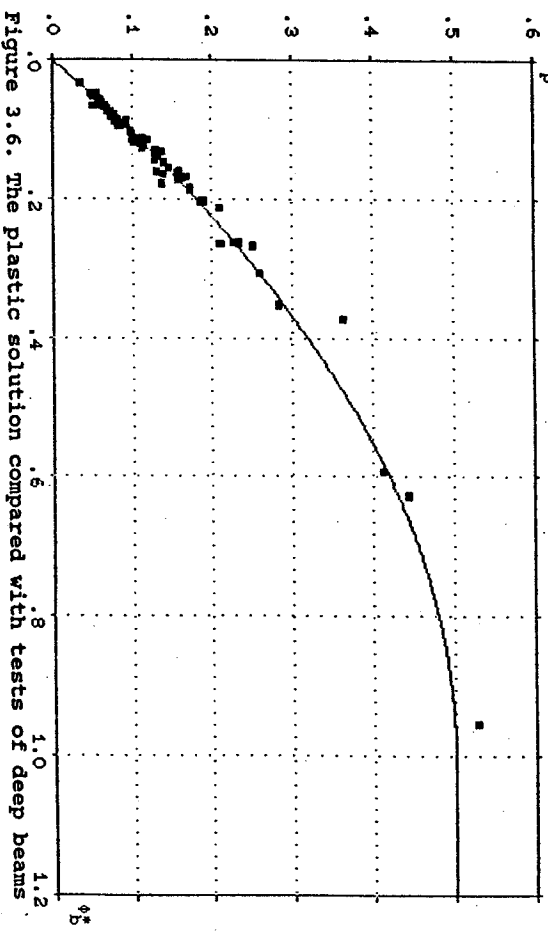


Figure 3.6. The plastic solution compared with tests of deep beams

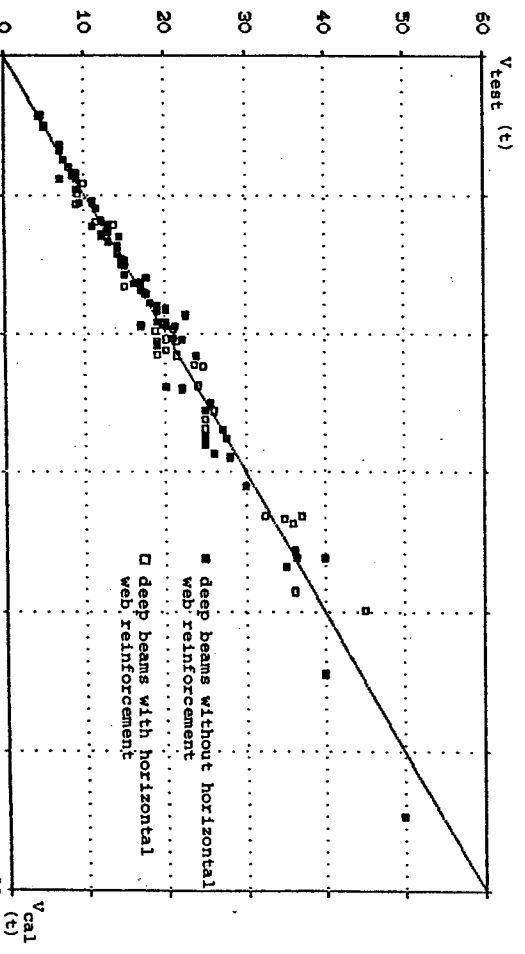


Figure 3.7. The comparison of tests with theory for deep beams.

CHAPTER IV. SHEAR CARRYING CAPACITY OF BEAMS, DEEP BEAMS AND CORBELS WITHOUT WEB REINFORCEMENT

In this chapter we will only treat beams subjected to concentrated loading. Consider a horizontal, simply supported rectangular concrete beam loaded by two symmetrical loads P , (Fig. 4.1).

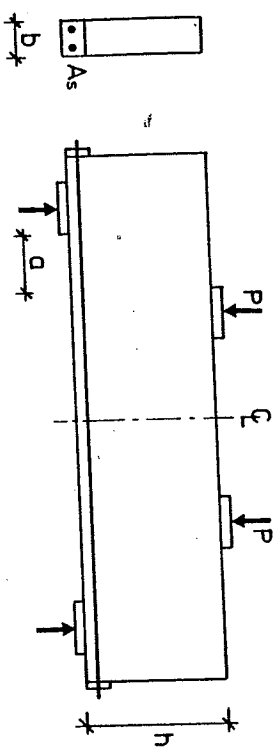


Figure 4.1. Rectangular reinforced concrete beam subjected to concentrated loads.

The beam is reinforced with the area A_s along the bottom face of the beam. The breadth and depth of the beam are termed b and h , respectively. The quantity a denotes the clear shear span, which is defined as the distance between the inside edge of support platen and the outside edge of load platen.

4.1 Shear capacity considering the tensile strength of concrete

In this section we will derive coinciding upper and lower bound solutions of non-webreinforced beams taking account of the tensile strength of concrete.

The coincident upper and lower bounds in the over reinforced case was found by J.F. Jensen in [81.3]. The complete solutions with their boundaries were derived by the author. These solutions can

be used not only for conventional beams but also for deep beams, corbels and joints. The solutions are compared with a great number of test series on non-webreinforced slender beams, deep beams and corbels subjected to concentrated loads on the top compression face.

A really good agreement has been found.

4.1.1 Lower bound solution

Let us consider the beam element A-B between the loading and supporting platen in a stringer beam.

The stress distribution is as shown in Fig. 4.2.

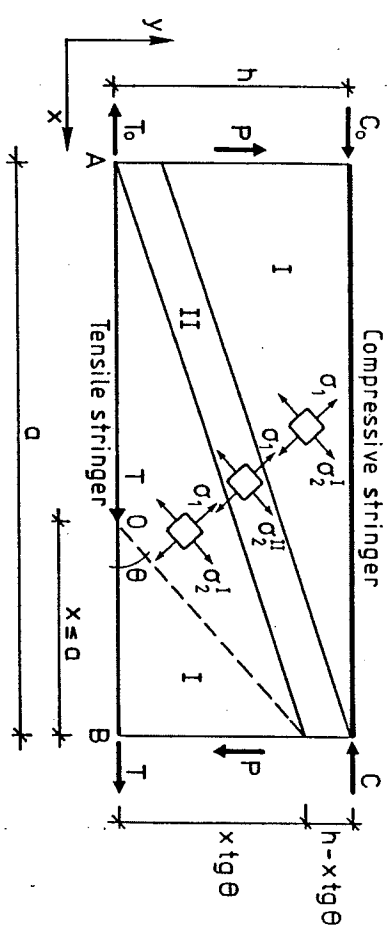


Figure 4.2. Stress distribution along the clear shear span.

We assume that if the tensile stringer is not strong enough, it will yield at a point O. The distance between point O and the section B is denoted x . The tensile force at point O is T .

We must have

$$x \leq a$$

$$(4.1.0)$$

When point O reaches point A, i.e. $x = a$, the stress distribution in the shear span may change into the case shown in Fig. 4.3.

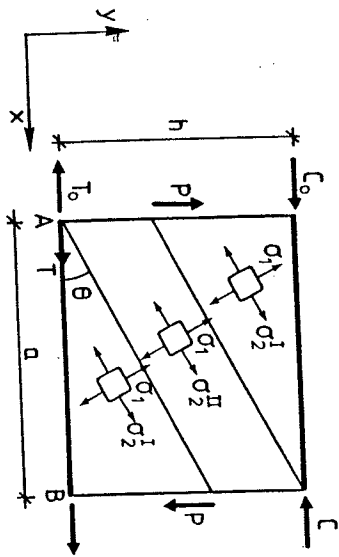


Figure 4.3. Stress distribution along the clear shear span of a stringer beam with small shear span.

In the areas marked I, the stresses are

$$\sigma_x^I = \sigma_2^I \cos^2 \theta + \sigma_1^I \sin^2 \theta \quad (4.1.1)$$

$$\sigma_y^I = \sigma_1^I \cos^2 \theta + \sigma_2^I \sin^2 \theta \quad (4.1.2)$$

$$|\tau_{xy}^I| = |\sigma_1^I - \sigma_2^I| \sin \theta \cos \theta \quad (4.1.3)$$

As mentioned in our basic assumptions, the stringers can not resist any lateral forces.

This leads to

$$\sigma_y^I = 0 \quad (4.1.4)$$

Inserting (4.1.4) into equation (4.1.2) yields

$$\sigma_2^I = -\sigma_1^I \cot^2 \theta \quad (4.1.5)$$

From equations (4.1.1), (4.1.3) and (4.1.5) we easily get

$$\sigma_x^I = \sigma_1^I (1 - \cot^2 \theta) \quad (4.1.6)$$

$$|\tau_{xy}^I| = \sigma_1^I \cot \theta \quad (4.1.7)$$

In area marked II, the stresses are

$$\sigma_2^{II} = k\sigma_1 - f_c^* \quad (4.1.8)$$

$$\sigma_x^{II} = \sigma_2^{II} \cos^2 \theta + \sigma_1^I \sin^2 \theta = \sigma_1^I + (k\sigma_1 - f_c^* - \sigma_1^I) \cos^2 \theta \quad (4.1.9)$$

$$|\tau_{xy}^{II}| = |\sigma_1^I - \sigma_2^{II}| \sin \theta \cos \theta = (\sigma_1^I - k\sigma_1 + f_c^*) \sin \theta \cos \theta \quad (4.1.10)$$

The first principal stress σ_1 in Fig. 4.2 and Fig. 4.3 is depending on the angle θ .

As mentioned in section 2.3, the first principal axis bisects the angle between the relative displacement vector and the yield line normal. It is demonstrated in Fig. 4.4.

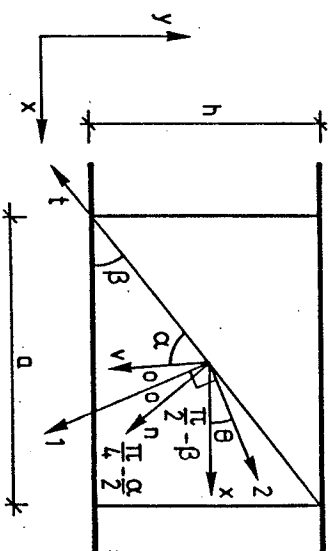


Figure 4.4. The relations between β , α and θ .

The relations between β , α and θ can be easily found to be

$$\theta = \beta + \frac{\alpha}{2} - \frac{\pi}{4} \quad (4.1.11)$$

$$\cot \beta = \frac{a}{h} \quad (4.1.12)$$

The magnitude of the first principal stress σ_1 is

$$\sigma_1 = f_t^* = \rho^* f_c^* \quad \text{when } \alpha > \varphi \quad (4.1.13)$$

$$0 \leq \sigma_1 \leq f_t^* \quad \text{when } \alpha = \varphi \quad (4.1.14)$$

$$\sigma_1 = 0 \quad \text{when } \alpha < \varphi \quad (4.1.15)$$

The relation between σ_1 and θ may then be found to be

$$\sigma_1 = \rho^* f_c^* \quad \text{when } \theta > \beta + \frac{\alpha}{2} - \frac{\pi}{4} \quad (4.1.16)$$

$$0 \leq \sigma_1 \leq f_t^* \quad \text{when } \theta = \beta + \frac{\alpha}{2} - \frac{\pi}{4} \quad (4.1.17)$$

$$\sigma_1 = 0 \quad \text{when } \theta < \beta + \frac{\alpha}{2} - \frac{\pi}{4} \quad (4.1.18)$$

At first, let us consider the case of $x = a$.

Using equilibrium conditions to section B in Fig. 4.3, we find that

$$P = |r_{xy}^I| b a \operatorname{tg} \theta + |r_{xy}^{II}| b (h - a \operatorname{tg} \theta) \quad \text{valid for } x \geq a \quad (4.1.19)$$

$$\pi + b a \operatorname{tg} \theta \sigma_x^I + b (h - a \operatorname{tg} \theta) \sigma_x^{II} + b a |r_{xy}^I| = 0 \quad (4.1.20)$$

Inserting equations (4.1.6), (4.1.7), (4.1.9) and (4.1.10) into equation (4.1.19) and (4.1.20) yields

$$\cot \theta = \frac{\sqrt{\left(\frac{a}{h}\right)^2 + 1 - D_0^2} + \frac{a}{h}}{1 + D_0} \quad (4.1.21)$$

$$\frac{\tau}{f_c^*} = \frac{\lambda_0 \sqrt{\left(\frac{a}{h}\right)^2 + 1 - D_0^2} - \mu_0 \frac{a}{h}}{2} \quad (4.1.22)$$

Here, $\tau = \frac{P}{h}$ has been introduced as the average shear stress in the section in question.

The parameters λ_0 , μ_0 and D_0 in formulae (4.1.21) and (4.1.22) are as follows

$$\lambda_0 = 1 - k \frac{\sigma_1^I}{f_c^*} + \frac{\sigma_1^I}{f_c^*} \quad (4.1.23)$$

$$\mu_0 = 1 - k \frac{\sigma_1^I}{f_c^*} - \frac{\sigma_1^I}{f_c^*} \quad (4.1.24)$$

$$D_0 = \frac{\mu_0 - 2 \frac{T}{b h f_c^*}}{\lambda_0} \quad (4.1.25)$$

Inserting equation (4.1.21) into equations (4.1.16), (4.1.17) and (4.1.18) yields

$$\sigma_1 = \rho^* f_c^* \quad \text{valid for } \operatorname{tg} \varphi - \frac{D}{\cos \varphi} < \frac{a}{h} \quad (4.1.26)$$

$$0 \leq \sigma_1 \leq f_t^* \quad \text{valid for } \operatorname{tg} \varphi - \frac{C}{\cos \varphi} \leq \frac{a}{h} \leq \operatorname{tg} \varphi - \frac{D}{\cos \varphi} \quad (4.1.27)$$

$$\sigma_1 = 0 \quad \text{valid for } \frac{a}{h} < \operatorname{tg} \varphi - \frac{C}{\cos \varphi} \quad (4.1.28)$$

Here, the parameters

$$C = 1 - 2 \frac{T}{b h f_c^*} \quad (4.1.29)$$

and

$$D = \frac{\mu - 2 \frac{T}{b h f_c^*}}{\lambda} \quad (4.1.30)$$

have been introduced.

The parameters λ and μ are as follows

$$\lambda = 1 - k\rho^* + \rho^* \quad (4.1.31)$$

$$\mu = 1 - k\rho^* - \rho^* \quad (4.1.32)$$

In the case of $\frac{a}{h} > \text{tg}\varphi - \frac{D}{\cos\varphi}$, we have

$$\cot\theta = \frac{\sqrt{\left(\frac{a}{h}\right)^2 + 1 - D^2} + \frac{a}{h}}{1 + D} \quad (4.1.33)$$

$$\frac{T}{f_c^*} = \frac{\lambda \sqrt{\left(\frac{a}{h}\right)^2 + 1 - D^2} - \mu \frac{a}{h}}{2} \quad (4.1.34)$$

Now we determine the highest lower bound by maximizing equation (4.1.34) with respect to the tensile force T.

For $T \leq \frac{\mu}{2} bhf_c^*$, the highest lower bound is obtained with the maximum tensile reinforcement force, i.e.

$$T = \phi^* bhf_c^* \quad (4.1.35)$$

Here, the effective reinforcement degree $\phi^* = \frac{A_s f_y}{bh f_c^*}$ has been introduced.

For $T > \frac{\mu}{2} bhf_c^*$, the highest lower bound is obtained with $T = \frac{\mu}{2} bhf_c^*$, i.e. $D = 0$.

Thus, the highest lower bound is

$$\frac{T}{f_c^*} = \frac{\lambda \sqrt{\left(\frac{a}{h}\right)^2 + 1 - D^2} - \mu \frac{a}{h}}{2} \quad (4.1.36)$$

with

$$D = \begin{cases} \frac{\mu - 2\phi^*}{\lambda} & \text{valid for } \phi^* \leq \frac{\mu}{2} \\ 0 & \text{valid for } \phi^* > \frac{\mu}{2} \end{cases} \quad (4.1.37)$$

In the case of $\frac{a}{h} < \text{tg}\varphi - \frac{C}{\cos\varphi}$, we easily find that

$$\cot\theta = \frac{\sqrt{\left(\frac{a}{h}\right)^2 + 1 - C^2} + \frac{a}{h}}{1 + C} \quad (4.1.38)$$

$$\frac{T}{f_c^*} = \frac{1}{2} \left[\sqrt{\left(\frac{a}{h}\right)^2 + 1 - C^2} - \frac{a}{h} \right] \quad (4.1.39)$$

with

$$C = \begin{cases} 1 - 2\phi^* & \text{valid for } \phi^* \leq \frac{1}{2} \\ 0 & \text{valid for } \phi^* > \frac{1}{2} \end{cases} \quad (4.1.40)$$

In the case of $\text{tg}\varphi - \frac{C}{\cos\varphi} \leq \frac{a}{h} \leq \text{tg}\varphi - \frac{D}{\cos\varphi}$, the highest lower bound may be found by maximizing equation (4.1.22) with respect to $\frac{\sigma_1}{f_c^*}$.

Through lengthy and tedious derivations, we get

$$\frac{\sigma_1}{f_c^*} = \frac{(1 - \sin\varphi)[(1 - 2\phi^*) - (\sin\varphi - \frac{a}{h} \cos\varphi)]}{2\cos\varphi[\cos\varphi - \frac{a}{h} \sin\varphi]} \quad (4.1.41)$$

Inserting equation (4.1.41) into equation (4.1.22) yields

$$\frac{T}{f_c^*} = \frac{[(\frac{a}{h})^2 + 1](1 - \sin\varphi) - 2\phi^* (\frac{a}{h} \cos\varphi - \sin\varphi)}{2[\frac{a}{h} \sin\varphi + \cos\varphi]} \quad (4.1.42)$$

Solutions (4.1.36), (4.1.39) and (4.1.42) are only valid when the condition

$$\sigma_2^I > K f_t^* - f_c^* \quad (4.1.43)$$

is satisfied.

Inserting equations (4.1.5) and (4.1.33) into (4.1.43), we get the condition

$$\frac{a}{h} \leq \mu \sqrt{\frac{1 - D^2}{\lambda^2 - \mu^2}} \quad (4.1.44)$$

When the equation (4.1.44) is not satisfied, the location of the yielding point of the tensile reinforcement 0 may depart from A and vary between A and B.

Inserting $x = a$ into equations (4.1.33) and (4.1.34), we find solution in this case

$$\cot \theta = \frac{\sqrt{\left(\frac{x}{h}\right)^2 + 1 - D^2} + \frac{x}{h}}{1 + D} \quad \text{valid for } x < a \quad (4.1.45)$$

$$\frac{T}{f_c^*} = \frac{\lambda \sqrt{\left(\frac{x}{h}\right)^2 + 1 - D^2} - \mu \frac{x}{h}}{2} \quad \text{valid for } x < a \quad (4.1.46)$$

The optimum value of $\frac{x}{h}$ can be found by maximizing equation (4.1.44) with respect to $\frac{x}{h}$. It's easy to find that

$$\frac{x}{h} = \mu \sqrt{\frac{1 - D^2}{\lambda^2 - \mu^2}} \quad \text{valid for } x < a \quad (4.1.47)$$

This value coincides with the equation (4.1.44). It means that when the shear span ratio reaches and surpasses some special value, the inclination of the principal direction and the lower bound will be independent of the shear span ratio.

Inserting equation (4.1.47) into (4.1.46) yields

$$\frac{T}{f_c^*} = \frac{1}{2} \sqrt{(\lambda^2 - \mu^2)(1 - D^2)} \quad (4.1.48)$$

It's worth noticing that when $\phi^* \geq \frac{h}{2}$ ($D = 0$), i.e. in the case of an over reinforced beam, the stress distribution in the shear span may become homogeneous, as shown in Fig. 4.5.

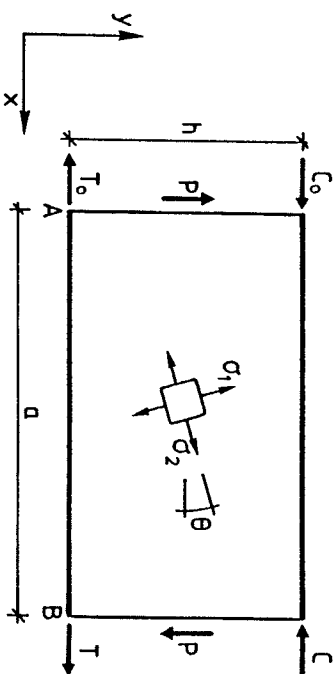


Figure 4.5. Stress distribution in the shear span of an over reinforced beam with large shear span ratio.

Solution (4.1.48) is valid only when the condition

$$\mu \sqrt{\frac{1 - D^2}{\lambda^2 - \mu^2}} > \text{tg} \psi - \frac{D}{\text{cos} \psi} \quad (4.1.49)$$

is satisfied. It yields

$$\lambda + \mu + D > 1 \quad (4.1.50)$$

Inserting equations (4.1.31), (4.1.32) and (4.1.37) into (4.1.50), we get

$$p^* \leq \frac{k - \sqrt{k(1 + K\phi^* - \phi^*)}}{k(x - 1)} \quad \text{valid for } \phi^* \leq \frac{k - 1}{4k} \quad (4.1.51)$$

and

$$p^* \leq \frac{1}{2K} \quad \text{valid for } \phi^* > \frac{K-1}{4K} \quad (4.1.52)$$

The highest lower bound may be found by differentiating equation (4.1.48) with respect to p^* .

It is found that for $\lambda + \mu + D \geq 1$, the highest lower bound is given by formulae (4.1.36), (4.1.39), (4.1.42), and (4.1.48). For $\lambda + \mu + D < 1$, the highest lower bound will be obtained when

$$p^* = \frac{K - \sqrt{K(1 + K\phi^* - \phi^*)}}{K(K-1)} \quad \text{for } \phi^* \leq \frac{K-1}{4K} \quad (4.1.53)$$

$$p^* = \frac{1}{2K} \quad \text{for } \phi^* \geq \frac{K-1}{4K} \quad (4.1.54)$$

It's coincident with the equations (4.1.51) and (4.1.52).

In this case the highest lower bound is

$$\frac{T}{f_c} = 2 \frac{[K - \sqrt{K(1 + \phi^*(K-1))}] \sqrt{K(1 + \phi^*(K-1))} - 1}{\sqrt{K(K-1)}^2} \quad \text{valid for } \phi^* \leq \frac{K-1}{4K} \quad (4.1.55)$$

$$\frac{T}{f_c} = \frac{1}{2\sqrt{K}} \quad \text{valid for } \phi^* > \frac{K-1}{4K} \quad (4.1.56)$$

When equation

$$\frac{a}{h} \geq \frac{1 + 2 \frac{\sin \phi^*}{1 - \sin \phi^*} \phi^*}{\sin \phi^*} - \cot \phi^* \quad (4.1.57)$$

is satisfied.

In the case of $\frac{a}{h} < \frac{1 + 2 \frac{\sin \phi^*}{1 - \sin \phi^*} \phi^*}{\sin \phi^*} - \cot \phi^*$, solutions (4.1.39) and (4.1.42) are valid.

4.1.2 Upper bound solution

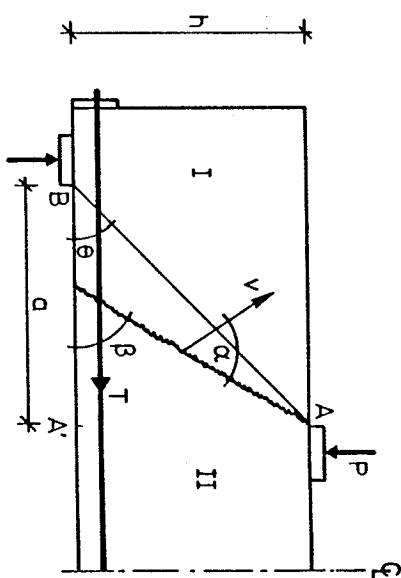


Figure 4.6. Failure mechanism in shear span for beams without web reinforcement.

Fig. 4.6 shows the shear span of a concrete beam subjected to the concentrated load P. Consider a failure mechanism consisting of a single straight yield line inclined at the angle β to the beam axis and running from A, which is the outside edge of the load platen, to point O, which may vary along the clear shear span. This yield line subdivides the beam into two rigid parts marked I and II in Fig. 4.6. Failure is assumed to take place along this yield line. The relative displacement rate is v , inclined at the angle α to the yield line. This mechanism is kinematically admissible, since it does not violate any support condition.

We assume that the reinforcement is yielding in tension, i.e.

$$\frac{T}{\sigma} \leq (\alpha + \beta) \leq \pi \quad (4.1.58)$$

The range of the angle β is

$$0 \leq \beta \leq \frac{\pi}{2} \quad (4.1.59)$$

The lower limit of β is imposed by the geometry of the beam, where

$$\cot \theta = \frac{a}{h} \quad (4.1.60)$$

The upper limit of β ensures that the reinforcement is yielding in tension.

The rate of internal work dissipated by this failure mechanism is

$$W_I = \frac{V}{2}(\lambda - \mu) \frac{bh f_C^*}{\sin \beta} - T V \cos(\alpha + \beta) \quad \text{valid for } \phi \leq \alpha \leq \pi - \phi \quad (4.1.61)$$

$$W_I = \frac{V}{2}(1 - \sin \alpha) \frac{bh f_C^*}{\sin \beta} - T V \cos(\alpha + \beta) \quad \text{valid for } \alpha \leq \phi \quad \text{or } \alpha \geq \pi - \phi \quad (4.1.62)$$

where T is the tensile force of the reinforcement at the intersection with the yield line.

Here, the parameters λ and μ defined as

$$\lambda = 1 - 2 \frac{f_t^*}{f_C^*} \frac{\sin \phi}{1 - \sin \phi} = 1 - \rho^* (k - 1) \quad (4.1.63)$$

and

$$\mu = 1 - 2 \frac{f_t^*}{f_C^*} \frac{1}{1 - \sin \phi} = 1 - \rho^* (k + 1) \quad (4.1.64)$$

have been introduced.

It is obvious that when $(\alpha + \beta) > \frac{\pi}{2}$, the reinforcement must be yielding. In this case we have

$$T = A_s f_y \quad (4.1.65)$$

When $\alpha + \beta = \frac{\pi}{2}$, we are in the over reinforced case.

The rate of external work done by the reaction is

$$W_E = p \cdot v \cdot \sin(\alpha + \beta) \quad (4.1.66)$$

The work equation $W_I = W_E$ yields the upper bound

$$\frac{T}{f_C^*} = \frac{\lambda - \mu \sin(\alpha + \beta) \cos \beta + (\mu - 2\phi^*) \sin \beta \cos(\alpha + \beta)}{2 \sin \beta \sin(\alpha + \beta)} \quad \text{valid for } (\phi \leq \alpha \leq \pi - \phi) \quad (4.1.67)$$

$$\frac{T}{f_C^*} = \frac{1 - \sin(\alpha + \beta) \cos \beta + (1 - 2\phi^*) \sin \beta \cos(\alpha + \beta)}{2 \sin \beta \sin(\alpha + \beta)} \quad \text{valid for } (\alpha \leq \phi \quad \text{or } \alpha \geq \pi - \phi) \quad (4.1.68)$$

Here, the effective reinforcement degree ϕ^* has been introduced

$$\phi^* = \begin{cases} \frac{A_s f_y}{bh f_C^*} & \text{for } (\alpha + \beta) > \frac{\pi}{2} \\ \frac{T}{bh f_C^*} & \text{for } (\alpha + \beta) = \frac{\pi}{2} \end{cases} \quad (4.1.69)$$

It appears that $\frac{\partial (T/f_C^*)}{\partial \alpha} = 0$, for

$$\lambda \cos(\alpha + \beta) = -(\mu - 2\phi^*) \sin \beta \quad (\phi \leq \alpha \leq \pi - \phi) \quad (4.1.70)$$

$$\cos(\alpha + \beta) = -(1 - 2\phi^*) \sin \beta \quad (\alpha \leq \phi \quad \text{or } \alpha \geq \pi - \phi) \quad (4.1.71)$$

$\frac{\partial (T/f_C^*)}{\partial \beta} = 0$, for

$$(\lambda - \mu) \sin \alpha \sin(\alpha + 2\beta) = 2\phi^* \sin^2 \beta \quad (\phi \leq \alpha \leq \pi - \phi) \quad (4.1.72)$$

$$(1 - \sin \alpha) \sin(\alpha + 2\beta) = 2\phi^* \sin^2 \beta \quad (\alpha \leq \phi \quad \text{or } \alpha \geq \pi - \phi) \quad (4.1.73)$$

Solving equations (4.1.70) and (4.1.72), we find that

$$\sin(\alpha + \beta) = \eta \cos\beta \quad \text{valid for } \phi^* \leq \frac{\mu}{\lambda} \quad (4.1.74)$$

$$\cot\beta = \frac{\sqrt{1 - D^2}}{\sqrt{\eta^2 - 1}} \quad \beta \geq \theta \quad (4.1.75)$$

$$\sin\alpha = \frac{1 + \eta D}{\eta + D} \quad \text{and } \varphi \leq \alpha \leq \pi - \varphi \quad (4.1.76)$$

Here, the parameters η and D are defined by

$$\eta = \frac{\lambda}{\mu} \quad (4.1.77)$$

$$D = \begin{cases} \frac{\mu - 2\phi^*}{\lambda} & \text{for } \phi^* < \frac{\mu}{2} \\ 0 & \text{for } \phi^* \geq \frac{\mu}{2} \end{cases} \quad (4.1.78)$$

Inserting equations (4.1.70), (4.1.74) and (4.1.75) into equation (4.1.67) we get the lowest upper bound

$$\frac{T}{f_c} = \frac{1}{2} \sqrt{(\lambda^2 - \mu^2)(1 - D^2)} \quad (4.1.79)$$

It should be pointed out that equation (4.1.79) is only valid when

$$\beta > \theta \quad (4.1.80)$$

and

$$\alpha \geq \varphi \quad (4.1.81)$$

Inserting equations (4.1.75) and (4.1.60) into equation (4.1.80) and inserting equation (4.1.76) into equation (4.1.81) yield the following condition for equation (4.1.79) to be valid

$$\frac{a}{h} > \sqrt{\frac{1 - D^2}{\eta^2 - 1}} \quad (4.1.82)$$

and

$$\lambda + \mu + D \geq 1 \quad (4.1.83)$$

If equation (4.1.82) is not satisfied, it means that $\beta \leq \theta$. Thus β must be restricted to the value (4.1.60), i.e.

$$\cot\beta = \frac{a}{h} \quad (4.1.84)$$

Solving equations (4.1.70) and (4.1.84) yields

$$\sin\alpha = \frac{\frac{a}{h} \sqrt{\left(\frac{a}{h}\right)^2 + 1 - D^2} + D}{\left(\frac{a}{h}\right)^2 + 1} \quad \text{valid for } \varphi \leq \alpha \leq \pi - \varphi \quad (4.1.85)$$

The lowest upper bound is obtained by inserting equations (4.1.70) and (4.1.84) into equation (4.1.67).

$$\frac{T}{f_c} = \frac{1}{2} \sqrt{\lambda \left[\left(\frac{a}{h}\right)^2 + 1 - D^2 - \mu \frac{a}{h} \right]} \quad (4.1.86)$$

The condition for equation (4.1.86) to be valid can easily be found by inserting equation (4.1.85) into equation (4.1.81). This leads to

$$\frac{a}{h} \geq \operatorname{tg}\varphi - \frac{D}{\cos\varphi} \quad (4.1.87)$$

When equation (4.1.87) is not satisfied, it means that α must be equal to or less than φ and equation (4.1.70) is not valid anymore.

Solving equations (4.1.71) and (4.1.84) yields the solutions.

$$\sin\alpha = \sin\varphi \quad \text{valid for } \operatorname{tg}\varphi - \frac{C}{\cos\varphi} \leq \frac{a}{h} \leq \operatorname{tg}\varphi - \frac{D}{\cos\varphi} \quad (4.1.88)$$

$$\sin\alpha = \frac{\frac{a}{h} \sqrt{\left(\frac{a}{h}\right)^2 + 1 - C^2} + C}{\left(\frac{a}{h}\right)^2 + 1} \quad \text{valid for } \frac{a}{h} \leq \operatorname{tg}\varphi - \frac{C}{\cos\varphi} \quad (4.1.89)$$

Here, the parameter C has been introduced

$$C = \begin{cases} 1 - 2\phi^* & \text{when } \phi^* < \frac{1}{2} \\ 0 & \text{when } \phi^* \geq \frac{1}{2} \end{cases} \quad (4.1.90)$$

As in the case corresponding to equation (4.1.88), the lowest upper bound can be easily found by inserting equations (4.1.84) and (4.1.88) into equation (4.1.68).

$$\frac{T}{f_C} = \frac{\left(\frac{a}{h}\right)^2 + 1 \left[(1 - \sin\varphi) - 2\phi^* \left(\frac{a}{h}\right) \cos\varphi - \sin\varphi \right]}{2 \left[\left(\frac{a}{h}\right) \sin\varphi + \cos\varphi \right]} \quad (4.1.91)$$

When $\frac{a}{h} \leq \text{tg}\varphi - \frac{C}{\cos\varphi}$, we find the lowest upper bound by inserting equations (4.1.84) and (4.1.89) into equation (4.1.68)

$$\frac{T}{f_C} = \frac{1}{2} \left[\sqrt{\left(\frac{a}{h}\right)^2 + 1 - C^2} - \frac{a}{h} \right] \quad (4.1.92)$$

In the over reinforced case, i.e. when $\phi^* \geq \frac{1}{2}$ corresponding to $\varphi \leq \alpha \leq \pi - \varphi$, or when $\phi^* \geq \frac{1}{2}$ corresponding to $\alpha \leq \varphi$ or $\alpha \geq \pi - \varphi$, we may find the lowest upper bound in two ways.

One way is to use the same procedure as above which is done first.

When the beam is over reinforced, it appears that

$$\frac{\partial (T/f_C^*)}{\partial \alpha} > 0 \quad (4.1.93)$$

It means that we find the lowest upper bound when α equals the smallest possible value. From the condition (4.1.58), we have

$$\alpha + \beta = \frac{\pi}{2} \quad (4.1.94)$$

Inserting equation (4.1.94) into equation (4.1.67) yields

$$\frac{T}{f_C} = \frac{\lambda - \mu \cos\beta}{2 \sin\beta} \quad \text{valid for } \varphi \leq \alpha \leq \pi - \varphi \quad (4.1.95)$$

It appears that

$$\left[\frac{\partial (T/f_C^*)}{\partial \beta} \right] = 0$$

for

$$\cot\beta = \frac{1}{\sqrt{\eta^2 - 1}} = \text{tg}\alpha \quad (4.1.96)$$

Inserting equation (4.1.96) into equation (4.1.95) yields

$$\frac{T}{f_C} = \frac{1}{2} \sqrt{\lambda^2 - \mu^2} \quad \text{valid for } \phi^* \geq \frac{1}{2} \quad (4.1.97)$$

This solution is only valid if equations (4.1.80) and (4.1.81) are satisfied. From equations (4.1.80), (4.1.81) and (4.1.96), we get the condition for equation (4.1.97) to be valid:

$$\frac{a}{h} \geq \frac{1}{\sqrt{\eta^2 - 1}} \quad (4.1.98)$$

and

$$\lambda + \mu \geq 1 \quad (4.1.99)$$

When equation (4.1.98) is not fulfilled, we find the lowest upper bound by inserting equation (4.1.84) into equation (4.1.95)

$$\frac{T}{f_C} = \frac{1}{2} \left[\lambda \sqrt{1 + \left(\frac{a}{h}\right)^2} - \mu \frac{a}{h} \right] \quad \text{valid for } \phi^* \geq \frac{1}{2} \quad (4.1.100)$$

The condition for equation (4.1.81) to be valid in this case becomes

$$\frac{a}{h} \geq \operatorname{tg} \varphi \quad (4.1.101)$$

In the case of $\frac{a}{h} \leq \operatorname{tg} \varphi$, we can easily find the solution by inserting equations (4.1.94) and (4.1.84) into equation (4.1.68).

$$\frac{T}{f_c} = \frac{1}{2} \left[\sqrt{1 + \left(\frac{a}{h}\right)^2} - \frac{a}{h} \right] \quad \text{valid for } \phi^* \geq \frac{1}{2} \quad (4.1.102)$$

Another way to find the lowest upper bound in the case of an overreinforced beam is minimizing the equations (4.1.79), (4.1.86) and (4.1.92) with respect to ϕ^* . The same solutions as equations (4.1.97), (4.1.100) and (4.1.102) have been found in this way.

As mentioned above solutions (4.1.79) and (4.1.97) are valid only when equations (4.1.83) and (4.1.99) are fulfilled. When they are not satisfied, the lowest upper bound may be obtained by differentiating equations (4.1.79) and (4.1.97) with respect to ϕ^* .

It has been found that for $\lambda + \mu + D \leq 1$, the lowest upper bound can be reached only when

$$\lambda + \mu + D = 1 \quad (4.1.103)$$

Inserting equations (4.1.63), (4.1.64) and (4.1.78) into equation (4.1.103) yields

$$\rho^* = \begin{cases} \frac{\sqrt{k-1} + \phi^*(k-1)}{\sqrt{k}(k-1)} & \text{valid for } \phi^* < \frac{k-1}{4k} \\ \frac{1}{2k} & \text{valid for } \phi^* \geq \frac{k-1}{4k} \end{cases} \quad (4.1.104)$$

In this case curves corresponding to equations (4.1.82) and (4.1.98) are overlapping the curves corresponding to equations (4.1.87) and (4.1.101). Inserting equation (4.1.104) into solutions (4.1.79) and (4.1.97), we find that

$$\frac{T}{f_c} = 2 \frac{\left[\sqrt{k-1} - \sqrt{1 + \phi^*(k-1)} \right] \left[\sqrt{k(1 + \phi^*(k-1))} - 1 \right]}{(k-1)^2} \quad \phi^* \leq \frac{k-1}{4k} \quad (4.1.105)$$

$$\frac{T}{f_c} = \frac{1}{2\sqrt{k}} \quad \phi^* \geq \frac{k-1}{4k} \quad (4.1.106)$$

Now equation (4.1.87) becomes

$$\frac{a}{h} \geq \frac{\sqrt{1 + \phi^*(k-1)}}{\sin \varphi} - \cot \varphi \quad \text{for } \phi^* \leq \frac{k-1}{4k} \quad (4.1.107)$$

$$\frac{a}{h} \geq \operatorname{tg} \varphi \quad \text{for } \phi^* \geq \frac{k-1}{4k} \quad (4.1.108)$$

When equations (4.1.107) and (4.1.108) are not satisfied, solutions (4.1.91), (4.1.92) and (4.1.102) will still be valid.

Fig. 4.7 shows the domains of the different failure mechanisms in our upper bound analysis with the ρ^* -value satisfying equation (4.1.83). The boundaries are plotted for $\varphi = 37^\circ$, i.e. $k = 4$ and $\rho^* = 0.1$.

In the case of large ρ^* -values, i.e. when condition (4.1.83) is violated, the failure mechanism marked 3 and 4 in Fig. 4.7 will disappear, because their upper and lower boundaries overlap, while the failure mechanism marked 1, 2, 5, 6 and 7 remain applicable.

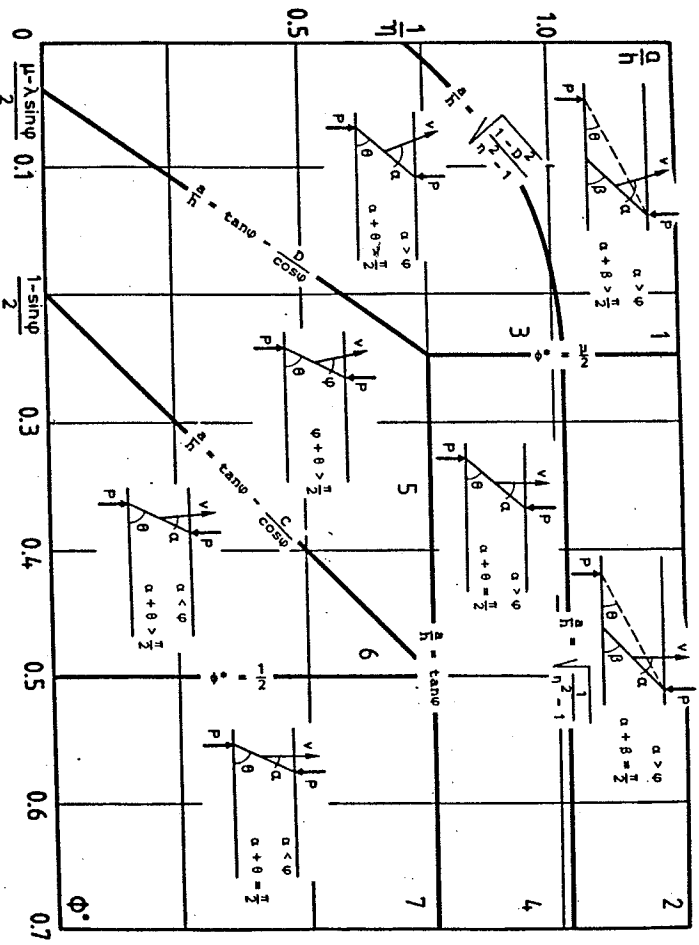


Figure 4.7. Domains of the different failure mechanisms for small p^* -values.

4.1.3 The complete plastic solutions

We have derived both the highest lower bound solutions and the lowest upper bound solutions. It is easy to note that they are identical. These solutions thus are exact according to our assumptions in section 2.6.

The complete plastic solutions are summarized in Fig. 4.8 and Fig. 4.9.

$\frac{D}{h}$	$\frac{1}{h} \leq \frac{D}{h} \leq \frac{1}{\sqrt{1-D^2}}$	$\frac{1}{h} \leq \frac{D}{h} \leq \frac{1}{\sqrt{1-D^2}}$	$\lambda + \mu + D \geq 1$	
			$\phi^* \leq \frac{1}{2}$	$\phi^* \geq \frac{1}{2}$
$\frac{1}{h} \leq \frac{D}{h} \leq \frac{1}{\sqrt{1-D^2}}$	$\frac{1}{h} \leq \frac{D}{h} \leq \frac{1}{\sqrt{1-D^2}}$	$\frac{1}{2} \sqrt{\lambda^2 - \mu^2} (1 - D^2)$	$\frac{1}{2} \sqrt{\lambda^2 - \mu^2}$	$\frac{1}{2} \sqrt{\lambda^2 - \mu^2}$
$\frac{1}{h} \leq \frac{D}{h} \leq \frac{1}{\sqrt{1-D^2}}$	$\frac{1}{h} \leq \frac{D}{h} \leq \frac{1}{\sqrt{1-D^2}}$	$\frac{1}{2} [\lambda \sqrt{\lambda^2 + 1 - D^2} - \mu \frac{\lambda}{h}]$	$\frac{1}{2} \sqrt{\lambda^2 - \mu^2}$	$\frac{1}{2} [\lambda \sqrt{\lambda^2 + 1 - \mu \frac{\lambda}{h}}]$
$\frac{1}{h} \leq \frac{D}{h} \leq \frac{1}{\sqrt{1-D^2}}$	$\frac{1}{h} \leq \frac{D}{h} \leq \frac{1}{\sqrt{1-D^2}}$	$\frac{1}{2} [(\frac{\lambda}{h})^2 + 1] (1 - \sin \phi) - 2\phi^* (\frac{\lambda}{h} \cos \phi - \sin \phi)$		
$\frac{1}{h} \leq \frac{D}{h} \leq \frac{1}{\sqrt{1-D^2}}$	$\frac{1}{h} \leq \frac{D}{h} \leq \frac{1}{\sqrt{1-D^2}}$	$\frac{1}{2} (\frac{\lambda}{h} \sin \phi + \cos \phi)$		
$\frac{1}{h} \leq \frac{D}{h} \leq \frac{1}{\sqrt{1-D^2}}$	$\frac{1}{h} \leq \frac{D}{h} \leq \frac{1}{\sqrt{1-D^2}}$	$\frac{1}{2} [(\frac{\lambda}{h})^2 + 1 - C^2 - \frac{\lambda}{h}]$		$\frac{1}{2} [(\frac{\lambda}{h})^2 + 1 - \frac{\lambda}{h}]$

Figure 4.8. The complete plastic solutions for small p^* -values.

In Fig. 4.8 and 4.9, the parameters are defined as follows.

$$p^* = \frac{f_t^*}{f_c^*}, \quad k = \frac{1 + \sin \phi}{1 - \sin \phi}$$

$$\lambda = 1 - p^* (k - 1), \quad \eta = \frac{\lambda}{\mu}$$

$$\mu = 1 - p^* (k + 1), \quad \phi^* = \frac{A S^* Y}{b h f_c^*}$$

$$\frac{T}{f_c^*} = \frac{V}{b h f_c^*}$$

$$C = \begin{cases} 1 - 2\phi^* & \text{for } \phi^* \leq \frac{1}{2} \\ 0 & \text{for } \phi^* > \frac{1}{2} \end{cases}$$

$$D = \begin{cases} \frac{\mu - 2\phi^*}{\lambda} & \text{for } \phi^* \leq \frac{\mu}{2} \\ 0 & \text{for } \phi^* > \frac{\mu}{2} \end{cases}$$

$\lambda + \mu + D < 1$		$\lambda + \mu + D \geq 1$	
$\frac{a}{h}$	$\frac{T}{T_c}$	$\phi^* \leq \frac{K-1}{4K}$	$\frac{K-1}{4K} \leq \phi^* \leq \frac{1}{2}$
$\sqrt{1 + \frac{K-1}{K^2}} \sin \omega - \cot \omega \leq \frac{a}{h}$	$\cot \omega \leq \frac{a}{h}$	$\frac{2}{\sqrt{K}}$	
$\tan \omega = \frac{C}{\cos \omega} \leq \frac{a}{h} \leq \frac{\sqrt{1 + \frac{K-1}{K^2}} \sin \omega - \cot \omega}{\sin \omega}$	$\frac{a}{h} \leq \tan \omega - \frac{C}{\cos \omega}$	$\frac{1}{2} \left[\frac{(\frac{a}{h})^2 + 1}{(K-1)^2} \sqrt{K(1 + \frac{K-1}{K^2})} (\sqrt{K(1 + \frac{K-1}{K^2})} - 1) \right]$	
		$\frac{1}{2} \left[\frac{(\frac{a}{h})^2 + 1}{(K-1)^2} \sqrt{K(1 + \frac{K-1}{K^2})} (\sqrt{K(1 + \frac{K-1}{K^2})} + 1) \right]$	
		$\frac{1}{2} \left[\frac{(\frac{a}{h})^2 + 1}{(K-1)^2} \sqrt{K(1 + \frac{K-1}{K^2})} (\sqrt{K(1 + \frac{K-1}{K^2})} + \cos \omega) \right]$	
		$\frac{1}{2} \left[\frac{(\frac{a}{h})^2 + 1}{(K-1)^2} \sqrt{K(1 + \frac{K-1}{K^2})} (\sqrt{K(1 + \frac{K-1}{K^2})} - \cos \omega) \right]$	
		$\frac{1}{2} \left[\frac{(\frac{a}{h})^2 + 1}{(K-1)^2} \sqrt{K(1 + \frac{K-1}{K^2})} (\sqrt{K(1 + \frac{K-1}{K^2})} - 1) \right]$	

Figure 4.9. The complete plastic solutions for large ρ^* -values.

These solutions are also valid when $\rho^* = 0$, which correspond to the so-called square yield locus (Fig. 2.15). It is easy to find that in this case the complete solutions will be very much simplified and we get

$$\frac{T}{T_c} = \begin{cases} \frac{1}{2} \left[\left(\frac{a}{h} \right)^2 + 1 - C^2 - \frac{a}{h} \right] & \text{for } \phi^* \leq \frac{1}{2} \\ \frac{1}{2} \left[\left(\frac{a}{h} \right)^2 + 1 - \frac{a}{h} \right] & \text{for } \phi^* > \frac{1}{2} \end{cases} \quad \begin{matrix} (4.1.92) \\ (4.1.102) \end{matrix}$$

In what follows we will name equations (4.1.92) and (4.1.102) the simple solutions to distinguish them from the complete solutions considering the tensile strength of concrete.

Fig. 4.10 shows the domains of the complete plastic solutions for small ρ^* -values in the $(\phi^*, \frac{a}{h})$ parameter plane. The boundaries are plotted for $\varphi = 37^\circ$, i.e. $K = 4$ and $\rho^* = 0.1$.

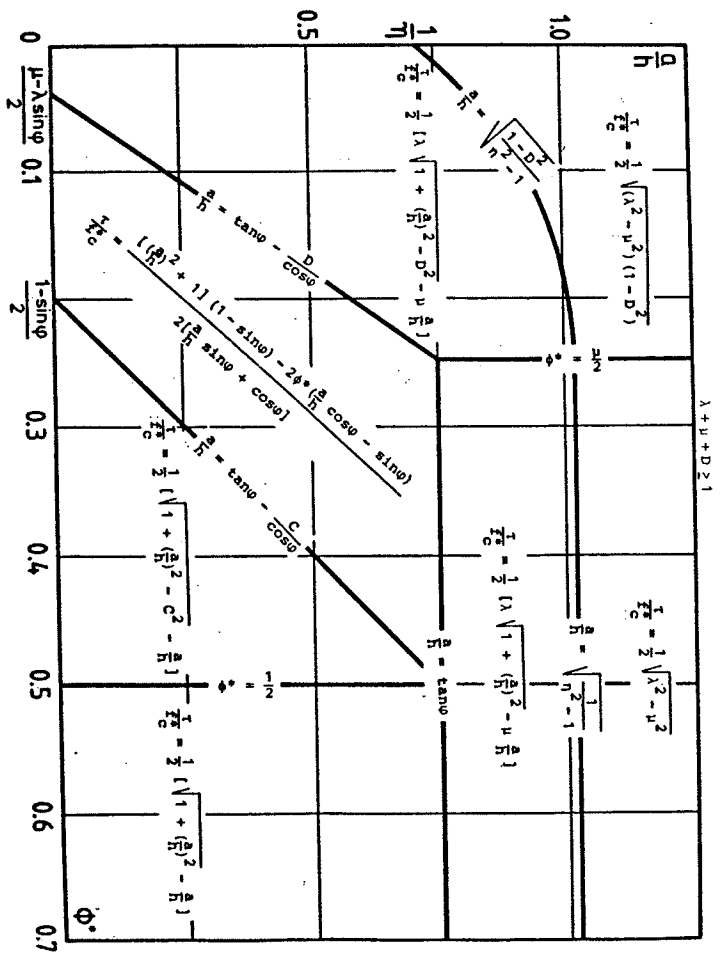


Figure. 4.10. Domains of the complete plastic solutions for beams subjected to point loading and without web reinforcement.

Fig. 4.11 shows the domains of the complete plastic solutions for large ρ^* -values in the $(\phi^*, \frac{a}{h})$ coordinate plane. The boundaries are plotted for $\psi = 37^\circ$, i.e. $k = 4$ and $\rho^* = 0.2$.

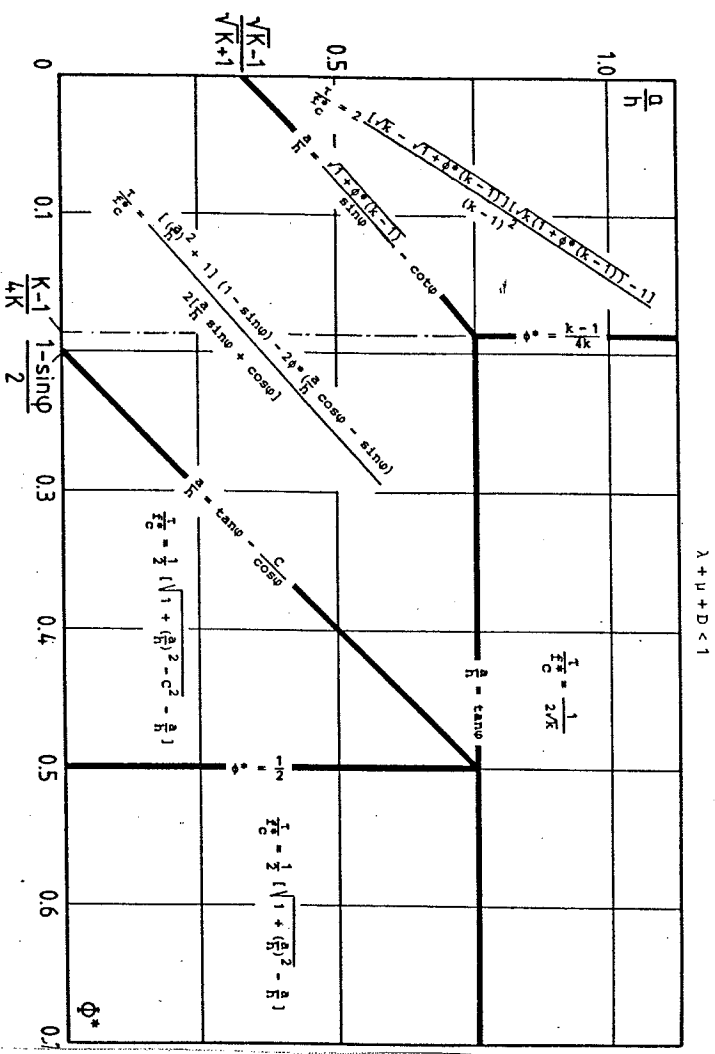


Figure 4.11. Domains of the complete plastic solutions for large ρ^* - values.

In Fig. 4.12 the shear carrying capacity τ/f_c^* is plotted against a/h for different values of ϕ^* and ρ^* .

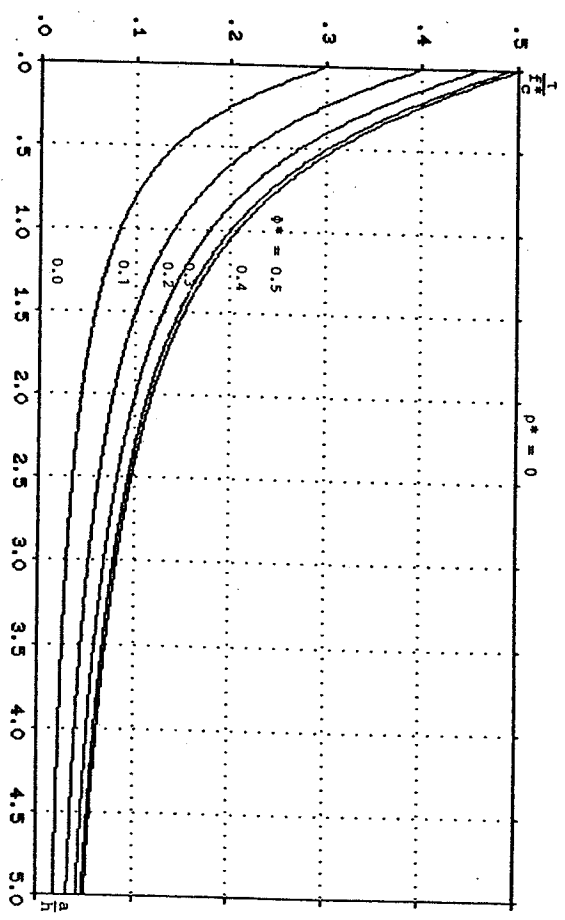


Figure 4.12. Shear carrying capacity of a beam subjected to concentrated loads versus clear shear span and longitudinal reinforcement degree.

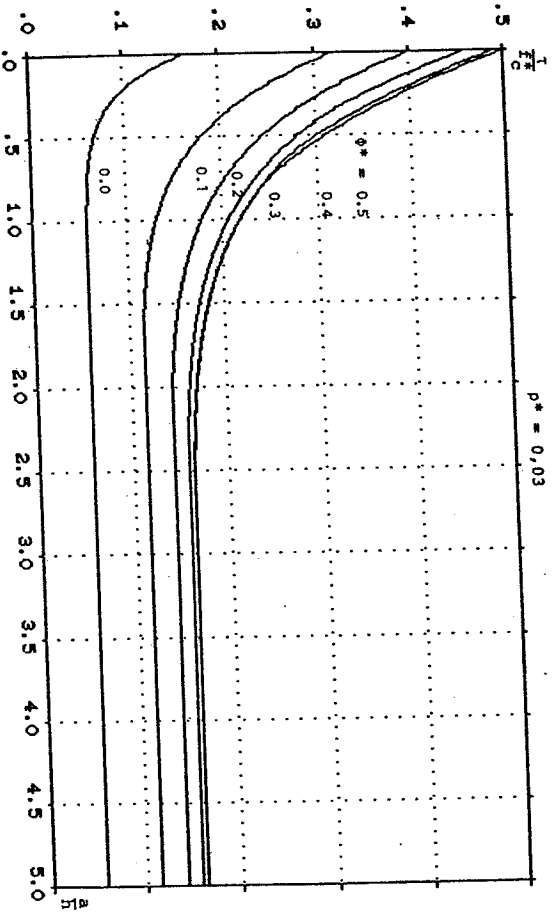


Figure 4.12 (continued).

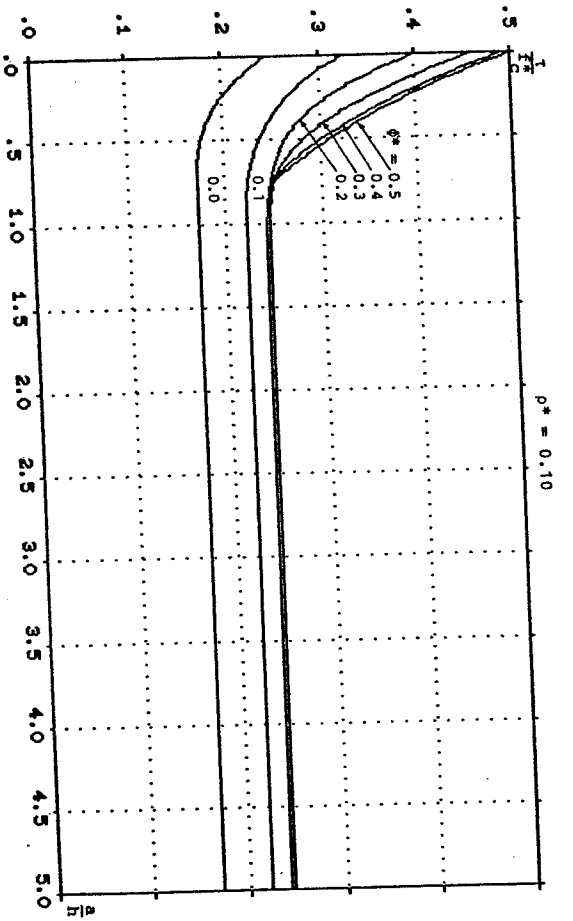


Figure 4.12 (continued).

Fig. 4.13 shows the relation between the shear capacity and the longitudinal reinforcement degree for different shear span ratios and p^* values.

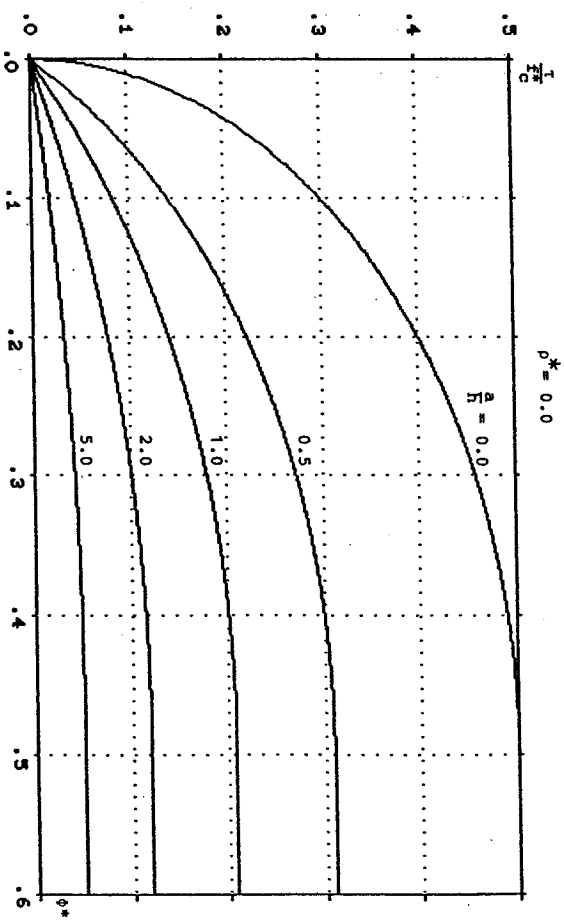


Figure 4.13. Shear capacity of a beam loaded by concentrated force versus longitudinal reinforcement degree.

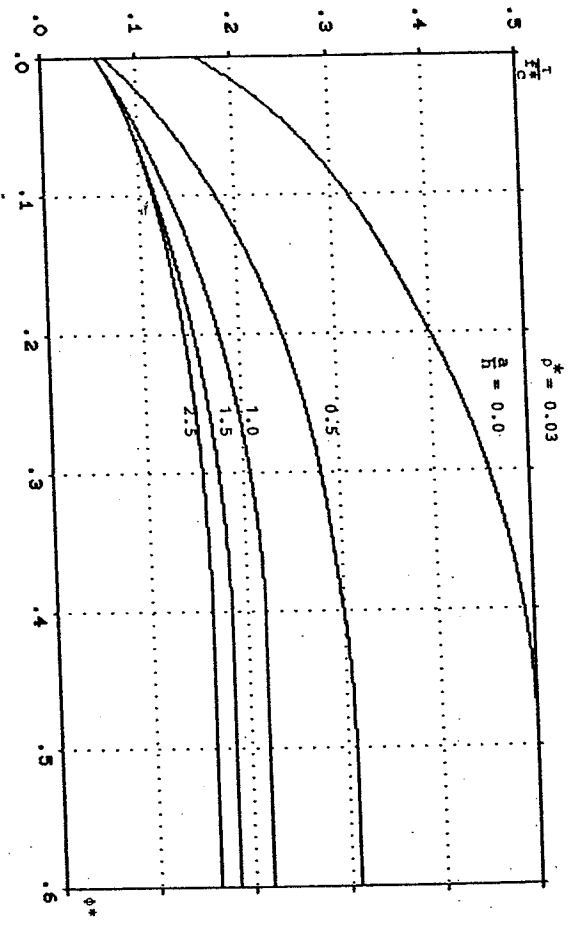


Figure 4.13 (continued).

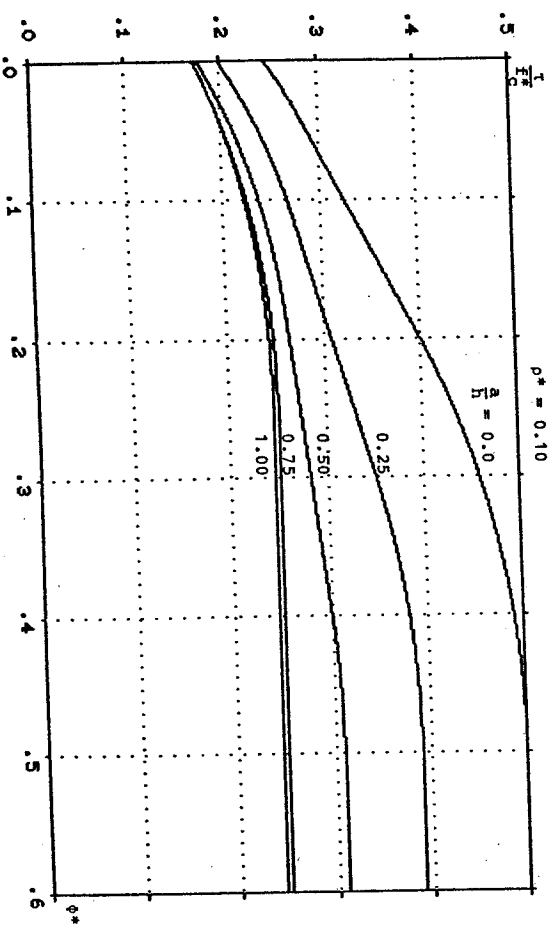


Figure 4.13 (continued).

From Fig. 4.12 and 4.13, it is very clear that the shear carrying capacity, in general, increases with an increase of the longitudinal reinforcement degree and decreases with an increase of the clear span ratio before it reaches some special value. This special value is very much influenced by the ρ^* value. In Fig. 4.14 the influence of the ρ^* value to the shear capacity has been shown in different values of $\frac{h}{\bar{h}}$ and ϕ^* .

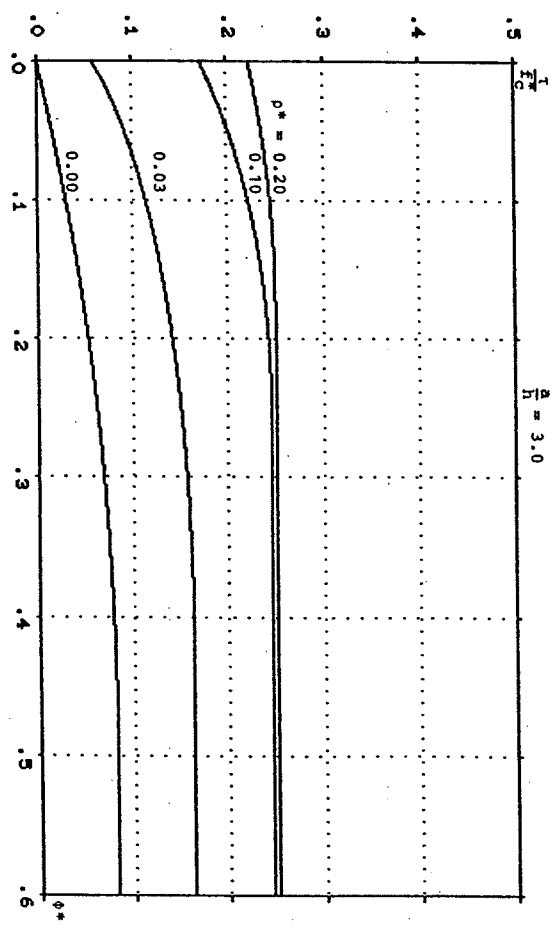


Figure 4.14. The influence of ρ^* to shear capacity for different values of $\frac{h}{\bar{h}}$ and ϕ^* .

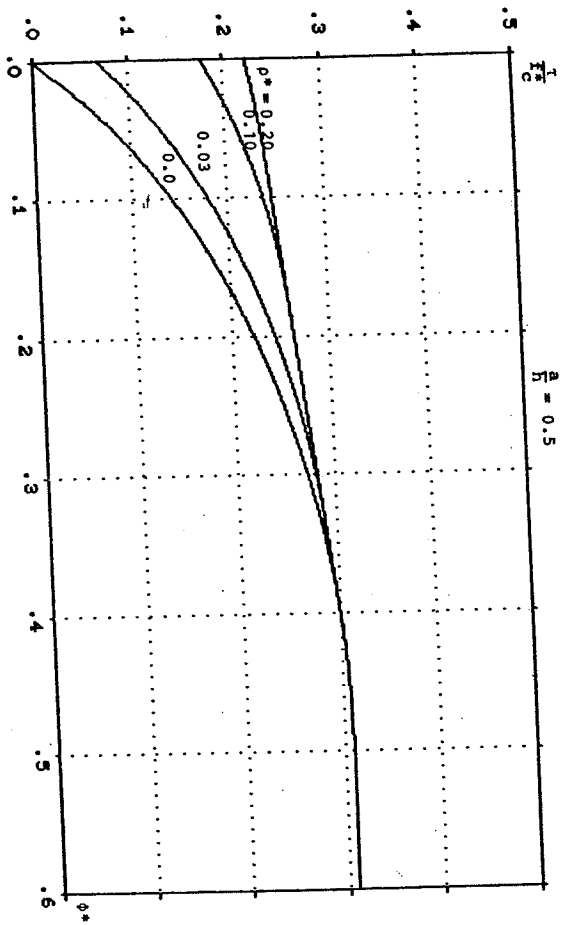


Figure 4.14 (continued).

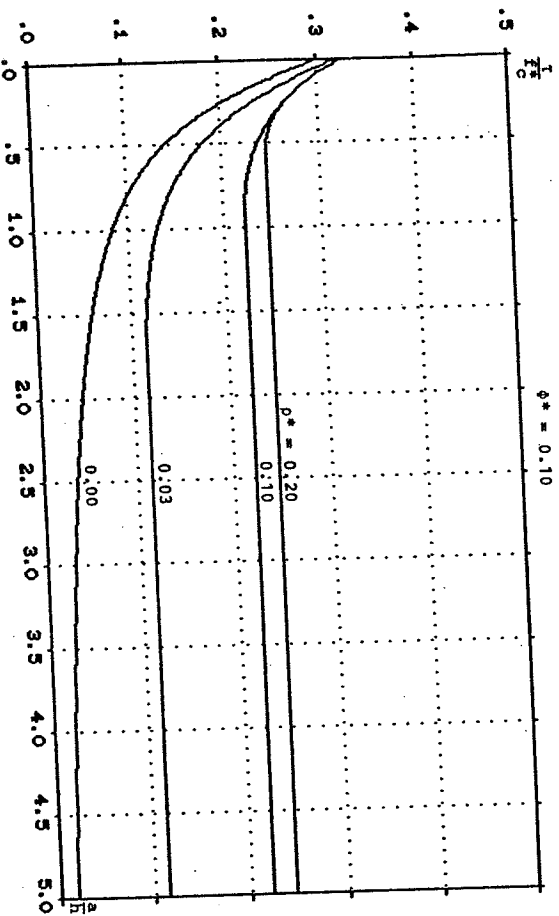


Figure 4.14 (continued).

The difference between the cases of considering the tensile strength of concrete and neglecting it can be seen very clearly in Fig. 4.14, especially for beams with large shear span ratio and for corbels with low reinforcement degrees.

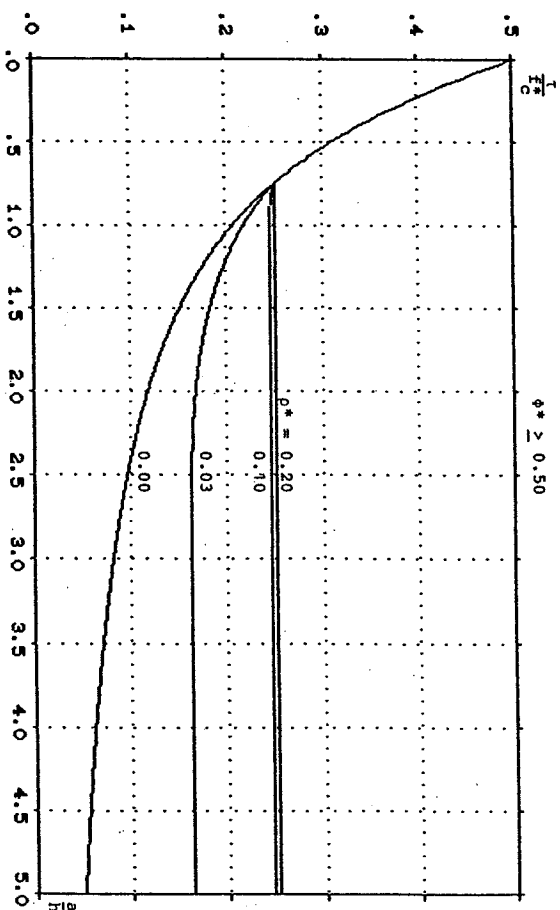


Figure 4.14 (continued).

4.1.1.4 The ρ^* and ν values in the plastic solutions

As mentioned before, the effectiveness factors ν and ρ^* in our complete solutions must be determined by experiments.

Inserting $f_c^* = \nu f_c$ into the complete plastic solutions shown in Fig. 4.8 and solving it with respect to ν , we find the corresponding domains of the ν -formulae as shown in Fig. 4.15. The boundaries are plotted for $\varphi = 37^\circ$, i.e. $K = 4$ and $\rho^* = 0.1$.

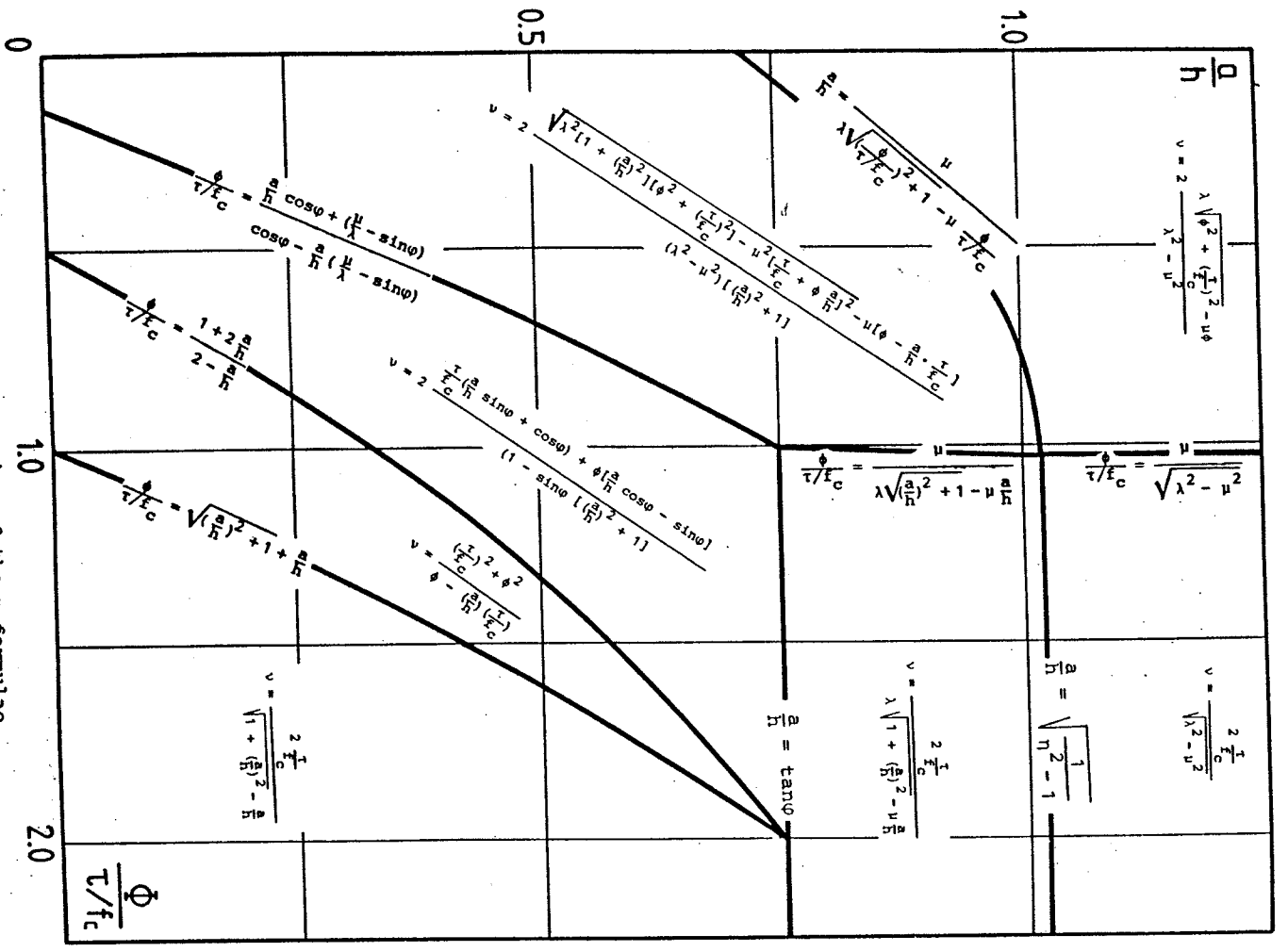


Figure 4.15. The domains of the v-formulae.

It is worth noticing that when we determine the v-value for shear from test results, we should exclude flexural failures and local failures and preferably use the test data from test specimen with high reinforcement ratios. Otherwise, it may produce very unreliable results especially in the case of tests with very low reinforcement ratios.

A great number of test data for non-shear reinforced beams, deep beams and corbels subjected to concentrated loads have been found in literature. The detailed test data, including the dimensions, material properties and measured ultimate loads of beams, deep beams and corbels, and the sources are shown in Appendix B.

It is obvious that the v-value is very much dependent on the ρ^* -value that we have chosen. We may decide the ρ^* -value from the beam failure model. According to our plastic solutions, for the overreinforced case, when equation (4.1.98) is satisfied, the τ/f_c^* is independent from a/h. This conclusion has been verified by the tests. A great number of tests have shown that τ/f_c is almost a constant for beams with relatively big shear span ratios failed in shear. When the shear span ratio is less than a definite value, the τ/f_c is decreasing with increasing shear span ratio. The critical shear span ratio is about 2.5.

Inserting $a/h = 2.5$ into equation

$$\frac{a}{h} = \sqrt{\frac{1}{2 - \eta}} \quad (4.1.109)$$

we get the ρ^* -value about 0.03. This value satisfies the requirement of equations (4.1.51) and (4.1.52).

Parametric analysis indicates that the effectiveness factor v mainly is a function of the uniaxial compressive strength f_c , the ratio of reinforcement ϕ , defined as $\phi = A_s/bh$, the clear shear span ratio a/h and the absolute depth of the specimen.

Fig. 4.16 and Fig. 4.17 show some examples of the dependence of v

on f_c . It is very clear that ν decreases with the increase of the uniaxial compressive strength of concrete.

For simplicity, the relation between ν and f_c may be described empirically by assuming that ν is inversely proportional to $\sqrt{f_c}$. That is

$$\nu = \frac{k_1}{\sqrt{f_c}} \quad (4.1.110)$$

Here, k_1 is a constant and f_c is in MPa.

For comparison, such kind of curves is drawn in Fig. 4.16 and Fig. 4.17 together with the tests. A good agreement is found.

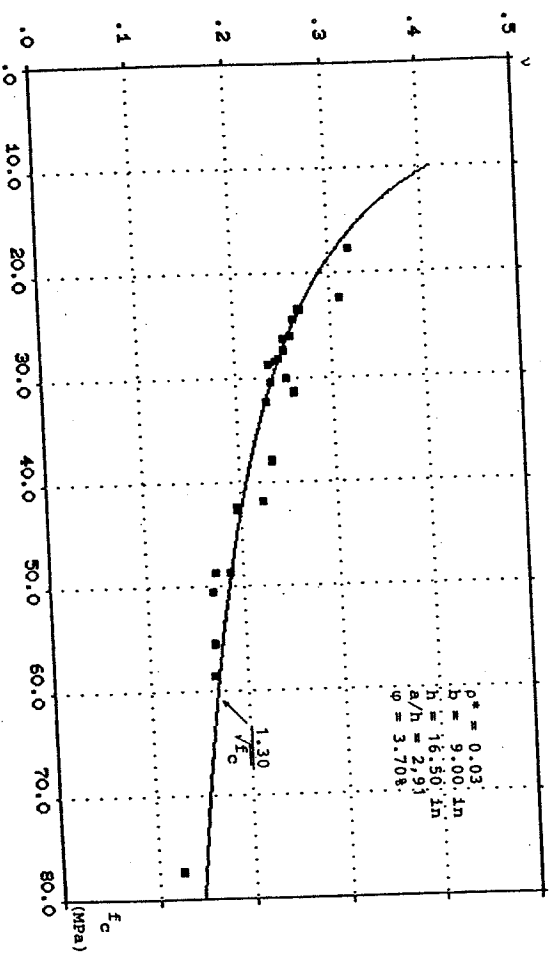


Figure 4.16. The ν -dependence on f_c , [62.2].

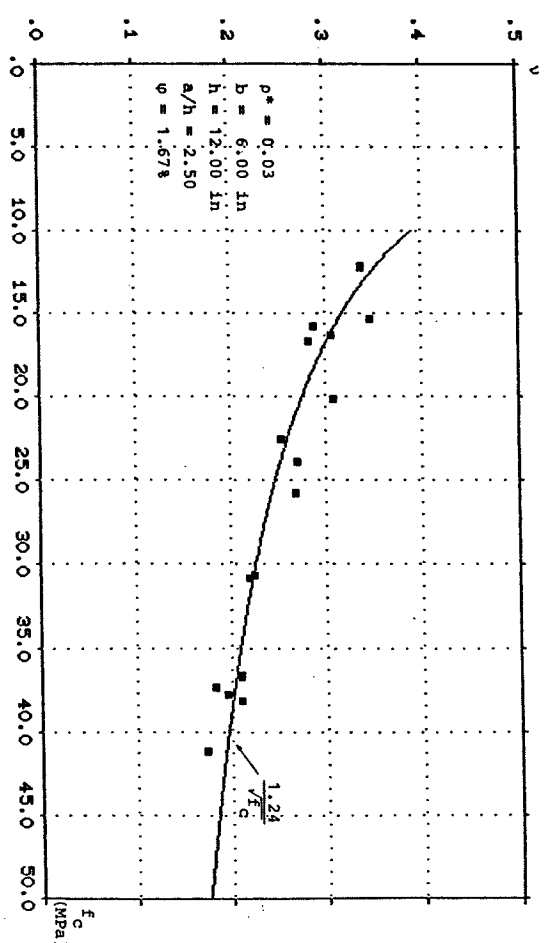


Figure 4.17. The ν -dependence on f_c , [54.2].

For high strengths of concrete, the ν -dependence on f_c may be better expressed as

$$\nu = \frac{3}{\sqrt{f_c^2}} K \quad (4.1.111)$$

The comparison of equations (4.1.110) and (4.1.111) with some tests with high strength of concrete can be seen in Fig. 4.18. Unfortunately, we have only found a few shear tests with high strength of concrete. In the following sections we will only use (4.1.110) to describe approximately the ν -dependence on f_c .

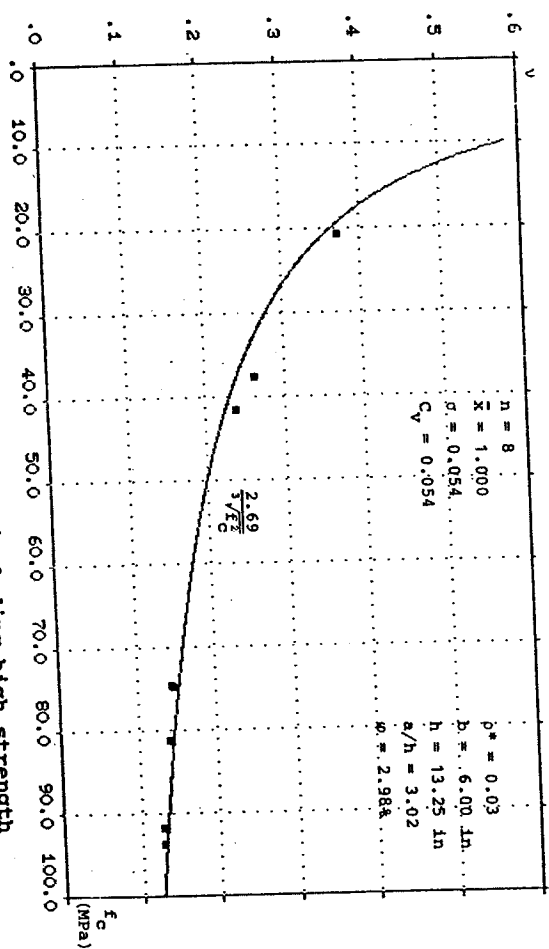
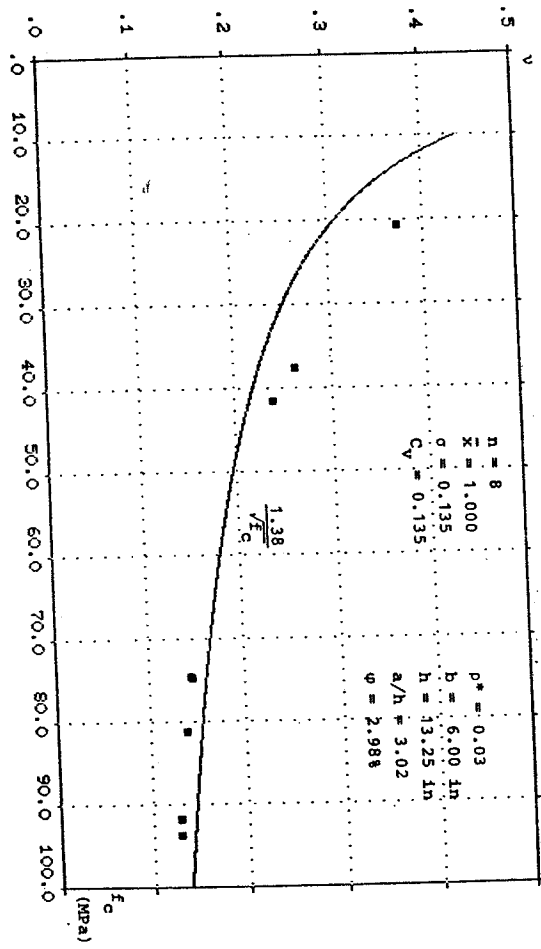


Figure 4.18. The v -dependence on f_c including high strength concrete [84.5].

Some v - ϕ relations are depicted in Fig. 4.19.

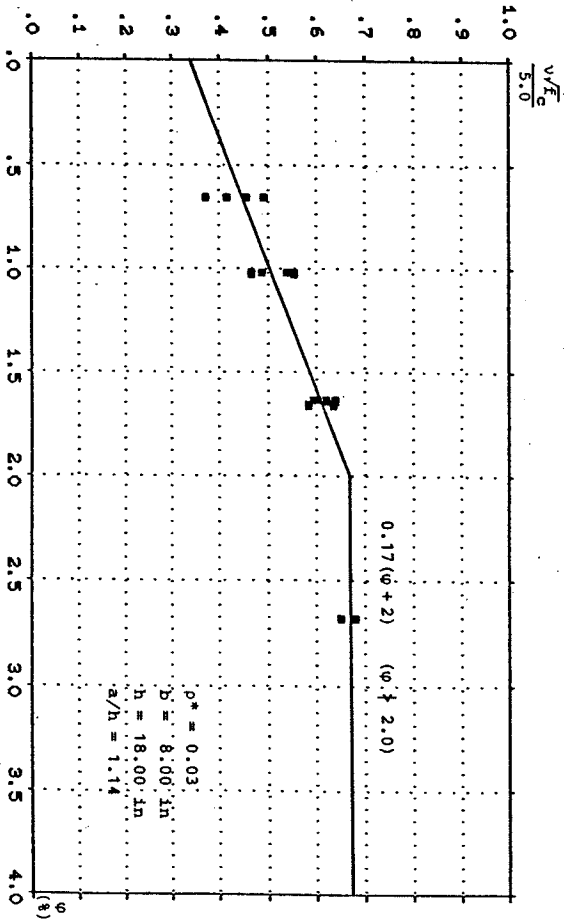


Figure 4.19. The v -dependence on ϕ [63.2].

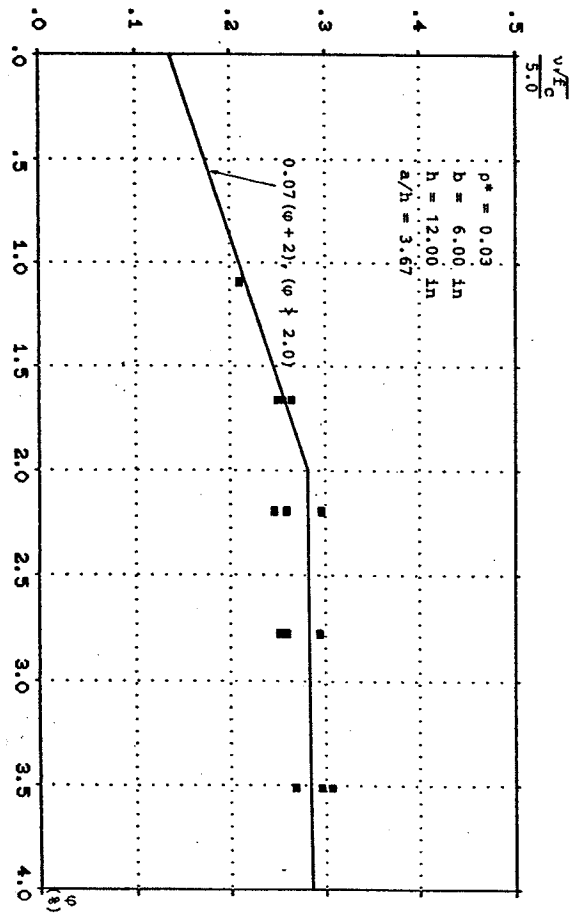


Figure 4.19. (continued) [66.1].

As clearly shown in Fig.4.19, the v -value is increasing almost linearly with ϕ for lower reinforcement ratios, for example $\phi < 2.0$, and is independent of ϕ for higher ratios, i.e. $\phi \geq 2.0$.

The v -dependence on a/h may be expressed as

$$v = k_2 \left(3.5 - \frac{a}{h} \right), \quad \left(\frac{a}{h} \leq 2.5 \right) \quad (4.1.112)$$

Here k_2 is a constant

Some experimental evidence is shown in Fig. 4.20.

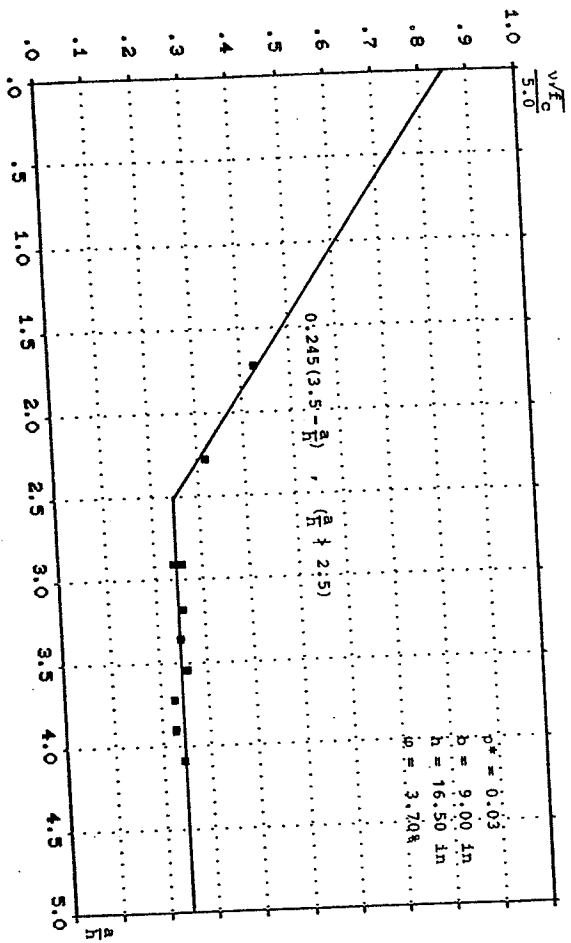


Figure 4.20. The v -dependence on $\frac{a}{h}$. [62.2].

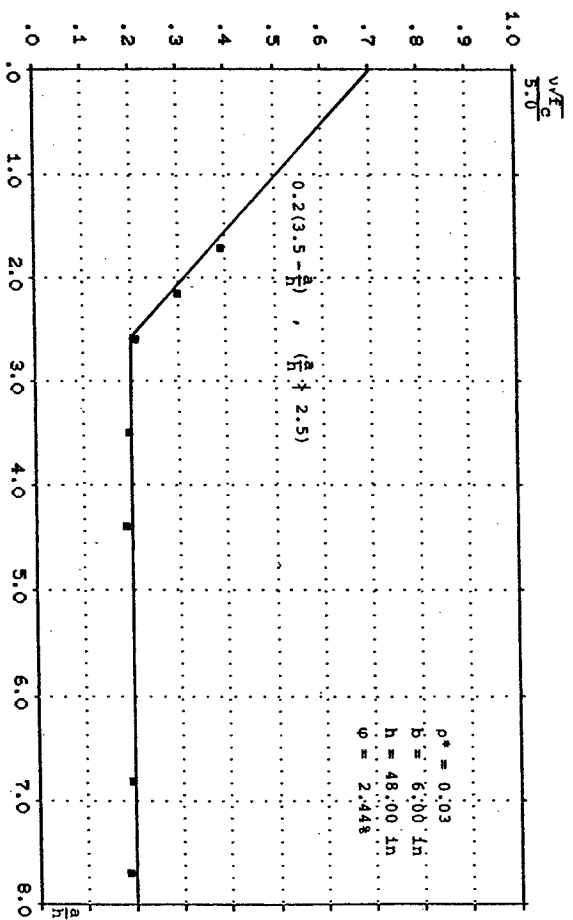


Figure 4.20. (continued) [67.3].

A parametric analysis has shown that the v -value decreases with increasing specimen depth. Some evidence is provided in Fig. 4.21.

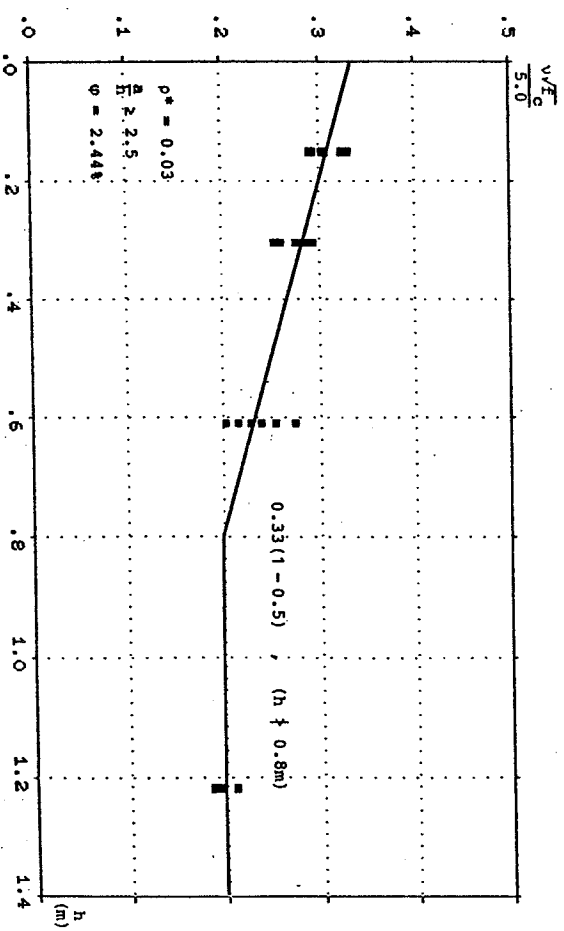


Figure 4.21. The v -dependence on h (m). [67.3].

From the parametric analysis of 657 observed shear failures of beams, deep beams and corbels, the following empirical ν formula with $\rho^* = 0.03$ is suggested

$$\nu = \frac{0.35(3.5 - \frac{a}{h})(\varphi + 2)(1 - 0.2n)}{\sqrt{f_c}} \leq 1.0 \quad \left[\begin{array}{l} \frac{a}{h} \neq 2.5 \\ \varphi \neq 2.0 \\ h \neq 1.25 \end{array} \right] \quad (4.1.113)$$

Here f_c is in MPa, φ in percent and h in meter.

Formula (4.1.113) is verified by tests having $f_c \leq 100$ MPa, $a/h \leq 10.0$ and $h \leq 1.20$ m. Out of these ranges, more tests are needed. Results of 657 beams, deep beams and corbels from 30 available references were compared to the complete solutions in Fig. 4.8 using (4.1.113).

The statistical values of the ratios of test to theory are presented in Fig. 4.22. A very good agreement has been found.

Item	Observed shear failure				Theoretical shear failure			
	number	mean	standard deviation	coeff. of variation	number	mean	standard deviation	coeff. of variation
Cases	n	\bar{x}	σ	C_v	n	\bar{x}	σ	C_v
beams	412	1.004	0.152	0.151	353	1.015	0.148	0.146
deep beams	127	1.018	0.146	0.143	101	1.022	0.136	0.133
corbels	118	1.002	0.140	0.140	110	1.008	0.142	0.141
total	657	1.006	0.149	0.148	564	1.015	0.145	0.143

Figure 4.22. The statistical values of the ratios of test to theory.

The comparison between theory and test results is also shown in Fig. 4.23.

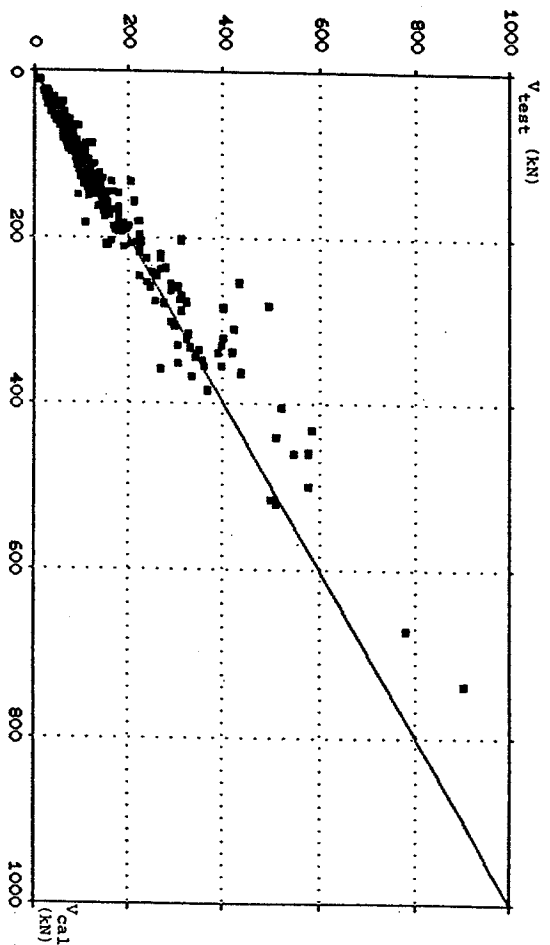


Figure 4.23. The comparison between theory and tests of beams.

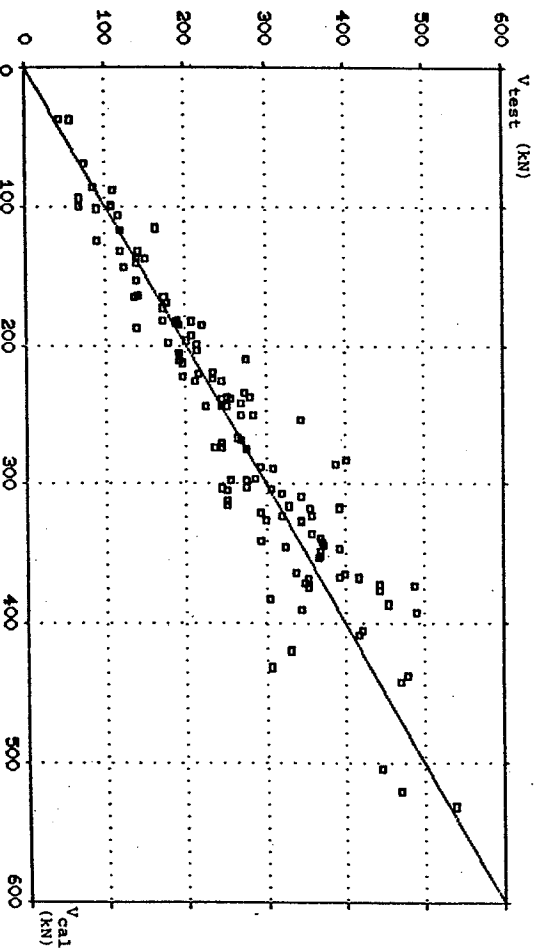


Figure 4.23. The comparison between theory and tests of deep beams (continued).

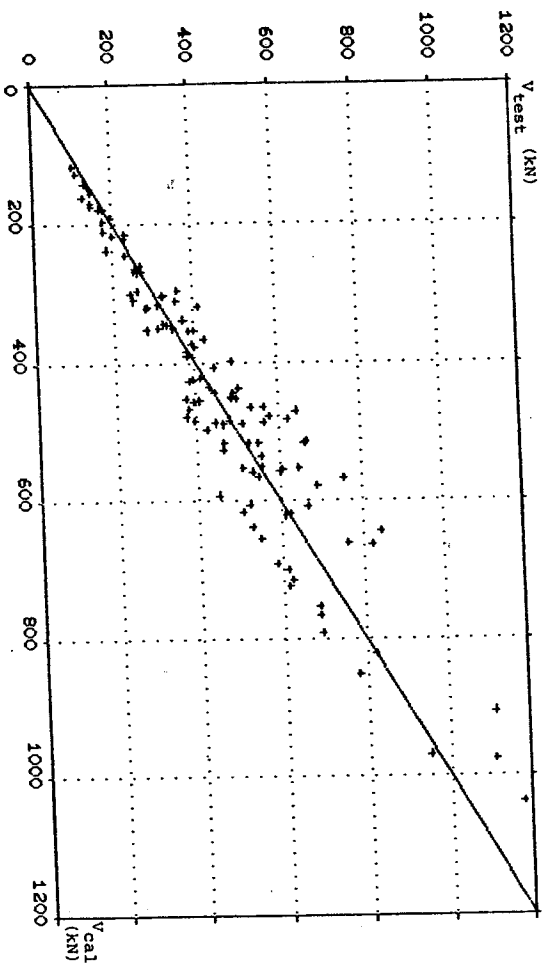


Fig. 4.23 (continued).

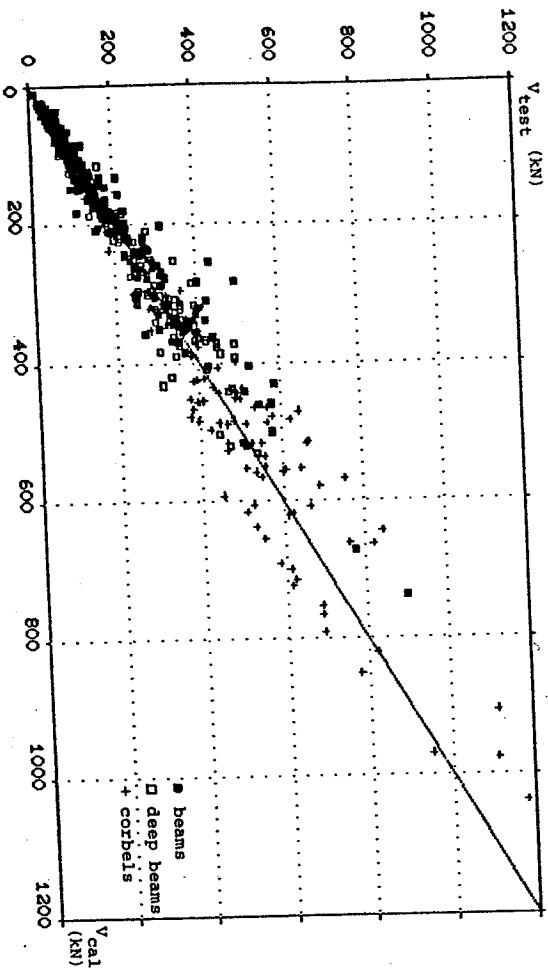


Fig. 4.23. (continued).

To demonstrate the general applicability of the complete plastic solutions, Fig. 4.24 shows the comparison of theory with the results of the shear tests of beams, deep beams and corbels for different shear span ratios. The ν -value has been calculated from (4.1.113).

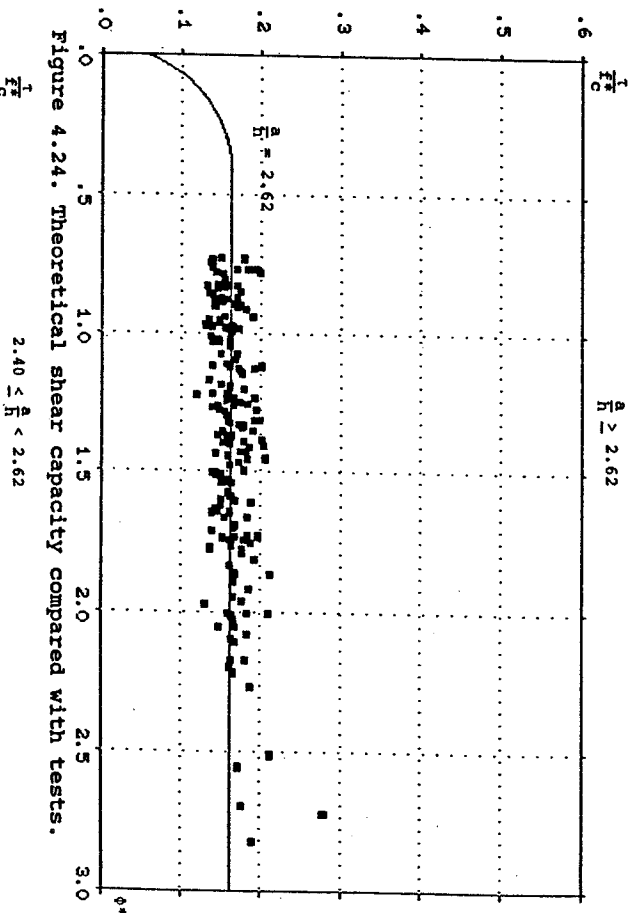


Figure 4.24. Theoretical shear capacity compared with tests.

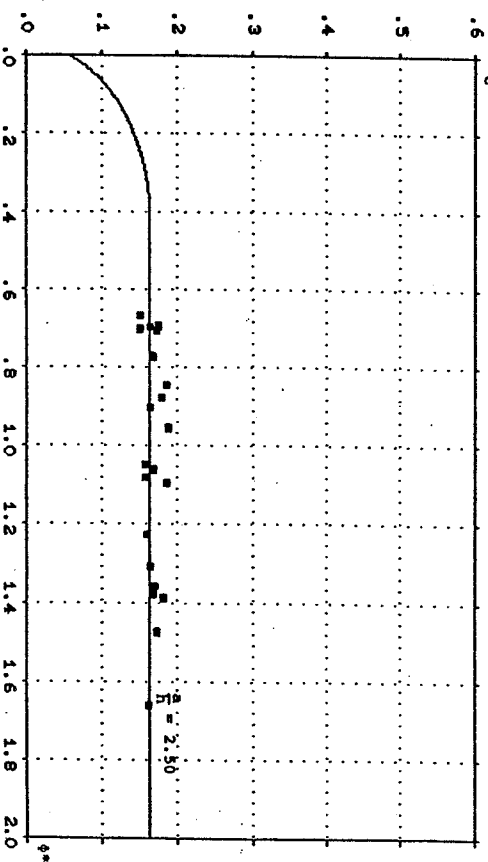


Figure 4.24. (continued).

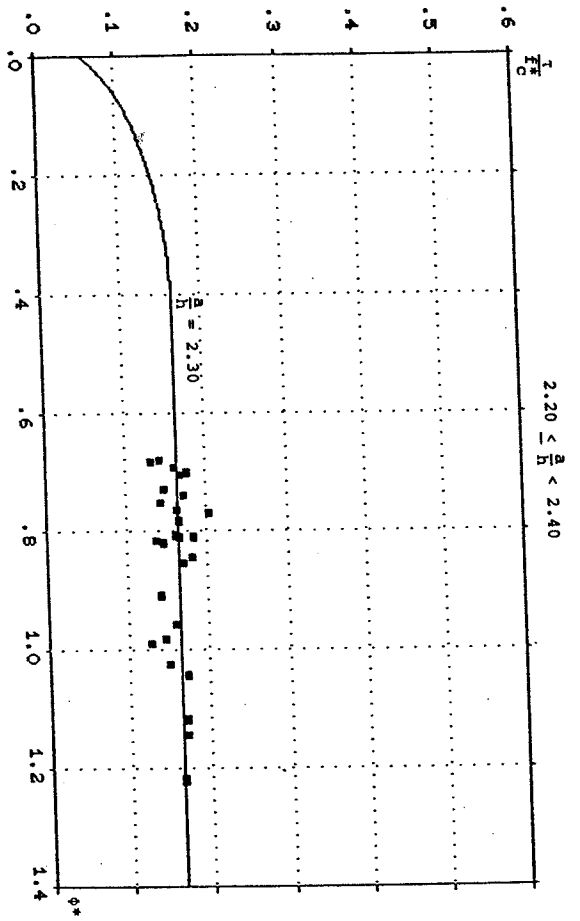


Figure 4.24. (continued).

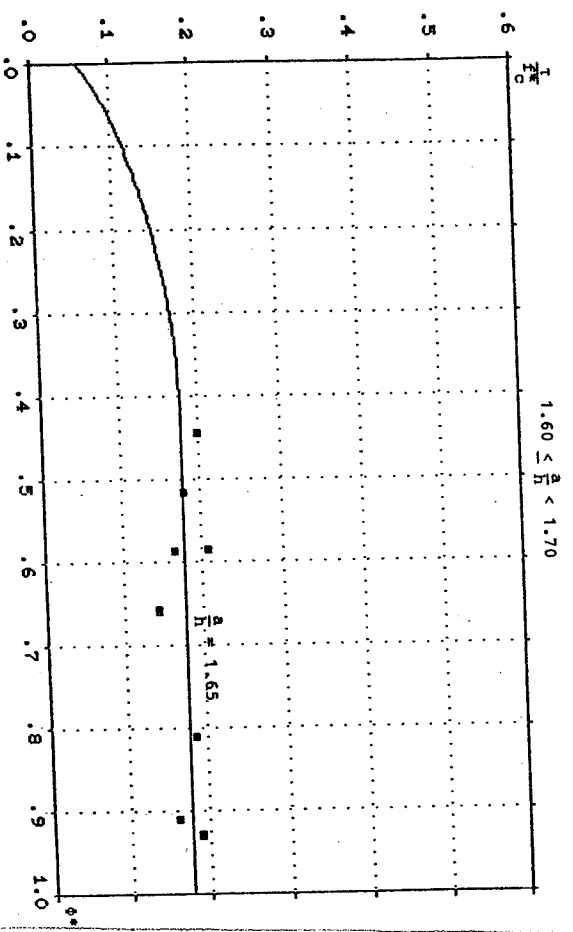


Figure 4.24. (continued).

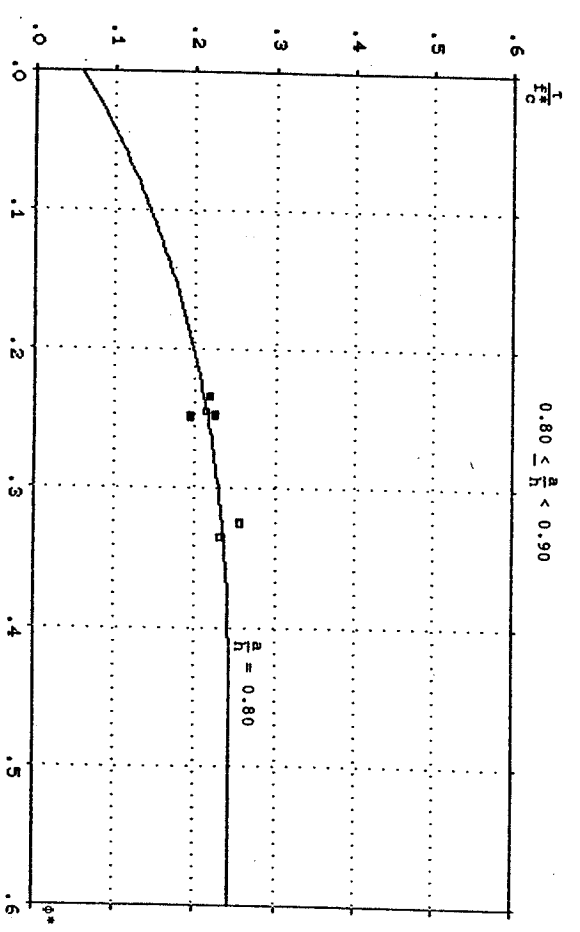


Figure 4.24. (continued).

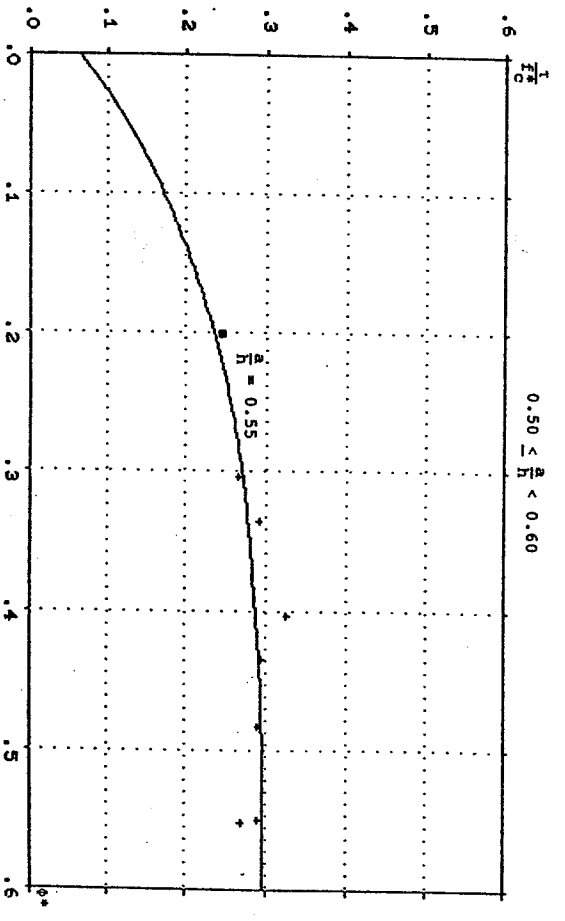


Figure 4.24. (continued).

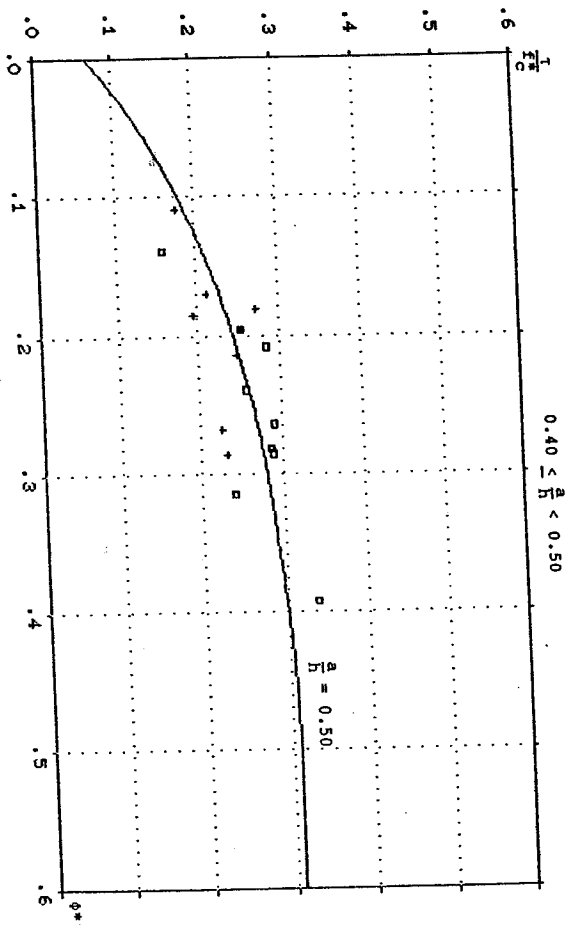


Figure 4.24. (continued).

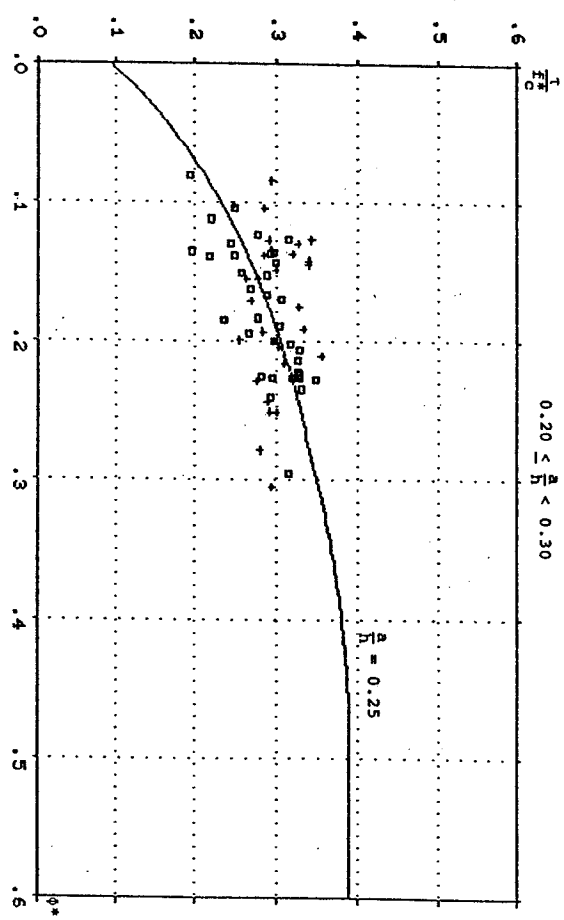


Figure 4.24. (continued).

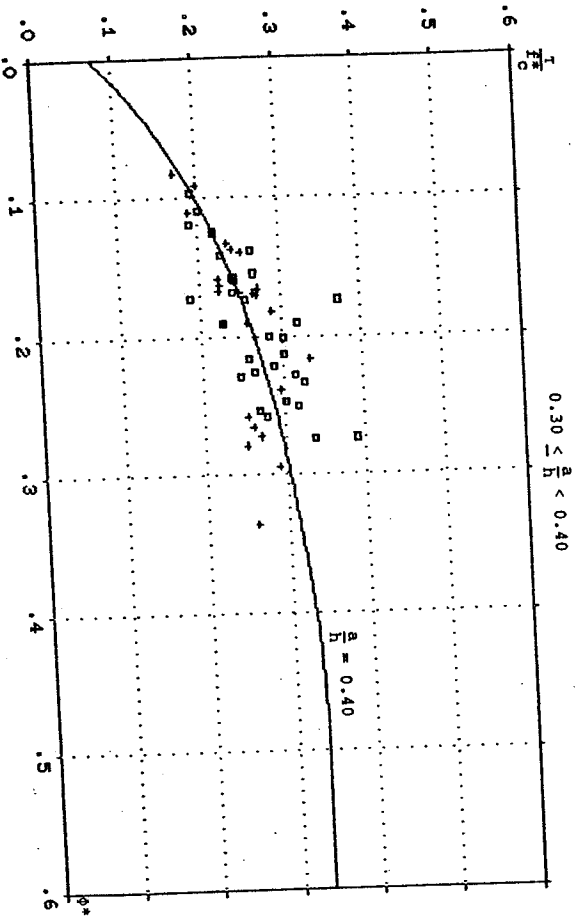


Figure 4.24. (continued).

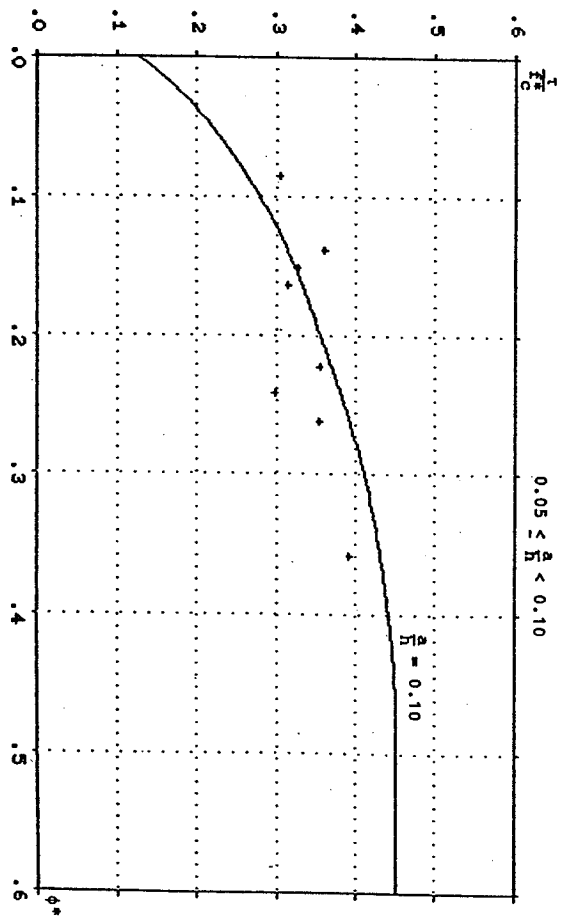


Figure 4.24. (continued).

4.2 Shear capacity neglecting the tensile strength of concrete

In section 4.1 we have derived the complete exact beam shear solutions for structural members without web reinforcement and subjected to concentrated loads. For practical use, it may often be considered to be too complicated to use. Further as a matter of fact, the behaviour of concrete in tension is almost brittle. Therefore, in most cases, it is reasonable to neglect the tensile strength of concrete. The exact simple solutions of beam shear based on the yield condition reducing to the so-called square yield locus (Fig. 2.15) were presented by Nielsen and Brastrup [78.2] and [78.3]. The corresponding empirical v formula were proposed by Rokkjar [79.4].

In this section, an alternative derivation giving identical solutions is developed.

4.2.1 Lower bound solution

Fig. 4.25 shows a stress distribution in a rectangular concrete beam with concentrated loading. The longitudinal reinforcement is firmly connected with the lateral steel plate. The beam is subdivided into a number of areas with homogeneous stress conditions. The shaded regions are in a state of biaxial, hydrostatic compression with a stress termed σ_b . The part I is in a state of biaxial compression with horizontal stress σ_b and vertical stress termed σ_v . The part II is also in a state of compression with stress σ_b . The part III is in a state of uniaxial compression with stress σ_b , but along line AB there is some bond stress with the reinforcement. In the bending section, the reinforcement force is termed T and the resultant compression force of concrete is termed C . This stress state is statically admissible in the sense that it satisfies the equilibrium equations and the statical boundary conditions on the upper and lower face.

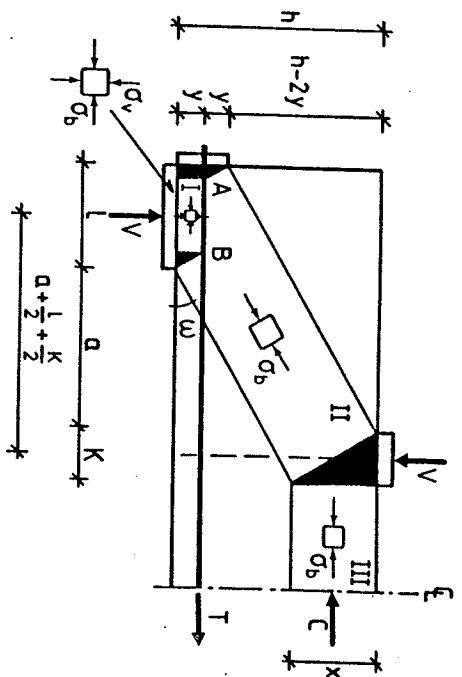


Fig. 4.25. Stress distribution in a rectangular beam subjected to symmetrical two-point loads.

The length of the load platen K is determined by the geometrical relation

$$\frac{K}{x} = \tan \omega = \frac{h-x}{a+x} \quad (4.2.1)$$

with the solution

$$k = \frac{1}{2} \left[\sqrt{a^2 + 4x(h-x)} - a \right] \quad (4.2.2)$$

The depth x of the compressive concrete zone is determined by horizontal equilibrium

$$x = \frac{T}{b\sigma_b} \quad (4.2.3)$$

The shear load V corresponding to this stress distribution is found by equilibrium of vertical forces

$$V = bc\sigma_b k = \frac{bc\sigma_b}{2} \left[a^2 + 4x(h-x) - a \right] \quad (4.2.4)$$

Inserting equation (4.2.3) into (4.2.4) yields

$$V = \frac{1}{2} \left[\sqrt{a^2 b^2 \sigma_b^2 + 4T(hb\sigma_b - T)} - ab\sigma_b \right] \quad (4.2.5)$$

We now determine the highest lower bound by maximizing (4.2.5) with respect to the statical variables σ_b and T . It appears that:

$$\frac{dV}{d\sigma_b} > 0 \quad \text{always} \quad (4.2.6)$$

$$\frac{dV}{dT} \geq 0 \quad \text{for } T \leq \frac{1}{2} hb\sigma_b$$

Thus the highest lower bound is obtained with the maximum concrete stress, i.e. $\sigma_b = f_c^*$. For $T \leq \frac{1}{2} hb f_c^*$, the highest lower bound is obtained when the reinforcement force is maximum, i.e. $T = \phi^* bh f_c^*$. Inserting into equation (4.2.5), we get

$$\frac{T}{f_c^*} = \frac{1}{2} \left[\sqrt{\left(\frac{a}{h}\right)^2 + 4\phi^* (1-\phi^*)} - \frac{a}{h} \right] \quad \text{for } \phi^* \leq \frac{1}{2} \quad (4.2.7)$$

For $T > \frac{1}{2} hb f_c^*$, the highest lower bound is obtained with $T = \frac{1}{2} bh f_c^*$ and we find

$$\frac{T}{f_c^*} = \frac{1}{2} \left[\sqrt{\left(\frac{a}{h}\right)^2 + 1} - \frac{a}{h} \right] \quad \text{for } \phi^* > \frac{1}{2} \quad (4.2.8)$$

This solution coincides with the solution derived by Nielsen et al using different stress distributions [78.2], [78.3].

4.2.2. Upper bound solution

Consider a failure mechanism consisting of a curved yield line in the shear span of the rectangular concrete beam subjected to the concentrated load V , (Fig. 4.26). The yield line is running from A , which is the outside edge of the load platen, to B , which is the inside edge of the support platen. The part I rotates relatively round an arbitrary point O with angular velocity of η . The inclination of the straight line AB is determined by the angle θ , where $\cot\theta = \frac{a}{h}$. M is the centre of line AB and the relative displacement of point M is δ_m , inclined at the angle α_m to the line AB . The length of line OM is termed r_m , inclined at the angle β to the horizontal direction. The means of the parameters t , l and y can be clearly found in Fig. 4.26.

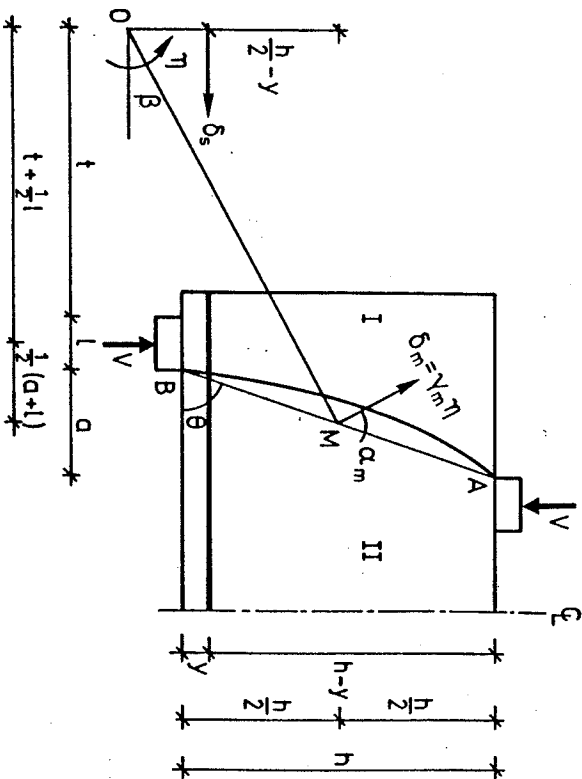


Fig. 4.26. Failure mechanism for shear span subjected to concentrated load.

We assume that the reinforcement is yielding in tension, i.e.

$$\alpha_m + \theta \leq \frac{\pi}{2} \quad (4.2.9)$$

The rate of internal work dissipated by this mechanism is

$$W_I = \frac{1}{4} b f_C^* \eta \left\{ (2t+2l+a) \left[\sqrt{a^2+h^2} \cdot \sqrt{1+\tan^2 \beta - h \tan \beta - a} \right] + 2 \frac{A_s f_C^* \eta}{b f_C^*} \left[(2t+2l+a) \tan \beta - (h-2y) \right] \right\} \quad (4.2.10)$$

where we have used equation (2.4.12) to compute the contribution from the web concrete.

The external work is

$$W_E = \frac{1}{2} (2t+l) \eta V \quad (4.2.11)$$

The work equation $W_I = W_E$ then yields an upper bound for the ultimate shear stress:

$$\frac{T}{f_C^*} = \frac{(2t+2l+a) \left[\sqrt{a^2+h^2} \cdot \sqrt{1+\tan^2 \beta - h \tan \beta - a} \right] + 2 \phi^* h \left[(2t+2l+a) \tan \beta - (h-2y) \right]}{2h(2t+l)} \quad (4.2.12)$$

The lowest upper bound can then be found by minimizing equation (4.2.12) with respect to the variables t and $\tan \beta$.

It appears that

$$\frac{\partial (T/f_C^*)}{\partial (\tan \beta)} = 0 \quad \text{for } \sin \beta = \sin \theta \cdot (1-2\phi^*) \quad (\text{valid for } \phi^* \leq \frac{1}{2}) \quad (4.2.13)$$

$$\frac{\partial (T/f_C^*)}{\partial t} = 0 \quad \text{for } t \rightarrow \infty \quad (4.2.14)$$

Inserting equations (4.2.13) and (4.2.14) and $\cot \theta = \frac{a}{h}$ into (4.2.12), we get the lowest upper bound

$$\frac{T}{f_C^*} = \frac{1}{2} \left[\sqrt{\left(\frac{a}{h}\right)^2 + 4\phi^* (1-\phi^*)} - \frac{a}{h} \right] \quad \text{for } \phi^* \leq \frac{1}{2} \quad (4.2.15)$$

For $\phi^* > \frac{1}{2}$, minimum is obtained with $\beta=0$ and $t \rightarrow \infty$ since the reinforcement can not be in compression.

In this case the lowest upper bound is easily found to be

$$\frac{T}{f_C^*} = \frac{1}{2} \left[\sqrt{\left(\frac{a}{h}\right)^2 + 1} - \frac{a}{h} \right] \quad \text{for } \phi^* > \frac{1}{2} \quad (4.2.16)$$

This solution is valid when the longitudinal reinforcement is sufficiently strong, it no longer contributes to the shear capacity, which is determined by the web concrete alone.

Solutions (4.2.15) and (4.2.16) coincide with the solutions derived by Nielsen et al assuming a different failure mechanism, which consists of a straight yield line running from the load to the support and with a relative displacement inclined at an angle to the yield line, [78.2]. We note that the lowest upper bound is identical with the highest lower bound. This means that we have determined the correct value of ultimate shear strength corresponding to our assumptions.

It should be noticed, as only the shear problem is concerned in our analysis here, that the ultimate shear capacity is independent from the location of the horizontal reinforcement. But, the distance y in Fig. 4.25 and Fig. 4.26, which is measured from the bottom of the cross section to the centroid of horizontal reinforcement, does strongly influence the bending carrying capacity of the beam, because the increasing of y leads to decrease of the effective depth d of the beams and then to decrease of the ultimate bending capacity.

Compare equations (4.2.7) and (4.2.8), or (4.2.15) and (4.2.16), with solution (3.1.1), which is the moment capacity formula, $y_{o'}$ may find the critical position of the horizontal reinforcement $y_{o'}$. For $y < y_{o'}$ the shear will govern the carrying capacity of the beam, while for $y > y_{o'}$ the beam will fail in flexure. Same influence can be found for the length of supporting platen ℓ in Fig. 4.25 and Fig. 4.26. In [81.2] and [81.3], some solutions had been derived by J.F. Jensen and B.C. Jensen for the combinations of bending, shear and bearing carrying capacity of the beam. Those solutions are the functions of many parameters, such as the clear shear span a , the length of supporting platen ℓ , the beam depth h , the distance y and the reinforcement degree ϕ^* , and are somewhat complicated.

It has been found that Jensen's solution are fully identical with the combining equations (3.1.1) and (4.2.7), (4.2.8). But the way of the latter, i.e. to calculate the bending and shear carrying capacity separately, is more easy, convenient and preferable from a practical point of view.

4.2.3 Modified simple formula

The comparison of the simple solutions with the complete solutions can be seen in Fig. 4.14. It appears that the simple solutions have some obvious disadvantages. In the first place, it declares that the shear capacity will continuously decrease along with the increase of the shear span to depth ratio. According to the simple formula in the case of an overreinforced beam, the shear capacity of beams with shear span ratio equal to 5 will only be half that of beams with shear span ratio equal to 2.5. It does not agree with the tests. In order to fill up the shortage of the simple formula, the corresponding empirical ν formula [79.4] consists of a parabolic contribution with the purpose of increasing the ν value in the case of big shear span ratios. The ν value is very often bigger than unit in such cases.

Secondly, it gives zero shear capacity for beams without any reinforcement and underestimate the shear carrying capacity of beams with low reinforcement degrees, especially when the shear span ratio is rather small. In conventional beams it perhaps makes no problem at all since the requirement of reinforcement is governed by the bending design. But for specimens with very small shear span ratio, such as deep beams, corbels and joints, it may result in too conservative results.

Furthermore, for the reason given above, it is not possible to extend the simple solutions into fibre concrete beams and to shear in corbels with tensile normal force, in which an example can be found in section 4.3.

By utilizing the properties of the complete solutions, we may modify the simple solutions to eliminate the first mentioned shortage of the simple solutions. The simplest way is giving a limit of 2.5 to the shear span ratio when using the simple solutions, i.e. when the shear span ratio is larger than 2.5 it is put equal to 2.5. It means that the modified simple solutions now are

$$\frac{T}{f_c} = \begin{cases} \frac{1}{2} \left[\left(\frac{a}{h} \right)^2 + 4\phi^* (1 - \phi^*) - \frac{a}{h} \right] & \text{for } \phi^* \leq \frac{1}{2} \\ \frac{1}{2} \left[\left(\frac{a}{h} \right)^2 + 1 - \frac{a}{h} \right] & \text{for } \phi^* > \frac{1}{2} \end{cases} \quad (4.2.17)$$

The ν formula corresponding to the modified simple solutions (4.2.17) has been found by the parametric analysis of 412 conventional beams from 21 references in the literature (see Appendix B). The result is

$$\nu = \frac{0.60(2 - 0.4 \frac{a}{h})(\phi^* + 2)(1 - 0.25h)}{\sqrt{f_c}} \leq 1.0 \quad \left[\begin{array}{l} \frac{a}{h} \dagger 2.5 \\ \phi \dagger 2.0 \\ h \dagger 1.0 \end{array} \right] \quad (4.2.18)$$

As in equation (4.1.123), f_c is in MPa, ϕ in percent and h in meter.

The statistical data of the ratios of tests to modified simple theory are presented in Fig. 4.27. If we compare them to the values shown in Fig. 4.22, the equations (4.2.17) and (4.2.18) are seen to be satisfactory for beams. For deep beams and corbels, the complete solutions are somewhat better. Comparisons of the modified simple formulae with test results can also be seen in Fig. 4.28.

Item	Observed shear failure				Theoretical shear failure			
	number	mean	standard deviation	coeff. of variation	number	mean	standard deviation	coeff. of variation
Statistical values	n	\bar{x}	σ	C_v	n	\bar{x}	σ	C_v
Cases								
beams	412	1.028	0.155	0.151	380	1.038	0.155	0.149
deep beams	127	1.103	0.192	0.174	118	1.094	0.151	0.138
corbels	118	1.086	0.186	0.171	116	1.088	0.187	0.172
total	657	1.053	0.172	0.163	614	1.058	0.163	0.154

Fig. 4.27. The statistics of the ratios of tests to the modified simple theory.

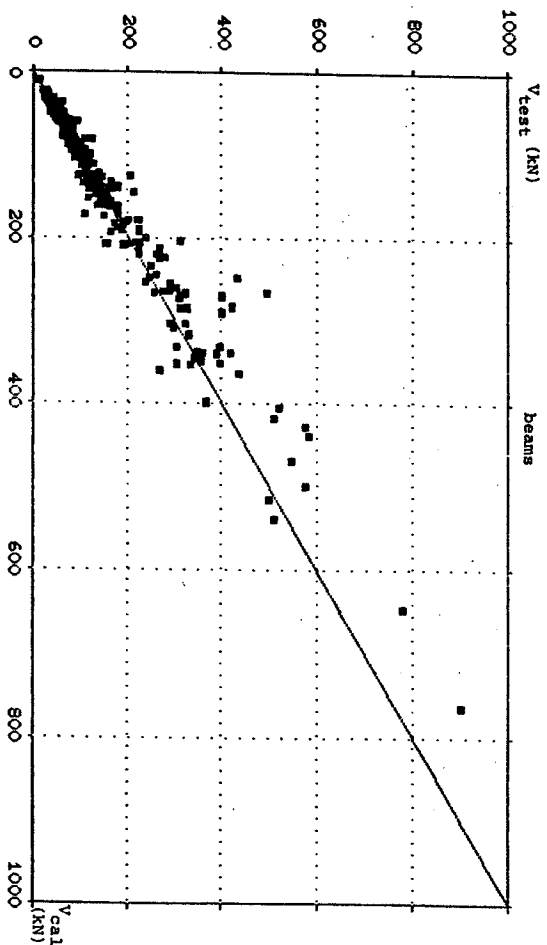


Fig. 4.28. Comparison of beam tests with modified simple theory.

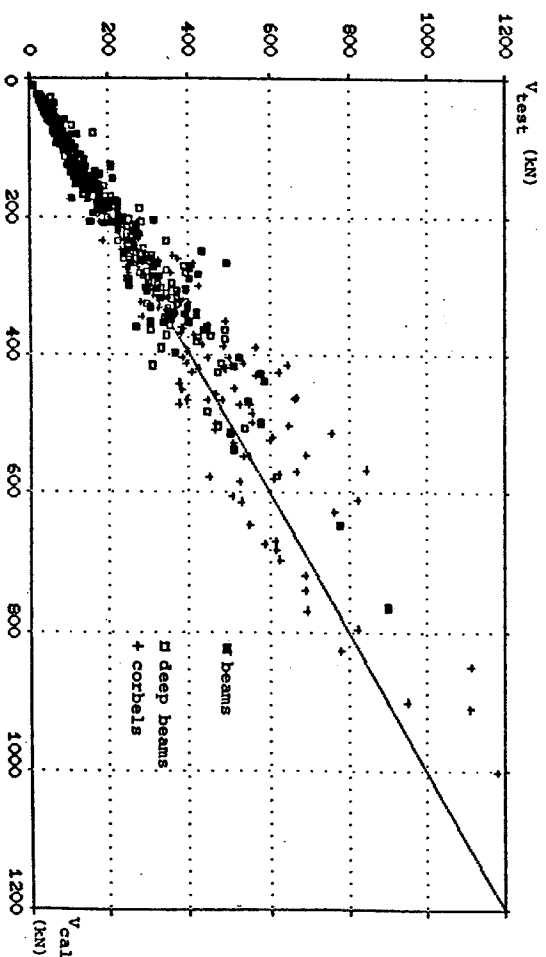


Fig. 4.28. The comparison of beam, deep beam and corbel tests with modified simple theory (continued).

4.3 The influence of normal force on the shear capacity

In this section the problem how normal forces influence the shear capacity of reinforced concrete beams is treated. The best upper bound solution considering the tensile strength of concrete for rectangular beams is presented in what follows. The theory then is compared with the tests of corbels with tensile normal force and beams with compressive normal force. A rather good agreement has been found.

4.3.1 Theoretical solutions

Fig. 4.29 shows a shear span of a rectangular beam, subjected to the concentrated load P and the normal force N.

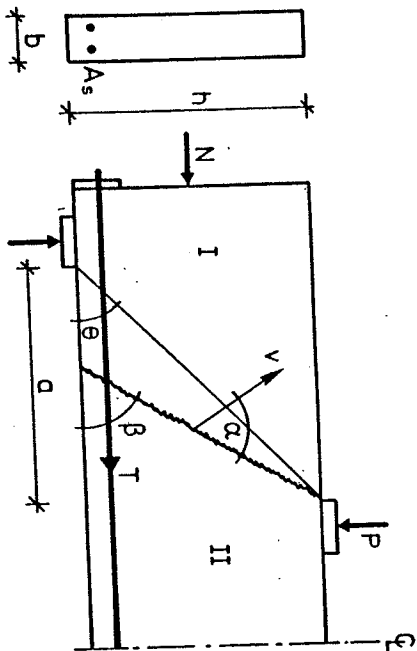


Fig. 4.29. Failure mechanism for a shear span with normal force.

The yield line pattern is the same as in 4.1.2.

The range of the variables alpha and beta in this case is

$$\alpha + \beta \leq \pi \tag{4.3.1}$$

and

$$\theta \leq \beta \tag{4.3.2}$$

The rate of external work is

$$W_E = P v \sin(\alpha + \beta) + N v \cos(\alpha + \beta) \tag{4.3.3}$$

Here, N is the normal force, positive as a compressive force.

The rate of internal work dissipated by this failure mechanism is

$$W_I = \frac{V}{2} (\lambda - \mu \sin \alpha) \frac{b h f_c^*}{\sin \beta} + T v |\cos(\alpha + \beta)| \quad \text{for } \psi \leq \alpha \leq \pi - \psi \tag{4.3.4}$$

$$W_I = \frac{V}{2} (1 - \sin \alpha) \frac{b h f_c^*}{\sin \beta} + T v |\cos(\alpha + \beta)| \quad \text{for } \alpha \leq \psi \text{ or } \alpha \geq \pi - \psi \tag{4.3.5}$$

The work equation $W_I = W_E$ yields the upper bound

$$\frac{T}{f_c^*} = \frac{\lambda - \mu \sin(\alpha + \beta) \cos \beta + (\lambda - 2\chi) \sin \beta \cos(\beta + \alpha)}{2 \sin \beta \sin(\alpha + \beta)} \quad \text{for } \psi \leq \alpha \leq \pi - \psi \tag{4.3.6}$$

$$\frac{T}{f_c^*} = \frac{1 - \sin(\alpha + \beta) \cos \beta + (1 - 2\chi) \sin \beta \cos(\beta + \alpha)}{2 \sin \beta \sin(\alpha + \beta)} \quad \text{for } \alpha \leq \psi \text{ or } \alpha \geq \pi - \psi \tag{4.3.7}$$

Here the parameter chi and the normal force degree $n^* = \frac{N}{b h f_c^*}$ has been introduced. The parameter x is defined by

$$x = \begin{cases} \frac{T}{b h f_c^*} + \frac{N}{b h f_c^*} = \phi^* + n^* & \text{for } (\alpha + \beta) \geq \frac{\pi}{2} \\ \frac{T}{b h f_c^*} - \frac{N}{b h f_c^*} = n^* - \phi^* & \text{for } (\alpha + \beta) \leq \frac{\pi}{2} \end{cases} \tag{4.3.8}$$

$$\tag{4.3.9}$$

In the case of $\beta > 0$ and $\alpha > \varphi$, we may find the lowest upper bound by minimizing equation (4.3.6) with respect to α and β . Following the same procedure as in 4.1.2, we find the lowest upper bound

$$\frac{T}{f_C} = \frac{1}{2} \sqrt{(\lambda^2 - \mu^2)(1 - D_1^2)} \quad (4.3.10)$$

Here the parameter D_1 is defined as

$$D_1 = \begin{cases} \frac{\mu - 2(n^* + \phi^*)}{\lambda} & \text{for } n^* + \phi^* < \frac{\mu}{2} \\ 0 & \text{for } n^* + \phi^* \geq \frac{\mu}{2} \\ \frac{\mu - 2(n^* - \phi^*)}{\lambda} & \text{for } \frac{\mu}{2} < n^* - \phi^* \end{cases} \quad (4.3.11)$$

The range of validity of equation (4.3.10) has been found to be

$$\frac{a}{h} > \sqrt{\frac{1 - D_1^2}{\eta^2 - 1}} \quad (4.3.12)$$

$$n^* + \phi^* > -\rho^* \quad (\text{it means } D_1 \leq 1.0) \quad (4.3.13)$$

and

$$\lambda + \mu + D_1 > 1.0 \quad (4.3.14)$$

For the case of $\beta = 0$ and $\alpha > \varphi$, the lowest upper bound may be obtained by differentiation of equation (4.3.6) with respect to α and making β equal to 0. It yields

$$\frac{T}{f_C} = \frac{1}{2} \left[\lambda \left(\frac{a}{h} \right)^2 + 1 - D_1^2 - \mu \frac{a}{h} \right] \quad (4.3.15)$$

which is valid for

$$\frac{a}{h} \leq \sqrt{\frac{1 - D_1^2}{\eta^2 - 1}} \quad (4.3.16)$$

$$n^* + \phi^* > -\rho^* \quad (4.3.17)$$

and

$$\frac{a}{h} \tan \varphi > \frac{D_1}{\cos \varphi} \quad (4.3.18)$$

Using the condition $\beta = 0$ and $\alpha = \varphi$, the lowest upper bound is easily found by inserting $\beta = 0$ and $\alpha = \varphi$ into equation (4.3.7). It appears that

$$\frac{T}{f_C} = \frac{[(\frac{a}{h})^2 + 1](1 - \sin \varphi) - 2x(\frac{a}{h} \cos \varphi - \sin \varphi)}{2(\frac{a}{h} \sin \varphi + \cos \varphi)} \quad (4.3.19)$$

In this case x becomes

$$x = \begin{cases} n^* + \phi^* & \text{for } \frac{a}{h} \leq \tan \varphi \\ n^* - \phi^* & \text{for } \frac{a}{h} > \tan \varphi \end{cases} \quad (4.3.20)$$

$$\text{for } \frac{a}{h} > \tan \varphi \quad (4.3.21)$$

The necessary condition for equation (4.3.19) to be applicable is

$$\tan \varphi - \frac{C_1}{\cos \varphi} < \frac{a}{h} \leq \tan \varphi - \frac{D_1}{\cos \varphi} \quad (4.3.22)$$

and the conditions (4.3.13) and (4.3.14). Here the parameter C_1 has been introduced as

$$C_1 = \begin{cases} 1 - 2(n^* + \phi^*); & n^* + \phi^* < \frac{1}{2} \\ 0 & ; \\ 1 - 2(n^* - \phi^*); & n^* + \phi^* \geq \frac{1}{2} \end{cases} \quad (4.3.23)$$

When we are in the case of $\beta=0$ and $\alpha < \varphi$, the lowest upper bound can be found by minimizing equation (4.3.7) with respect to α and keeping $\beta=0$. Following the same step as in 4.1.2, we get

$$\frac{T}{f_c} = \frac{1}{2} \left[\sqrt{\left(\frac{\alpha}{h}\right)^2 + 1 - C_1^2} - \frac{\alpha}{h} \right] \quad (4.3.24)$$

which is identical to the expressions derived by Rolikjar [78.3] using the so-called square yield locus as yield condition.

The condition for solution (4.3.24) to be valid is:

$$\frac{\alpha}{h} \leq \tan \varphi - \frac{C_1}{\cos \varphi} \quad (4.3.25)$$

and

$$n^{+\phi^*} > -\rho^* \quad (4.3.26)$$

$$n^{-\phi^*} \leq 1.0 \quad (4.3.27)$$

In the situation when $\lambda + \mu + D_1 \leq 1.0$, the lowest upper bound can only be obtained with $\alpha \leq \varphi$. We may find the lowest upper bound by differentiation of equation (4.3.7) with respect to β and keeping $\alpha = \varphi$. It has been found that

$$\frac{T}{f_c} = 2 \frac{\sqrt{K-1} + (K-1)\xi}{(K-1)^2} \frac{[\sqrt{K-1} + (K-1)\xi]^{-1}}{\xi} \quad (4.3.28)$$

Here the parameter ξ is defined as

$$\xi = \begin{cases} n^{+\phi^*} > \frac{K-1}{4K} & ; & n^{+\phi^*} < \frac{K-1}{4K} \\ \frac{K-1}{4K} & & n^{+\phi^*} > \frac{K-1}{4K} \\ n^{+\phi^*} > \frac{K-1}{4K} & & n^{+\phi^*} > \frac{K-1}{4K} \\ n^{-\phi^*} & & \frac{K-1}{4K} < n^{-\phi^*} \end{cases} \quad (4.3.29)$$

The condition for solution (4.3.28) to be valid is

$$\frac{\alpha}{h} > \frac{1}{\sin \varphi} \left[\sqrt{1 + (K-1)\chi} - \cos \varphi \right] \quad (4.3.30)$$

$$n^{+\phi^*} > -\rho^* \quad (4.3.31)$$

and

$$n^{-\phi^*} \leq 1.0 \quad (4.3.32)$$

If equation (4.3.30) is not satisfied, β is limited by the geometrical condition and it is necessary that it equals θ . In this situation, solution (4.3.19) is valid, but the necessary condition is changed into

$$\tan \varphi - \frac{C_1}{\cos \varphi} < \frac{\alpha}{h} < \frac{1}{\sin \varphi} \left[\sqrt{1 + (K-1)\chi} - \cos \varphi \right] \quad (4.3.33)$$

and equation (4.3.13).

In the case of $\beta=0$ and $\alpha < \varphi$, the solution (4.3.24) and the range of validity of equations (4.3.25), (4.3.26) and (4.3.27) are still valid.

The regions for the different failure mechanisms for small ρ^* -values in the upper bound analysis and the corresponding plastic solutions are depicted in Fig. 4.30 and Fig. 4.31 in a $(n^*, \frac{\alpha}{h})$ coordinate system. The boundaries are plotted for $\rho^* = 0.06$ and $\phi^* = 0.15$.

The conditions for big ρ^* -values and the corresponding plastic solutions are depicted in Fig. 4.32 and Fig. 4.33. The boundaries are plotted for $\rho^* = 0.25$ and $\phi^* = 0.15$.

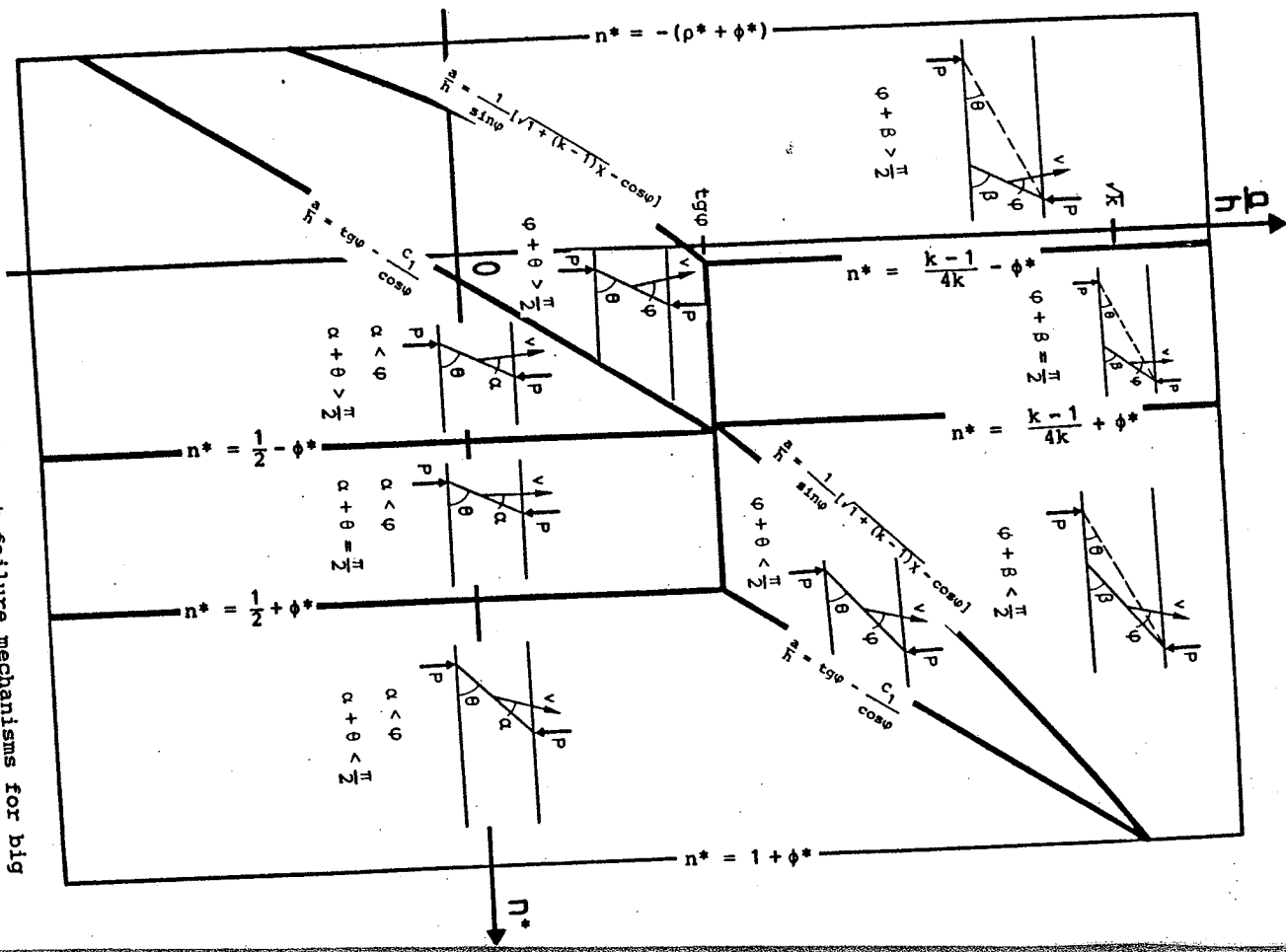


Fig. 4.32. Regions of the different failure mechanisms for big p^* -values in the case of beam shear with normal force.

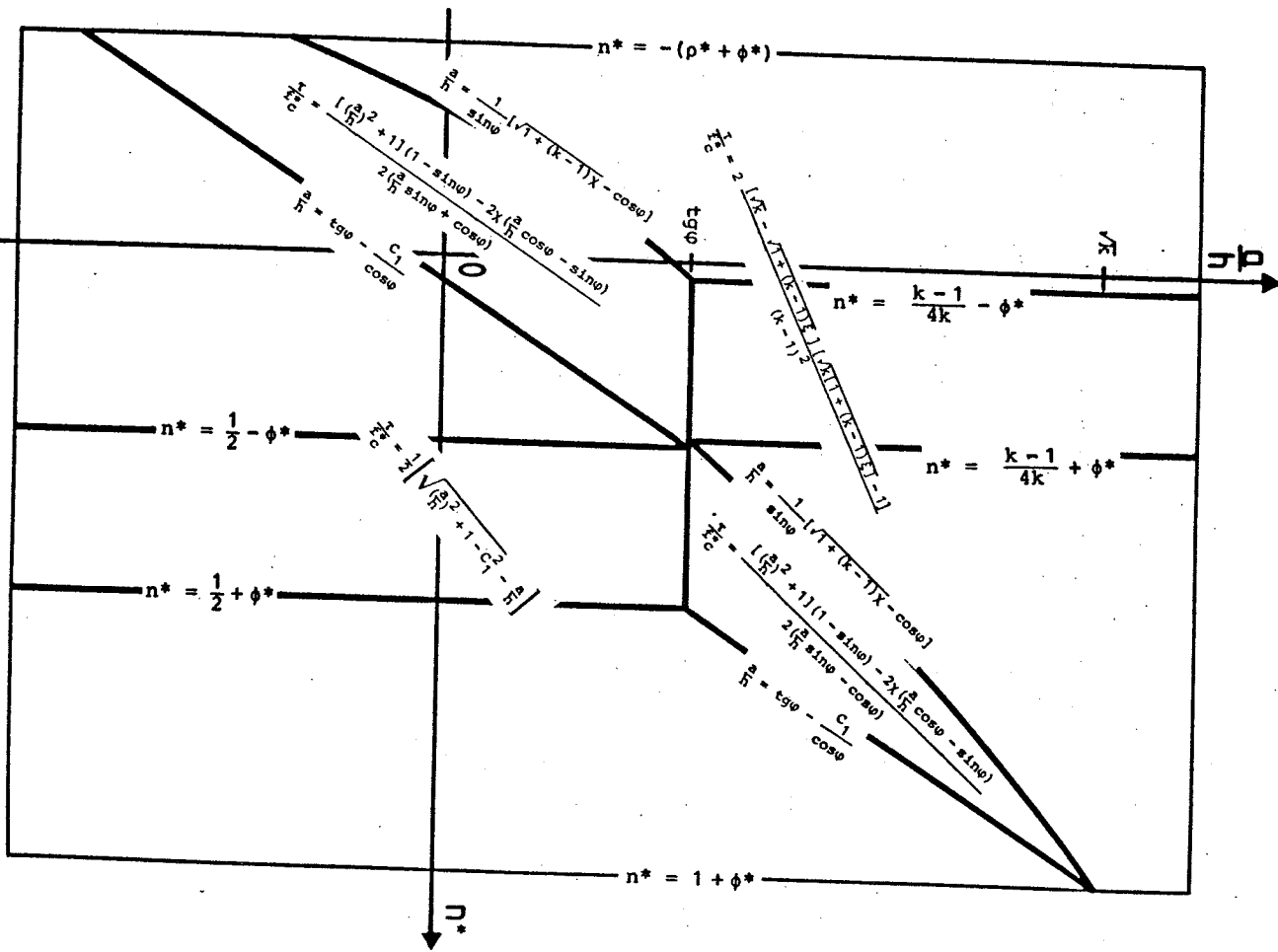


Fig. 4.33. Regions of the different plastic solutions for big p^* -values in the case of beam shear with normal force.

The solutions are shown in Fig. 4.34, Fig. 4.35 and Fig. 4.36 for some values of the parameters. For low values of the normal force, the shear capacity increases with increasing normal force, while for high values of the normal force the shear capacity decreases with increasing normal force.

In Fig. 4.36 the influence of the ρ^* -values to the shear capacity has been shown for different $\frac{a}{h}$ and ϕ^* .

The difference between the case of considering the tensile strength of concrete or neglecting it can be seen very clearly in Fig. 4.37.

In the case of beam shear with normal tensile forces, the simple solutions ($\rho^* = 0$) may underestimate the shear carrying capacity throughout all ranges of shear span ratio. In the case of big normal compressive forces, the simple solutions may overestimate the shear capacity in beams for large shear span ratios.

The flexural capacity of course might govern the load carrying capacity in some regions of the parameters. For the calculation of bending with normal force, see [84.1].

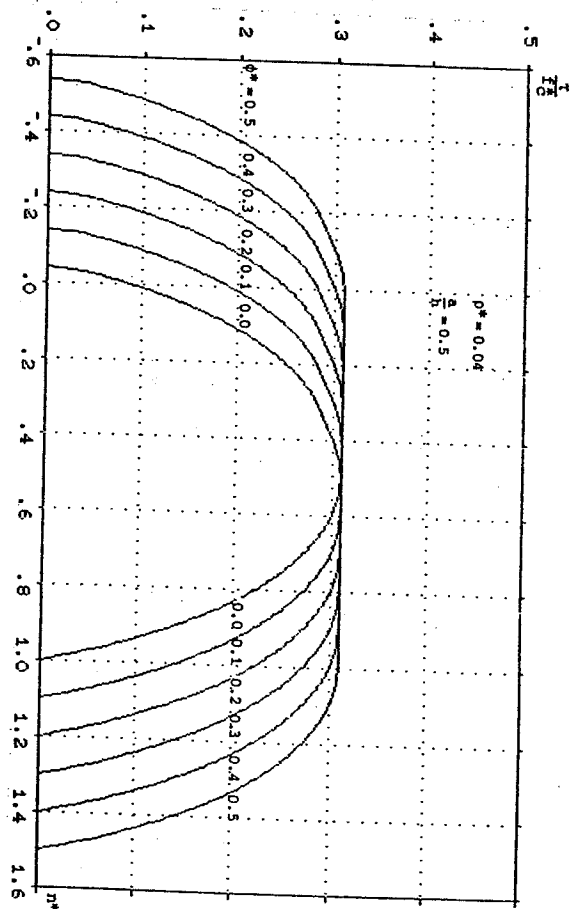


Fig. 4.34. Shear carrying capacity of beams subjected to concentrated loads and normal force versus the normal force degree for different longitudinal reinforcement degrees.

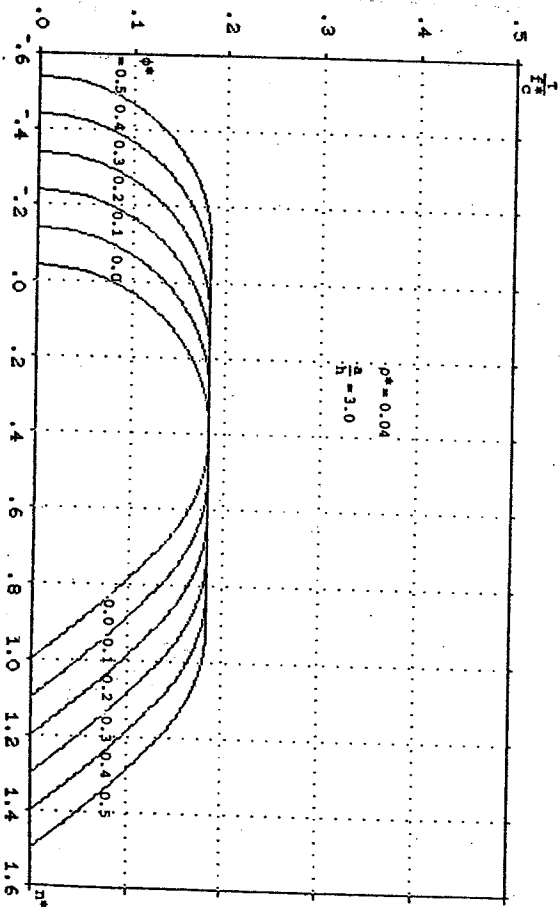


Fig. 4.34. (continued).

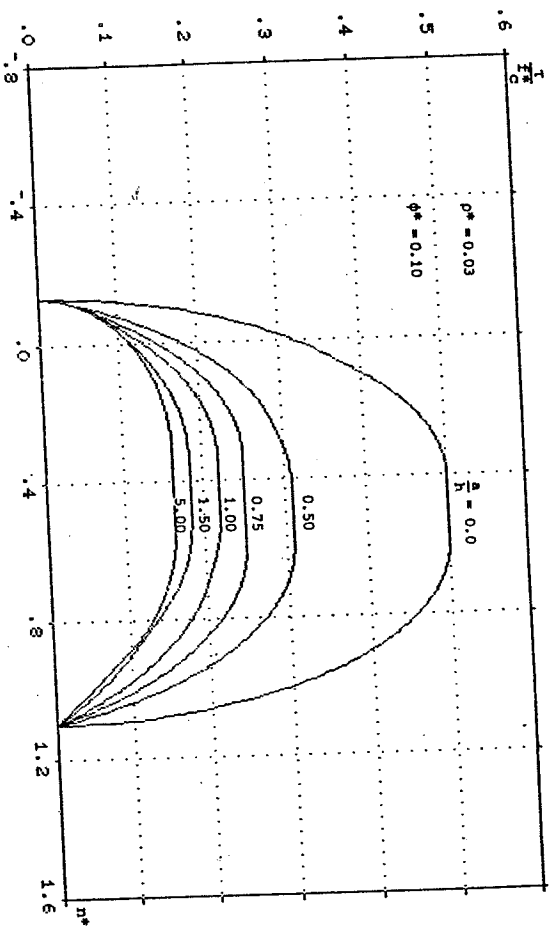


Fig. 4.35. Shear carrying capacity versus the normal force degree for different shear span ratios.

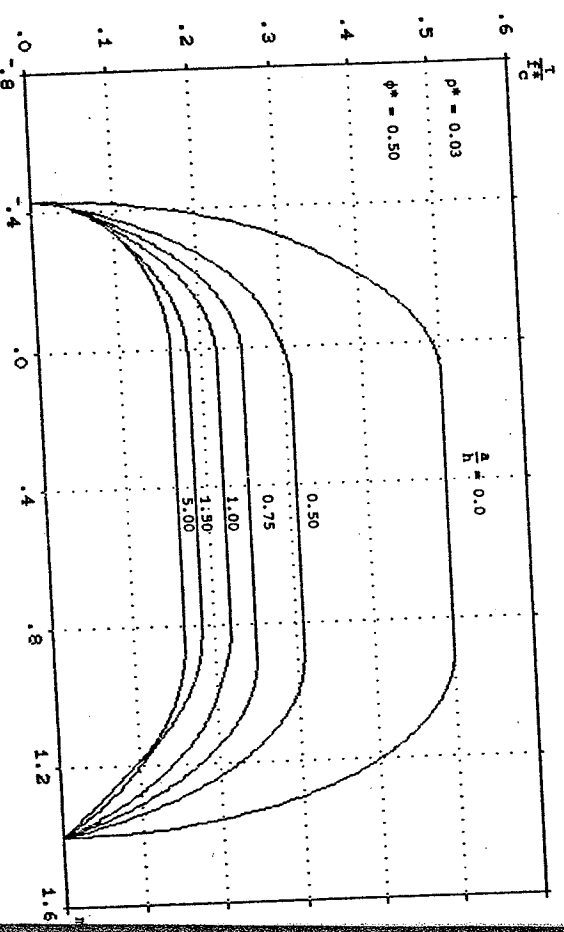


Fig. 4.35. (continued).

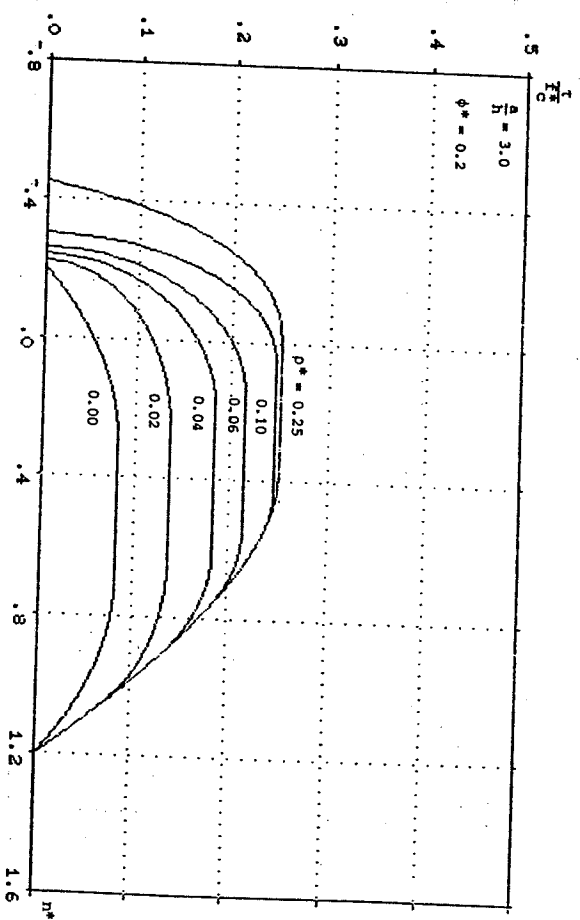


Fig. 4.36. The influence of ρ^* -values to the shear capacity of beams subjected to combined shear forces and normal forces.

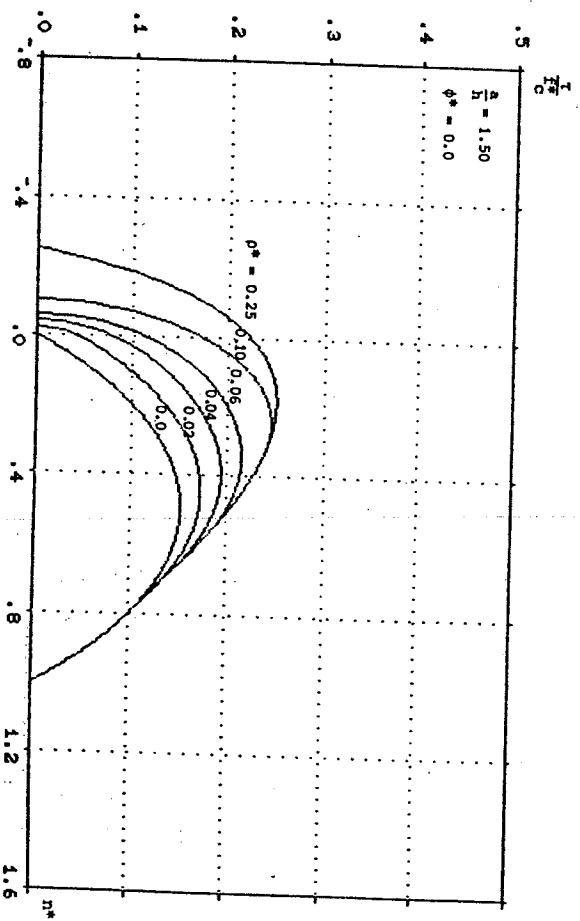


Fig. 4.36. (continued).

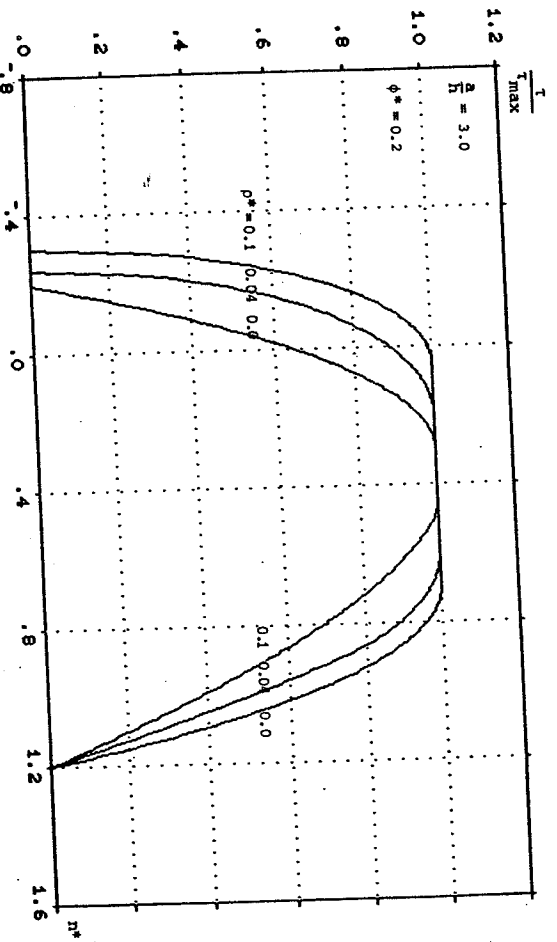


Fig. 4.37. The influence of ρ^* on shear capacity with various $\frac{h}{h_{max}}$ and ϕ^* .

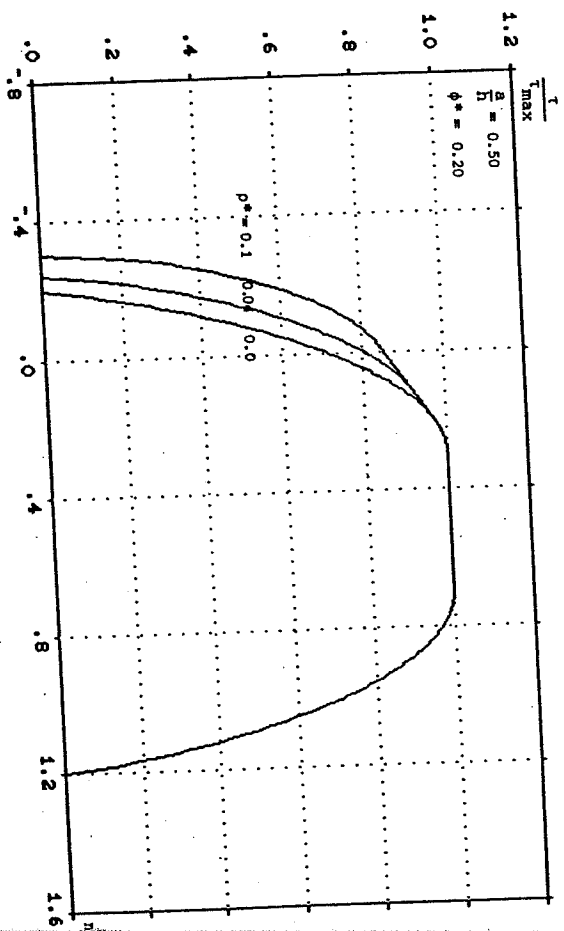


Fig. 4.37. (continued).

4.3.2 Experimental verification

To test the validity of the complete set of equations in Fig. 4.31 for shear specimens with normal force, an investigation has been made for corbels with tensile normal force and beams with compressive normal force reported in the literature, [65.1], [60.1] and [57.1].

The detailed test data are shown in Appendix C.

A parametric analysis of 24 observed shear failures of corbels with normal force has given the following best empirical ν formula with $\rho^* = 0.1$ as

$$\nu = 0.055(2.0 - 0.8 \frac{h}{h}) (\varphi + 4) (1 - 0.25 h) \leq 1.0 \quad (4.3.34)$$

Here ν should be in percent and h in meter.

The mean value \bar{x} of the ratios of test to theory is 1.000, while the standard deviation σ is 0.076 and the coefficient of variation C_v is 0.076.

The comparison of test results with theory is shown on Fig. 4.38.

The very good agreement between tests and theory can also be seen from Fig. 4.39.

The complete solutions shown in Fig. 4.31 may be a little complicated for practical use. For the shear specimens with tensile normal force, we are forced to consider the tensile strength of concrete to get the agreement with tests, especially when the tensile normal force is bigger than the force that the reinforcement can take.

However, in some cases we may simplify the calculation according to the actual situation. For example we may only use equation (4.3.15) in stead of the complete solutions to calculate the shear capacity of corbels subjected to the combined shear and normal tensile force.

Using (4.3.15) with $p^* = 0.1$ and (4.3.34) for 24 observed shear failures of corbels, the mean value \bar{x} is 1.014, while the standard deviation σ is 0.092 and the coefficient of variation C_v is 0.090. The results is still quite satisfactory and the calculation becomes more easy and simple.

For the specimens subjected to combined shear and compressive normal force, we may simplify the complete solutions by modifying equation (4.3.24) for $\frac{\bar{a}}{h} \pm 2.5$, just as we did in section 4.2.

In this case the corresponding v formula has been found by the parametric analysis of 47 stub beams with axial loads and knee frames from 2 reports in the literature, [60.1], [57.1].

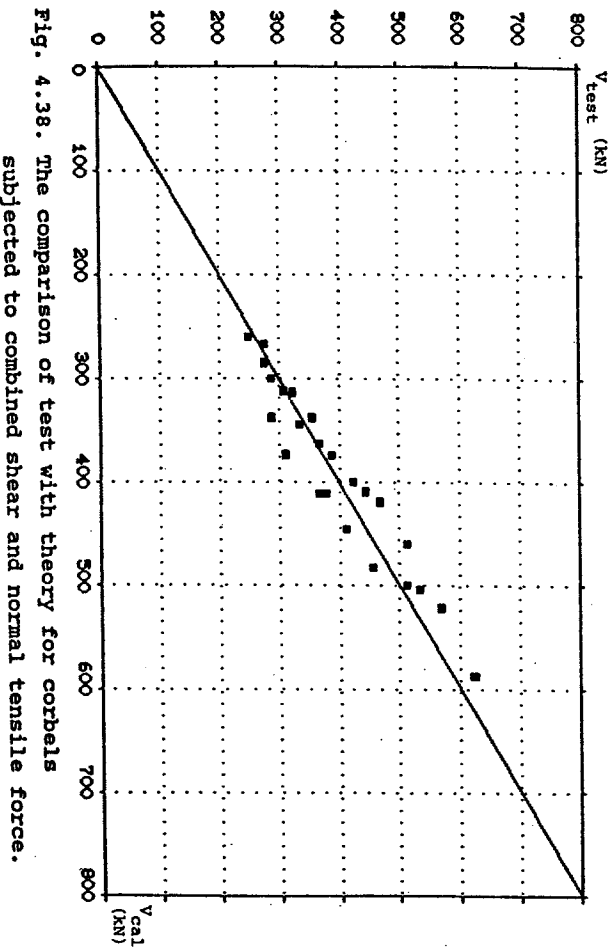


Fig. 4.38. The comparison of test with theory for corbels subjected to combined shear and normal tensile force.

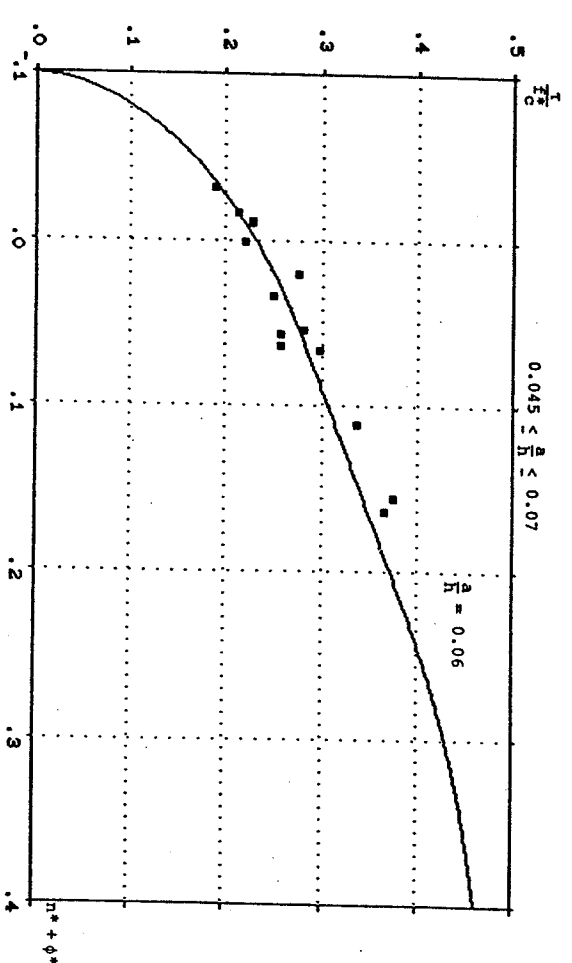


Fig. 4.39. The plastic solutions for beam shear with normal force compared with corbel test results. $0.15 < \frac{\bar{a}}{h} < 0.25$

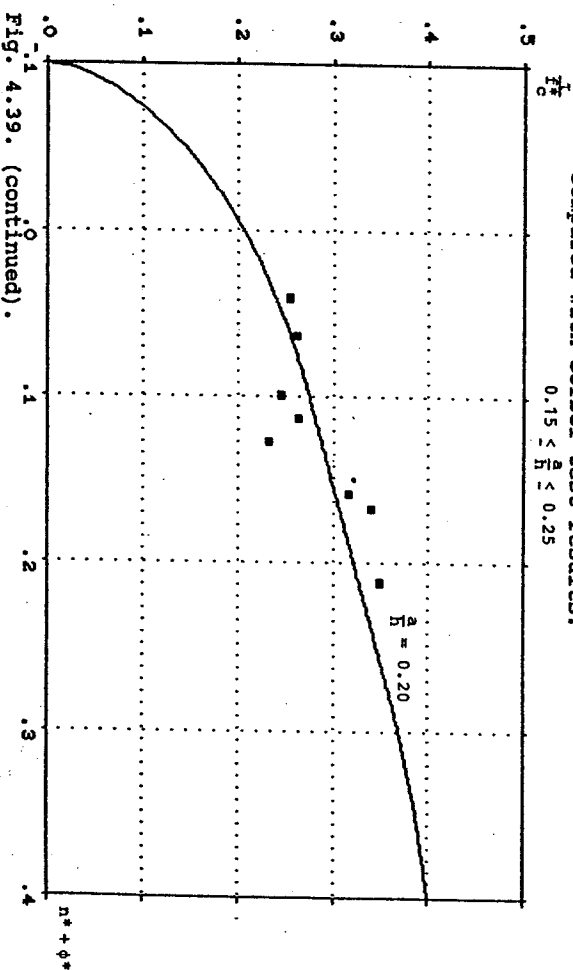


Fig. 4.39. (continued).

The result is

$$v = \frac{0.58(\phi+2)(2-0.4\frac{h}{h})(1-0.25h)(1+0.75\frac{N}{A_s F_y})}{\sqrt{F_c}} \leq 1.0 \quad (4.3.35)$$

$$[\frac{h}{h} \dagger 2.5, \phi \dagger 2.0 \text{ and } h \dagger 1.0]$$

As before f_c is in MPa, ϕ in percent and h in meter.

The mean value \bar{x} of the ratios of 47 observed shear tests to theory is 0.997, while the standard deviation σ is 0.094 and the coefficient of variation C_v is 0.095.

The comparison of test results with theory is shown on Fig. 4.40.

To demonstrate the general applicability of the theory, Fig. 4.41 shows the results of shear tests of stub beams with axial loads and knee frames for different shear span ratios. The v value has been calculated from (4.3.35).

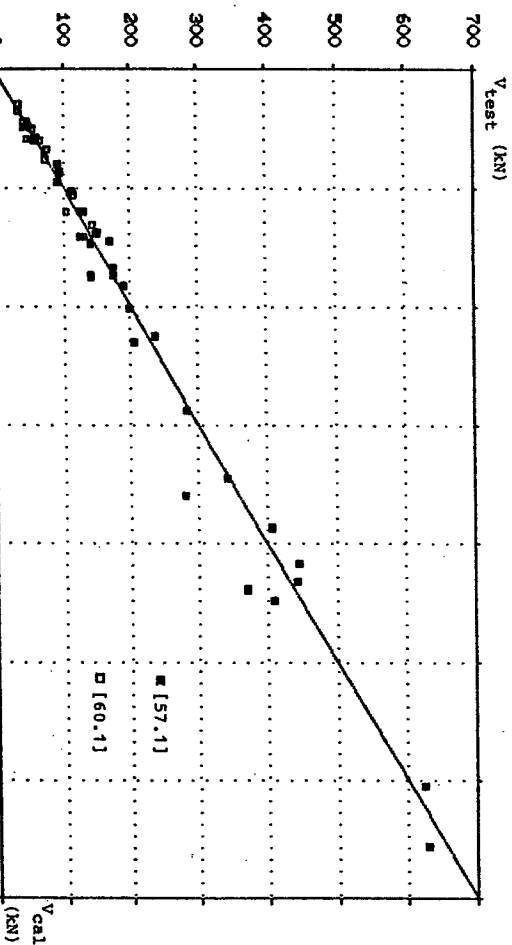


Fig. 4.40. The comparison of tests with theory of stub beams with axial loads and knee frames.

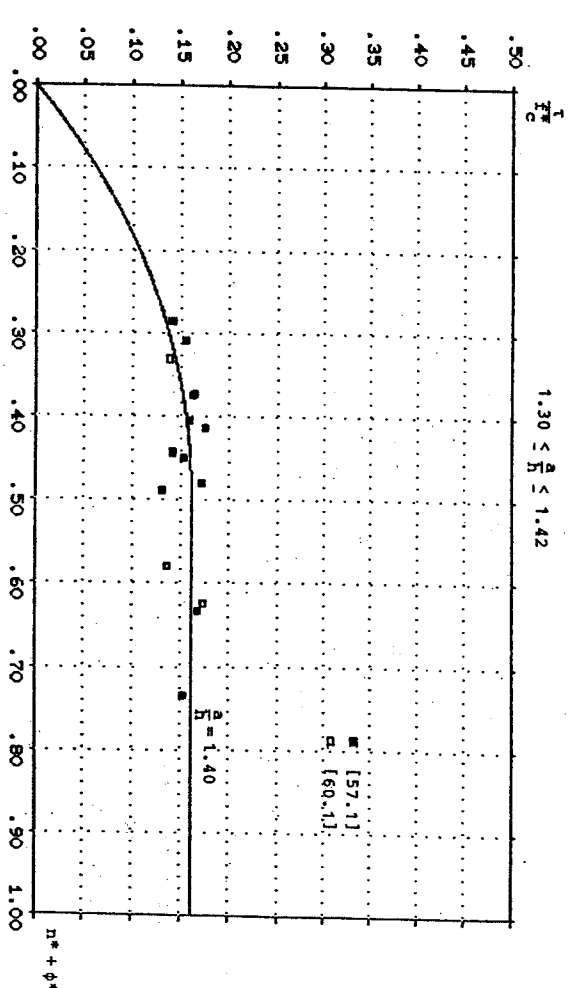


Fig. 4.41. Theoretical shear capacity compared with test results of stub beams with axial loads and knee frames.

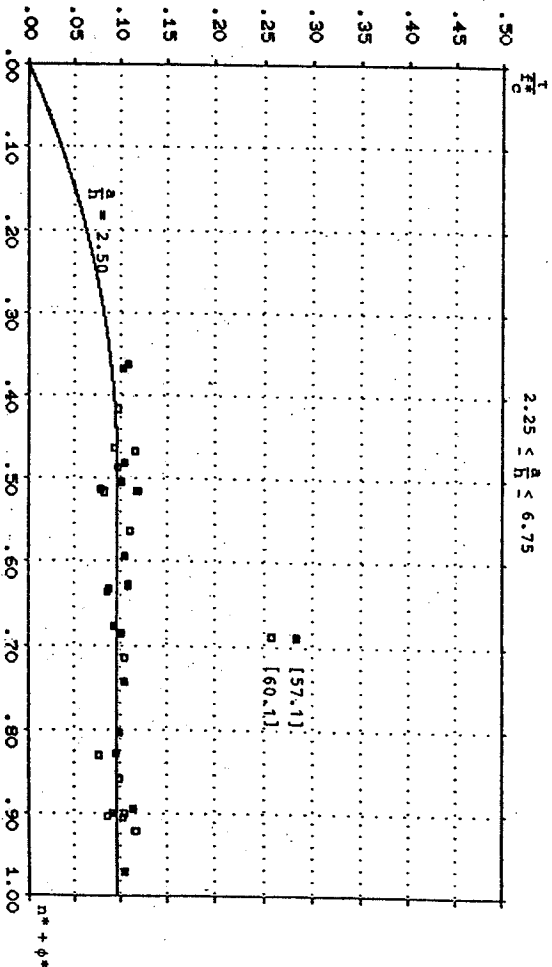


Fig. 4.41. (continued).

4.4. The influence of prestress to shear capacity of beams

The problem how prestress influences the shear capacity of concrete beams without web reinforcement has only been very preliminarily studied. According to plastic theory, prestress does not influence the theoretical shear solution in any way. The reason is that the prestress introduces an internal, self-equilibrated stress system, which does not affect either the failure mechanism, nor the stress distribution at collapse.

However, the existence of an initial, non-zero stress state does influence the amount of stress redistribution which must take place before failure, and this has an effect on the ultimate load.

In the following, we will use the complete plastic solutions in Fig. 4.10 and we will try to modify the ν expression for prestressed beams.

The effect of prestress seems to be that it increases the effectiveness factor with increasing level of effective prestress.

An investigation how the prestress influences the effectiveness factor ν has been made for 286 prestressed beams without web reinforcement reported in the literature [58.2], [59.2], [60.3], [60.9], [63.3], [65.5] and [69.4].

The detailed test data are shown in Appendix D.

A treatment similar to that reported in 4.1.4 has shown that the effective prestress in the section increases the ν value and that prestressed beams do not exhibit an a/h dependence to a degree that has been found for non-prestressed beams. In fact for a carefully chosen ρ^* -value, we may consider the influence of the shear span to the ν value for prestressed beams to be non-existent. A proper ρ^* value is found to be 0.003 - 0.005 for prestressed rectangular beams reported in [59.2].

Fig. 4.42 shows an example of the dependence of ν on $F_{se}/A_c f_c$, which is the average effective prestress ratio in the section of the beams. Here A_c is the area of the section and F_{se} is the effective prestress acting on the section. Similar to the ν - ψ relation shown in Fig. 4.42, the ν value is increasing almost linearly with increasing the average effective prestress ratio $F_{se}/A_c f_c$. Beyond a certain limit of $F_{se}/A_c f_c$ the ν value seems to be independent of $F_{se}/A_c f_c$. This limit may be chosen as 0.15 for simplicity.

A parametric analysis of 54 observed shear failures of prestressed beams with rectangular section [59.2] and [69.4] has given the following empirical ν formula assuming $\rho^* = 0.003$

$$\nu = \frac{0.575(\psi+1.5)(1-0.2h)}{\sqrt{F_c}} \left[\frac{F_{se}}{A_c f_c} \right] \left[\begin{array}{l} \psi \neq 2.0 \\ h \neq 1.0 \\ \frac{F_{se}}{A_c f_c} \neq 0.15 \end{array} \right] \quad (4.4.1)$$

Here ψ should be in percent, f_c in MPa and h in meter.

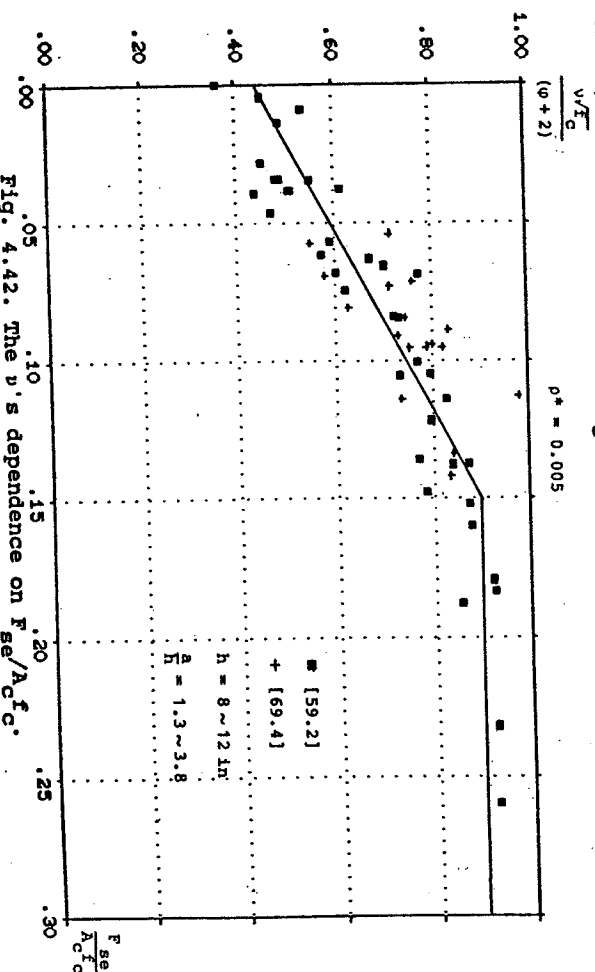


Fig. 4.42. The ν 's dependence on $F_{se}/A_c f_c$.

The mean value \bar{x} of the ratios of test to theory is 1.007, while the standard deviation σ is 0.089 and the coefficient of variation C_V is 0.088. The comparison of tests with theory is shown in Fig. 4.43.

The good agreement between tests and theory can also be seen from Fig. 4.44.

For practical use, we may simplify our theory by neglecting the tensile strength of concrete, i.e. let $\rho^* = 0$ and use the simple formulae (4.2.15) and (4.2.16). The corresponding ν formula then is

$$\nu = \frac{0.52(\psi+2)(1-0.25h)}{\sqrt{F_C}} \left[1 + 6 \frac{F_{Se}}{A_C F_C} \right] \quad (4.4.2)$$

ψ	\neq	2.0
h	\neq	1.0
$\frac{F_{Se}}{A_C F_C}$	\neq	0.15

Units are as before.

In this case the mean value \bar{x} of the ratios of test to theory is 1.007, while the standard deviation σ is 0.133 and the coefficient of variation C_V is 0.132. The comparison of tests to theory is shown in Fig. 4.45. The agreement between tests and theory can also be seen from Fig. 4.46.

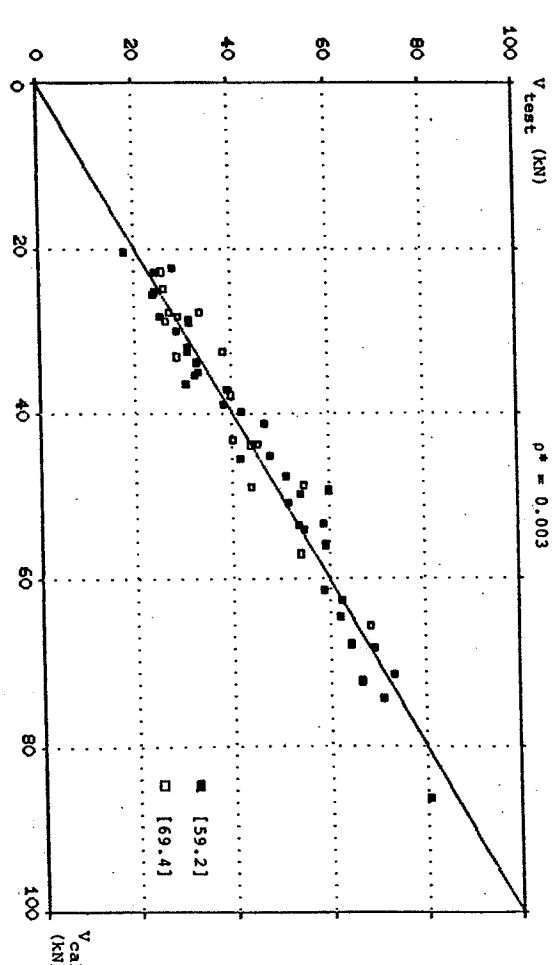


Fig. 4.43. The comparison of theory with tests of prestressed beams with rectangular section.

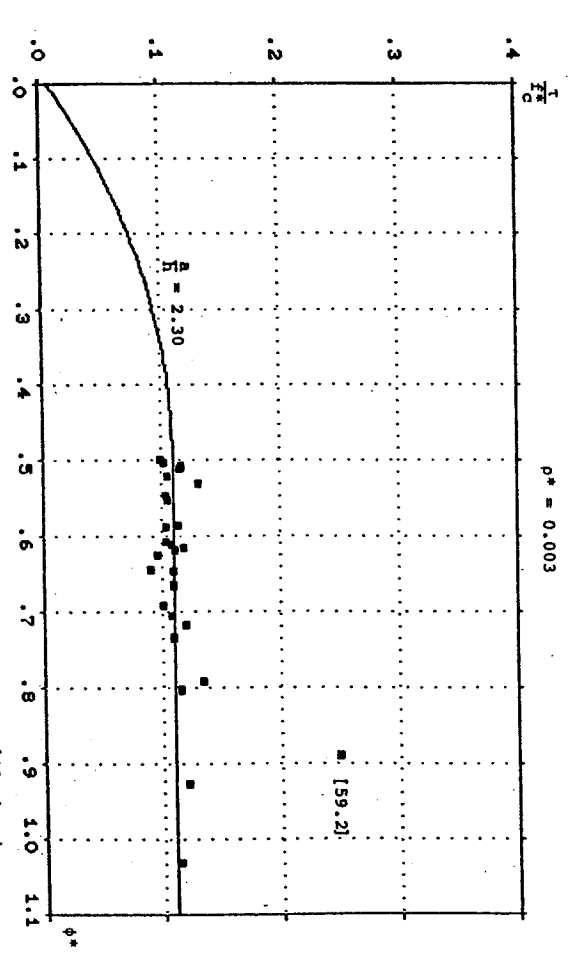


Fig. 4.44. The plastic beam shear solutions compared with test results of prestressed beam with rectangular section.

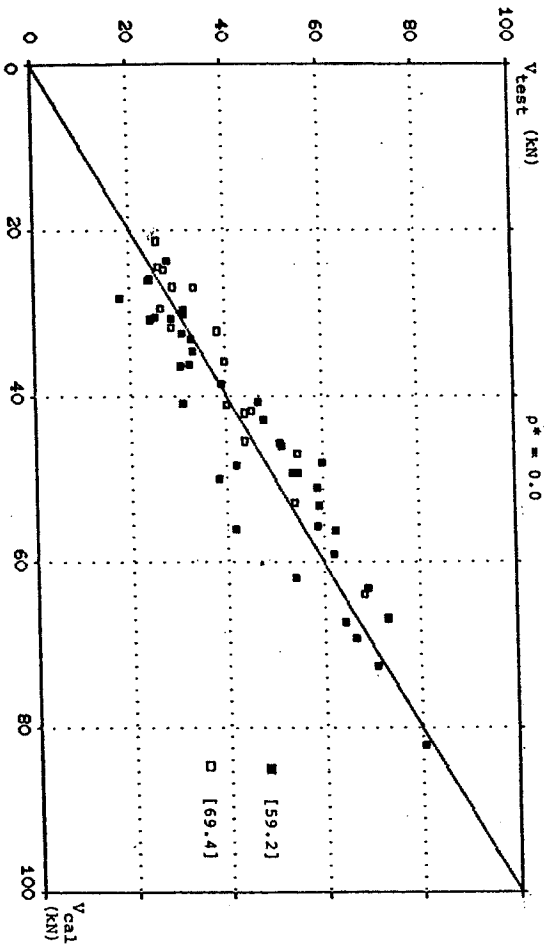


Fig. 4.45. The comparison of simplified theory with tests of prestressed beams.

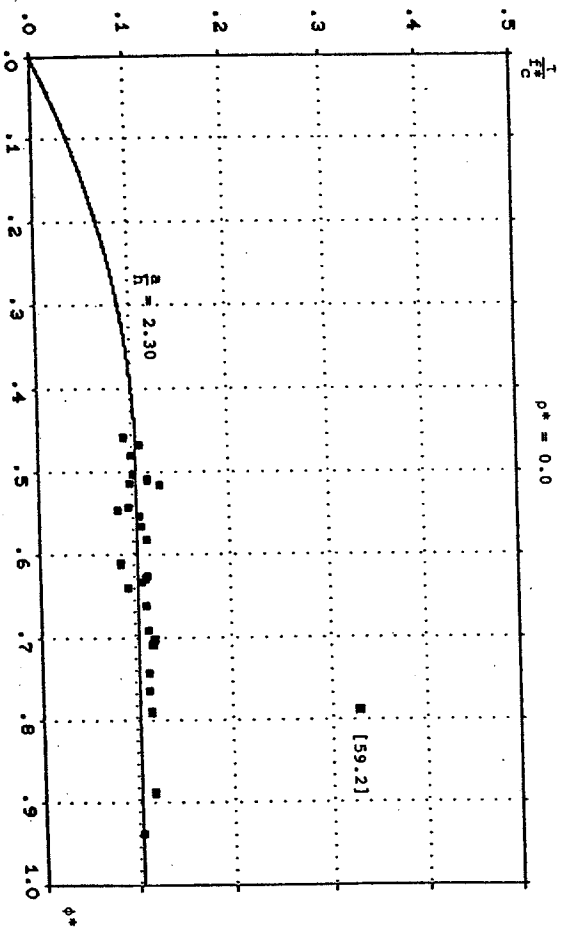


Fig. 4.46. The simplified plastic solutions compared with tests.

In practice, a lot of prestressed beams are with T cross section or I cross section. The considerable influence of tension or compression flanges on the maximum shear capacity of beams without shear reinforcement has been studied in [78.3]. The upper bound technique for such beams is somewhat complicated. An alternative method has been developed in this section. We may employ the complete plastic shear solutions shown in Fig. 4.10 for the web and take account of the influence of the flanges in the v formula.

A parametric analysis of 286 observed shear failure of prestressed beams without web reinforcement has shown a relatively simple and quite good empirical v formula assuming $\rho^* = 0.007$

$$v = \frac{0.445(\varphi+2) \left[\frac{F_{Se}}{A_C F_C} \right] \left[\frac{A_C}{bh} \right]}{\sqrt{F_C}} \left[\begin{array}{l} \varphi \uparrow 2.0 \\ \frac{F_{Se}}{A_C F_C} \uparrow 0.10 \\ \frac{A_C}{bh} \uparrow 1.8 \end{array} \right] \quad (4.4.3)$$

Units are as before.

The mean value \bar{x} of the 286 ratios of test to theory is 1.000, while the standard deviation σ and the coefficient of variation γ are 0.166. The comparison of tests with theory is shown in Fig. 4.47.

In practice, it's more convenient to use the modified simple solutions (4.2.17) to calculate the shear capacity of prestressed beams. The corresponding v formula can be taken as

$$v = \frac{0.505(\varphi+2) \left[\frac{F_{Se}}{A_C F_C} \right] \left[\frac{A_C}{bh} \right]}{\sqrt{F_C}} \left[\begin{array}{l} \varphi \uparrow 2.0 \\ \frac{A_C}{bh} \uparrow 1.8 \\ \frac{F_{Se}}{A_C F_C} \uparrow 0.12 \end{array} \right] \quad (4.4.4)$$

Using formulae (4.2.17) and (4.4.4), the mean value \bar{x} of the 286 ratios of the test to theory is 1.004, while the standard deviation is 0.188 and the coefficient of variation C_V is 0.187. The comparison of tests with theory is depicted in Fig. 4.48.

The simplified plastic solution (4.2.15) and (4.2.16) may also be used for prestressed beams. In this case we may use the corresponding ν formula as

$$\nu = \frac{0.655(\varphi \neq 1.5) \left[\frac{F_{se}}{A_C F_C} \right] \left[\frac{A_C}{bh} \right]}{\sqrt{F_C}} \quad (4.4.5)$$

$$\left[\begin{array}{l} \varphi \neq 2.0 \\ A_C \neq 1.8 \\ D_n \\ F_{se} \neq 0.12 \\ A_C F_C \end{array} \right]$$

The calculation using formulae (4.2.15), (4.2.16) and (4.4.5) has been carried out for 286 prestressed beams. The mean value \bar{x} is 1.005, while the standard deviation σ is 0.200 and the coefficient of variation C_V is 0.199. Fig. 4.49 shows the comparison of theory with tests.

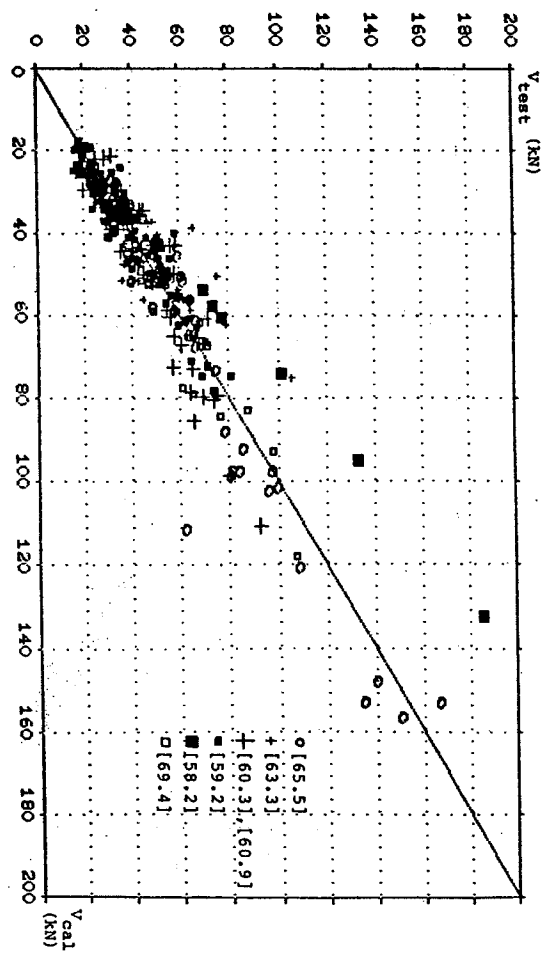


Fig. 4.47. The comparison of theory with tests of 286 prestressed beams without web reinforcement.

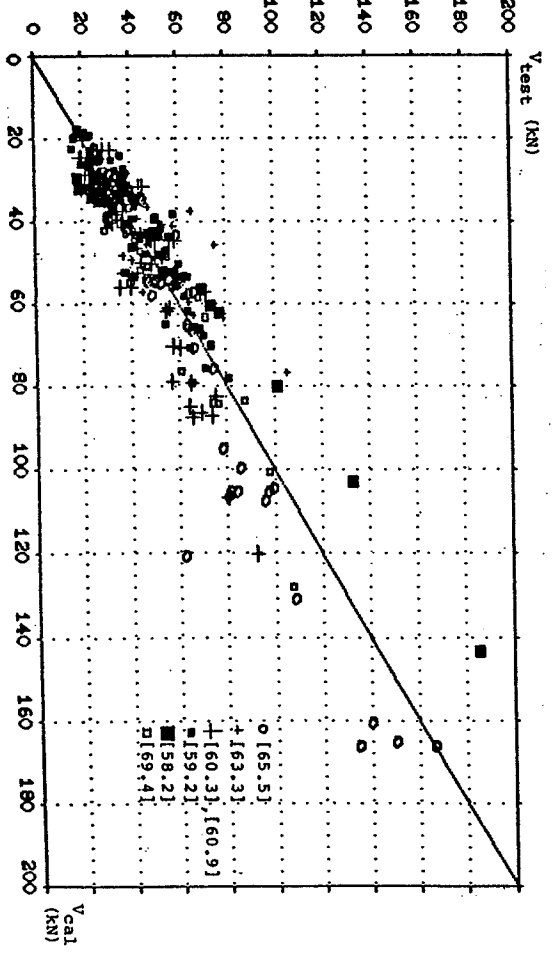


Fig. 4.48. The comparison of theory with tests of prestressed beams using the modified simple formula (4.2.17) and corresponding ν formula (4.4.4).

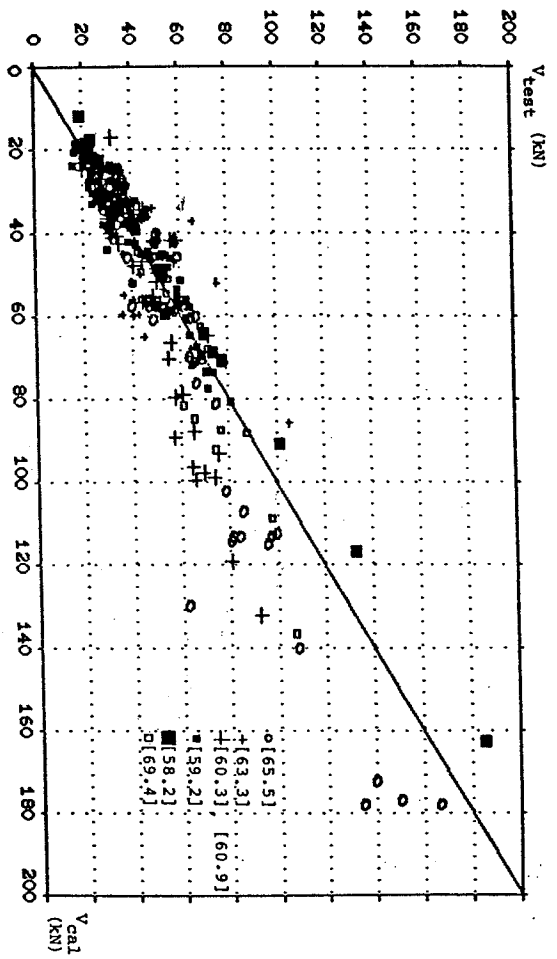


Fig. 4.49. The comparison of theory with tests of prestressed beams using the simplified formulae (4.2.15), (4.2.16) and the corresponding ν formula (4.4.5).

4.5. Shear capacity of joints

The complete plastic shear solutions listed in Fig. 4.8 can be easily extended to solve the shear problem of concrete joints, which are shown in Fig. 4.50.

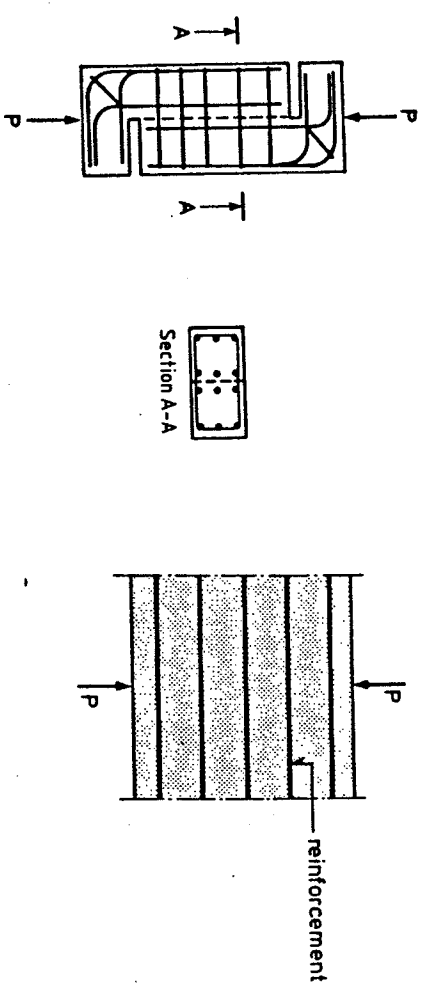


Fig. 4.50. Joints of monolithic concrete.

Inserting $\frac{a}{h} = 0$ into the relevant formulae along the line $\frac{a}{h} = 0$ in Fig. 4.10, we get the shear carrying capacity of reinforced monolithic concrete as follows:

$$\frac{T}{F_c} = \begin{cases} \frac{1}{2} \cdot \lambda \sqrt{1-D^2} & \phi^* \leq \frac{\mu \cdot \lambda \cdot \sin \nu}{2} & (4.5.1) \\ \frac{1 - \sin \nu + \phi^* \cdot \operatorname{tg} \nu}{2 \cos \phi} & \frac{\mu \cdot \lambda \cdot \sin \nu}{2} < \phi^* \leq \frac{1 - \sin \nu}{2} & (4.5.2) \\ \frac{1}{2} \sqrt{1-C^2} & \frac{1 - \sin \nu}{2} < \phi^* \leq \frac{1}{2} & (4.5.3) \\ \frac{1}{2} & \frac{1}{2} < \phi^* & (4.5.4) \end{cases}$$

Inserting equations (4.1.31), (4.1.32), (4.1.37) and (4.1.40) into equations (4.5.1) - (4.5.4), we may rewrite the shear capacity into

$$\frac{T}{F_c} = \begin{cases} \sqrt{(\rho^* + \phi^*) [(1 - 3\rho^*) - (\rho^* + \phi^*)]} & \phi^* \leq 0.2 - 1.6\rho^* & (4.5.5) \\ 0.25 + 0.75\phi^* & 0.2 - 1.6\rho^* < \phi^* \leq 0.2 & (4.5.6) \\ \sqrt{\phi^* (1 - \phi^*)} & 0.2 < \phi^* \leq 0.5 & (4.5.7) \\ 0.5 & 0.5 < \phi^* & (4.5.8) \end{cases}$$

Solutions (4.5.5) - (4.5.8) are identical with the solutions given firstly by B.C. Jensen [77.2].

The shear carrying capacity of joints versus effective reinforcement degree for some ρ^* -values is depicted in Fig. 4.51.

It is obvious that the tensile strength of concrete plays an important part in shear carrying capacity when the reinforcement degree is rather low.

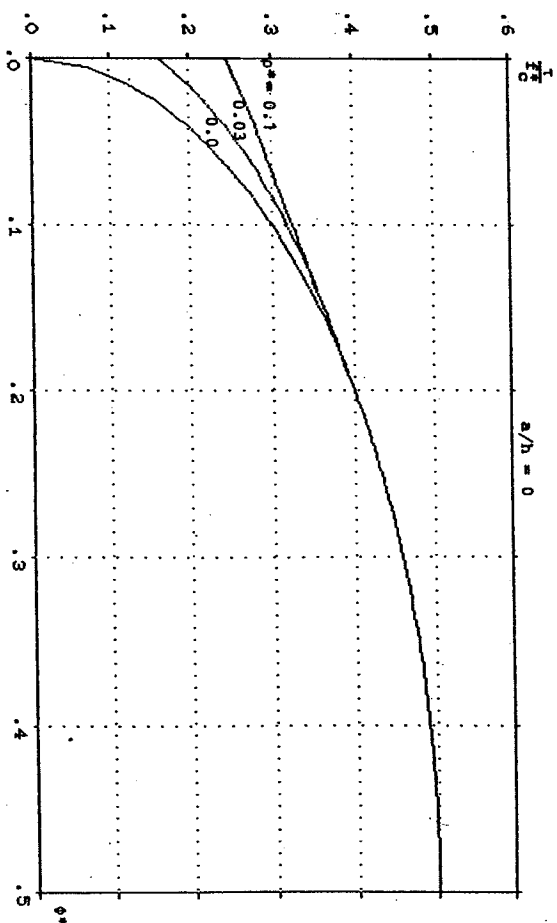


Fig. 4.51. Shear carrying capacity of joints versus effective reinforcement degree for some ρ^* -values.

The theory with $\rho^* = 0.035$ and $\nu = 0.665$ has been compared with joint tests of monolithic concrete performed by Hofbeck et al. [69.1]. The agreement between the formulae for the carrying capacity and the test results is exceptionally good.

The comparison between theory and test results is depicted in Fig. 4.5.2. To demonstrate the applicability of the complete plastic shear solutions to the monolithic concrete joints, Fig. 4.5.3 shows how better the test results fit the theoretical curves.

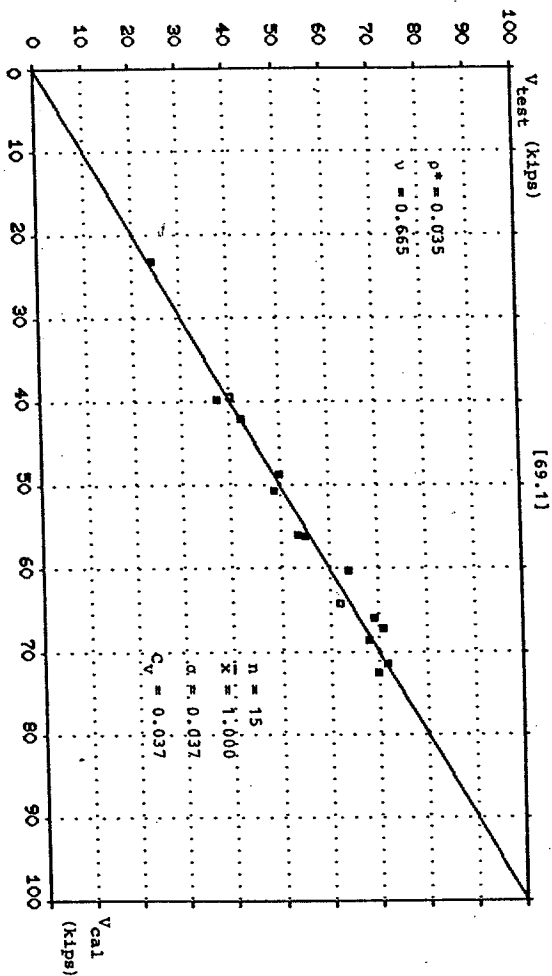


Fig. 4.52. The comparison between theoretical calculations and test results.

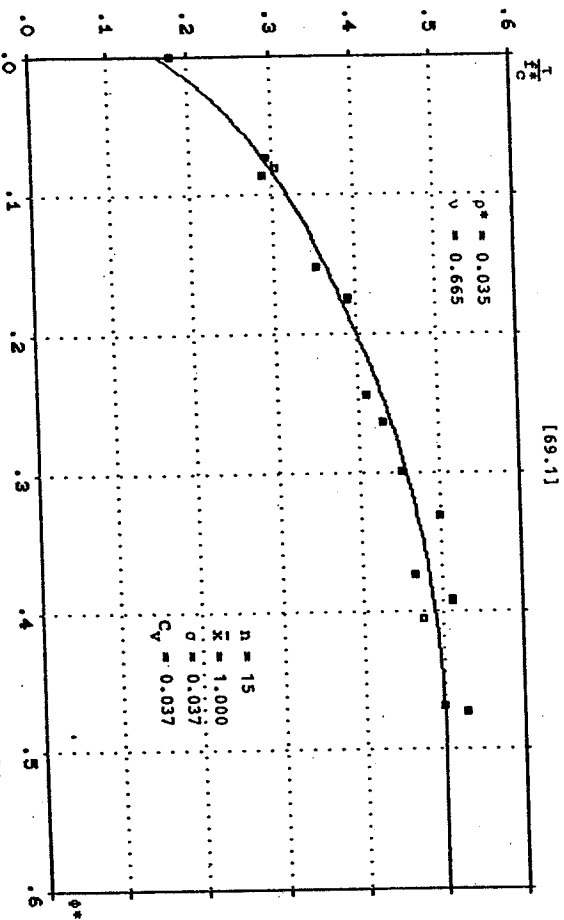


Fig. 4.53. The theoretical curve compared with test results.

CHAPTER V. SHEAR CARRYING CAPACITY OF BEAMS WITH WEB REINFORCEMENT

In this chapter we will only treat beams with vertical stirrups and subjected to point loading. Besides the assumptions that we have made in section 2.6, we further assume:

- 5) The web reinforcements is rigid, perfectly plastic. The stirrup spacing is sufficiently small to permit a continuous distribution of the stirrup forces. The cross-sectional steel area per unit length in both directions is A_{swh} and A_{swv} , respectively. The yield stress of the web reinforcement is f_{yw} .

Fig. 5.1 shows a shear span of a concrete beam subjected to the shear force V . The breadth and depth of the beam are termed b and h^* , respectively. The failure mechanism is assumed to be consisting of a single yield line inclined at angle β to the beam axis.

The relative displacement rate is v inclined at the angle α to the beam normal. For the beams with web reinforcement, it is reasonable to neglect the tensile strength of concrete.

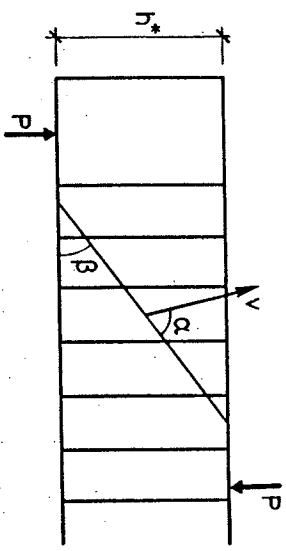


Fig. 5.1. Failure mechanism of beam with vertical stirrups subjected to point loading.

On the above assumptions, the following upper bound solutions were

derived by Nielsen and Bræstrup [76.7]. Most of these upper bounds are backed by coincident lower bound solutions, but some of them are still missing the lower bound solutions [79.1].

5.1 Theoretical solutions

The complete lowest upper bounds can be summarized as following:

$\frac{\tau/f_c^*}{\phi_v^*}$	ϕ_h^*	$\phi_h^* \leq \frac{1}{2}$	$\phi_h^* = \frac{1}{2}$
$\phi_v^* < \phi_{vo}^*$		$\frac{1}{2} \left[\sqrt{\left[\frac{a}{h^*} \right]^2 + 4\phi_h^*(1-\phi_h^*)} - \frac{a}{h^*} \right] + \phi_v^* \frac{a}{h^*}$	$\frac{1}{2} \left[\sqrt{\left[\frac{a}{h^*} \right]^2 + 1 - \frac{a}{h^*}} \right] + \phi_v^* \frac{a}{h^*}$
$\phi_{vo}^* \leq \phi_v^* \leq \frac{1}{2}$		$2 \sqrt{\phi_h^*(1-\phi_h^*)} \phi_v^*(1-\phi_v^*)$	$\sqrt{\phi_v^*(1-\phi_v^*)}$
$\phi_v^* > \frac{1}{2}$		$\sqrt{\phi_h^*(1-\phi_h^*)}$	$\frac{1}{2}$

(5.1)

Here

$$\phi_{vo}^* = \begin{cases} \frac{\left[\frac{a}{h^*} \right]^2 + 4\phi_h^*(1-\phi_h^*) - \frac{a}{h^*}}{h^*} & \text{valid for } \phi_h^* \leq \frac{1}{2} \\ 2 \left[\frac{a}{h^*} \right]^2 + 4\phi_h^*(1-\phi_h^*) & \\ \frac{2 \left[\frac{a}{h^*} \right]^2 + 1 - \frac{a}{h^*}}{2 \left[\frac{a}{h^*} \right]^2 + 1} & \text{for } \phi_h^* > \frac{1}{2} \end{cases} \quad (5.2)$$

$$\phi_h^* = \frac{A_s f_y}{b h^* f_c^*} + \frac{A_{sv} f_{yv}}{b f_c^*} \quad (5.3)$$

Solutions (5.1) is also visualized in Fig. 5.2 for deep beams with $a/h^* = 0.3$.

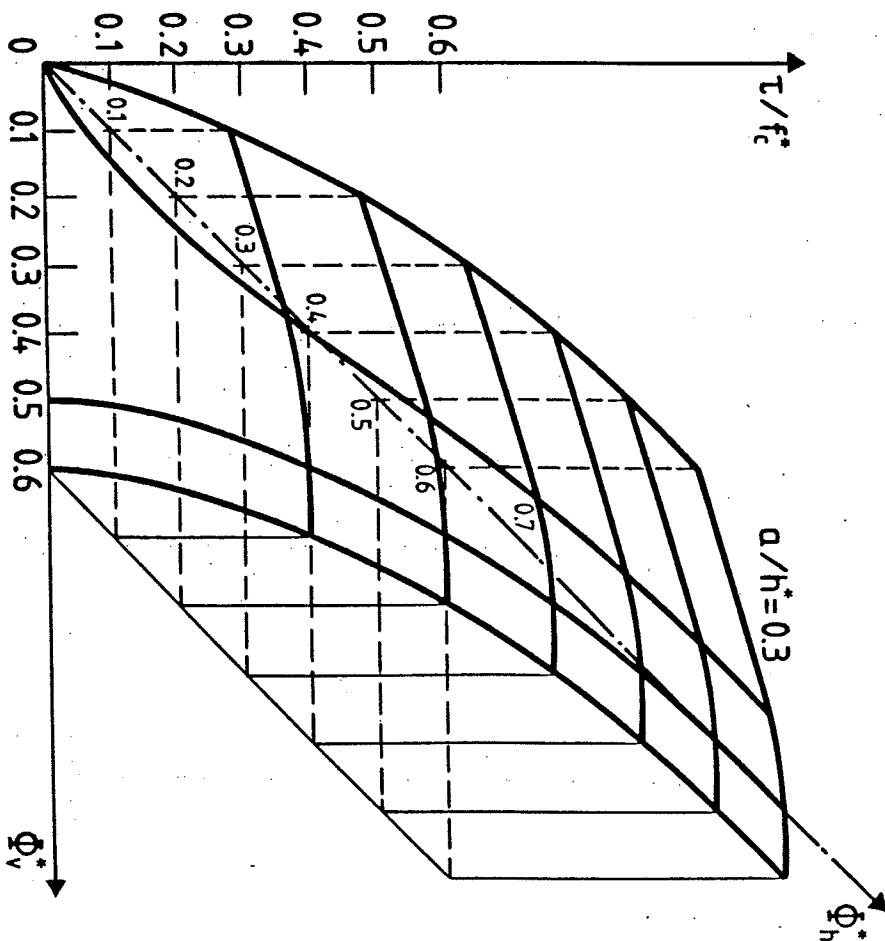


Fig. 5.2. Shear capacity of beams with vertical stirrups versus the reinforcement degree in both directions.

Fig. 5.3. Regions of complete plastic solutions of beams subjected to point loading and with shear reinforcement.

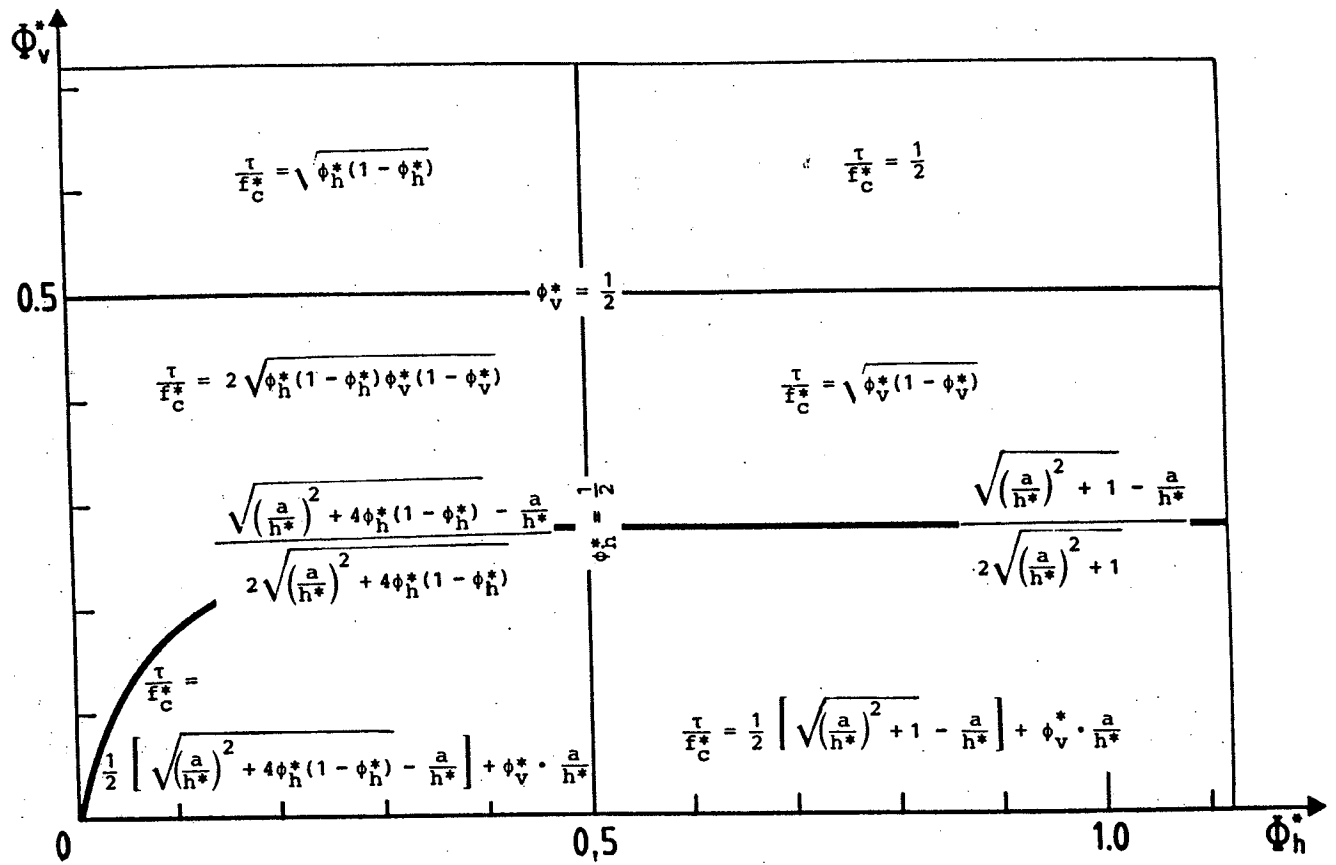
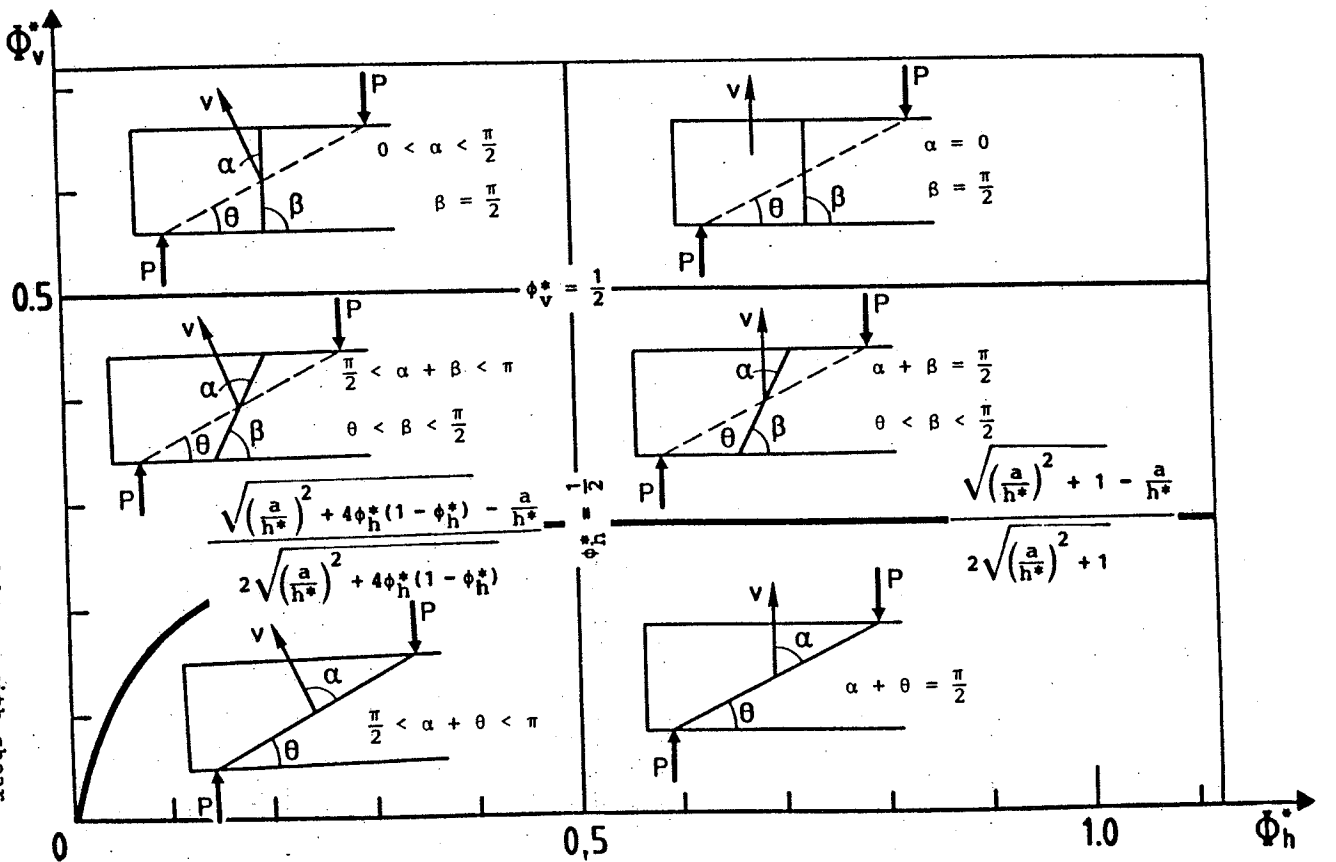


Fig. 5.4. Regions of the failure mechanisms of beams with shear reinforcement.



The regions of complete upper bound solutions and the corresponding failure mechanisms are illustrated in Fig. 5.3 and Fig. 5.4, respectively. The boundaries are plotted for $a/h^* = 0.5$.

5.2 The effective shear depth h^* and the effectiveness factor ν

In order to be able to use the theoretical solutions (5.1) in practice we need to assess the values of the effectiveness factor ν and the effective shear depth h^* . These two parameters are interrelated in the sense that an assessment of the effectiveness factor ν from experimental results of shear tests is influenced by the choice of h^* and vice versa.

In our plastic analysis, the effective shear depth h^* is defined as the distance between the tension and compression stringers. It's rational to consider the tensile reinforcement as the tension stringer. Concerning the compression stringer, things become more complicated and vague. For T-beams, we may take the compression stringer as being identical to the compression flange. If for conventional rectangular beams, the compression zone is choiced, iteration must be used in the analysis of existing tests.

Besides the distance between the two stringers there may be another possibility of defining the effective shear depth h^* . The usual practice and standards are to relate the nominal shear stress to the effective depth of the beam. The Danish Code of Practice requires the use of the internal moment lever arm Z calculated at the section of maximum moment. It has been found that the internal moment lever arm may not be suitable for the effective shear depth h^* in the analysis of existing shear tests of rectangular beams with both strong tensile reinforcement and shear reinforcement. A more rational way may be to define the effective shear depth h^* as the stirrup depth d_s , as illustrated in Fig. 5.5. Unfortunately, up to now we cannot propose a rational and convenient way to de-

side h^* for rectangular beams, since the experimental documentation is lacking.

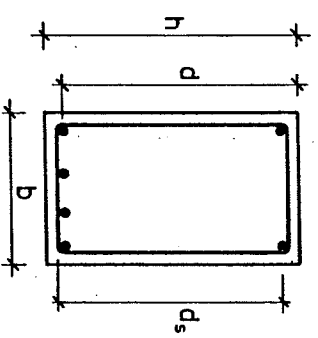


Fig. 5.5. Illustration of effective shear depth h^* .

With the view of combining the physics of our theory with practice in the analysis of test results described below, the effective shear depth h^* is defined as the distance measured from the centroid of the tensile reinforcement to the centre of the compressive flange for T-section beams and as the $0.85 d$ for the rectangular beams.

Having decided upon h^* , we can proceed to determine ν . Towards this end we need test results covering a wide range of various parameters such as concrete strengths from weak to strong, both tensile reinforcement degrees and shear reinforcement degrees from lower to higher, shear span ratio from small to large and so on.

Unfortunately, not very many available web failure tests have been found in the literature.

In order to assess the effectiveness factor ν from the existing experimental results of shear tests, inserting $f_c^* = \nu f_c$ into the complete plastic equations (5.1) and solving them with respect to ν , we get the ν formulae and the corresponding regions as shown in Fig. 5.6. The boundaries are plotted for $a/h^* = 0.5$.

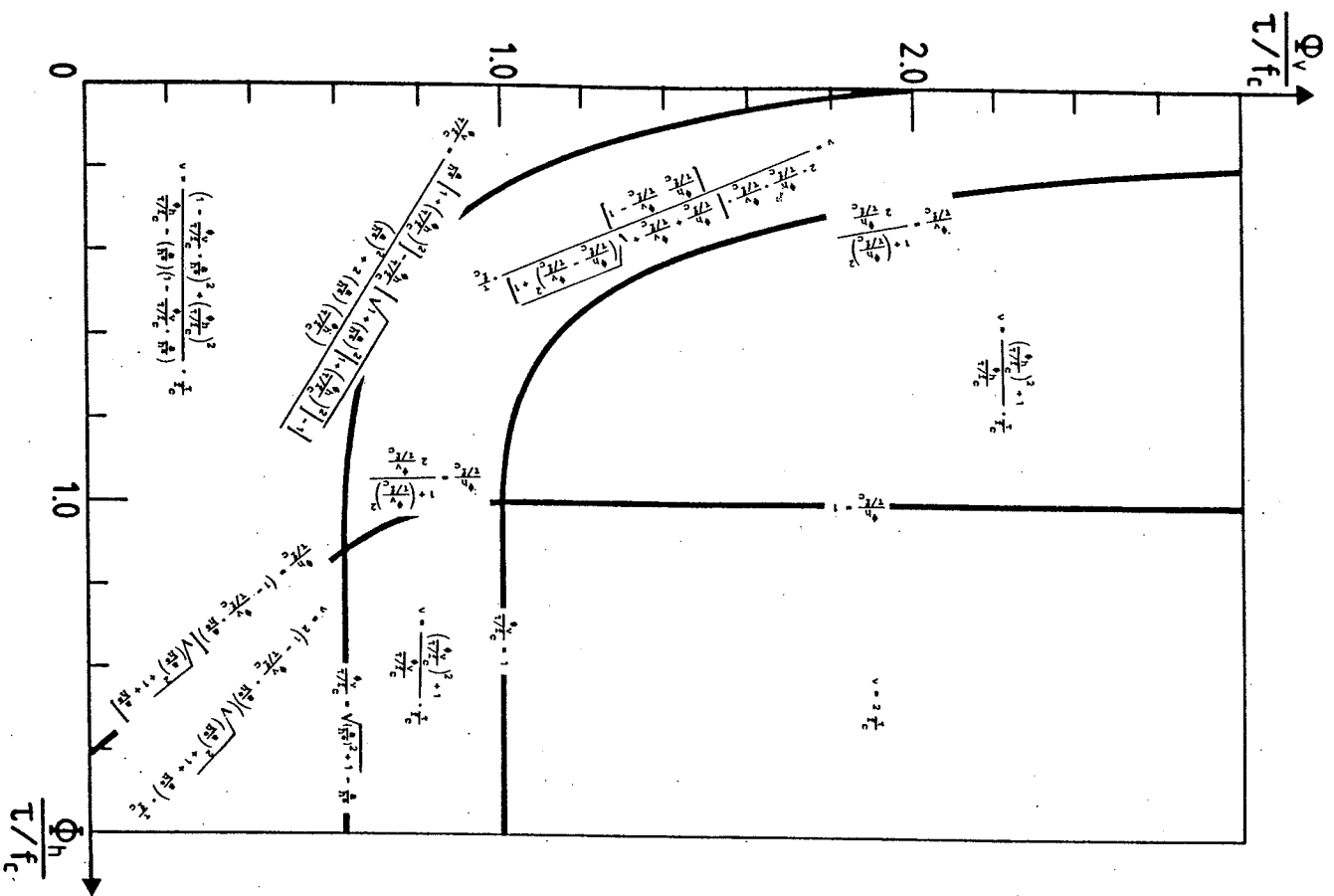


Fig. 5.6. Regions of the ν formulae of beams with shear reinforcement.

5.3 Experimental verification of the theory

5.3.1 Conventional thin-webbed beams

In order to verify the plastic solutions for the web failure mechanism and to investigate the dependence of the web effectiveness factor ν on the concrete strength, the width of the web and the reinforcement details, (i.e. the number and dimensions of the longitudinal bars, their distances from the edges of the beam, and whether they are supported by stirrups), several series of T-beams with shear reinforcement had been tested at the Structural Research Laboratory of the Technical University of Denmark since 1973, [76.6], [80.2].

The test data are summarized in Appendix E.

The results are generally in good agreement with the web crushing criterion (Eq. (5.1)). Because all these tested beams are with the same shear span ratio, it's impossible to investigate whether the web effectiveness factor ν is dependent or independent upon the shear span ratio from these tests.

The concrete strengths of most beams in these tests are between 5 ~ 25 MPa, only very few beams are with concrete strength around 35 MPa, therefore even using the constant ν value the coefficient of variation C_ν is nearly the same as the case considering the ν dependence on f_c .

For 106 observed shear failures, the best correspondence between test results and the theory are obtained for $\nu = 0.725$, when the shear effective depth is defined as in 5.2. The mean value $\bar{\nu}$ is 1.001, while the standard deviation σ is 0.120 and the coefficient of variation C_ν is 0.120.

The tendency of ν to decrease with increasing concrete strength has been found even though it's not very clear since the tests

didn't cover a wide range of concrete strength. A linear relationship

$$v = 0.79 - \frac{f_c \text{ (MPa)}}{200} \quad (5.4)$$

may be used when h^* is defined as in 5.2.

If the experimental results are compared with this model, the correspondence is reasonably good, (see Fig. 5.7).

The mean value is 1.003, while both the standard deviation σ and the coefficient of variation C_v are 0.113.

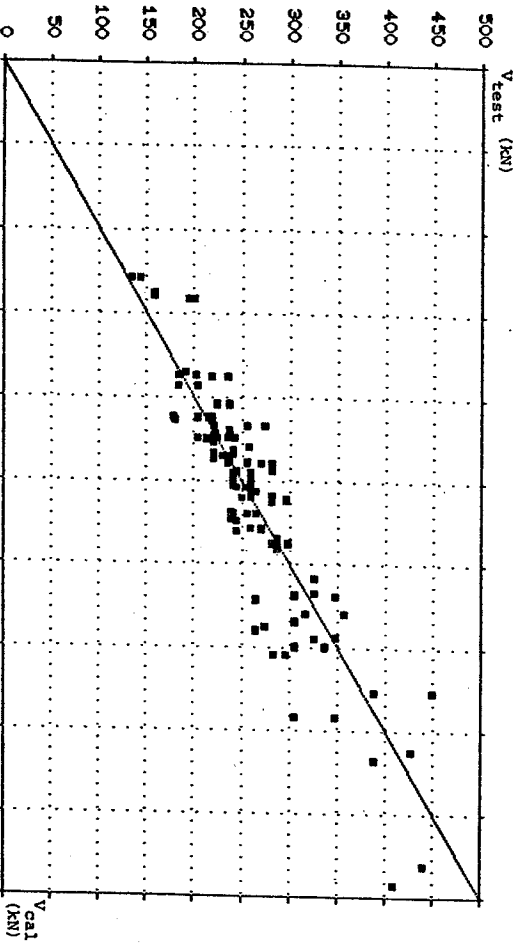


Fig. 5.7. The comparison of theory with tests of T-beams with shear reinforcement and subjected to point loads.

To demonstrate the general applicability of the web crushing criterion (Eq. (5.1)), Fig. 5.8 shows how the test results fit the theoretical curve.

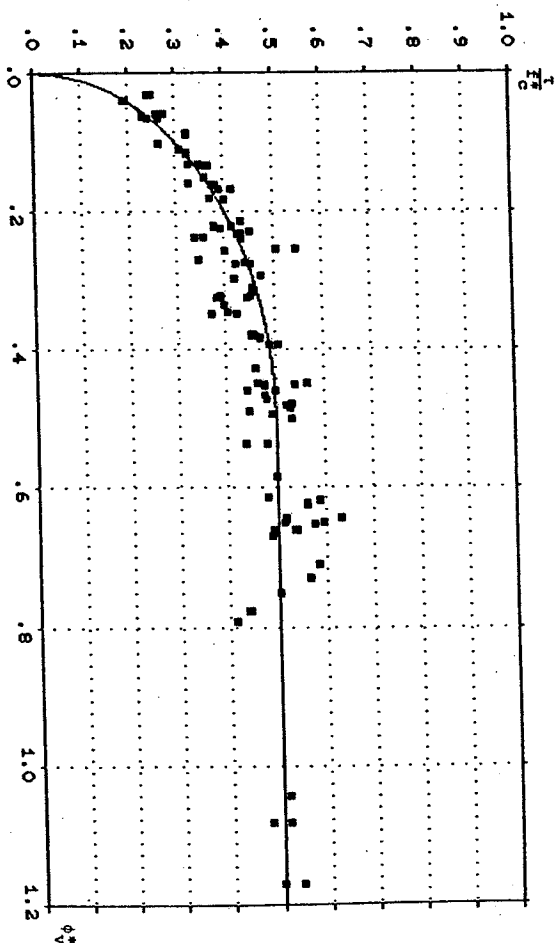


Fig. 5.8. Theoretical shear capacity compared with tests.

Results from previous applications of the plasticity theory to shear in beams without shear reinforcement have shown that the variation of v may be described by an inverse square root dependence $v = k_1/\sqrt{f_c}$ where k_1 is a constant (see Fig. 4.16 to 4.18). However, it has been found from the shear test series mentioned above that such model may underestimate the v -value for the concrete strength $f_c > 20$ MPa when h^* is defined as in section 5.2. But, if the whole beam depth h is used instead of h^* , just like we do for beams without shear reinforcement, this inverse square root dependence model may also give a satisfactory agreement with tests. For all these series of tests, the best correspondence between test results and the theory is obtained for

$$v = 1.86/\sqrt{f_c} \quad (f_c \text{ in MPa}) \quad (5.5)$$

With ν according to (5.5), and comparing tests with theory (5.1), we find the mean value is 1.001, while both the standard deviation σ and the coefficient of variation C_V are 0.107. It's a little better than using the ν model (5.4).

To establish a final conclusion, more test data which cover a wide range of concrete strength are needed.

5.3.2. Deep beams with web reinforcement

Here only 35 deep beam tests reported by Prof. F.K. Kong et al [70.2] are analyzed. These tests consist of seven different types of web reinforcement. The detailed test data are shown in Appendix F. Twenty beams subdivided into 4 types, have only the horizontal web reinforcement. For such deep beams, which have no vertical web reinforcement, the failure mechanism shown in Fig. 4.7 and the corresponding complete theoretical solutions presented in Fig. 4.8 together with the empirical ν equation (4.1.123) are available. The comparisons of test to theoretical calculation prove our confidence. A rather good agreement has been found in the statistics of ratios of test to theory.

If we exclude the horizontal web reinforcement in calculation of the mechanical reinforcement degree ϕ defined by

$$\phi = \frac{A_{gY} f_Y}{b h f_c} \quad (5.6)$$

for 20 beams, the mean value is 1.051, while the standard deviation and the coefficient of variation C_V are 0.113 and 0.108, respectively. The comparison of tests with calculated results is shown in Fig. 5.9.

However, if we include the horizontal web reinforcement in the reinforcement degree ϕ defined by

$$\phi = \frac{A_{gY} f_Y}{b h f_c} + \frac{A_{sw} f_{Ywh}}{b f_c} \quad (5.7)$$

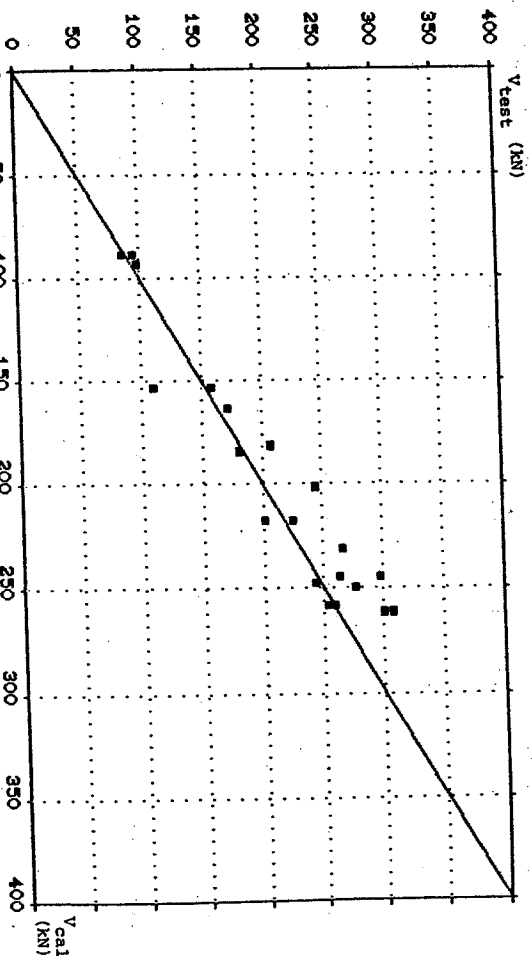


Fig. 5.9. The comparison of theory with tests of 20 deep beams with only horizontal web reinforcement.

where A_{sw} and f_{Ywh} are the area per unit length and the yield strength of horizontal web reinforcement, respectively, then the calculated results are a little higher than the tests. In this case, the mean value \bar{x} is 0.936, while the standard deviation σ and the coefficient of variation C_V are 0.107 and 0.114, respectively. We note no considerable difference between the two statistics, except the mean value. The former calculation is too conservative and the latter is too unsafe. It may be that the horizontal web reinforcement is not so effective on shear capacity as the main reinforcement, (of course it may be useful in decreasing the shear crack width in the web). Until more decisive experimental evidence is available, for the safe reason, we prefer to use the former way to calculate the shear carrying capacity of such deep beams, i.e. excluding the horizontal web reinforcement in the calculation of the reinforcement degree.

For the other 15 deep beams with vertical web reinforcement, which consist of 3 types of vertical web reinforcement arrangements, a

statistical analysis has been shown that the best agreement between theory and test may be reached by using

$$v = \frac{2.35}{\sqrt{f_c}} \quad (f_c \text{ in MPa}) \quad (5.8)$$

when the whole depth of the deep beam is used as the shear depth. The mean value is 0.999, while both the standard deviation σ and the coefficient of variation C_v are 0.100.

The comparison of theoretical calculations with tests is shown in Fig. 5.1. In these tests the concrete strength only varied in a small range, whereby the v dependence on f_c is also not quite clear.

If we put the effective shear depth of rectangular beams equal to $0.85d$, the statistics for different v expressions can be seen in Table 5.3.1.

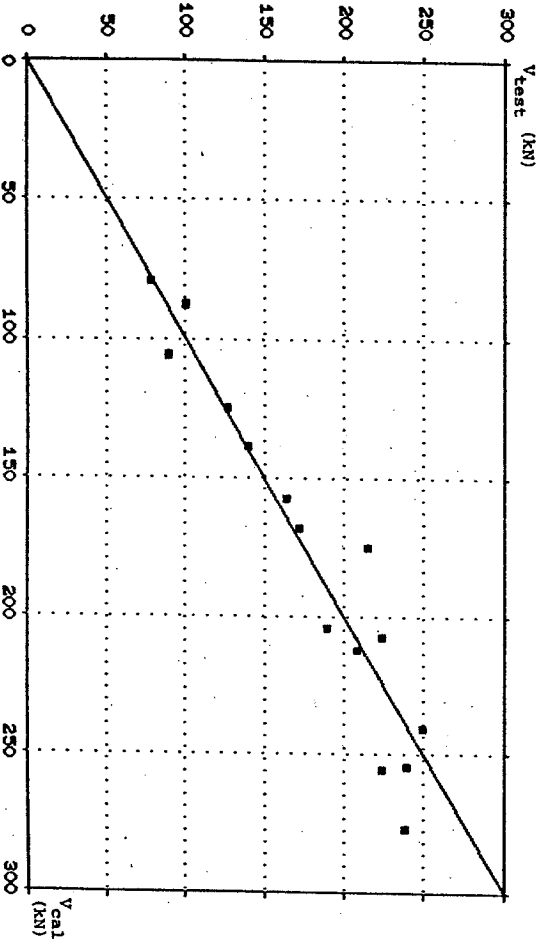


Fig. 5.10. The plastic solution for beam shear with web reinforcement compared with deep beam test results.

v	0.72	$0.8 - \frac{f_c}{200}$	$\frac{3.3}{\sqrt{f_c}}$
\bar{x}	1.006	1.030	1.002
σ	0.146	0.146	0.139
C_v	0.145	0.142	0.139

Table 5.3.1. Statistics of the ratios of tests to theoretical calculations for different v expressions.

It seems that the difference can hardly be said to be striking. However, in order to be unique and identical with the T-beams described in 5.3.1, equation (5.4) appears preferable to the inverse square root model $v = k_1/\sqrt{f_c}$, where k_1 is a constant, since k_1 , in these two cases deviate too much from each other.

5.3.3. Prestressed beams with web reinforcement

As we have mentioned in Section 4.4, according to the theory of plasticity, prestressing should have no effect on the shear carrying capacity of a perfectly plastic structure. However, for concrete beams, the existence of prestressing does influence the stress redistribution before failure and results in the change of the ultimate load.

How the prestress influences the effectiveness factor v of concrete beams with web reinforcement has only been very preliminarily investigated for 93 observed shear failure tests of prestressed beams reported in the literature [64.2], [71.2], [73.3], [73.4], and [76.3].

The detailed test data are shown in Appendix G.

The experimental investigation of the shear capacity of prestressed concrete beams with shear reinforcement has shown that the effective prestress in the section does increase the ν value but the dependence of ν on the average effective prestress in the section is smaller than for beams without shear reinforcement. For the available test results, defining the effective shear depth h^* as in Section 5.2, the best correspondence between tests and theoretical calculations is obtained for

$$\nu = \left[0.8 - \frac{F}{200C} \right] \left[1 + 2.2 \frac{F_{se}}{A_C F_C} \right] \left[\frac{F_{se}}{A_C F_C} \right] \pm 0.5 \quad (5.9)$$

The mean value \bar{x} is 1.002, while both the standard deviation σ and the coefficient of variation C_v are 0.151.

The comparison of tests with calculations is shown in Fig. 5.11.

The applicability of the plastic solutions for beams with shear reinforcement can also be seen in Fig. 5.12, although the scatter is considerable. However, it is believed that as long as the effectiveness factor ν is only considered to be depending on the concrete compressive strength and the average effective prestress on the section, it will be difficult to obtain better results from any theory.

If the inverse square root model of concrete strength is considered in the ν expression, the best correspondence between tests and theory is found to be

$$\nu = \frac{3.8}{\sqrt{F_C}} \left[1 + 2 \frac{F_{se}}{A_C F_C} \right] \left[\frac{F_{se}}{A_C F_C} \right] \pm 0.5 \quad (5.10)$$

Now the statistical results are: mean value \bar{x} is 1.006, and the standard deviation σ and the coefficient of variation C_v are 0.159 and 0.158, separately.

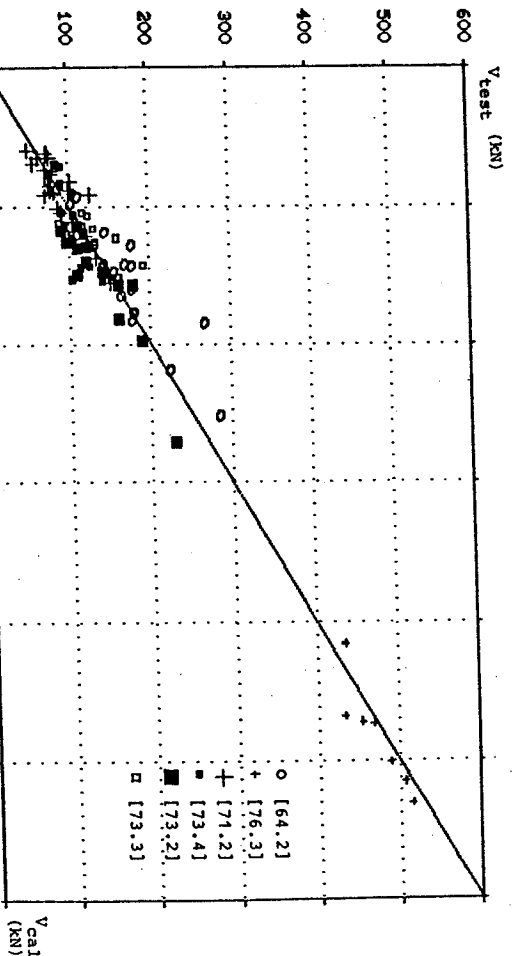


Fig. 5.11. The comparison of calculations with tests of prestressed beams with web reinforcement.

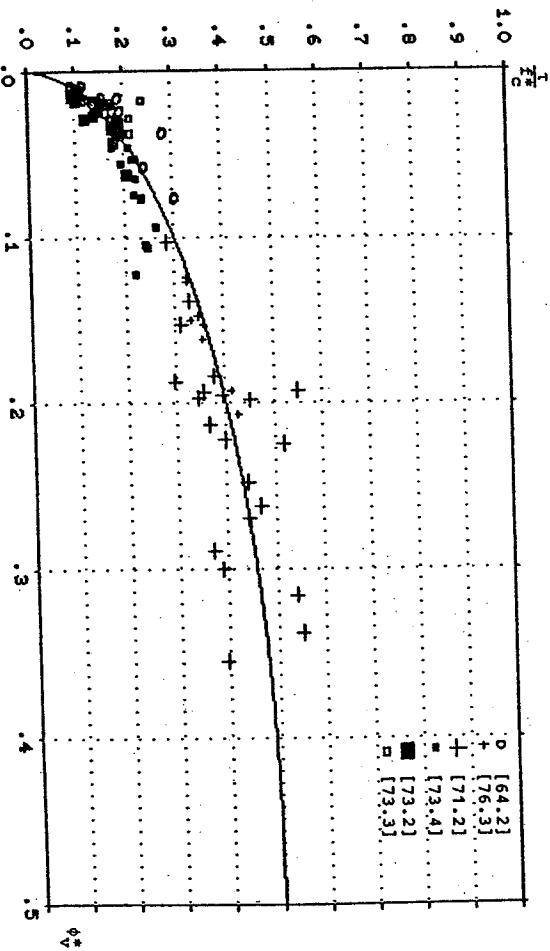


Fig. 5.12. Theoretical shear capacity for beams with shear reinforcement compared with tests of prestressed beams.

5.4 Some discussion on ν

In Chapter IV it is shown that the main parameters governing the ν -value for ordinary beams with rectangular section and without shear reinforcement are the concrete strength, the amount of longitudinal reinforcement and the shear span/depth-ratio. Besides the above major factors, the scale effect, represented by the absolute value of the depth, also gives a smaller effect on the ν -value.

The dependence on the concrete strength is easily understood, since increasing concrete strength leads to decreasing ductility.

The dependence on the reinforcement ratio is probably due to the dowel action of the reinforcement, which is neglected in the plastic theory model according to our assumptions in Section 2.6, and to the fact, that increasing reinforcement ratios leads to decreasing crack widths at rupture.

The decreasing ν -value for increasing a/h -values up to about 2.5 is probably due to the dowel action and to the fact that the required stress redistribution is strongly increasing for increasing a/h -values in this interval.

The slight decreasing ν -value for increasing depth of the section may be explained as a result of an unstable crack propagation at a lower load if the crack is longer, therefore the shear compression capacity is not proportional to the depth of the section but less.

For prestressed beams with rectangular section and without shear reinforcement, the main parameters governing the ν -value are the same as for ordinary beams except that the shear span/depth-ratio has only a small influence and that the average effective prestress on the section has an influence.

The experimental investigation has shown the ν -value is increasing almost proportional to the average effective prestressing of the section up to about 0.15. This phenomenon is probably due to the

fact that the prestressing effectively delays the formation and prevents the propagation of the inclined shear cracks. Therefore prestressing increases the depth of shear compressive zone of concrete and raises the shear carrying capacity of the beams.

Indeed, pre-tensioned prestressed beams do not exhibit such a strong a/h -ratio dependence like that found for ordinary beams.

The explanation may be that small span-to-depth ratios enable the dowel action to develop in ordinary beams, provided that there is a well anchored reinforcement. However, in pretensioned prestressed beams the anchoring capacity of the strands will limit the dowel effects. But some tests still show more or less the dependence of ν on the a/h -ratio. To draw a more convincing and definite conclusion, more available test data are needed. Before these are available, and in order to be on the safe side and finally to be convenient in practice, the slight increasing of ν for small a/h -ratio should not be taken into account.

The precise plastic shear solutions for beams with T-section or I-section and without web reinforcement are somewhat complicated. To find a more rational and precise ν dependence is even more difficult. For the sake of simplicity and in order to utilize the existing conclusions for beams with rectangular section, we may employ the plastic solutions to the web area of such beams but include the favourable effects of the compressive flange into the ν expression. We must point out that the physical meaning of ν here is somewhat different from its original definition, i.e. it's not only an empirical measure of concrete ductility and the absorbent of other shortcomings of the theory (for example, the neglecting of dowel action), but also a conversion factor of an alternative simple method. This is the reason why in such cases the ν -value may become larger than unit.

A parametric analysis of prestressed beams without web reinforcement has shown the ν -value in such cases increase approximately proportional to the (whole area)/(web area) ratio until about 1.8.

It's an unfortunate consequence of the above mentioned conclusions that the resulting empirical formulae of v for beams without shear reinforcement are rather different from the v expressions for beams with shear reinforcement in Chapter V. Among the possible reasons for the difference found, we would like to mention the following:

- 1) The ductility is probably increased and the dowel action may be decreased by supplying shear reinforcement.
- 2) Different measures of the shear depth are used for beams with shear reinforcement and beams without shear reinforcement, i.e. for beams without shear reinforcement we use the whole depth of the beam as the shear depth, while for beams with shear reinforcement we use the effective depth h^* as the shear depth.
- 3) In order to determine the v dependence for high concrete strengths and shear span/depth ratios more available data are needed.

In order to unify the v expression in various cases, more research is needed in this field.

SUMMARY

This paper deals with some elementary problems in reinforced concrete theory. Shear resistance of beams, deep beams, corbels and joints are mainly treated.

The classical plastic theory has been used under the assumptions of the modified Coulomb failure criterion with non-zero tension cut-off as yield condition and the associated flow rule (normality condition) as constitutive equations for the concrete.

For plane structural members without shear reinforcement an exact solution (i.e. with corresponding upper and lower bounds) has been found for beams, deep beams, corbels and joints.

Moreover an upper bound solution is presented for members subjected to combined shear and normal force, which is proved to be identical to the exact shear solution without normal force.

Due to the well-known fact that concrete is not the perfect plastic material the exact plastic solutions are then modified by replacing the compressive strength of concrete f_c and the tensile strength of concrete f_t by the reduced values $v \cdot f_c$ and $\rho^* \cdot f_c$ respectively. The v and ρ^* are called effectiveness factors.

A lot of work has been done to develop a more general and rational method for the assessment of approximate v -value in various shear cases, especially for members without shear reinforcement.

The theoretical predictions are lastly compared with a great number of experimental results from the literature.

A good agreement has been found.

RESUME

Rapporten omhandler en beskrivelse af nogle elementære teoretiske problemer i armeret beton.

Der behandles forskydningsproblemer i slanke bjælker, høje bjælker, konsoller og fuger.

Den klassiske plasticitetsteori anvendes under forudsætning af, at den associerede flydelov gælder. (Normalitetsbetingelsen).

Betonen antages at være et modificeret Coulomb materiale med en trækstyrke, der er forskellig fra nul.

For plane elementer uden forskydningsarmering udledes en eksakt løsning (dvs. med sammenfaldende øvre- og nedreværdi), der finder anvendelse både for slanke bjælker, konsoller samt fuger.

Ligeledes præsenteres en øvre værdiløsning for konstruktioner belastet med kombineret forskydning og normalkraft, der ses at være identisk med den eksakte forskydningsløsning uden normalkraft.

På grund af forskellen mellem den rigtige spændings-tøjningssammenhang for beton og det sammenhæng der eksisterer for et stift plastisk materiale, skal de eksakte plastiske løsninger reduceres.

Dette gøres ved at indsætte de reducerede værdier $v \cdot f_c$ og $p \cdot f_c$ for henholdsvis den plastiske trykstyrke f_c og trækstyrken f_t .

v og p kaldes effektivitetsfaktorer.

Der er blevet lagt et stort arbejde i at udvikle en mere generel og rationel metode til at vurdere tilnærmede v -værdier for forskydningsilfældet, især for forskydningspåvirkede legemer uden forskydningsarmering.

De teoretiske beregninger er herefter sammenlignet med et stort antal forsøgsresultater fra litteraturen omhandlende slanke bjælker, høje bjælker og konsoller.

Der er fundet udmærket overensstemmelse.

REFERENCES

- [51.1] Clark, A.: Diagonal tension in reinforced concrete beams. Journal of the ACI, Oct. 1951, pp. 145-156.
- [53.1] Ferguson, P.M. and Thomson, J.N.: Diagonal tension in T-beams without stirrups. Journal of the ACI, May 1953, pp. 665-575.
- [54.1] Zwoyer, E.M. and Siess, C.P.: Ultimate strength in shear of simply-supported prestressed concrete beams without web reinforcement. Journal of the ACI, Oct. 1954, pp. 181-200.
- [54.2] Moody, K.G., Viest, I.M., Eistner, R.C. and Hognestad, E.: Shear strength of reinforced concrete beams. Part 1 - Test of simple beams. Journal of the ACI, Dec. 1954, pp. 317-332.
- [56.1] Ferguson, P.M.: Some implications of recent diagonal tension tests. Journal of the ACI, Aug. 1956, pp. 157-172.
- [57.1] Morrow, J. and Viest, I.M.: Shear strength of reinforced concrete frame members without web reinforcement. Journal of the ACI, March 1957, pp. 833-868.
- [57.2] Al-Alusi, A.F.: Diagonal tension strength of reinforced concrete T-beams with varying shear span. Journal of the ACI, May 1957, pp. 1067-1077.
- [58.1] Hanson, J.A.: Shear strength of lightweight reinforced concrete beams. Journal of the ACI, Sept. 1958, pp. 387-403.
- [58.2] Hicks, A.B.: The influence of shear span and concrete strength upon the shear resistance of a pre-tensioned prestressed concrete beam. Magazine of Concrete Research, Nov. 1958, pp. 115-122.
- [58.3] Watstein, D. and Mathey, R.G.: Strains in beams having diagonal cracks. Journal of the ACI, Dec. 1958, pp. 717-728.
- [59.1] Guralnick, S.: Shear strength of reinforced concrete beams. Journal of the ASCE, St. 1, Jan. 1959, pp. 1-42.
- [59.2] Soren, M.A., Zwoyer, E.M. and Siess, C.P.: Strength in shear in beams without web reinforcement. University of Illinois, Engineering Experiment Station Bulletin, No. 452, 1959, pp. 69.
- [60.1] Cossio, R.D.D. and Siess, C.P.: Behavior and strength in shear of beams and frames without web reinforcement, Journal of the ACI, Feb. 1960, pp. 695-735.
- [60.2] De Pavia, H.A.R. and Austin, W.J.: Tests of reinforced concrete deep beams. University of Illinois, Department of Civil Engineering, March 1960.
- [60.3] Sethunaryanan, R.: Ultimate strength of pre-tensioned I beams in combined bending and shear. Magazine of Concrete Research, Vol. 12, No. 35, July, 1960, pp. 83-90.
- [60.4] Bower, J.E. and Viest, I.M.: Shear strength of restrained concrete beams without web reinforcement. Journal of the ACI, July 1969, pp. 73-98.

- [60.5] Taub, J. and Neville, A.M.:
Resistance to shear of reinforced concrete beams. Part I
Beams without web reinforcement. Journal of the ACI, Aug.
1960, pp. 193-220.
- [60.6] Winemiller, J.R. and Austin, W.J.:
Tests of reinforced concrete deep beams with web and
compression reinforcement. University of Illinois
Department of Civil Engineering, Aug. 1960.
- [60.7] Guralnick, S.A.:
High-strength deformed steel bars for concrete
reinforcement. Journal of the ACI, Aug. 1960, pp.
241-282.
- [60.8] Taylor, R.:
Some shear tests on reinforced concrete beams without
shear reinforcement. Magazine of Concrete Research, Vol.
12, No. 36, Nov. 1969, pp. 18.
- [60.9] Rusch, H. and Vigerust, G.:
Schubversuche und Spannbetonbalken. Deutscher Ausschuss
für Stahlbeton, Heft 137, Berlin, 1960, pp. 18.
- [62.1] Hognestad, E.:
Shear and diagonal tension. Report of ACI-ASCE Committee
326, Journal of the ACI, Jan. 1962, pp. 3-30; Feb. 1962,
pp. 279-333; March 1962, pp. 355-395.
- [62.2] Van den Berg, F.J.:
Shear strength of reinforced concrete beams without web
reinforcement. Part 2 - Factors affecting load at
diagonal cracking. Journal of the ACI, No. 1962, pp.
1587-1600.
- [63.1] Bressler, B. and Scordelis, A.C.:
Shear strength of reinforced concrete beams. Journal of
the ACI, Jan. 1963, pp. 51-72.
- [63.2] Mathey, R.G. and Watstein, D.:
Shear strength of beams without web reinforcement
containing deformed bars of different yield strengths.
Journal of the ACI, Feb. 1963, pp. 183-207.
- [63.3] Evans, R.H. and Schumacker, Z.G.:
Shear strength of prestressed beams without web
reinforcement. Journal of the ACI, Nov. 1963, pp.
1621-1642.
- [64.1] Kani, G.N.J.:
The riddle of shear failure and its solution. Journal of
the ACI, Apr. 1964, pp. 441-466.
- [64.2] Hanson, J.M. and Hulsbos, C.L.:
Ultimate shear tests of prestressed concrete I-beams
under concentrated and uniform loadings. Journal of the
PCI, June, 1964, pp. 15-28.
- [65.1] Krilz, L.B. and Taths, C.H.:
Connections in precast concrete structures - strengths
of corbels. Journal of the PCI, Feb. 1965, pp. 16-53.
- [65.2] Lorentsen, M.:
Theory for the combined action of bending moment and
shear in reinforced and prestressed concrete beams.
Journal of the ACI, Apr. 1965, pp. 403-420.
- [65.3] Arthur, P.D. and Ganguli, S.:
Tests on end-zone stresses in pre-tensioned concrete I
beams. Magazine of Concrete Research, Vol. 17, No. 51,
June 1965, pp. 85-96.
- [65.4] de Pavis, H.A.R. and Sless, C.P.:
Strength and behavior of deep beams in shear. Journal of
the ASCE, SMS, Oct. 1965.

[65.5] Arthur, P.D.:
The shear strength of pre-tensioned I beams with unreinforced webs. Magazine of Concrete Research, Vol. 17, No. 53, Dec. 1965, pp. 199-210.

[65.6] Leonhardt, F.:
Reducing the shear reinforcement in reinforced concrete beams and slabs. Magazine of Concrete Research, Vol. 17, No. 53, Dec. 1965, pp. 187-198.

[66.1] Krefeld, W.J. and Thurston, C.W.:
Contribution of longitudinal steel to shear resistance of reinforced concrete beams. Journal of the ACI, Apr. 1966, pp. 451-476.

[66.3] Kani, G.N.J.:
Basic facts concerning shear failure. Journal of the ACI, June 1966, pp. 675-690.

[66.4] Taylor, R.:
Some shear tests on reinforced concrete T beams with stirrups. Magazine of Concrete Research, Vol. 18, No. 57, Dec. 1966, pp. 221-230.

[67.1] Nielsen, M.P.:
Om forskydningsarmering af jernbetonbjælker. Bygningsstatistiske Meddelelser, Vol. 38, Nr. 2, pp. 33-58.

[67.2] Bresler, B. and MacGregor, J.G.:
Review of concrete beams failing in shear. Journal of the ASCE, ST1, Feb. 1967, pp. 343-372.

[67.3] Kani, G.N.J.:
How safe are our large reinforced concrete beams. Journal of the ACI, March 1967, pp. 128-141.

[68.1] Kar, J.N.:
Diagonal cracking in prestressed concrete beams. Journal of the ASCE, ST1, Jan. 1968, pp. 83-109.

[68.2] Ramakrishnan, V. and Ananthanarayana, Y.:
Ultimate strength of deep beams in shear. Journal of the ACI, Feb. 1968.

[68.3] Rajagopalan, K.S. and Ferguson, P.M.:
Exploratory shear tests emphasizing percentage of longitudinal steel. Journal of the ACI, Aug. 1968, pp. 634-638.

[68.4] Fenwick, R.C. and Paulay, T.:
Mechanisms of shear resistance of concrete beams. Journal of the ASCE SM10, Oct. 1968, pp. 2325-2350.

[69.1] Hofbeck, J.A., Ibrahim, I.O. and Mattock, A.H.:
Shear transfer in reinforced concrete. Journal of the ACI, Feb. 1969, pp. 119-128.

[69.2] Kani, G.N.J.:
A rational theory for the function of web reinforcement. Journal of the ACI, March 1969, pp. 185-197.

[69.3] Regan, P.E.:
Shear in reinforced concrete beams. Magazine of Concrete Research, Vol. 21, No. 66, March 1969, pp. 31-42.

[69.4] Kar, J.N.:
Shear strength of prestressed concrete beams without web reinforcement. Magazine of Concrete Research, Vol. 21, No. 68, Sep. 1969, pp. 159-170.

[70.1] Chen, W.F.:
Extensibility of concrete and theorems of limit analysis. Journal of the Engineering Mechanics Division EM3, June 1970, pp. 341-351.

- [70.2] Kong, F.K., Robins, P.J. and Cole, D.F.:
Web reinforcement effects on deep beams. Journal of the
ACI, Proc. Vol. 67, No. 11, Dec. 1970.
- [71.1] Zsutty, T.:
Shear strength prediction for separate categories of
simple beam test. Journal of the ACI, Feb. 1971, pp.
138-143.
- [71.2] Bennett, E.M. and Balasooriya, B.M.
Shear strength of prestressed beams with thin webs
failing in inclined compression. Journal of the ACI,
March 1971, pp. 204-212.
- [71.3] Suter, G.T. and Manuel, R.F.:
Diagonal crack width control in short beams. Journal of
the ACI, June 1971, pp. 451-455.
- [71.4] Kong, F.K. and Robins, P.J.:
Web reinforcement effects on lightweight concrete deep
beams. Journal of the ACI, Proc. Vol. 68, No. 7, July
1971.
- [71.5] Sheikh, M.A., de Pavia, H.A.R. and Neville, A.M.:
Flexure - shear strength of reinforced concrete deep
beams. Journal of the Structural Engineer, Proc. Vol. 49,
No. 8, Aug. 1971, pp. 359-363.
- [71.6] Haddadin, M.J., Sheu-Tjern, H. and Mattock, A.H.:
Stirrup effectiveness in reinforced concrete beams with
axial force. Journal of the ASCE, ST9, Sep. 1971, pp.
2277-2297.
- [71.7] Placas, A. and Regan, P.E.:
Shear failure of reinforced concrete beams. Journal of
the ACI, Oct. 1971, pp. 763-773.
- [71.8] Manuel, R.F., Slight, B.W. and Suter G.T.:
Deep beam behavior affected by length and shear span
variations. Journal of the ACI, Proc. Vol. 68, No. 12,
Dec. 1971.
- [72.1] Kong, F.K. and Robins, P.J.:
Shear strength of reinforced concrete deep beams. Journal
of Concrete, Proc. Vol. 6, No. 3, March 1972.
- [72.2] Kong, F.K. and Singh, A.:
Diagonal cracking and ultimate loads of lightweight
concrete deep beams. Journal of the ACI, Proc. Vol. 69,
No. 8, Aug. 1972.
- [72.3] Kong, F.K., Robins, P.J., Singh, A. and Sharp, G.R.:
Shear analysis and design of reinforced concrete deep
beams. Journal of the Structural Engineer, Proc. Vol. 50,
No. 10, Oct. 1972.
- [72.4] Santhakumar, A.R. and Arunachalam, N.V.:
Strength and behavior of single-span, deep reinforced
concrete beams. Indian Concrete Journal, Nov. 1972, pp.
459-465.
- [72.5] Taylor, H.P.J.:
Shear strength of large beams. Journal of the ASCE, ST11,
Nov. 1972, pp. 2473-2490.
- [73.1] Swamy, R.N. and Andriopoulos, A.D.:
Contribution of aggregate interlock and dowel forces to
the shear resistance of reinforced beams with web
reinforcement. ACI, sp 42-6, pp. 129-166.
- [73.2] Moayer, M. and Regan, P.E.:
Shear strength of prestressed and reinforced concrete
T-beams. ACI, sp 42-8, pp. 183-213.

- [73.3] Cederwall, K. Hedman, O. and Losberg, A.:
Shear strength of partially prestressed beams with pretensioned reinforcement of high grade deformed bars. ACI, sp 42-9, pp. 215-230.
- [73.4] Bennett, E.W. and Debalky, S.Y.:
High strength steel as shear reinforcement in prestressed concrete beams. ACI sp 42-10, pp. 231-248.
- [73.5] Manuel, R.F.:
Failure of deep beams. ACI sp 42-19, Vol. 2.
- [73.6] Smith, K.N. and Fereidj, S.M.:
Effect of loading and supporting conditions on the shear strength of deep beams. ACI sp 42-20, Vol. 2.
- [73.7] Sørensen, H.C.:
Shear in reinforced concrete beams with high strength stirrups. Shear tests on 12 reinforced concrete T-beams. Technical University of Denmark, Structural Research Laboratory. Intern. Report I 27, 1973.
- [74.1] Hermansen, B.R. and Cowan, J.:
Modified shear-friction theory for bracket design. Journal of the ACI, Feb. 1974, pp. 55-60.
- [74.2] Desayi, P.:
A method for determining the shear strength of reinforced concrete beams with small a_v/d ratios. Magazine of Concrete Research, Vol. 26, No. 86, March 1974, pp. 29-38.
- [74.3] Bræstrup, M.W.:
Plastic analysis of shear in reinforced concrete. Magazine of Concrete Research, Vol. 26, No. 89, Dec. 1974.
- [75.1] Nielsen, M.P. and Bræstrup, M.W.:
Plastic shear strength of reinforced concrete beam. Bygningstat. Medd., Vol. 46, No. 3, 1975, pp. 61-99.
- [75.2] Jensen, B.C. and Nielsen M.P.:
Om spalteforsøget og om koncentrerede kræfter på narmerede betongprisme. (Splitting tests and concentrated loads on unreinforced concrete prisms). Nordisk Beton 9, March 1975, pp. 9-13.
- [75.3] Kong, F.K., Robins, P.J. and Sharp, G.R.:
The design of reinforced concrete deep beam in current practice. Journal of The Structural Engineer, Vol. 53, No. 4, April 1974, pp. 173-180.
- [75.4] Jensen B.C.:
Lines of discontinuity of displacements in the theory of plasticity of plain and reinforced concrete. Magazine of Concrete Research, Vol. 21, No. 92, Sep. 1975, pp. 143-150.
- [75.5] Mahgoub, M.O.:
Shear strength of prestressed concrete beams without web reinforcement. Magazine of concrete Research, Vol. 21, No. 93, Dec. 1975, pp. 219-228.
- [75.6] Grant, G. and Sokal, Y.:
Deep web reinforcement. Journal of Concrete, Dec. 1975, pp. 28-31.
- [76.1] Prabhath Kumar.:
Collapse load of deep reinforced concrete beams. Magazine of Concrete Research, Vol. 28, No. 94, March 1976.
- [76.2] Mattock, A.H., Chen K.C. and Soongswang, K.:
The behavior of reinforced concrete corbels. Journal of the PCI, March-April 1976, pp. 52-77-

- [76.3] Lynberg, B.S.: Ultimate shear resistance of partially prestressed reinforced concrete I-beams. Journal of the ACI, April 1976, pp. 214-222.
- [76.4] Mattock, A.H.: Design proposals for reinforced concrete corbels. Journal of the PCI, May-June 1976, pp. 18-42.
- [76.5] Selvam, V.K.M.: Shear strength of reinforced concrete deep beams. Building and Environment, Vol. 11, pp. 211-214.
- [76.6] Bræstrup, M.W., Nielsen, M.P., Bach, F. and Jensen, B.C.: Shear tests on reinforced T-beams, series T. Technical University of Denmark, Structural Research Laboratory, Report R 72, 1976, pp. 114.
- [77.1] Bræstrup, M.W., Nielsen M.P. and Bach, F.: Plastic analysis of shear in concrete. Danish Center for Applied Mathematics and Mechanics, Report No. 120, May 1977, pp. 24 + figs.
- [77.2] Jensen, B.C.: Some applications of plastic analysis to plain and reinforced concrete. Technical University of Denmark, Institute of Building Design, Report No. 123, 1977, pp. 119.
- [77.3] Taner, N. Fazio, P.P. and Zielinski, Z.A.: Strength and behavior of beam - Panel tests and analysis. Journal of the ACI, Oct. 1977, pp. 511-520.
- [77.4] Macgregor, J.G. and Hawkins, N.M.: Suggested Revisions to ACI Building Code clauses dealing with shear friction and shear in deep beams and corbels. Journal of the ACI, Nov. 1977, pp. 537-545.
- [77.5] Roikjar, M., Nielsen, M.P., Bræstrup, M.W. and Bach, F.: Forskydningsforsøg med spændbetonbjælker uden forskydningsarmering. Technical University of Denmark, Structural Research Laboratory, Intern Rapport Nr. I 51, 1977, pp. 15.
- [77.6] Jensen, J.F., Bræstrup, M.W., Bach, F. and Nielsen, M.P.: Præfabrikerede sandwichelementer af letbeton. Technical University of Denmark, Structural Research Laboratory, Intern Rapport Nr. I 54, 1977, pp.28.
- [77.7] Bach, F., Nielsen, M.P. and Bræstrup, M.W.: Forskydningsforsøg med jernbetonbjælker. Technical University of Denmark, Structural Research Laboratory, Intern Rapport, I 49, 1977, pp. 18.
- [78.1] Kumar, P.: Optimal force transmission in reinforced concrete deep beams. Computers and Structures, Vol. 8, 1978, pp. 223-229.
- [78.2] Nielsen, M.P. and Bræstrup, M.W.: Shear strength of prestressed concrete beams without web reinforcement. Magazine of Concrete Research, Vol. 30, No. 104, Sep. 1978.
- [78.3] Nielsen, M.P. Bræstrup, M.W., Jensen, B.C. and Bach, F.: Concrete plasticity: Beam shear - shear in joints - punching shear. Danish Society for Structural Science and Engineering/Structural Research Laboratory, Lyngby, 1978, pp. 129.
- [78.4] Jensen, J.F., Jensen V., Christensen H.H., Bach, F., Bræstrup, M.W. and Nielsen, M.P.: On the behavior of cracked reinforced concrete beams in the elastic range. Technical University of Denmark, Structural Research Laboratory, Report R 103, 1978, pp. 21.

- [78.5] Jensen, J.F., Pedersen C., Bræstrup, M.W., Bach, F. and Nielsen, M.P.: Rapport over forskydningsforsøg med 6 spændbetonbjælker. Technical University of Denmark, structural Laboratory, Report R 102, 1978, pp. 28.
- [78.6] Pedersen, C., Jensen, J.F., Nielsen, M.P. and Bach, F.: Ophøjet længdearmring som forskydningsarmring. Technical University of Denmark, Structural Research Laboratory, Report R 100, 1978, pp. 21.
- [78.7] Jensen, J.F., Bræstrup, M.W., Bach, F. and Nielsen, M.P.: Nogle plasticitetsteoretiske bjælkeløsninger. Technical Report R 101, 1978, pp. 50.
- [79.1] Bræstrup, M.W.: Effect of main steel strength on the shear capacity of reinforced concrete beams with stirrups. Technical University of Denmark, Structural Research Laboratory, Report R 110, 1979.
- [79.2] Ray, S.P. and Reddy, C.S.: Strength of reinforced concrete deep beams with and without opening in the web. Indian Concrete Journal, Sep. 1979, pp. 242-246.
- [79.3] Mirza, S.A. and Macgregor, J.G.: Statistical study of shear strength of reinforced concrete slender beams. Journal of the ACI, Nov. 1979, pp. 1159-1177.
- [79.4] Roikjær, M., Pedersen, C., Bræstrup, M.W., Nielsen, M.P. og Bach, F.: Bestemmelse af Ikke-forskydningsarmerede bjælkers forskydningsbæreevne. Technical University of Denmark, Structural Research Laboratory, Intern Rapport, I 62, 1979.
- [79.5] Exner, H.: On the effectiveness factor in plastic analysis of concrete. IABSE Colloquium, Copenhagen 1979, Final Report, pp. 35-42.
- [79.6] Nielsen, M.P.: Some examples of lower-bound design of reinforcement in plane stress problems. IABSE Colloquium, Copenhagen 1979, Final Report, pp. 317-324.
- [79.7] Jensen, B.C.: Reinforced Concrete Corbels - some exact solutions. IABSE Colloquium, Copenhagen 1979, Final Report, pp. 293-300.
- [79.8] Jensen, J.F.: Plastic solutions for reinforced concrete beams in shear. IABSE Colloquium, Copenhagen 1979, Final Report, pp 71-78.
- [80.1] Singh, R., Ray, S.P. and Reddy, C.S.: Some tests on reinforced concrete deep beams with and without opening in the web. Indian Concrete Journal, July 1980, pp. 189-194.
- [80.2] Bach, F., Nielsen, M.P. and Bræstrup, M.W.: Shear tests on reinforced concrete T-beams, Series V, U, X, B and S. Technical University of Denmark, Structural Research Laboratory, Report R 120, 1980, pp. 86.
- [80.3] Bræstrup, M.W.: Shear strength of reinforced concrete beams. 3. Edition. Technical University of Denmark, Structural Research Laboratory, Series F, No. 53, 1980, pp. 60.
- [81.1] Batchelor, B. dev. and Kwun, M.: Shear in RC beams without web reinforcement. Journal of the ASCE, ST5, May 1981, pp. 907-921.

- [81.2] Jensen, J.F. and Jensen, B.C.: Forsøg med armerede og uarmerede betonkonsoller. DIAB F: 88, Oct. 1981, pp. 56.
- [81.3] Jensen, J.F.: Plasticitetssteoretiske løsninger for skiver og bjælker af jernbeton. Technical University of Denmark, Structural Research Laboratory, Series R, No. 141, 1981.
- [82.1] Hara, T. and Otsuka, T.: The applicability of plasticity theory on the shear strength of reinforced concrete corbels. Transactions of the Japan Concrete Institute, Vol. 4, 1982, pp. 287-296.
- [82.2] Smith, K.N. and Vantsiotis, A.S.: Shear Strength of deep beams. Journal of the ACI, May-June 1982.
- [82.3] Bræstrup, M.W.: Ten lectures on concrete plasticity. Technical University of Denmark, Structural Research Laboratory, Serie R, No. 159, 1983.
- [82.4] Research group of deep beams: Tests and researches of simple supported reinforced concrete deep beams. Summing-up reports. Internal report to the "Design code for reinforced concrete structures". (In Chinese). Oct. 1982.
- [83.1] Hara, T. and Kitada, Y.: Experimental comparison for the shear failure of reinforced concrete cantilevers with smaller a/d ratios. Transactions of the Japan Concrete Institute, Vol. 5, 1983, pp. 247-254.
- [83.2] Kotsovos, M.D.: Mechanisms of 'shear' failure. Magazine of Concrete Research, Vol. 35, No. 123, June 1983, pp. 99-106.
- [84.1] Feddersen, B. and Nielsen, M.P.: Plastic analysis of reinforced concrete beams in pure bending or pure torsion. Bygningsstatistiske Meddelelser, Vol. 55, No. 2, 1984.
- [84.2] Kotsovos, M.D.: Behavior of reinforced concrete beams with a shear span to depth ratio between 1.0 and 2.5. Journal of the ACI, May-June 1984, pp. 279-286.
- [84.3] Maruyama, K. Sawamura, S. and Maekawa, K.: Shear cracking behaviors of reinforced concrete simple supported beams. Transactions of the Japan Concrete Institute, Vol. 6, 1984, pp. 379-386.
- [84.4] Hara, T.: The shear strength of reinforced concrete deep beams. Transactions of the Japan Concrete Institute, Vol. 6, 1984.
- [84.5] Mphonde, A.G. and Frantz, G.C.: Shear tests of high - and low - strength concrete beams without stirrups. Journal of the ACI, July-Aug. 1984, pp. 350-357.
- [84.6] Nielsen, M.P.: Limit analysis and concrete plasticity. Prentice-Hall, Inc. Englewood Cliffs, New Jersey, 1984.
- [85.1] Chen, G.W.: Some tests of reinforced concrete deep beams. Department of Civil Engineering, Nanjing Institute of Technology, 1985. (to be published).
- [86.1] Pettersson, T.: The shear capacity of prestressed concrete beams in regions of plastic hinges. Nordic Concrete Research publication, No. 5, 1986, pp. 129-140.

- [86.2] Gurlley, C.: Shear in reinforced beams. Civil Engineering Transactions, 1987, The Institute of Engineers, Australia.
- [86.3] Bernhardt, C.J. and Fynboe, C.C.: High strength concrete beams. Nordic Concrete Research publication, No. 5, 1986, pp. 19-26.
- [86.4] Rogowsky, D.M., Macgregor, J.G. and Ong, S.Y.: Tests of reinforced concrete deep beams. Journal of the ACI, July-Aug. 1986, pp. 614-623.
- [86.5] Batchelor, B.V., George, H.K. and Campbell, T.I.: Effectiveness factor for shear in concrete beams. Journal of Structural Engineering, Vol. 112, No. 6, June 1986, pp. 1464-1477.
- [86.6] Rogowsky, D.M. and Macgregor, J.G.: Design of reinforced concrete deep beams. Journal of Concrete International, Aug. 1986, pp. 49-58.
- [86.7] Maruyama, K. Yoshida, T., Mukai, T. and Hashimoto, C.: Some consideration on shear behavior of reinforced concrete beams. Transactions of the Japan Concrete Institute, Vol. 8, 1986, pp. 275-282.
- [86.8] Kotsyvos, M.D.: Behavior of beams with shear span-to-depth ratios greater than 2.5. Journal of the ACI, Nov.-Dec. 1986, pp. 1026-1034.
- [86.9] Subedi, N.K., Vardy, A.E. and Kubota, N.: Reinforced concrete deep beams - some test results. Magazine Concrete Research, Vol. 38, No. 137, Ced. 1986, pp. 206-219.
- [87.1] Kotsyvos, M.D.: Shear failure of reinforced concrete beams. Eng. Struct., Vol. 9, Jan. 1987, pp. 32-38.
- [87.2] Chen, W.F. and Han, D.J.: Plasticity in structural engineering. (To be published).
- [87.3] Lim, T.Y., Paramasivam, P. and Lee, S.L.: Shear and moment capacity of reinforced steel-fibre-concrete beams. Magazine of Concrete Research, Vol. 39, No. 140, Sep. 1987.
- [87.4] Solanki, H. and Sabnis, G.M.: Reinforced concrete corbels - simplified. Journal of the ACI, Sep.-Oct. 1987, pp. 428-432.
- [87.5] Man, S.T. and Hsu, T.T.C.: Shear strength prediction for deep beams with web reinforcement. Journal of the ACI, Nov.-Dec. 1987, pp. 513-523.
- [87.6] Chana, P.S.: Investigation of the mechanism of shear failure of reinforced concrete beams. Magazine of Concrete Research, Vol. 39, No. 141, Dec. 1987, pp. 196-204.

APPENDIX A

TEST DATA OF DEEP BEAMS FAILED IN FLEXURE

BEAM MARK	L0 CM	b CM	h CM	d CM	acc CM	l CM	fc KG/CM2	As CM2	Fy KG/CM2	Vt T
M-III-0	110	12.1	60.3	55.0	55.0	10	198	8.04	2800	21.20
M-III-1	110	12.3	60.2	55.0	55.0	10	198	8.04	2800	20.00
M-III-2	120	12.5	60.3	55.0	45.0	10	301	2.03	3983	9.00
M-III-3	120	12.5	60.5	53.0	45.0	10	301	2.04	3810	7.00
M-III-4	120	12.0	60.5	57.0	45.0	10	301	3.08	2785	9.50
M-III-1	120	12.5	60.5	57.0	45.0	10	301	3.08	2785	9.50
M-III-2	120	12.6	59.1	55.0	45.0	10	293	3.31	3153	11.00
M-III-3	120	12.6	59.8	54.0	45.0	10	293	3.17	4158	14.50
M-III-4	120	12.7	60.4	53.5	45.0	10	293	3.13	4045	14.00
M-III-1	120	12.2	60.9	57.5	45.0	10	313	3.95	2767	13.00
M-III-2	120	13.0	59.5	56.0	45.0	10	313	4.09	3124	15.00
M-III-3	120	12.9	60.6	54.5	45.0	10	313	3.77	3367	14.50
M-III-4	120	12.6	60.7	53.0	45.0	10	313	4.23	4158	20.00
M-IV-3	120	12.8	61.0	55.0	45.0	10	313	5.86	2851	19.00
M-IV-4	120	12.8	59.3	52.0	45.0	10	313	5.03	3367	20.00
M-V-5	120	12.2	119.5	115.0	45.0	10	211	4.64	2712	30.00
M-0.5-17	100	12.0	49.5	47.0	37.5	10	330	2.26	2473	7.00
M-0.5-18	100	12.2	50.2	45.0	37.5	10	330	5.34	2830	17.00
M-0.5-19	100	12.1	50.0	45.0	37.5	10	330	6.16	2851	17.00
M-1.0-2A	100	12.4	100.4	95.0	37.5	10	282	6.04	3040	40.00
M-0.6-1	80	10.5	48.0	45.3	30.0	10	239	3.08	2944	12.00
M-0.6-2	80	10.5	48.6	43.3	30.0	10	239	3.02	2127	9.00
M-0.6-3	80	10.7	48.7	41.2	30.0	10	239	4.02	2127	11.50
M-0.6-4	80	11.1	48.5	44.3	30.0	10	261	4.52	2549	15.00
M-0.6-5	80	10.7	64.4	57.0	32.0	10	261	3.02	2288	12.00
M-0.8-1	80	10.5	64.4	57.0	32.0	10	344	4.02	2288	15.00
M-0.8-2	80	10.5	64.2	53.3	32.0	10	344	4.02	2288	15.00
M-0.8-3	80	10.2	63.2	59.5	32.0	10	344	5.34	2732	25.00
M-0.8-4	80	10.7	80.0	77.4	32.0	10	337	3.08	2662	19.50
M-1.0-1	80	10.3	80.1	71.2	32.0	10	337	3.02	2433	17.50
M-1.0-2	80	10.3	80.1	77.4	32.0	10	337	4.02	2670	25.50
M-1.0-3	80	10.3	80.1	69.0	32.0	10	353	4.02	2288	20.00
M-1.0-4	80	10.3	80.1	75.5	32.0	10	353	6.16	2662	35.00
M-1.0-5	80	10.7	80.0	75.5	32.0	10	321	6.18	2597	40.00
M-1.0-6	80	12.3	80.3	75.5	32.0	10	321	3.16	2468	8.50
M-0.4-1	120	11.1	48.0	46.7	40.0	10	150	4.52	2850	14.00
Z-109	116	8.0	60.0	54.0	42.0	10	150	12.06	2900	50.00
Z-202	90	12.0	90.0	81.0	45.0	15	214	12.06	2900	27.50
Z-204	180	12.0	90.0	81.8	90.0	15	214	12.06	3050	22.50
Z-208	180	12.0	60.0	54.0	90.0	15	253	7.60	2850	36.25
Z-700A	110	10.0	75.0	67.0	37.5	15	341	7.60	2850	36.25
Z-801	125	10.3	75.0	67.5	40.0	20	269	7.79	3067	36.40

APPENDIX A (CONTINUED)

TEST DATA OF DEEP BEAMS FAILED IN FLEXURE

BEAM MARK	L0 CM	b CM	h CM	d CM	acc CM	l CM	fc KG/CM2	As CM2	Fy KG/CM2	Vt T
I-7	150	10.0	60.0	57.0	75.0	12	277	7.60	2620	14.00
I-8	150	10.0	60.0	57.0	50.0	12	277	7.60	2620	21.00
I-9	150	10.0	60.0	57.0	37.5	12	331	7.60	2620	27.50
I-10	150	10.0	60.0	57.0	50.0	12	313	6.28	2580	17.40
I-12	150	10.0	60.0	54.0	50.0	12	318	8.54	2630	23.70
I-14	240	10.0	60.0	57.0	80.0	12	343	7.60	2620	14.20
I-15	240	10.0	60.0	57.0	60.0	12	310	7.60	2620	17.60
A1-1	48	12.0	47.8	43.0	16.0	10	264	1.57	3090	13.00
A1-2	72	12.0	47.5	42.8	24.0	10	264	4.02	2400	17.50
A1-5	72	12.0	47.0	42.3	24.0	10	223	0.77	3170	4.50
A1-5-1	72	12.0	47.5	42.6	24.0	10	240	3.14	3090	16.00
A1-5-2	72	12.8	48.0	43.2	24.0	10	252	4.71	3090	22.00
A1-5-3	72	13.0	48.0	43.2	24.0	10	252	4.71	3090	20.00
A1-5-4	72	12.5	47.5	43.0	24.0	10	248	3.11	2448	12.00
A1-5-5	96	12.5	48.0	43.2	32.0	10	292	1.57	3090	7.00
A2-1	96	13.0	48.0	43.2	32.0	10	207	4.02	2400	13.00
A2-2	96	13.0	47.5	42.7	32.0	10	305	6.28	2650	22.00
A2-3	120	12.0	47.5	42.7	40.0	10	292	1.57	3090	5.00
A2-4	120	12.0	47.0	42.3	40.0	10	207	4.02	2680	11.00
A2-5	120	12.5	47.0	42.3	40.0	10	305	6.28	2680	17.00
A2-6	50	16.0	50.3	45.3	25.0	10	317	4.27	3984	28.00
B1-1	50	16.2	50.0	45.0	25.0	10	309	4.27	3888	25.00
B1-2	50	16.0	50.5	45.0	25.0	10	415	4.27	3918	26.00
B1-3	75	16.0	50.3	45.3	25.0	10	317	4.27	3692	27.00
B1-4	75	16.5	50.0	45.0	37.5	10	309	4.27	3720	19.00
B1-5	75	16.1	50.0	45.0	25.0	10	415	4.27	3741	25.00
F1.5-1	68	15.0	45.0	40.5	22.5	10	425	4.27	2621	20.00
SL-B-2	90	11.0	60.0	56.5	30.0	15	266	3.08	3812	19.00
SL-C-2	90	11.0	45.0	41.5	30.0	15	266	3.08	4612	18.00
SL-D-3	90	11.0	30.0	26.5	30.0	15	266	7.60	4003	19.00
SL-E-1	90	10.0	20.0	15.2	45.0	10	266	8.54	2820	4.50
SL-E-2	90	10.0	20.0	16.5	30.0	10	266	3.08	3141	4.30
SL-E-3	90	10.0	22.5	18.0	30.0	10	266	6.28	2823	7.40

APPENDIX B (CONTINUED)

TEST DATA OF CONVENTIONAL BEAMS FAILED IN SHEAR

BEAM MARK	b IN	h IN	d IN	acc IN	l IN	fc KSI	As IN2	Fy KSI	Vt KIPS
B---14B2	12.00	16.00	14.50	17.50	5.50	2.12	3.220	67.60	82.50
B---14E2	12.00	16.13	14.75	17.50	5.50	1.84	1.014	67.50	62.50
B---14A4	12.00	16.00	14.25	17.50	5.50	3.27	4.272	61.70	115.00
B---14B4	12.00	16.00	14.50	17.50	5.50	3.82	3.220	58.60	112.50
B---14E4	12.00	16.00	14.50	17.50	5.50	4.19	2.150	61.20	115.00
B---14A6	12.00	16.00	14.00	17.50	5.50	6.59	6.431	65.00	202.50
B---14B6	12.00	16.00	14.50	17.50	5.50	6.78	3.220	65.90	175.00
B---21B2	12.00	16.00	14.44	24.50	5.50	2.01	3.220	63.40	53.50
B---21E2	12.00	16.00	14.75	24.50	5.50	1.64	1.014	67.20	47.50
B---21A4	12.00	16.00	14.50	24.50	5.50	4.32	4.272	58.70	117.50
B---21B4	12.00	16.00	14.50	24.50	5.50	3.93	3.220	61.30	89.00
B---21E4	12.00	16.00	14.38	24.50	5.50	3.51	2.150	62.40	90.00
B---21F4	12.00	16.00	14.56	24.50	5.50	4.63	2.150	60.40	90.00
B---21A6	12.00	16.00	14.00	24.50	5.50	4.56	1.953	66.20	95.00
B---21B6	12.00	16.00	14.75	24.50	5.50	6.57	6.431	64.90	130.00
B---28B2	12.00	16.00	14.25	31.50	5.50	2.13	3.220	68.30	45.00
B---28E2	12.13	16.00	14.63	31.50	5.50	1.99	1.014	67.20	29.00
B---28A4	12.00	16.00	14.50	31.50	5.50	3.99	4.272	48.20	72.50
B---28B4	12.00	16.00	14.50	31.50	5.50	4.69	3.220	64.00	57.50
B---28E4	12.00	16.00	14.50	31.50	5.50	4.80	2.150	62.20	60.00
B---28A6	12.13	16.00	13.88	31.50	5.50	6.84	6.431	66.00	75.00
B---40B6	12.00	16.00	14.50	43.50	5.50	6.36	3.220	65.50	72.50
B---56B2	12.00	16.00	14.50	59.50	5.50	5.04	3.220	64.80	35.00
B---56E2	12.00	16.00	14.50	59.50	5.50	2.13	3.220	68.30	22.50
B---56A4	12.00	16.00	14.75	59.50	5.50	3.62	4.272	47.80	31.00
B---56B4	12.00	16.00	14.50	59.50	5.50	3.95	3.220	63.90	27.50
B---56E4	12.00	16.00	14.50	59.50	5.50	4.12	2.150	62.20	24.50
B---56A6	12.13	16.00	14.00	59.50	5.50	5.78	6.431	63.60	40.00
B---56B6	12.00	16.00	14.63	59.50	5.50	6.63	3.220	67.00	17.15
B---70B2	12.00	16.00	14.38	73.50	5.50	2.37	3.220	67.00	20.75
B---70A4	12.00	16.00	14.50	73.50	5.50	3.95	4.272	63.20	29.75
B---84B4	12.00	16.00	14.00	87.50	5.50	6.52	6.431	63.10	40.00
B---113B4	12.00	16.00	14.38	116.50	5.50	3.95	3.220	67.40	25.00
I-----1	8.00	18.00	15.86	24.00	3.50	3.68	3.864	38.70	70.35
I-----2	8.00	18.00	15.86	24.00	3.50	3.33	3.864	38.70	69.85
I-----3	8.00	18.00	15.86	24.00	3.50	3.17	2.391	67.50	58.85
I-----4	8.00	18.00	15.86	24.00	3.50	3.83	2.391	67.50	70.35
I-----5	8.00	18.00	15.86	24.00	3.50	3.73	2.352	71.00	64.85

APPENDIX B (CONTINUED)

TEST DATA OF CONVENTIONAL BEAMS FAILED IN SHEAR

BEAM MARK	b IN	h IN	d IN	acc IN	l IN	fc KSI	As IN2	Fy KSI	Vt KIPS
IIT-----6	8.00	18.00	15.86	24.00	3.50	3.71	2.352	71.00	65.35
IIV-----7	8.00	18.00	15.86	24.00	3.50	3.50	2.361	64.30	65.38
IIV-----8	8.00	18.00	15.86	24.00	3.50	3.61	2.361	64.30	68.35
V-----9	8.00	18.00	15.86	24.00	3.50	3.35	1.476	101.20	50.35
V-----10	8.00	18.00	15.86	24.00	3.50	3.91	1.476	101.20	60.35
VI-----11	8.00	18.00	15.86	24.00	3.50	3.68	1.479	105.20	50.35
VI-----12	8.00	18.00	15.86	24.00	3.50	3.72	1.479	105.20	60.35
V-----13	8.00	18.00	15.86	24.00	3.50	3.25	0.954	103.20	50.00
V-----14	8.00	18.00	15.86	24.00	3.50	3.87	0.954	103.20	50.35
VI-----15	8.00	18.00	15.86	24.00	3.50	3.70	0.951	101.20	40.35
VI-----16	8.00	18.00	15.86	24.00	3.50	3.31	0.951	101.20	42.40
IITIA---17	8.00	18.00	15.86	60.00	3.50	4.24	3.229	73.20	19.80
IITIA---18	8.00	18.00	15.86	60.00	3.50	3.65	3.229	73.20	18.15
VA-----19	8.00	18.00	15.86	60.00	3.50	3.41	1.182	100.00	14.23
VA-----20	8.00	18.00	15.86	60.00	3.50	3.71	1.182	100.00	14.83
VIB---21	8.00	18.00	15.86	45.00	3.50	3.79	1.067	102.50	16.05
VIB---22	8.00	18.00	15.86	45.00	3.50	3.74	1.067	102.50	14.03
VIB---23	8.00	18.00	15.86	45.00	3.50	4.43	1.067	102.50	16.88
VIA---24	8.00	18.00	15.86	60.00	3.50	3.82	0.594	100.90	12.25
VIA---25	8.00	18.00	15.86	60.00	3.50	3.74	0.594	100.90	11.23

APPENDIX B (CONTINUED)

TEST DATA OF CONVENTIONAL BEAMS FAILED IN SHEAR

BEAM MARK	b IN	h IN	d IN	acc IN	l IN	fc KSI	As IN2	Fy KSI	Vt KIPS
R-----1	6.00	12.00	10.70	36.00		3.80	0.630		10.10
R-----2	6.00	12.00	10.70	36.00		3.80	0.940		10.60
R-----3	6.00	12.00	10.70	36.00		3.60	0.900		10.10
R-----7	6.00	12.00	10.70	36.00		4.07	0.940		12.20
D-----2	6.00	12.00	10.70	36.00		4.40	0.940		11.80
3---S---1	6.06	12.00	10.03	30.00	3.00	5.40	0.114	169.00	6.50
IIB-----1	6.00	14.00	12.50	42.00	4.00	3.58	1.148	46.80	10.20
IIB-----2	6.00	14.00	12.25	48.00	4.00	3.03	1.148	46.40	9.15
IIB-----3	6.00	14.00	12.12	54.00	4.00	2.85	1.148	46.60	8.30
IA-----1A	6.00	14.00	12.06	30.00	4.00	3.30	1.148	47.00	13.30
---1-----	6.00	13.00	10.70	16.00	1.50	4.56	1.570	65.80	42.37
---4-----	6.00	13.00	10.70	16.00	1.50	5.19	0.614	56.00	21.37
---7-----	6.00	13.00	10.70	21.40	1.50	4.29	1.570	65.80	22.24
---10-----	6.00	13.00	10.70	21.40	1.50	4.36	0.614	56.00	15.28
A-----1	15.70	39.40	36.80	110.30	6.00	5.28	7.744	62.50	80.70
A-----2	15.70	39.40	36.80	110.30	6.00	4.62	7.744	62.50	73.90
B-----1	7.85	19.70	18.40	55.15	3.00	4.93	1.936	62.50	23.40
B-----2	7.85	19.70	18.40	55.15	3.00	4.50	1.936	62.50	19.60
B-----3	7.85	19.70	18.40	55.15	3.00	5.81	1.936	62.50	19.20
C-----1	3.93	9.85	9.20	27.58	1.50	4.64	0.484	62.50	5.06
C-----2	3.93	9.85	9.20	27.58	1.50	4.64	0.484	62.50	5.39
C-----3	3.93	9.85	9.20	27.58	1.50	4.98	0.484	62.50	6.18
C-----4	3.93	9.85	9.20	27.58	1.50	3.77	0.484	62.50	5.06
C-----5	3.93	9.85	9.20	27.58	1.50	4.06	0.484	62.50	6.06
C-----6	3.93	9.85	9.20	27.58	1.50	5.22	0.484	62.50	6.18
D-----1	2.36	5.91	5.52	16.55	0.90	5.80	0.174	62.50	2.62
D-----2	2.36	5.91	5.52	16.55	0.90	5.80	0.174	62.50	2.72
D-----3	2.36	5.91	5.52	16.55	0.90	5.80	0.174	62.50	2.38
D-----4	2.36	5.91	5.52	16.55	0.90	5.80	0.174	62.50	2.56
S1C1//4	3.94	7.87	6.65	2.66		3.36	0.380	39.85	22.48
S1C2//1	3.94	7.87	6.65	3.33		3.89	0.380	39.85	17.92
S1C2//2	3.94	7.87	6.65	3.99		3.89	0.380	39.85	19.58
S1C2//3	3.94	7.87	6.65	4.66		3.89	0.380	39.85	18.39
S1C2//4	3.94	7.87	6.65	5.32		3.89	0.380	39.85	15.22
S1C3//1	3.94	7.87	6.65	5.99		3.67	0.380	39.85	13.47
S1C3//2	3.94	7.87	6.65	6.65		3.67	0.380	39.85	12.34
S1C3//3	3.94	7.87	6.65	7.32		3.67	0.380	39.85	14.12
S1C3//4	3.94	7.87	6.65	7.98		3.67	0.380	39.85	10.75

APPENDIX B (CONTINUED)

TEST DATA OF CONVENTIONAL BEAMS FAILED IN SHEAR

BEAM MARK	b IN	h IN	d IN	acc IN	l IN	fc KSI	As IN2	Fy KSI	Vt KIPS
T-B-----1	5.91	11.81	9.84	19.69		2.55	0.616	55.47	20.72
T-B-----2	5.91	11.81	9.84	19.69		3.00	0.616	55.47	18.74
T-B-----5	5.91	11.81	9.84	19.69		3.40	0.889	55.47	24.80
T-B-----6	5.91	11.81	9.84	19.69		3.40	0.889	55.47	27.56
T-B-----9	5.91	11.81	9.84	29.53		3.67	0.889	55.47	13.01
T-B-----10	5.91	11.81	9.84	29.53		3.71	0.889	55.47	10.47
B-18-----1	8.00	18.00	15.90	24.00	3.50	3.68	3.880	38.70	70.00
B-18-----2	8.00	18.00	15.90	24.00	3.50	3.33	3.880	38.70	69.50
C-18-----1	8.00	18.00	15.90	24.00	3.50	3.71	2.353	71.00	65.00
C-18-----2	8.00	18.00	15.90	24.00	3.50	3.83	2.391	67.50	70.00
D-18-----1	8.00	18.00	15.90	24.00	3.50	3.72	1.488	105.20	60.00
D-18-----2	8.00	18.00	15.90	24.00	3.50	3.91	1.476	96.90	60.00
E-18-----1	8.00	18.00	15.90	24.00	3.50	3.25	0.954	99.50	49.65
E-18-----2	8.00	18.00	15.90	24.00	3.50	3.87	0.954	99.50	50.00

APPENDIX B (CONTINUED)

TEST DATA OF CORBELS FAILED IN SHEAR

BEAM MARK	b IN	h IN	d IN	acc IN	l IN	fc KSI	As IN2	Fy KSI	Vt KIPS
CO-----2E	8.00	26.00	24.10	[65.1]	2.50	4.44	1.195	44.90	144.79
CO-----3E	8.00	26.00	24.10	6.00	2.50	3.98	1.195	43.00	124.93
CO-----4E	8.00	26.00	24.10	6.00	2.50	4.20	1.195	44.90	145.56
CO-----5E	8.00	18.00	16.10	2.75	2.50	4.01	1.198	44.50	114.50
CO-----6E	8.00	18.00	16.20	6.00	2.50	4.14	0.622	48.10	63.89
CO-----7E	8.00	18.00	16.10	6.00	2.50	4.49	1.198	44.50	109.48
CO-----8E	8.00	26.00	24.10	9.50	2.50	4.58	1.195	46.50	139.97
CO-----9E	8.00	26.00	24.10	9.50	2.50	4.79	1.195	53.30	148.84
CO-----10E	8.00	26.00	24.10	9.50	2.50	4.75	1.195	46.50	127.06

APPENDIX B (CONTINUED)

TEST DATA OF DEEP BEAMS FAILED IN SHEAR

BEAM MARK	b IN	h IN	d IN	acc IN	l IN	fc KSI	As IN2	Fy KSI	Vt KIPS
R10-----1	4.00	18.00	16.00	[73.5]	6.00	4.90	0.620	59.40	100.00
R10-----2	4.00	18.00	16.00	4.80	6.00	5.10	0.620	59.40	100.00
R10-----3	4.00	18.00	16.00	4.80	6.00	4.37	0.620	56.80	82.50
R10-----4	4.00	18.00	16.00	4.80	6.00	4.63	0.620	59.40	90.00
R11-----1	4.00	18.00	16.00	4.00	6.00	4.60	0.400	44.60	87.50
R11-----4	4.00	18.00	16.00	4.00	6.00	4.60	0.620	58.60	102.00
R11-----5	4.00	18.00	16.00	8.00	6.00	4.60	0.620	58.10	90.50
R11-----7	4.00	18.00	16.00	8.00	6.00	5.35	0.880	62.60	109.50
R11-----10	4.00	18.00	16.00	14.40	6.00	5.52	1.200	54.20	66.00
R11-----11	4.00	18.00	16.00	17.00	6.00	4.68	1.200	54.20	61.50
A-----4	3.00	30.00	28.50	[68.2]	4.00	3.96	0.110	46.00	36.50
A-----4R	3.00	30.00	28.50	8.50	4.00	1.78	0.110	46.00	24.40
B-----1	3.00	15.00	13.50	8.50	4.00	2.96	0.307	46.00	15.25
B-----2	3.00	20.00	18.50	8.50	4.00	3.09	0.307	46.00	20.25
B-----3	3.10	22.50	21.00	8.50	4.00	3.60	0.307	46.00	27.80
B-----4	3.10	30.00	28.50	8.50	4.00	4.11	0.307	46.00	42.55
C-----1	3.00	15.00	13.50	8.50	4.00	3.12	0.307	46.00	20.25
C-----2	3.10	20.00	18.50	8.50	4.00	3.54	0.307	46.00	31.60
C-----3	3.00	22.50	21.00	8.50	4.00	2.84	0.307	46.00	26.65
C-----4	3.10	30.00	28.50	8.50	4.00	2.38	0.307	46.00	31.15
K1-----1	3.09	15.00	13.50	13.50	4.00	2.21	0.110	46.00	12.55
G33S11	3.00	9.00	8.00	[65.4]	4.00	3.38	0.400	47.30	19.20
G33S31	3.00	9.00	8.00	8.00	4.00	2.89	0.620	45.20	24.05
OAO-----44	4.00	14.00	12.00	[82.2]	4.00	2.97	0.930	62.50	31.37
OAO-----48	4.00	14.00	12.00	12.00	4.00	3.035	0.930	61.13	30.60
OBO-----49	4.00	14.00	12.00	14.50	4.00	3.145	0.930	61.13	33.50
OCO-----50	4.00	14.00	12.00	18.00	4.00	3.000	0.930	61.13	26.00
ODO-----47	4.00	14.00	12.00	25.00	4.00	2.830	0.930	61.13	16.50

APPENDIX B (CONTINUED)

TEST DATA OF CORBELS FAILED IN SHEAR

BEAM MARK	b CM	h CM	d CM	acc CM	l CM	fc KG/CM2	As CM2	Fy KG/CM2	Vt T
7.5-0.84-3	14.9	24.7	20.0	6.0	3.75	240.5	2.53	3325	18.15
7.5-0.84-5	15.1	25.0	20.0	10.0	3.75	240.5	2.53	3325	14.25
7.5-0.84-7	15.2	23.7	20.0	14.0	3.75	240.5	2.53	3325	10.425
7.5-1.32-3	14.9	24.3	20.0	6.0	3.75	240.5	3.97	3848	18.80
7.5-1.32-5	15.0	24.6	20.0	10.0	3.75	240.5	3.97	3848	18.25
7.5-1.32-7	14.9	24.4	20.0	14.0	3.75	240.5	3.97	3848	12.90
10--0.42-3	15.3	25.0	20.0	6.0	5.00	240.5	1.27	3325	13.50
10--0.84-3	14.9	24.8	20.0	6.0	5.00	240.5	2.53	3325	20.00
10--0.84-5	14.9	24.8	20.0	10.0	5.00	240.5	2.53	3325	15.00
10--0.84-7	14.9	24.9	20.0	14.0	5.00	240.5	2.53	3325	11.50
10--1.32-3	15.5	25.2	20.0	6.0	5.00	240.5	3.97	3848	26.00
10--1.32-5	15.2	24.8	20.0	10.0	5.00	240.5	3.97	3848	18.10
10--1.32-7	15.2	24.6	20.0	14.0	5.00	240.5	3.97	3848	15.00
A-----2	16.4	35.0	25.0	[81.2]	5.0	202.9	4.51	3212	15.09
A-----3	16.4	35.0	25.0	22.5	5.0	177.4	4.02	4864	17.13
A-----4	16.4	35.0	25.0	22.5	5.0	177.4	6.03	4864	23.66
A-----5	16.4	35.0	25.0	22.5	5.0	177.4	8.04	4864	23.55
A-----6	16.2	35.0	25.0	22.5	5.0	177.4	10.04	4864	25.80
B-----2	16.5	35.0	25.0	22.5	5.0	217.2	9.03	3518	27.53
B-----3	16.5	35.0	25.0	22.5	5.0	217.2	8.04	4864	26.51
B-----4	16.5	35.0	25.0	22.5	5.0	217.2	12.05	4864	28.55
B-----5	20.3	52.5	45.0	5.5	5.0	177.4	2.26	3426	33.14
C-----2	20.2	52.5	45.0	5.5	5.0	177.4	3.39	3426	40.79
C-----3	20.3	52.5	45.0	5.5	5.0	107.1	4.52	3589	33.14
C-----4	20.2	52.5	45.0	5.5	5.0	107.1	9.05	3589	40.38
C-----5	20.3	52.5	45.0	7.88	5.0	157.0	10.05	4864	54.04
D-----1	20.5	52.5	45.0	5.0	5.0	157.0	10.06	4864	53.53
D-----2	20.3	52.5	45.0	13.5	5.0	217.2	10.05	4864	45.89
D-----3	20.2	52.5	45.0	22.5	5.0	217.2	10.09	4864	38.24

APPENDIX B (CONTINUED)

TEST DATA OF DEEP BEAMS FAILED IN SHEAR

BEAM MARK	b CM	h CM	d CM	acc CM	l CM	fc KG/CM2	As CM2	Fy KG/CM2	Vt T
II-----0	12.0	90.6	82.0	57.5	12.0	206.0	12.06	2790	30.00
III-----0	12.1	60.3	55.0	45.0	12.0	196.0	8.04	2800	21.20
M---V-----1	12.2	72.0	68.0	45.0	12.0	257.0	3.65	3392	14.00
M---V-----2	12.2	85.1	80.1	45.0	12.0	257.0	4.64	2712	20.00
M---V-----3	12.3	95.4	91.0	45.0	12.0	257.0	4.64	2712	23.00
M---V-----4	12.8	108.4	104.0	45.0	12.0	257.0	4.64	2712	25.00
M---0.8---2A	12.4	80.0	75.0	37.5	12.0	318.0	6.16	2850	28.00
M---1.0---2A	12.4	80.0	75.0	37.5	12.0	313.0	10.18	3820	48.00
M---1.0---3A	12.4	100.4	95.0	37.5	12.0	282.0	6.04	3040	40.00
M---1.0---4A	12.2	80.0	75.0	30.0	12.0	314.0	6.16	2920	37.50
M---1.0---5A	12.0	80.0	75.0	30.0	12.0	355.0	7.82	3060	43.00
M---0.6---3	10.5	48.4	45.0	30.0	12.0	239.0	4.02	3092	17.60
M---0.6---6	10.5	48.5	44.8	30.0	12.0	261.0	5.34	2944	20.50
M---0.6---7	12.4	48.5	44.8	30.0	12.0	258.0	6.16	2859	25.00
M---0.8---3	10.4	64.0	61.5	32.0	12.0	344.0	4.02	2780	19.50
M---0.8---6	10.2	63.2	59.5	32.0	12.0	344.0	5.34	2732	25.00
M---0.8---7	12.4	63.8	58.0	32.0	12.0	359.0	6.78	2434	31.50
M---0.8---8	12.7	64.7	57.8	32.0	12.0	359.0	7.60	2632	30.50
M---0.8---9	12.4	64.5	58.2	32.0	12.0	359.0	8.54	2622	33.00
M---1.0---10	12.4	64.7	59.0	32.0	12.0	359.0	9.10	3286	35.00
M---1.0---11	10.7	80.0	77.4	32.0	12.0	337.0	3.08	2662	19.50
M---1.0---12	10.3	80.1	77.4	32.0	12.0	337.0	4.02	2670	25.50
M---1.0---13	10.7	80.0	75.5	32.0	12.0	353.0	6.16	2662	35.00
M---1.0---14	10.7	80.0	75.8	32.0	12.0	353.0	8.16	3268	33.80
M---1.0---15	12.3	81.0	75.5	32.0	12.0	321.0	7.10	2804	37.50
M---1.0---16	12.3	80.3	75.3	32.0	12.0	321.0	7.10	2804	37.50
M---1.0---17	12.3	81.0	75.8	32.0	12.0	353.0	8.16	3268	33.80
M---1.0---18	12.3	80.3	75.5	32.0	12.0	321.0	6.16	2662	35.00
M---1.0---19	12.5	81.0	73.2	32.0	12.0	353.0	7.60	2597	40.00
M---1.0---20	12.5	81.0	73.2	32.0	12.0	353.0	7.60	2597	40.00
M---1.0---21	12.0	90.0	81.0	45.0	15.0	214.0	12.06	2900	50.00
M---1.0---22	12.0	90.0	81.0	45.0	15.0	214.0	12.06	2900	50.00
M---1.0---23	12.0	90.0	81.0	45.0	15.0	214.0	12.06	2900	50.00
M---1.0---24	12.0	90.0	81.0	45.0	15.0	214.0	12.06	2900	50.00
M---1.0---25	12.0	90.0	81.0	45.0	15.0	214.0	12.06	2900	50.00
M---1.0---26	12.0	90.0	81.0	45.0	15.0	214.0	12.06	2900	50.00
M---1.0---27	12.0	90.0	81.0	45.0	15.0	214.0	12.06	2900	50.00
M---1.0---28	12.0	90.0	81.0	45.0	15.0	214.0	12.06	2900	50.00
M---1.0---29	12.0	90.0	81.0	45.0	15.0	214.0	12.06	2900	50.00
M---1.0---30	12.0	90.0	81.0	45.0	15.0	214.0	12.06	2900	50.00
M---1.0---31	12.0	90.0	81.0	45.0	15.0	214.0	12.06	2900	50.00
M---1.0---32	12.0	90.0	81.0	45.0	15.0	214.0	12.06	2900	50.00
M---1.0---33	12.0	90.0	81.0	45.0	15.0	214.0	12.06	2900	50.00
M---1.0---34	12.0	90.0	81.0	45.0	15.0	214.0	12.06	2900	50.00
M---1.0---35	12.0	90.0	81.0	45.0	15.0	214.0	12.06	2900	50.00
M---1.0---36	12.0	90.0	81.0	45.0	15.0	214.0	12.06	2900	50.00
M---1.0---37	12.0	90.0	81.0	45.0	15.0	214.0	12.06	2900	50.00
M---1.0---38	12.0	90.0	81.0	45.0	15.0	214.0	12.06	2900	50.00
M---1.0---39	12.0	90.0	81.0	45.0	15.0	214.0	12.06	2900	50.00
M---1.0---40	12.0	90.0	81.0	45.0	15.0	214.0	12.06	2900	50.00
M---1.0---41	12.0	90.0	81.0	45.0	15.0	214.0	12.06	2900	50.00
M---1.0---42	12.0	90.0	81.0	45.0	15.0	214.0	12.06	2900	50.00
M---1.0---43	12.0	90.0	81.0	45.0	15.0	214.0	12.06	2900	50.00
M---1.0---44	12.0	90.0	81.0	45.0	15.0	214.0	12.06	2900	50.00
M---1.0---45	12.0	90.0	81.0	45.0	15.0	214.0	12.06	2900	50.00
M---1.0---46	12.0	90.0	81.0	45.0	15.0	214.0	12.06	2900	50.00
M---1.0---47	12.0	90.0	81.0	45.0	15.0	214.0	12.06	2900	50.00
M---1.0---48	12.0	90.0	81.0	45.0	15.0	214.0	12.06	2900	50.00
M---1.0---49	12.0	90.0	81.0	45.0	15.0	214.0	12.06	2900	50.00
M---1.0---50	12.0	90.0	81.0	45.0	15.0	214.0	12.06	2900	50.00
M---1.0---51	12.0	90.0	81.0	45.0	15.0	214.0	12.06	2900	50.00
M---1.0---52	12.0	90.0	81.0	45.0	15.0	214.0	12.06	2900	50.00
M---1.0---53	12.0	90.0	81.0	45.0	15.0	214.0	12.06	2900	50.00
M---1.0---54	12.0	90.0	81.0	45.0	15.0	214.0	12.06	2900	50.00
M---1.0---55	12.0	90.0	81.0	45.0	15.0	214.0	12.06	2900	50.00
M---1.0---56	12.0	90.0	81.0	45.0	15.0	214.0	12.06	2900	50.00
M---1.0---57	12.0	90.0	81.0	45.0	15.0	214.0	12.06	2900	50.00
M---1.0---58	12.0	90.0	81.0	45.0	15.0	214.0	12.06	2900	50.00
M---1.0---59	12.0	90.0	81.0	45.0	15.0	214.0	12.06	2900	50.00
M---1.0---60	12.0	90.0	81.0	45.0	15.0	214.0	12.06	2900	50.00
M---1.0---61	12.0	90.0	81.0	45.0	15.0	214.0	12.06	2900	50.00
M---1.0---62	12.0	90.0	81.0	45.0	15.0	214.0	12.06	2900	50.00
M---1.0---63	12.0	90.0	81.0	45.0	15.0	214.0	12.06	2900	50.00
M---1.0---64	12.0	90.0	81.0	45.0	15.0	214.0	12.06	2900	50.00
M---1.0---65	12.0	90.0	81.0	45.0	15.0	214.0	12.06	2900	50.00
M---1.0---66	12.0	90.0	81.0	45.0	15.0	214.0	12.06	2900	50.00
M---1.0---67	12.0	90.0	81.0	45.0	15.0	214.0	12.06	2900	50.00
M---1.0---68	12.0	90.0	81.0	45.0	15.0	214.0			

APPENDIX B (CONTINUED)

TEST DATA OF DEEP BEAMS FAILED IN SHEAR

BEAM MARK	b CM	h CM	d CM	acc CM	l CM	fc KG/CM2	AS CM2	Fy KG/CM2	Vt T
801	10.3	75.0	67.5	40.0	20.0	269.0	7.79	3067	36.40
802	10.5	75.0	67.5	40.0	20.0	319.0	7.79	3067	38.00
803	10.3	75.0	67.5	40.0	20.0	278.0	7.79	3067	35.00
803A	10.0	75.0	67.5	40.0	20.0	263.0	7.79	3067	33.50
802A	10.0	75.0	67.5	40.0	20.0	317.0	7.79	3067	36.50
801A	10.7	75.0	67.5	40.0	20.0	324.0	7.79	3067	37.50
804A	10.7	75.0	67.5	40.0	20.0	267.0	7.79	3067	35.00
805A	10.4	75.0	67.5	70.0	15.0	273.0	7.79	3067	21.80
806A	10.5	75.0	67.5	70.0	15.0	252.0	7.79	3067	21.80
I-----1	10.0	60.0	57.0	45.0	12.0	236.0	7.72	2620	18.10
I-----2	10.0	60.0	57.0	30.0	12.0	284.0	7.72	2620	24.05
I-----3	10.0	60.0	57.0	22.5	12.0	283.0	7.72	2620	40.10
I-----4	10.0	60.0	57.0	30.0	12.0	330.0	6.34	2580	35.00
I-----5	10.0	60.0	57.0	30.0	12.0	248.0	9.78	2440	29.25
I-----6	10.0	60.0	54.0	30.0	12.0	298.0	8.85	2630	25.00
I-----7	10.0	60.0	57.0	75.0	12.0	277.0	7.72	2620	14.00
I-----8	10.0	60.0	57.0	50.0	12.0	276.0	7.72	2620	21.00
I-----9	10.0	60.0	57.0	37.5	12.0	331.0	7.72	2620	27.50
I-----10	10.0	60.0	57.0	50.0	12.0	348.0	6.34	2580	17.40
I-----11	10.0	60.0	57.0	50.0	12.0	297.0	9.78	2440	23.75
I-----12	10.0	60.0	54.0	50.0	12.0	318.0	8.85	2630	23.70
I-----13	10.0	60.0	57.0	110.0	12.0	286.0	7.72	2620	6.90
I-----14	10.0	60.0	57.0	80.0	12.0	348.0	7.72	2620	14.20
I-----15	10.0	60.0	57.0	60.0	12.0	310.0	7.72	2620	17.55
II-----2	10.0	75.0	69.0	25.0	12.0	317.0	10.17	2920	31.25
II-----3	10.0	75.0	69.0	75.0	12.0	308.0	15.20	2620	27.50
II-----4	10.0	75.0	69.0	90.0	12.0	301.0	15.20	2620	21.60
II-----5	10.0	75.0	69.0	102.5	12.0	326.0	15.20	2620	19.50
II-----6	10.0	75.0	69.0	25.0	12.0	288.0	8.04	2900	34.40
II-----9	10.0	75.0	69.0	50.0	12.0	362.0	10.17	2920	25.50
II-----10	10.0	75.0	69.0	50.0	12.0	277.0	12.57	2670	25.50
II-----11	10.0	75.0	69.0	12.0	12.0	345.0	15.20	2680	31.00
II-----21	10.0	75.0	69.0	15.0	12.0	225.0	12.57	2670	25.50
II-----22	10.0	75.0	69.0	50.0	21.0	317.0	12.57	2670	36.00
II-----23	10.0	75.0	69.0	50.0	15.0	389.0	12.57	2670	36.00
II-----24	10.0	75.0	69.0	50.0	12.0	285.0	6.16	2770	28.00
A1.5-----7A	13.0	48.0	43.2	24.0	10.0	252.0	4.71	3090	22.00
A1.5-----7A	12.0	48.0	43.2	24.0	10.0	252.0	4.71	3090	20.00
B1-----1	16.0	50.3	45.3	25.0	10.0	317.0	4.27	3984	28.00
B1-----2	16.2	50.0	45.0	25.0	10.0	309.0	4.27	3888	25.00
B1-----3	16.0	50.5	45.0	25.0	10.0	415.0	4.27	3918	26.00
B1.5-----1	16.0	50.3	45.3	25.0	10.0	317.0	4.27	3692	27.00

APPENDIX B (CONTINUED)

TEST DATA OF DEEP BEAMS FAILED IN SHEAR

BEAM MARK	b CM	h CM	d CM	acc CM	l CM	fc KG/CM2	AS CM2	Fy KG/CM2	Vt T
SL---A---1	10.0	90.0	85.5	45.0	10.0	223.0	9.36	2823	28.00
SL---A---2	11.0	90.0	86.5	30.0	15.0	223.0	3.08	3141	28.50
SL---A---3	10.0	90.0	85.5	30.0	10.0	223.0	8.54	2823	30.00
SL---A---4	11.0	90.0	86.5	30.0	15.0	223.0	7.60	2473	37.90
SL---A---5	11.0	90.0	86.5	30.0	20.0	223.0	7.60	2473	42.50
SL---A---6	10.0	90.0	86.5	30.0	10.0	266.0	7.60	2473	32.50
SL---B---1	11.0	60.0	55.5	45.0	15.0	223.0	9.36	3141	29.00
SL---B---3	10.0	60.0	56.5	30.0	15.0	223.0	6.28	2823	23.00
SL---B---4	10.0	60.0	56.5	30.0	15.0	223.0	6.28	2823	25.60
SL---B---5	10.0	60.0	56.5	30.0	15.0	223.0	6.28	2823	25.00
SL---C---1	10.0	45.0	40.5	45.0	15.0	266.0	8.54	2823	19.00
SL---C---2	10.0	45.0	41.5	30.0	15.0	266.0	3.08	4612	18.00
SL---C---3	11.0	45.0	41.5	30.0	10.0	266.0	7.60	2473	26.00
SL---C---4	11.0	45.0	41.5	30.0	10.0	223.0	6.28	2823	19.60
SL---D---1	11.0	30.0	25.5	45.0	15.0	223.0	8.54	2823	11.00
SL---D---3	11.0	30.0	26.5	30.0	15.0	266.0	7.60	4003	19.00
SL---E---1	10.0	20.0	16.5	45.0	10.0	266.0	8.54	2823	4.50

APPENDIX C

TEST DATA OF BEAMS SUBJECTED TO SHEAR AND NORMAL COMPRESSION

BEAM MARK	b IN	h IN	d IN	acc IN	l IN	fc KSI	as IN2	Fy KSI	Vt KIPS	N KIPS
A-----1	6.00	12.00	10.00	23.00	6.00	4.07	0.60	66.50	16.50	0.00
A-----2	6.00	12.00	10.00	33.00	6.00	4.57	0.60	68.00	9.40	0.00
A-----3	6.00	12.00	10.00	43.00	6.00	2.82	0.60	65.60	7.70	0.00
A-----4	6.00	12.00	10.00	53.00	6.00	3.89	0.60	66.60	7.90	0.00
B-----1	6.00	12.00	10.00	23.00	6.00	3.78	0.60	66.50	25.70	20.00
B-----2	6.00	12.00	10.00	33.00	6.00	4.14	0.60	66.50	14.75	20.00
B-----3	6.00	12.00	10.00	43.00	6.00	3.82	0.60	57.10	10.90	20.00
B-----4	6.00	12.00	10.00	53.00	6.00	4.10	0.60	66.50	9.45	20.00
A-----11	6.00	12.00	10.00	23.00	6.00	4.10	2.00	49.50	23.25	0.00
A-----12	6.00	12.00	10.00	33.00	6.00	3.87	2.00	45.50	13.25	0.00
A-----13	6.00	12.00	10.00	43.00	6.00	3.21	2.00	57.00	10.55	0.00
A-----14	6.00	12.00	10.00	53.00	6.00	3.99	2.00	52.80	12.30	0.00
A-----15	6.00	12.00	10.00	63.00	6.00	3.63	2.00	48.10	11.10	0.00
B-----11	6.00	12.00	10.00	23.00	6.00	3.66	2.00	48.10	32.25	20.00
B-----12	6.00	12.00	10.00	33.00	6.00	3.93	2.00	56.80	16.85	20.00
B-----13	6.00	12.00	10.00	43.00	6.00	4.05	2.00	51.40	13.90	20.00
B-----14	6.00	12.00	10.00	53.00	6.00	4.25	2.00	52.60	11.90	20.00
B-----15	6.00	12.00	10.00	63.00	6.00	4.11	2.00	47.30	10.55	20.00

APPENDIX C (CONTINUED)

TEST DATA OF KNEE FRAMES [57.1]

BEAM MARK	b IN	h IN	d IN	a IN	fc KSI	as IN2	Fy KSI	Vt KIPS	N KIPS
F-21B2	12.00	16.50	14.50	21.60	1.47	3.262	54.60	46.30	46.30
F21B2R	12.00	16.50	14.50	21.60	2.04	3.262	54.60	63.60	63.60
F21-B4	12.00	16.50	14.50	21.60	4.31	3.262	54.80	83.10	83.10
F21B4R	12.00	16.50	14.50	21.60	4.23	3.262	54.80	91.90	91.90
F21-C4	12.00	16.25	14.50	21.60	3.86	2.769	62.90	62.90	62.90
F21C4R	12.00	16.25	14.75	21.60	4.48	2.769	64.80	99.70	99.70
F21-D4	12.00	16.25	14.50	21.60	4.57	2.114	65.60	100.10	100.10
F21-E4	12.25	16.50	15.00	21.60	4.45	1.470	62.60	91.20	91.20
F21-F4	12.00	16.50	14.50	21.60	4.35	1.299	62.00	77.10	77.10
F21-A6	12.00	16.50	14.50	21.60	7.02	4.113	54.60	141.40	141.40
F21-B6	12.00	16.50	14.50	21.60	6.52	3.262	54.80	140.00	140.00
F38-B2	12.00	16.50	14.25	38.60	1.80	3.262	54.20	25.50	25.50
F38-E2	12.00	16.50	14.50	38.60	2.05	0.866	56.30	20.60	20.60
F38-B4	12.00	16.38	14.75	38.60	4.55	3.262	55.90	38.90	38.90
F38-D4	12.13	16.38	15.00	38.60	3.90	2.401	53.40	38.00	38.00
F38-E4	12.00	16.50	14.88	38.60	4.66	1.631	53.40	33.20	33.20
F38-A6	12.00	16.50	14.00	38.60	6.61	4.885	52.80	53.00	53.00
F38-B6	12.00	16.50	15.00	38.60	6.03	3.262	54.90	44.50	44.50
F55-B2	12.00	16.50	14.50	55.60	1.72	3.262	54.30	21.20	21.20
F55-A4	12.13	16.13	14.63	55.60	3.83	3.514	58.80	33.90	33.90
F55-B4	12.00	16.50	15.00	55.60	4.28	3.262	55.70	28.30	28.30
F55-D4	12.13	16.13	15.00	55.60	3.71	2.638	62.70	28.30	28.30
F55-E4	12.13	16.88	15.25	55.60	4.11	1.732	61.30	29.30	29.30
F55-A6	12.00	16.50	13.75	55.60	6.10	5.484	55.00	42.40	42.40
F55-B6	12.00	16.50	14.50	55.60	6.34	3.262	54.50	31.80	31.80
F70-B2	12.00	16.50	14.25	70.00	2.09	3.262	55.50	20.50	20.50
F70-A4	12.00	16.13	14.25	70.00	4.21	3.692	54.50	31.80	31.80
F70-A6	12.00	16.50	14.50	70.00	5.61	5.808	51.40	38.90	38.90
F84-B4	12.00	16.38	14.75	84.00	4.30	3.262	55.30	29.30	29.30

APPENDIX C (CONTINUED)

TEST DATA OF CORBELS SUBJECTED TO SHEAR AND NORMAL TENSION

BEAM MARK	b IN	h IN	d IN	acc 1 IN	acc 1 IN	fc KSI	As IN ²	Fy KSI	Vt KIPS	N/Vt %
CO-104	8.00	18.0	16.20	2.75	1.50	4.21	0.622	45.70	56.25	0.50
CO-105	8.00	22.0	20.20	2.75	1.50	3.86	0.614	45.70	62.05	0.50
CO-106	8.00	26.0	24.20	2.75	1.50	4.04	0.620	47.30	69.31	0.50
CO-107	8.00	18.0	16.10	2.75	1.50	4.08	1.198	48.50	79.98	0.50
CO-108	8.00	22.0	20.10	2.75	1.50	3.86	1.206	47.70	82.81	0.50
CO-109	8.00	26.0	24.10	2.75	1.50	4.24	1.195	48.20	100.06	0.50
CO-110	8.00	18.0	16.10	2.75	1.50	4.25	2.396	47.50	120.04	0.50
CO-111	8.00	22.0	20.10	2.75	1.50	3.90	2.396	48.80	127.51	0.50
CO-112	8.00	26.0	24.10	2.75	1.50	4.31	2.391	48.70	139.97	0.50
CO-116	8.00	18.0	16.10	6.00	1.50	3.87	1.198	48.30	62.21	0.50
CO-117	8.00	22.0	20.10	6.00	1.50	3.88	1.206	44.70	72.52	0.50
CO-118	8.00	26.0	24.10	6.00	1.50	4.24	1.195	48.40	87.53	0.50
CO-119	8.00	18.0	16.10	6.00	1.50	4.21	2.396	48.50	104.97	0.50
CO-120	8.00	22.0	20.10	6.00	1.50	4.13	2.396	47.70	114.97	0.50
CO-121	8.00	26.0	24.10	6.00	1.50	3.97	2.391	48.20	114.91	0.50
CO-129	8.00	26.0	24.10	10.00	1.50	4.12	1.195	47.00	64.97	0.50
CO-135	8.00	14.0	12.10	3.00	1.50	6.43	1.200	46.80	75.02	0.75
CO-141	8.00	26.0	24.10	2.75	1.50	4.00	1.195	45.30	64.97	1.00
CO-142	8.00	18.0	16.10	2.75	1.50	4.27	2.396	44.30	85.01	1.00
CO-143	8.00	22.0	20.10	2.75	1.50	4.11	2.396	47.20	92.46	1.00
CO-144	8.00	26.0	24.10	2.75	1.50	4.25	2.391	48.80	102.57	1.00
CO-151	8.00	18.0	16.10	6.00	1.50	4.23	2.396	45.30	69.94	1.00
CO-152	8.00	22.0	20.10	6.00	1.50	4.13	2.396	48.50	82.49	1.00
CO-169	8.00	14.0	12.10	3.00	1.50	6.65	2.401	46.80	95.15	1.25

APPENDIX D

TEST DATA OF PRESTRESSED CONCRETE BEAMS FAILED IN SHEAR

BEAM MARK	b IN	h IN	d IN	Ac IN ²	acc 1 IN	fc KSI	As IN ²	Fy KSI	Fse KIPS	Vt KIPS
A-----2	2.00	9.00	7.90	34.00	36.00	4.400	0.119	5.120	20.50	5.600
A-----4	2.00	9.00	7.90	34.00	36.00	6.480	0.119	5.120	22.30	5.900
A-----5	2.00	9.00	7.90	34.00	18.00	6.480	0.119	5.200	23.00	11.000
A-----6	2.00	9.00	7.90	34.00	18.00	5.200	0.119	5.200	23.80	11.800
A-----7	2.00	9.00	7.90	34.00	18.00	5.200	0.119	5.200	22.00	12.000
A-----8	2.00	9.00	7.90	34.00	18.00	5.120	0.119	5.120	23.50	11.200
A-----9	2.00	9.00	7.90	34.00	18.00	4.960	0.119	5.120	24.50	10.600
A-----10	2.00	9.00	7.90	34.00	18.00	4.960	0.119	5.120	24.70	11.200
A-----11	2.00	9.00	7.90	34.00	18.00	5.120	0.119	5.120	23.90	9.000
A-----12	2.00	9.00	7.90	34.00	18.00	4.960	0.119	5.120	24.70	10.400
A-----13	2.00	9.00	7.90	34.00	18.00	6.080	0.119	5.120	22.90	14.500
A-----14	2.00	9.00	7.90	34.00	18.00	4.960	0.119	5.120	25.60	13.600
A-----15	2.00	9.00	7.90	34.00	18.00	5.120	0.119	5.120	24.70	13.800
A-----16	2.00	9.00	7.90	34.00	18.00	5.040	0.119	5.040	25.00	12.600
A-----17	2.00	9.00	7.90	34.00	36.00	5.600	0.119	5.600	24.70	7.200
A-----18	2.00	9.00	7.90	34.00	36.00	6.000	0.119	5.600	23.90	7.500
A-----19	2.00	9.00	7.90	34.00	36.00	5.600	0.119	5.600	22.60	7.000
A-----20	2.00	9.00	7.90	34.00	36.00	6.400	0.119	5.920	23.20	7.800
A-----21	2.00	9.00	7.90	34.00	36.00	5.840	0.119	5.840	23.80	7.700
A-----22	2.00	9.00	7.90	34.00	36.00	5.760	0.119	5.760	23.50	7.200
A-----23	2.00	9.00	7.90	34.00	27.00	6.240	0.119	5.440	24.80	10.100
A-----24	2.00	9.00	7.90	34.00	27.00	5.440	0.119	5.440	23.30	9.000
A-----25	2.00	9.00	7.90	34.00	27.00	5.920	0.119	5.920	24.70	10.000
A-----26	2.00	9.00	7.90	34.00	27.00	5.200	0.119	5.200	24.00	9.000
B-----2	2.00	12.00	10.70	40.00	36.00	5.920	0.222	7.040	32.80	10.900
B-----3	2.00	12.00	10.70	40.00	18.00	7.040	0.222	7.040	33.70	18.000
B-----4	2.00	12.00	10.70	40.00	27.00	7.200	0.222	7.200	36.00	14.800
B-----5	2.00	12.00	10.70	40.00	18.00	5.600	0.222	7.440	32.40	17.600
B-----6	2.00	12.00	10.70	40.00	18.00	7.440	0.222	7.440	31.90	22.400
B-----7	2.00	12.00	10.70	40.00	18.00	7.200	0.222	7.200	32.80	14.300
B-----8	2.00	12.00	10.70	40.00	27.00	7.200	0.222	7.200	32.80	14.300
B-----9	2.00	12.00	10.70	40.00	36.00	5.920	0.222	5.920	32.20	8.600
B-----10	2.00	12.00	10.70	40.00	12.00	7.520	0.222	7.520	33.80	33.800
B-----102	2.00	12.00	10.70	40.00	18.00	7.520	0.222	7.520	33.80	21.500
C-----1	2.00	12.00	10.70	40.00	18.00	6.160	0.222	6.160	32.40	19.300
C-----2	2.00	12.00	10.70	40.00	12.00	6.720	0.222	6.720	33.10	31.500
C-----3	2.00	12.00	10.70	40.00	24.00	6.160	0.222	6.160	33.70	15.000
C-----4	2.00	12.00	10.70	40.00	15.00	7.040	0.222	7.040	32.10	14.000
C-----5	2.00	12.00	10.70	40.00	15.00	7.040	0.222	7.040	35.20	24.400
C-----61	2.00	12.00	10.70	40.00	12.00	7.200	0.222	7.200	35.20	37.500
C-----62	2.00	12.00	10.70	40.00	12.00	7.200	0.222	7.200	35.20	30.300

APPENDIX D (CONTINUED)

TEST DATA OF PRESTRESSED CONCRETE BEAMS FAILED IN SHEAR

BEAM MARK	b IN	h IN	d IN	Ac IN ²	acc IN	I IN	fc KSI	As IN ²	Fy KSI	Fse KIPS	Vt KIPS
C---72	2.00	12.00	10.70	40.00	24.00	[65.5]	7.200	0.222		33.70	16.800
C---81	2.00	12.00	10.70	40.00	18.00		6.880	0.222		33.40	18.200
C---82	2.00	12.00	10.70	40.00	18.00		6.880	0.222		33.40	18.900
C---83	2.00	12.00	10.70	40.00	18.00		6.880	0.222		33.40	21.900
D---1	2.50	12.00	10.70	44.00	36.00		5.760	0.222		34.00	13.300
D---2	2.50	12.00	10.70	44.00	42.00		6.560	0.222		33.00	11.300
E---1	3.00	12.00	10.70	48.00	30.00		6.320	0.222		32.00	12.900
E---2	3.00	12.00	10.70	48.00	30.00		7.200	0.222		32.80	15.000
S---2	4.00	12.00	9.90	48.00	24.00	[63.3]	5.630	0.796		13.10	23.750
S---3	2.00	12.00	10.50	36.00	42.50		5.380	0.442		12.30	10.550
S---4	2.00	12.00	10.50	36.00	42.50		5.060	0.994		12.30	14.750
S---5	2.00	12.00	10.50	36.00	42.50		5.100	0.601		16.60	13.000
S---7	2.00	12.00	10.50	36.00	36.00		4.900	0.785		18.80	16.950
S---8	2.00	12.00	10.10	36.00	55.00		4.150	0.601		29.20	8.200
S---9	1.90	12.00	10.10	35.40	50.80		4.430	0.785		28.90	11.000
S---10	1.30	12.00	10.00	32.40	55.00		4.430	0.785		27.60	7.700
S---11	1.90	12.00	10.10	35.40	55.00		4.730	0.442		22.40	8.600
S---12	1.40	12.00	10.10	33.00	55.00		4.730	0.601		22.50	7.600
S---13	1.30	12.00	10.10	32.40	55.00		5.220	0.442		21.30	8.450
S---14	2.00	12.00	10.10	36.00	45.00		4.390	0.785		21.80	11.400
S---15	2.00	12.00	10.00	36.00	45.00		4.040	0.442		21.90	9.650
S---16	2.00	12.00	10.00	36.00	45.00		4.930	0.601		22.10	10.750
S---17	1.30	12.10	10.30	32.70	45.00		5.420	0.785		18.20	7.500
S---18	1.30	12.00	10.10	32.40	45.00		4.350	0.601		20.70	7.400
S---19	2.00	12.00	10.10	36.00	37.00		4.350	0.785		20.60	11.100
S---20	1.30	12.00	10.00	32.40	45.00		4.080	0.442		23.30	7.500
S---21	2.00	12.00	10.10	36.00	37.00		4.080	0.442		24.60	12.000
S---22	1.40	12.00	10.30	33.00	37.00		3.480	0.785		19.50	8.500
S---24	1.40	12.00	10.10	33.00	37.00		5.350	0.442		19.90	8.150
S---25	2.10	12.00	10.10	36.60	37.00		5.350	0.601		20.80	11.900
S---26	1.40	12.00	10.00	33.00	37.00		5.150	0.601		20.00	8.350
S---27	2.00	12.00	10.10	36.00	28.00		5.130	0.785		19.40	14.900
S---29	2.00	12.00	10.10	36.00	28.00		4.140	0.602		18.40	14.500
S---30	2.00	12.00	10.10	36.00	28.00		5.100	0.440		23.70	17.700
S---32	1.40	12.00	10.00	33.00	28.00		4.670	0.443		18.30	9.100
S---34	1.10	12.00	10.10	30.60	28.00		4.910	0.602		18.30	10.900
S---35	1.30	12.10	10.30	31.93	28.00		5.700	0.787		17.60	13.300
S---36	1.20	12.10	10.30	31.32	28.00		5.180	0.194		14.50	6.700

APPENDIX D (CONTINUED)

TEST DATA OF PRESTRESSED CONCRETE BEAMS FAILED IN SHEAR

BEAM MARK	b IN	h IN	d IN	Ac IN ²	acc IN	I IN	fc KSI	As IN ²	Fy KSI	Fse KIPS	Vt KIPS
S---42	2.10	6.00	5.00	17.10	20.00	[63.3]	6.330	0.559		12.40	7.050
S---43	2.20	6.00	4.80	17.40	20.00		7.010	0.785		11.70	6.500
S---44	1.20	12.20	10.40	32.64	28.00		4.710	0.118		11.30	6.850
S---46	3.10	6.00	4.30	18.60	20.00		4.790	0.119		11.80	3.950
S---48	3.10	6.00	4.00	18.60	20.00		4.790	0.119		14.10	4.200
S---49	1.30	12.00	10.00	32.40	28.00		5.260	0.443		24.10	8.050
S---50	1.40	11.80	9.40	33.92	28.00		5.740	0.441		24.20	10.050
S---51	1.30	12.00	10.00	32.40	28.00		5.300	0.443		24.60	9.600
S---52	1.10	12.20	10.40	30.82	28.00		4.910	0.441		22.70	9.700
S---53	1.20	12.00	10.00	31.80	28.00		5.500	0.443		22.70	9.050
S---54	1.20	12.00	10.00	31.80	28.00		5.260	0.443		24.00	8.250
P---1	1.50	10.04	7.05	40.00	20.40	[60.3]	4.800	0.314		36.00	12.290
P---2	1.50	10.04	7.05	40.00	30.20		4.800	0.314		36.00	7.850
P---3	1.50	9.57	6.57	36.60	30.20		4.240	0.314		34.20	6.750
P---4	1.50	9.57	6.57	36.60	15.10		4.240	0.314		34.20	12.800
P---5	1.50	9.06	6.10	33.00	15.30		4.160	0.314		36.00	12.880
P---6	1.50	9.06	6.10	33.00	29.90		4.160	0.314		36.00	6.020
P---7	1.50	10.00	7.09	34.50	14.90		4.280	0.314		35.90	15.550
P---8	1.50	10.00	7.09	34.50	29.80		4.280	0.314		35.90	7.630
P---9	1.50	9.92	7.05	36.70	29.60		4.400	0.314		38.00	7.150
P---10	1.50	9.92	7.05	36.70	14.80		4.400	0.314		38.00	16.550
P---11	2.40	9.80	6.93	43.40	14.60		4.720	0.314		36.45	20.800
P---12	2.45	9.80	6.93	43.40	29.10		4.720	0.314		36.45	11.000
P---13A	2.00	9.92	6.97	41.90	14.60		4.480	0.314		36.00	18.000
P---13B	2.00	9.92	6.97	41.90	30.00		4.480	0.314		36.00	9.160
P---14	2.00	9.92	6.97	41.90	20.20		4.480	0.314		36.00	13.650
P---15A	1.50	10.04	7.05	40.00	14.80		4.040	0.314		36.00	14.450
P---15B	1.50	10.04	7.05	40.00	30.30		4.040	0.314		36.00	7.250
P---16	1.50	10.04	7.05	40.00	45.10		4.040	0.314		36.00	5.320
P---17A	1.50	10.04	7.05	40.00	14.80		4.800	0.314		20.00	14.700
P---17B	1.50	10.04	7.05	40.00	30.30		4.800	0.314		20.00	6.990
P---18	1.50	10.04	7.05	40.00	45.10		4.800	0.314		20.00	4.480
P---19	1.50	10.04	7.05	40.00	14.80		4.120	0.314		0.00	10.000
P---20	1.50	10.04	7.05	40.00	30.30		4.120	0.314		0.00	4.650
P---21A	1.50	10.04	7.05	40.00	14.80		4.680	0.220		25.00	14.620
P---21B	1.50	10.04	7.05	40.00	30.30		4.680	0.222		25.00	7.070
P---22	1.50	10.04	7.05	40.00	45.10		4.680	0.314		25.00	4.800
P---23A	1.38	10.08	7.09	39.60	14.90		4.640	0.157		18.50	12.570
P---23B	1.38	10.08	7.09	39.60	30.50		4.640	0.157		18.50	6.000
P---24	1.44	10.04	7.05	40.00	45.10		4.640	0.157		18.50	7.200
P---25	2.00	9.92	6.97	41.90	39.70		4.480	0.314		36.00	7.620

APPENDIX D (CONTINUED)

TEST DATA OF PRESTRESSED CONCRETE BEAMS FAILED IN SHEAR

BEAM MARK	p	h	d	Ac	acc	l	fc	As	Fy	Fse	Vt
	IN	IN	IN	IN2	IN	IN	KSI	IN2	KSI	KIPS	KIPS
P--26A	2.05	9.92	6.97	41.90	44.60		4.720	0.314		36.00	7.800
P--26B	2.10	9.92	6.97	41.90	49.50		4.720	0.314		36.00	7.240
						[60.9]	(CONTINUED)				
B3001A	1.97	9.84	8.90	40.92	25.59	5.9	4.509	0.198	217.6	0.00	5.630
B3001B	1.97	9.84	8.90	40.92	25.59	5.9	4.509	0.198	217.6	0.00	6.512
B3002A	1.97	9.84	8.90	40.92	25.59	5.9	3.513	0.198	217.6	14.09	10.141
B3002B	1.97	9.84	8.90	40.92	25.59	5.9	3.513	0.198	217.6	14.09	9.700
B3003A	1.97	9.84	8.90	40.92	25.59	5.9	5.586	0.198	217.6	33.25	9.938
B3003B	1.97	9.84	8.90	40.92	25.59	5.9	5.586	0.198	217.6	33.25	9.938
B3004A	1.97	9.84	8.90	40.92	25.59	5.9	7.157	0.198	217.6	51.84	11.260
B3004B	1.97	9.84	8.90	40.92	25.59	5.9	7.157	0.198	217.6	51.84	11.900
B4501A	1.97	9.84	8.90	40.92	35.43	5.9	5.874	0.297	217.6	0.00	4.483
B4501B	1.97	9.84	8.90	40.92	35.43	5.9	5.874	0.297	217.6	0.00	4.311
B4502A	1.97	9.84	8.90	40.92	35.43	5.9	6.542	0.297	217.6	19.96	8.230
B4502B	1.97	9.84	8.90	40.92	35.43	5.9	6.542	0.297	217.6	19.77	8.230
B4503A	1.97	9.84	8.90	40.92	35.43	5.9	6.577	0.297	217.6	32.78	10.949
B4503B	1.97	9.84	8.90	40.92	35.43	5.9	6.577	0.297	217.6	34.04	11.219
B4504A	1.97	9.84	8.90	40.92	35.43	5.9	6.528	0.297	217.6	50.01	12.615
B4504B	1.97	9.84	8.90	40.92	35.43	5.9	6.528	0.297	217.6	48.98	13.154
B6001A	1.97	9.84	8.90	40.92	62.99	5.9	8.576	0.363	217.6	45.74	7.992
B6001B	1.97	9.84	8.90	40.92	51.18	5.9	8.576	0.363	217.6	45.74	8.971
B6002A	1.97	9.84	8.90	40.92	39.37	5.9	8.320	0.363	217.6	45.74	12.9263
B6002B	1.97	9.84	8.90	40.92	29.53	5.9	8.320	0.363	217.6	45.74	16.020
B6003A	1.97	9.84	8.90	40.92	19.69	5.9	6.713	0.363	217.6	45.74	16.975

APPENDIX D (CONTINUED)

TEST DATA OF PRESTRESSED CONCRETE BEAMS FAILED IN SHEAR

BEAM MARK	p	h	d	Ac	acc	l	fc	As	Fy	Fse	Vt
	IN	IN	IN	IN2	IN	IN	KSI	IN2	KSI	KIPS	KIPS
A14-39	6.00	12.00	8.35	72.00	24.00	8.0	3.350	0.218	218.0	25.51	14.475
A14-44	6.00	12.00	8.50	72.00	24.00	8.0	3.350	0.249	218.0	29.38	15.990
A14-55	6.00	12.00	8.53	72.00	24.00	8.0	3.320	0.311	218.0	36.39	18.125
A14-68	6.00	12.00	8.42	72.00	24.00	8.0	2.440	0.280	218.0	33.01	14.935
A21-29	6.00	12.00	8.45	72.00	54.00	8.0	3.350	0.156	218.0	9.53	4.000
A21-39	6.00	12.00	8.95	72.00	54.00	8.0	3.130	0.218	218.0	12.84	5.430
A21-51	6.00	12.00	8.12	72.00	54.00	8.0	5.630	0.467	218.0	27.60	8.575
A22-20	6.00	12.00	8.45	72.00	36.00	8.0	5.350	0.176	208.0	10.77	7.235
A22-24	6.00	12.00	8.80	72.00	36.00	8.0	3.470	0.147	208.0	8.66	7.020
A22-27	6.00	12.00	8.38	72.00	36.00	8.0	3.850	0.176	208.0	10.56	6.930
A22-28	6.10	12.00	8.75	73.20	36.00	8.0	3.480	0.176	208.0	8.68	6.440
A22-31	6.00	12.00	8.06	72.00	36.00	8.0	3.530	0.176	208.0	15.73	7.455
A22-34	6.00	12.00	8.31	72.00	36.00	8.0	4.150	0.234	208.0	13.81	6.875
A22-36	6.00	12.00	8.35	72.00	36.00	8.0	2.890	0.176	208.0	15.49	7.350
A22-39	6.00	12.00	8.80	72.00	36.00	8.0	2.580	0.176	208.0	6.35	5.350
A22-40	6.00	12.00	8.20	72.00	36.00	8.0	5.790	0.381	208.0	27.43	13.195
A22-49	6.00	12.00	8.20	72.00	36.00	8.0	4.760	0.381	208.0	21.64	11.465
A32-19	6.10	12.00	9.03	73.20	36.00	8.0	4.990	0.176	208.0	4.00	5.670
A32-22	6.00	12.00	9.38	72.00	36.00	8.0	4.290	0.176	208.0	0.22	7.020
A32-27	6.00	12.00	9.16	72.00	36.00	8.0	2.800	0.176	208.0	1.76	6.240
A32-37	6.00	12.00	8.20	72.00	36.00	8.0	6.120	0.381	208.0	12.95	10.450
A32-49	6.00	12.00	8.20	72.00	36.00	8.0	4.760	0.381	208.0	21.98	6.850
B11-20	2.95	12.00	10.21	52.63	54.00	8.0	4.525	0.239	199.0	29.64	8.570
B11-29	2.95	12.00	10.00	52.80	54.00	8.0	4.190	0.239	199.0	29.64	8.570
B11-40	2.95	12.00	10.00	52.80	54.00	8.0	4.500	0.359	199.0	42.00	10.350
B12-10	3.06	12.00	11.11	53.77	36.00	8.0	5.600	0.121	213.5	14.88	7.870
B12-12	3.00	12.00	11.13	53.40	36.00	8.0	4.570	0.121	213.5	15.13	8.425
B12-14	3.00	12.00	11.14	53.40	36.00	8.0	3.850	0.121	213.5	14.88	8.370
B12-19	2.98	12.00	11.09	53.28	36.00	8.0	2.890	0.121	213.5	14.79	8.590
B12-26	3.03	12.00	10.06	54.40	36.00	8.0	4.460	0.233	212.0	25.63	11.650
B12-29	3.00	12.00	9.76	53.40	36.00	8.0	4.180	0.238	236.0	28.98	12.550
B12-34	3.08	12.00	10.18	55.00	36.00	8.0	4.825	0.349	212.0	37.48	14.375
B12-35	3.08	12.00	9.99	55.64	36.00	8.0	3.210	0.238	236.0	28.80	11.390
B12-50	2.96	12.00	10.20	53.15	36.00	8.0	2.950	0.299	199.0	34.68	11.930
B12-61	3.00	12.00	9.90	53.40	36.00	8.0	2.980	0.359	199.0	41.11	11.930
B13-16	3.00	12.00	10.38	53.40	28.00	8.0	5.540	0.179	199.0	22.46	13.200
B13-26	2.94	12.00	10.03	53.03	28.00	8.0	4.600	0.239	199.0	29.54	14.425
B21-41	2.90	12.00	10.04	52.78	28.00	8.0	4.320	0.359	199.0	42.54	15.815
B21-26	2.96	12.00	10.21	53.15	54.00	8.0	4.470	0.238	236.0	14.83	6.150
B22-09	2.96	12.00	11.07	53.15	36.00	8.0	6.320	0.119	236.0	7.56	7.045

APPENDIX D (CONTINUED)

TEST DATA OF PRESTRESSED CONCRETE BEAMS FAILED IN SHEAR

BEAM MARK	b IN	h IN	d IN	Ac IN2	acc IN	I IN	fc KSI	As IN2	Fy KSI	Fse KIPS	Vt KIPS
B22-23	3.00	12.00	10.03	53.69	36.00	8.0	5.120	0.238	236.0	13.16	9.300
B22-30	3.11	12.00	10.15	54.95	36.00	8.0	2.770	0.175	212.0	9.92	7.500
B22-41	3.16	12.00	10.02	55.84	36.00	8.0	2.710	0.233	212.0	11.93	8.700
B22-65	3.12	12.00	9.95	55.30	36.00	8.0	1.750	0.233	212.0	13.96	5.450
B22-68	3.00	12.00	9.90	53.40	36.00	8.0	2.670	0.359	199.0	21.18	9.435
B31-15	2.95	12.00	10.21	52.97	54.00	8.0	5.820	0.178	236.0	0.00	4.400
B32-11	2.98	12.00	10.40	53.28	36.00	8.0	5.220	0.119	236.0	0.00	5.450
B32-19	3.12	12.00	10.21	55.07	36.00	8.0	4.330	0.175	212.0	0.00	5.250
B33-31	3.10	12.00	10.20	55.12	36.00	8.0	2.720	0.175	212.0	0.00	3.800
B32-34	3.20	12.00	10.11	56.15	36.00	8.0	2.510	0.178	236.0	0.00	4.835
B32-41	2.96	12.00	10.59	53.15	36.00	8.0	3.275	0.299	199.0	0.00	8.000
B32-54	2.78	12.00	10.38	52.04	36.00	8.0	3.200	0.358	199.0	0.00	7.225
B32-09	1.75	12.00	11.04	47.56	36.00	8.0	6.460	0.121	213.5	15.25	8.315
C12-18	1.75	12.00	9.69	47.56	36.00	8.0	5.310	0.187	218.0	21.26	9.045
C12-19	1.79	12.00	10.11	47.79	36.00	8.0	6.040	0.233	212.0	25.89	11.170
C12-32	1.86	12.00	9.86	49.26	36.00	8.0	3.620	0.233	208.0	24.00	8.150
C12-33	1.88	12.00	10.08	49.00	36.00	8.0	5.470	0.373	218.0	43.04	12.750
C12-40	1.75	12.00	9.69	48.19	36.00	8.0	2.390	0.187	218.0	21.60	6.050
C12-44	1.75	12.00	9.50	48.81	36.00	8.0	2.890	0.249	218.0	25.17	6.425
C12-50	1.80	12.00	10.00	47.85	36.00	8.0	3.020	0.299	199.0	34.89	9.050
C12-57	1.83	12.00	9.91	48.65	36.00	8.0	2.490	0.359	199.0	42.00	13.000
C22-29	1.84	12.00	10.40	49.27	36.00	8.0	2.700	0.181	213.5	11.22	6.200
C22-31	1.77	12.00	10.88	47.68	36.00	8.0	3.300	0.241	213.5	14.46	5.450
C22-36	1.86	12.00	10.23	48.63	36.00	8.0	2.150	0.176	208.0	9.59	3.610
C22-39	1.85	12.00	10.18	49.08	36.00	8.0	2.150	0.176	208.0	9.59	3.610
C22-40	1.75	12.00	9.85	48.81	36.00	8.0	4.620	0.373	218.0	33.12	8.995
C22-46	1.79	12.00	10.11	48.11	36.00	8.0	3.160	0.299	199.0	17.25	6.385
C22-62	1.89	12.00	9.00	48.99	36.00	8.0	2.060	0.233	208.0	12.65	5.125
C22-73	1.75	12.00	9.91	47.56	36.00	8.0	2.910	0.419	199.0	23.17	6.665
C32-11	1.77	12.00	11.06	48.55	36.00	8.0	7.310	0.179	199.0	0.00	5.000
C32-22	1.82	12.00	10.00	48.47	36.00	8.0	3.870	0.176	208.0	0.00	5.175
C32-37	1.83	12.00	10.01	48.90	36.00	8.0	3.060	0.233	208.0	0.00	4.640
C32-42	1.88	12.00	10.10	49.19	36.00	8.0	2.690	0.233	208.0	0.00	4.075
C32-50	1.84	12.00	10.68	48.71	36.00	8.0	3.230	0.356	236.0	0.00	5.300
C32-80	1.81	12.00	10.00	47.91	36.00	8.0	3.000	0.478	199.0	0.00	5.290

[58.2]

APPENDIX D (CONTINUED)

TEST DATA OF PRESTRESSED CONCRETE BEAMS FAILED IN SHEAR

BEAM MARK	b IN	h IN	d IN	Ac IN2	acc IN	I IN	fc KSI	As IN2	Fy KSI	Fse KIPS	Vt KIPS
2	1.50	10.00	7.09	39.75	20.00	4.400	0.314	211.6	25.18	11.460	9.350
1	1.50	10.00	7.09	39.75	25.00	4.400	0.314	211.6	25.18	8.220	8.220
5	1.50	10.00	7.09	39.75	30.00	4.400	0.314	211.6	25.18	6.130	6.130
6	1.50	10.00	7.09	39.75	43.00	4.400	0.314	211.6	25.18	5.290	5.290
9B	1.50	10.00	7.09	39.75	55.00	4.400	0.314	211.6	25.18	4.210	4.210
9A	1.50	10.00	7.09	39.75	81.50	4.400	0.314	211.6	25.18	17.280	17.280
11A	1.50	10.00	7.09	39.75	15.00	5.520	0.314	211.6	25.18	7.390	7.390
11B	1.50	10.00	7.09	39.75	47.50	5.520	0.314	211.6	25.18	6.040	6.040
12	1.50	10.00	7.09	39.75	15.00	3.760	0.314	211.6	25.18	12.040	12.040
13A	1.50	10.00	7.09	39.75	30.00	3.760	0.314	211.6	25.18	6.240	6.240
13B	1.50	10.00	7.09	39.75	47.50	3.760	0.314	211.6	25.18	4.060	4.060
14	1.50	10.00	7.09	39.75	15.00	5.040	0.314	211.6	25.18	16.420	16.420
15A	1.50	10.00	7.09	39.75	30.00	5.040	0.314	211.6	25.18	7.720	7.720
15B	1.50	10.00	7.09	39.75	47.50	5.040	0.314	211.6	25.18	5.420	5.420
16	1.50	10.00	7.09	39.75	30.00	5.040	0.314	211.6	25.18	5.420	5.420

[58.2] (CONTINUED)

[69.4]

BEAM MARK	b IN	h IN	d IN	Ac IN2	acc IN	I IN	fc KSI	As IN2	Fy KSI	Fse KIPS	Vt KIPS
A-1	5.00	10.00	7.00	50.00	35.00	5.210	0.157	201.0	18.00	5.941	5.941
A-2	5.00	10.00	7.00	50.00	27.00	4.950	0.300	214.0	28.30	9.864	9.864
A-3	5.00	10.00	7.00	50.00	27.00	4.900	0.300	214.0	32.77	12.112	12.112
A-4	5.00	10.00	7.00	50.00	24.50	4.180	0.300	214.0	23.56	15.400	15.400
A-5	5.00	10.00	7.00	50.00	21.00	5.000	0.300	214.0	11.00	8.583	8.583
A-6	5.00	10.00	7.00	50.00	28.00	4.065	0.240	214.0	11.00	9.791	9.791
A-7	5.00	10.00	7.00	50.00	27.00	4.380	0.300	214.0	18.57	10.122	10.122
A-8	5.00	10.00	7.00	50.00	29.00	4.950	0.300	214.0	10.86	6.492	6.492
A-9	5.00	10.00	7.00	50.00	27.00	4.900	0.300	214.0	9.26	5.722	5.722
A-10	5.00	10.00	7.00	50.00	35.00	4.610	0.300	214.0	13.40	6.053	6.053
A-11	5.00	10.00	7.00	50.00	28.00	5.060	0.240	214.0	23.10	9.791	9.791
A-12	5.00	10.00	7.00	50.00	28.00	4.230	0.240	214.0	11.00	6.385	6.385
B-3	4.00	8.00	6.00	32.00	21.00	4.640	0.240	214.0	10.86	6.492	6.492
B-4	4.00	8.00	6.00	32.00	24.00	4.065	0.240	214.0	13.40	6.053	6.053
B-5	4.00	8.00	6.00	32.00	28.00	4.380	0.300	214.0	13.40	6.053	6.053
B-6	4.00	8.00	6.00	32.00	28.00	4.810	0.240	214.0	14.72	8.914	8.914
B-7	4.00	8.00	6.00	32.00	21.00	4.830	0.240	214.0	14.72	8.914	8.914
B-9	4.00	8.00	6.00	32.00	30.00	5.140	0.240	214.0	18.59	7.481	7.481
B-10	4.00	8.00	6.00	32.00	29.00	5.125	0.300	214.0	23.49	15.400	15.400
B-11	3.00	12.00	9.00	55.50	29.75	5.600	0.300	214.0	28.37	15.951	15.951
B-12	3.00	12.00	9.00	55.50	29.75	5.000	0.300	214.0	32.72	15.513	15.513
B-14	3.00	12.00	9.00	55.50	29.75	4.410	0.300	214.0	18.70	14.743	14.743
B-15	3.00	12.00	8.50	55.50	21.25	5.640	0.240	214.0	23.13	19.582	19.582
B-16	3.00	12.00	9.00	55.50	21.25	4.900	0.300	214.0	32.89	24.202	24.202
B-18	3.00	12.00	8.50	55.50	17.00	4.900	0.300	214.0	32.89	24.304	24.304
B-19	3.00	12.00	9.00	55.50	29.75	5.100	0.300	214.0	24.00	13.754	13.754
B-20	3.00	12.00	8.50	55.50	24.00	5.100	0.300	214.0	24.00	13.754	13.754

APPENDIX D (CONTINUED)

TEST DATA OF PRESTRESSED CONCRETE BEAMS FAILED IN SHEAR

BEAM MARK	b IN	h IN	d IN	Ac IN ²	acc IN	I IN	fc KSI	As IN ²	Fy KSI	Fse KIPS	Vt KIPS
I---21	3.00	12.00	9.00	55.50	34.00	[69.4]	(CONTINUED)				
D-----1	2.00	12.00	8.50	43.50	17.00		5.100	0.300	214.0	28.79	11.005
D-----2	2.00	12.00	8.50	43.50	29.75		5.075	0.157	201.0	21.05	17.165
D-----3	2.00	12.00	8.50	43.50	21.25		5.075	0.157	201.0	21.05	9.572
D-----4	2.00	12.00	8.50	43.50	34.00		5.050	0.300	214.0	27.78	16.614
D-----5	2.00	12.00	8.50	43.50	29.75		5.050	0.300	214.0	27.78	10.454
D-----6	2.00	12.00	8.50	43.50	17.00		4.460	0.240	214.0	26.31	9.904
D-----7	2.00	12.00	8.50	43.50	34.00		4.460	0.240	214.0	26.31	22.005
D-----8	2.00	12.00	9.00	43.50	42.50		5.000	0.300	214.0	32.72	10.561
D-----9	2.00	12.00	9.00	41.88	54.00		5.050	0.300	214.0	32.11	9.353
										23.95	6.492

APPENDIX E

TEST DATA OF R.C.T-BEAMS WITH WEB REINFORCEMENT AND FAILED IN SHEAR

BEAM MARK	b CM	h CM	d CM	acc CM	I CM	fc KG/CM ²	As CM ²	Fy KG/CM ²	Asc CM ²	Fyc KG/CM ²	Dc CM	Sy KG/CM ²	Vt KG/CM ²		
T5214-W	20	80	40	9	35.9	105	15	105.5	12.06	5745	2.26	4562	3.1	19.4	21.9
T5218-W	20	80	40	9	35.9	105	15	105.2	12.06	5621	2.26	4562	3.1	24.6	22.4
T5218-E	20	80	40	9	35.9	105	15	105.2	12.06	5769	2.26	4562	3.1	25.4	21.7
T6005-W	20	80	40	9	35.9	105	15	107.9	12.06	7336	2.26	4562	3.1	6.9	16.1
T6005-E	20	80	40	9	35.9	105	15	107.9	12.06	7336	2.26	4562	3.1	7.1	16.1
T6010-E	20	80	40	9	35.9	105	15	105.0	12.06	7411	2.26	4562	3.1	14.2	19.4
T6014-W	20	80	40	9	35.9	105	15	115.9	12.06	7374	2.26	4562	3.1	19.5	24.2
T6014-E	20	80	40	9	35.9	105	15	115.9	12.06	7374	2.26	4562	3.1	19.9	22.7
T6018-W	20	80	40	9	35.9	105	15	112.0	12.06	7360	2.26	4562	3.1	24.2	24.5
T6018-E	20	80	40	9	35.9	105	15	112.0	12.06	7360	2.26	4562	3.1	25.7	23.5
T6022-W	20	80	40	9	35.9	105	15	105.5	12.06	7360	2.26	4562	3.1	30.7	23.9
T6022-E	20	80	40	9	35.9	105	15	105.5	12.06	7360	2.26	4562	3.1	29.7	22.4
T6025-W	20	80	40	9	35.9	105	15	104.5	12.06	7360	2.26	4562	3.1	34.7	22.4
T6025-E	20	80	40	9	35.9	105	15	104.5	12.06	7360	2.26	4562	3.1	35.6	24.2
T6029-W	20	80	40	9	35.9	105	15	107.6	12.06	7349	2.26	4562	3.1	39.8	26.5
T6029-E	20	80	40	9	35.9	105	15	107.6	12.06	7349	2.26	4562	3.1	39.2	24.5
T6032-W	20	80	40	9	35.9	105	15	119.8	12.06	7274	2.26	4562	3.1	40.3	24.3
T6032-E	20	80	40	9	35.9	105	15	119.8	12.06	7274	2.26	4562	3.1	43.0	24.5
T9025-W	20	80	40	9	35.9	105	15	127.9	12.06	9151	2.26	4562	3.1	35.8	27.5
T9025-E	20	80	40	9	35.9	105	15	127.9	12.06	9151	2.26	4562	3.1	35.4	26.5
T9032-E	20	80	40	9	35.9	105	15	100.6	12.06	9151	2.26	4562	3.1	46.5	26.3
T9036-W	20	80	40	9	35.9	105	15	107.3	12.06	9152	2.26	4562	3.1	51.7	28.6
T9040-W	20	80	40	9	35.9	105	15	114.8	12.06	9151	2.26	4562	3.1	49.2	26.5
T9040-E	20	80	40	9	35.9	105	15	114.8	12.06	9151	2.26	4562	3.1	51.7	25.4
T9043-W	20	80	40	9	35.9	105	15	105.2	12.06	9185	2.26	4562	3.1	55.2	28.6
T9043-E	20	80	40	9	35.9	105	15	105.2	12.06	9185	2.26	4562	3.1	56.7	27.6
T9047-W	20	80	40	9	35.9	105	15	128.5	12.06	9292	2.26	4562	3.1	62.6	28.6
T9047-E	20	80	40	9	35.9	105	15	128.5	12.06	9292	2.26	4562	3.1	60.3	30.4
T9060-W	20	80	40	9	35.9	105	15	121.3	12.06	9151	2.26	4562	3.1	68.9	24.5
T9060-E	20	80	40	9	35.9	105	15	121.3	12.06	9151	2.26	4562	3.1	68.9	24.3
T9065-W	20	80	40	9	35.9	105	15	102.4	12.06	9151	2.26	4562	3.1	78.9	24.5
T9065-E	20	80	40	9	35.9	105	15	102.4	12.06	9151	2.26	4562	3.1	78.9	24.5
T9071-W	20	80	40	9	35.9	105	15	111.3	12.06	9151	2.26	4562	3.1	88.4	26.5
T9071-E	20	80	40	9	35.9	105	15	111.3	12.06	9151	2.26	4562	3.1	88.4	24.5
T9078-W	20	80	40	9	35.9	105	15	114.7	12.06	9151	2.26	4562	3.1	98.5	28.6
T9078-E	20	80	40	9	35.9	105	15	114.7	12.06	9151	2.26	4562	3.1	98.5	26.5
T6018DW	20	80	40	9	35.9	105	15	98.1	12.06	7360	3.39	4562	3.1	24.5	18.2
T9029DW	20	80	40	9	35.9	105	15	109.9	12.06	9151	3.39	4562	3.1	38.3	24.5
T9029DE	20	80	40	9	35.9	105	15	109.9	12.06	9151	3.39	4562	3.1	39.0	26.5

APPENDIX E (CONTINUED)

TEST DATA OF R.C.T-BEAMS WITH WEB REINFORCEMENT AND FAILED IN SHEAR

BEAM MARK	b	h	d	acc	l	fc	As	Fy	Asc	Fyc	dc	Sy	Vt
	CM	CM	CM	CM	CM	KG/CM2	CM2	KG/CM2	CM2	KG/CM2	CM	KG/CM2	T
[76.6] (CONTINUED)													
T6018MW	20	80	40	9	35.9	105	15	106.8	12.06	7360	2.26	4562	3.1
T6018ME	20	80	40	9	35.9	105	15	106.8	12.06	7360	2.26	4562	3.1
T9029MW	20	80	40	9	35.9	105	15	116.2	12.06	8886	2.26	4562	3.1
T9029ME	20	80	40	9	35.9	105	15	116.2	12.06	8886	2.26	4562	3.1

[80.2]

V6002-W	20	80	40	9	34.3	105	15	198.8	19.63	6669	2.26	4660	3.1
V6002-E	20	80	40	9	34.3	105	15	198.8	19.63	6669	2.26	4660	3.1
V6004-W	20	80	40	9	34.3	105	15	215.2	19.63	6669	2.26	4660	3.1
V6004-E	20	80	40	9	34.3	105	15	215.2	19.63	6669	2.26	4660	3.1
U6007-W	20	80	40	9	34.3	105	15	149.9	19.63	6669	2.26	4660	3.1
U6007-E	20	80	40	9	34.3	105	15	149.9	19.63	6669	2.26	4660	3.1

U6010-W	20	80	40	9	34.3	105	15	168.3	19.63	6669	2.26	4660	3.1
U6010-E	20	80	40	9	34.3	105	15	168.3	19.63	6669	2.26	4660	3.1
U6013-W	20	80	40	9	34.3	105	15	126.4	19.63	6669	2.26	4660	3.1
U6013-E	20	80	40	9	34.3	105	15	126.4	19.63	6669	2.26	4660	3.1
U6017-W	20	80	40	9	34.3	105	15	187.6	19.63	6669	2.26	4660	3.1
U6017-E	20	80	40	9	34.3	105	15	187.6	19.63	6669	2.26	4660	3.1

U6017CE	20	80	40	9	34.3	105	15	187.6	19.63	6669	2.26	4660	3.1
U6023CW	20	80	40	9	34.3	105	15	175.4	19.63	6669	2.26	4660	3.1
U6023CE	20	80	40	9	34.3	105	15	175.4	19.63	6669	2.26	4660	3.1
U6029CW	20	80	40	9	34.3	105	15	203.9	19.63	6669	2.26	4660	3.1
U6029CE	20	80	40	9	34.3	105	15	203.9	19.63	6669	2.26	4660	3.1
U6044CW	20	80	40	9	34.3	105	15	154.0	19.63	6669	2.26	4660	3.1
U6044CE	20	80	40	9	34.3	105	15	154.0	19.63	6669	2.26	4660	3.1
U6007HW	20	80	40	9	34.3	105	15	158.1	19.63	6669	2.26	4660	3.1
U6007HE	20	80	40	9	34.3	105	15	158.1	19.63	6669	2.26	4660	3.1
U6010HE	20	80	40	9	34.3	105	15	182.5	19.63	6669	2.26	4660	3.1
U6017HW	20	80	40	9	34.3	105	15	207.0	19.63	6669	2.26	4660	3.1
U6017HE	20	80	40	9	34.3	105	15	207.0	19.63	6669	2.26	4660	3.1
U4213MW	20	80	40	9	34.0	105	15	144.8	38.48	4594	2.26	4660	3.1
U4213ME	20	80	40	9	34.0	105	15	144.8	38.48	4594	2.26	4660	3.1
U4222MW	20	80	40	9	34.0	105	15	161.1	38.48	4594	2.26	4660	3.1

APPENDIX E (CONTINUED)

TEST DATA OF R.C.T-BEAMS WITH WEB REINFORCEMENT AND FAILED IN SHEAR

BEAM MARK	b	h	d	acc	l	fc	As	Fy	Asc	Fyc	dc	Sy	Vt
	CM	CM	CM	CM	CM	KG/CM2	CM2	KG/CM2	CM2	KG/CM2	CM	KG/CM2	T
[80.2] (CONTINUED)													
U4222ME	20	80	40	9	34.0	105	15	161.1	38.48	4594	2.26	4660	3.1
U4230MW	20	80	40	9	34.0	105	15	171.3	38.48	4594	2.26	4660	3.1
U4230ME	20	80	40	9	34.0	105	15	171.3	38.48	4594	2.26	4660	3.1
U4244MW	20	80	40	9	34.0	105	15	168.3	38.48	4594	2.26	4660	3.1
U4244ME	20	80	40	9	34.0	105	15	168.3	38.48	4594	2.26	4660	3.1

X6009-W	20	80	40	9	35.8	105	15	74.4	9.05	9422	2.26	4660	3.1
X6009-E	20	80	40	9	35.8	105	15	74.4	9.05	9422	2.26	4660	3.1
X6018-W	20	80	40	9	35.3	105	15	95.9	9.05	9422	2.26	4660	3.1
X6018-E	20	80	40	9	35.3	105	15	95.9	9.05	9422	2.26	4660	3.1
X9032-W	20	80	40	9	34.9	105	15	86.7	9.05	9422	2.26	4660	3.1
X9032-E	20	80	40	9	34.9	105	15	86.7	9.05	9422	2.26	4660	3.1
X9043-W	20	80	40	9	34.9	105	15	83.6	9.05	9422	2.26	4660	3.1
X9043-E	20	80	40	9	34.9	105	15	83.6	9.05	9422	2.26	4660	3.1
B6009-W	38	80	40	9	35.4	105	15	109.1	16.08	7184	8.04	7184	3.3
B6009-E	38	80	40	9	35.4	105	15	109.1	16.08	7184	8.04	7184	3.3
B9025AW	38	80	40	9	35.4	105	15	125.4	16.08	9463	8.04	7184	3.3
B9025AE	38	80	40	9	35.4	105	15	125.4	16.08	9463	8.04	7184	3.3
B9029-W	38	80	40	9	35.4	105	15	98.9	16.08	9463	8.04	7184	3.3
B9029-E	38	80	40	9	35.4	105	15	98.9	16.08	9463	8.04	7184	3.3
B9040-W	38	80	40	9	35.4	105	15	87.7	16.08	9463	8.04	7184	3.3
B9040-E	38	80	40	9	35.4	105	15	87.7	16.08	9463	8.04	7184	3.3
U5617TW	20	80	40	9	34.5	105	15	182.5	19.63	7306	2.26	4660	3.1
U5617TE	20	80	40	9	34.5	105	15	182.5	19.63	7306	2.26	4660	3.1
U5604PW	20	80	40	9	34.5	105	15	245.7	8.04	6541	2.26	4660	3.1
U5604PE	20	80	40	9	34.5	105	15	245.7	8.04	6541	2.26	4660	3.1
R5651TW	20	80	40	9	35.9	105	15	94.8	16.08	6541	6.03	5715	3.3
R5651TE	20	80	40	9	35.9	105	15	94.8	16.08	6541	6.03	5715	3.3

APPENDIX G (CONTINUED)

TEST DATA OF PRESTRESSED BEAMS WITH WEB REINFORCEMENT

BEAM MARK	b IN	d IN	Ac IN2	acc IN	l IN	fc KSI	As IN2	Fy KSI	Sy KSI	Fse KIPS	Vt KIPS
[71.2] (CONTINUED)											
3-C-----5	1.00	8.88	32.5	26.63		4.58	0.359		1.259	13.9	10.98
3-D-----1	1.00	8.88	32.5	26.63		6.42	0.359		1.887	65.7	19.27
3-D-----2	1.00	8.88	32.5	26.63		5.90	0.359		1.259	67.8	17.25
3-D-----3	1.00	8.88	32.5	26.63		5.85	0.359		0.839	63.4	15.75
3-D-----4	1.00	8.88	32.5	26.63		5.71	0.359		0.628	65.0	13.72
[73.4]											
NL-6-240	2.00	12.00	44.0	36.00		5.54	0.801	127.2	0.104	50.0	18.52
NH-6-240	2.00	12.00	44.0	36.00		4.77	0.801	127.2	0.170	49.8	20.00
NL-6-160	2.00	12.00	44.0	36.00		5.26	0.801	127.2	0.156	49.6	20.34
NH-6-160	2.00	12.00	44.0	36.00		5.22	0.801	127.2	0.254	50.1	23.60
NL-6-80	2.00	12.00	44.0	36.00		5.35	0.801	127.2	0.313	50.0	23.91
[73.2]											
NH-6-80	2.00	12.00	44.0	36.00		5.21	0.801	127.2	0.509	49.9	25.62
NL10-160	2.00	12.00	44.0	36.00		5.18	0.801	127.2	0.355	49.2	23.03
NM10-160	2.00	12.00	44.0	36.00		5.14	0.801	127.2	0.584	50.9	23.03
PL-6-240	2.00	12.00	44.0	36.00		5.94	0.801	127.2	0.104	53.9	20.00
PH-6-160	2.00	12.00	44.0	36.00		5.43	0.801	127.2	0.254	70.5	21.01
PL-6-80	2.00	12.00	44.0	36.00		5.89	0.801	127.2	0.313	71.2	23.82
CH-6-240	2.00	12.00	44.0	36.00		7.77	0.801	127.2	0.170	49.9	23.03
CL-6-160	2.00	12.00	44.0	36.00		7.89	0.801	127.2	0.156	50.0	23.03
CH-6-160	2.00	12.00	44.0	36.00		7.98	0.801	127.2	0.254	49.8	25.17
CL-6-80	2.00	12.00	44.0	36.00		8.11	0.801	127.2	0.292	50.2	26.07
CM-6-80	2.00	12.00	44.0	36.00		8.00	0.801	127.2	0.424	50.7	28.31
CH-6-80	2.00	12.00	44.0	36.00		7.52	0.801	127.3	0.509	50.1	31.46

APPENDIX G (CONTINUED)

TEST DATA OF PRESTRESSED BEAMS WITH WEB REINFORCEMENT

BEAM MARK	b IN	d IN	Ac IN2	acc IN	l IN	fc KSI	As IN2	Fy KSI	Sy KSI	Fse KIPS	Vt KIPS
[73.2] (CONTINUED)											
P-----18	5.90	10.60	131.0	39.00		6.45	0.747	161.1	0.094	112.0	36.00
P-----19	5.90	10.60	131.0	39.00		6.58	0.747	161.1	0.064	112.0	24.50
P-----20	5.90	11.00	131.0	39.00		5.90	1.247	93.0	0.094	0.0	27.00
P-----21	5.90	11.00	131.0	39.00		6.21	1.247	93.0	0.064	0.0	20.20
P-----22	5.90	11.00	131.0	39.00		6.28	1.247	93.0	0.104	0.0	24.50
[73.3]											
P-----23	5.90	11.00	131.0	26.00		6.24	1.247	93.0	0.155	0.0	36.00
P-----41	5.90	11.00	131.0	39.00		6.38	1.247	93.0	0.000	0.0	15.70
P-----47	5.90	10.80	131.0	39.00		6.17	1.682	123.3	0.000	112.0	36.00
P-----48	5.90	10.60	131.0	39.00		5.97	0.747	161.1	0.000	70.0	31.70
P-----49	5.90	10.80	131.0	39.00		5.48	1.682	123.3	0.155	112.0	42.70
[73.4]											
P-----50	5.90	10.80	131.0	39.00		5.97	1.682	123.3	0.290	112.0	51.70

AFDELINGEN FOR BÆRENDE KONSTRUKTIONER
DANMARKS TEKNISKE HØJSKOLE

Department of Structural Engineering
Technical University of Denmark, DK-2800 Lyngby

SERIE R
(Tidligere: Rapporter)

- R 178. BJØRNBÆK-HANSEN og H. AGERSKOV: Udmattelsesforsøg med Ortotrop Broanepanel. 1983.
- R 179. KRISTIANSEN, NIELS ØRSKOV: Tryk- og Strømningsforhold i Siloer med Kohæsive Medier. 1984.
- R 180. NIELSEN, JOHN SANDER: The Effect of Stirrup Spacing on the Ultimate Load of Reinforced Concrete Beams Subjected to Pure Torsion. 1984.
- R 181. KERN, JENS CHR.: Numerisk Brudstadieberegning af Stift, Plastiske Materialer. 1984.
- R 182. FEDDERSEN, B., U. HESS, H. EXNER og M.P. NIELSEN: Gen-nemlokning af Huldåkelementer. 1984.
- R 183. BJERAGER, PETER: Reliability Analysis of Structural Systems. 1984.
- R 184. HESS, UWE: Plasticitetsteoretisk analyse af forankring og stød af forkommet armering i beton. 1984.
- R 185. NITTEGAARD-NIELSEN, PETER: Elementmetodebaserede beregningsmodeller for dæmpede konstruktionssvingninger. 1984.
- R 186. DAMKILDE, LARS: Beregning af plader af elastisk-plastisk materiale ved hjælp af elementmetoden. 1984.
- R 187. DAMKILDE, LARS: Stability of Plates of Elastic-plastic Material. 1984.
- R 188. NITTEGAARD-NIELSEN, PETER: Elementmetodebaseret beregningsmodel for dæmpede svingninger i 3-fase kontinuum: matrixmateriale - væske - luft. 1984.
- R 189. Resuméoversigt 1983 - Summaries of Papers 1983. 1984.
- R 190. JULIUS SOLNES: Vibration of Suspension Bridges under Earthquake Loads. 1984.
- R 191. MUNCH-ANDERSEN og V. ASKEGAARD: Results from Tests with Normal and Shear Strees Cells in Medium-Scale Model Silo. 1984.
- R 192. DITLEVSEN, OVE: Probabilistic Thinking: An Imperative in Engineering Modelling. 1984.
- R 193. STANG, HENRIK: En Kompositmaterialeteori og dens Anvendelse til Beskrivelse af Trækpåvirkede Cementkompositter. 1984.
- R 194. ARPE, ROBERT: Broers Dynamiske Respons på Trafiklast. Del 1. Teori. 1984. (Udsolgt), (Out of print).
- R 195. ARPE, ROBERT: Broers Dynamiske Respons på Trafiklast. Del 2. Modelforsøg. 1984.
- R 196. GERSTOFT, PETER: Simplified Methods for Dynamic Analysis of a Guyed Mast. 1984. (Udsolgt), (Out of print).
- R 197. DYRBYE, C.: Simulation of Earthquake Ground Motion on a Microcomputer. 1985.
- R 198. ABK Informationsdag 1985.
- R 199. RASMUSSEN, KIM: Elastic-Plastic Buckling of Long Plates in Compression. 1985.
- R 200. STANG, HENRIK: Dimensionering af limede konstruktive samlinger: En litteraturoversigt. 1985.
- R 201. Resuméoversigt 1984 - Summaries of Papers 1984. 1985.
- R 202. GIMSING, N.J.: Means of Improving the Deformational Characteristics of Cable Supported Bridges. 1985.
- R 203. SOB CZYK, KAZIMIERZ: Stochastic Differential Equations for Applications. 1985.
- R 204. STANG, HENRIK: The Fibre Pull-out Problem; An Experimental Investigation. 1985.
- R 205. STANG, HENRIK: The Fibre Pull-out Problem; An Experimental Investigation. 1985.
- R 206. STANG, HENRIK OG RUNE BRINCKER: Udmattelsesforsøg med limsamlinger mellem stål og glasfiberlaminater. Små prøver. 1985.
- R 207. GOLTERMANN, PER: Samvirken imellem lokal og global stabilitet i tyndvæggede bjælker. 1985.
- R 208. MÖLLMANN, H.: Theory of Thin-Walled Elastic Beams with Finite Displacements. 1985.
- R 209. HAHR, HENRIK: Materialeafhængig Stabilitetsopførsel af Simple Søjler. 1986.
- R 210. RIBERHOLT, H.: Glued Bolts in Glulam. 1986.
- R 211. Resuméoversigt 1985 - Summaries of Papers 1985. 1986.
- R 212. ANDREASEN, BENT og M.P. NIELSEN: Dome Effect in Reinforced Concrete Slabs. 1986.
- R 213. GERSTOFT, PETER: An Assessment of Wind Loading on Tower Shaped Structures. 1986.
- R 214. GIMSING, N.J.: Recent and Future Developments of Cable Supported Bridges. 1986.
- R 215. LANGE-HANSEN, P.: A Hybrid Upper Bound Theorem for the Limit Load in the Theory of Plasticity. 1986.
- R 216. MAGNUSSEN, GYLFI: Simulation Algorithms. 1987.
- R 217. Resuméoversigt 1986 - Summaries of Papers 1986. 1987.
- R 218. DYRBYE, C. Harmonic Vibrations of Plane Frames. 1987.
- R 219. WINTERSTEIN, STEVEN R.: Moment-based Hermite Models of Random Vibration. 1987.
- R 220. DØSSING, JENS: Stempelproblemer vedrørende cirkulær cylindriske skaller. 1987.
- R 221. DØSSING, JENS: Deformerbare dæknudepunkter i offshore stålkonstruktioner. 1987.
- R 222. RIBERHOLT, H.: De mekaniske egenskaber af plader oplimet af birkefiner. 1987.
- R 223. NIELSEN, LEIF OTTO: Forskydningsspændinger i homogene bjælketværsnit af symmetrisk materiale. 1987.
- R 224. LANGE-HANSEN, P. OG SØREN MØLLER NIELSEN: An Improved Upper Bound on the Residual Deflections in Elastic-Plastic Structures Subject to Variable Loading. 1988.
- R 225. THORUP, ERIK: User Guide and Documentation on the Program Fatsys (ver.3.0). 1988.
- R 226. DITLEVSEN, OVE: Uncertainty and Structural Reliability. Hocus Pocus or Objective Modelling. 1988.
- R 227. Resuméoversigt 1987 - Summaries of Papers 1987.
- R 228. RIBERHOLT, H.: Glued Bolts in Glulam. Part 2. 1988.
- R 229. RIBERHOLT, H.: Delamineringsprøvning. 1988.
- R 230. RIBERHOLT, H.: Woodflanges under tension, 1988.
- R 231. HOLKMANN OLSEN, N.: Implementation. 1988.
- R 232. HOLKMANN OLSEN, N.: Uniaxial. 1988.
- R 233. HOLKMANN OLSEN, N.: Anchorage. 1988.
- R 234. HOLKMANN OLSEN, N.: Heat Induced. 1988.
- R 235. SCHEEL, HELLE: Rotationskapacitet. 1988.
- R 236. NIELSEN, MONA: Arbejdslinier. 1988.
- R 237. Publication pending.
- R 238. ANDREASEN, BENT STEEN: Anchorage of Deformed Reinforcing bars. 1988.
- R 239. ANDREASEN, BENT STEEN: Anchorage Tests with Deformed Reinforcing Bars in more than one layer at a Beam Support. 1988.
- R 240. GIMSING, N.J.: Cable-Stayed Bridges with Ultra Long Spans. 1988.